THE DESIGN AND ANALYSIS OF MULTIRATE CONTROL SYSTEMS

Yoginee Patel

Submitted in accordance with the requirements of the award of the

D.Phil Degree

UNIVERSITY OF YORK

DEPARTMENT OF ELECTRONICS

SEPTEMBER 1991

CONTENTS

Page

CHAPTER TWO

State-Space Representation of Multivariable Multirate Systems

CHAPTER THREE

Sample Rate Selection

Page

CHAPTER SIX

Constrained and Optimised Solutions to the Multirate Eigenproblem

CHAPTER SEVEN

Deadbeat Control Using MIFO Sampled Feedback

NOMENCLATURE

$()^{\dagger}$	Moore-Penrose inverse (pseudoinverse).
$()^{*}$	Complex conjugate.
$\|\|K\|\|_2$	2-norm of K, i.e. maximum positive value of $(K^{*T}K)^{1/2}$.
α	Scalar contraction factor (see Section 3.6).
γ	Gain margin (see Section 3.6).
Δ	Multiplicative perturbation matrix.
B_C	Generalised sample rate selection criterion matrix (see Section 5.2).
$\alpha(i,j)$	Weighting element for cost function J_G.
β_i	Weighting element for cost function J_M.
$\gamma(i,j)$	Weighting element for cost function J_{D1}.
$\kappa(V)$	Conditioning of matrix V, i.e. $\kappa(V) = \|\|V\|\|_2\|\|V^{-1}\|\|_2$.
$\kappa_{mi}(V)$	Conditioning of multirate right eigenvector matrix V_{mi}.
$\{\mu_i\}$	Kronecker invariants (= input sample rate multiplicities).
$\bar{\sigma}[G(s)]$	Maximum singular value of G(s).

$\underline{\sigma}[G(s)]$	Minimum singular value of G(s).
λ_i	i'th eigenvalue.
v_i (v_{ai}, v_{di})	Right eigenvector associated with λ_i. (Subscripts a, d denote achieved and desired respectively).
Λ	Matrix diag$\{\lambda_1 \ ,.. \ \lambda_n\}$.
$\{\rho_i\}$	Input multiplicities produced by generalised sample rate selection criterion (see Section 5.2).
$\{\Phi,\Gamma,C,D\}$	Discrete system matrices.
$\Phi(T)=\Phi_T[1,0]$	Discrete system transition matrix for period T.
$\Gamma(T)=\Gamma_T[1,0]$	Discrete system control matrix for period T.
$\{\Phi_{MR1}, \Gamma_{MR1}\}$	State transition and control matrices for *general* multi-input, multi-output (MIMO) multirate system.
$\{\Phi_{MR2}, \Gamma_{MR2}\}$	State transition and control matrices for multiple input rate, fixed output rate (MIFO) MIMO multirate system.
$\ell_i = n_0/n_i$	Multiple of T_b contained within period T_i, i.e. $T_i = \ell_i T_b$.
{A,B,C,D}	Continuous system matrices.
A(t), B(t)	Continuous T-periodical system matrices.
c_i	Condition number of eigenvalue λ_i.

$c_{mj} = (c_{ji})$ Condition number of eigenvalue λ_{mi} for multirate system matrix Φ_{mj}.

E^{n+} Advance vector decomposition (Kranc) operator.

E^{n-} Delay vector decomposition (Kranc) operator.

$f^T(t)$ Continuous signal sampled at frequency 1/T.

$f(kT)$ Value of $f^T(t)$ at an instant kT.

$F(s)$ Laplace Transform of F.

$F^T(s)$ Discrete Laplace function (F(s) sampled at rate 1/T).

$F^T(z) = F(z)$ Z transform of function $F^T(s)$ for period T, i.e. Z[F(s)].

$F_h(z)$ Z transform of F(s) for period T, assuming input is held constant by a zero-order-hold (ZOH) of period T.

$F_h^T(z_n)$ Z transform of F(s) for period T/n, assuming input is held constant by a ZOH of period T.

$F^T(z,m)$ Modified Z transform, i.e. $Z[F(s)e^{sTm}]$.

$H(z)$ Singular pencil of open loop, single rate discrete system.

$H_c(z)$ Singular pencil of closed loop, single rate discrete system.

$H_{MOL}(z)$	Singular pencil of open loop, multirate discrete system.
$H_M(z)$	Singular pencil of closed loop, multirate discrete system.
I_n	Identitiy matrix of dimension (nxn).
$I_{n,i}$	Zero matrix of dimension (nxn) with diagonal unit entries starting on the (i+1)'th element.
J_G J_{D1} J_{D2} J_M	Optimisation Cost functions.
l_i	i'th left eigenvector.
Im(·)	Imaginary part of (·).
Im[C]	Image of C.
$L = V^{-1}$	Left eigenvector matrix $L = [l_1\ l_2\ ,..,\ l_n]^T$.
M_1, M_2	Block diagonal matrices of dimension $(n_0 x n_0)$ comprised of (nxn) dimension 0, I_n matrices.
n_i	Sample rate multiplicity (i.e. $T = n_0 T_b$, $T = n_i T_i$).
$N = \sum n_i$	Sum of multiplicities (i=1,..,m for input sample period multiplicities).
N[C]	Nullspace of C.
R[C]	Range space of C.

$Re(\cdot)$	Real part of $(\cdot)$.
$Res[F^T(z)]_{\lambda i}$	Residues of $F^T(z)$ at the poles, λ_i, of $F^T(z)$.
$R_{\lambda i}$	Nullspace of $S_{\lambda i}$, i.e. $N[S_{\lambda i}]$.
S_i	$[\Phi,\Gamma_i]$ invariant subspace (where Γ_i = i'th column of Γ).
$S_{\lambda i}$	Compatibly dimensioned (partitioned) matrix $[\lambda_i I-A : B]$.
T	Main sample interval.
T_b	Base sample interval.
T_i	Sample interval of i'th input (= T/n_i).
T_{c1}	Transformation matrix for canonical system which generates indices $\{l_i\}$.
T_{c2}	Transformation matrix for canonical system which generates indices $\{\mu_i\}$.
V	Matrix of right eigenvectors, $V = [\nu_1\ \nu_2\ ,..,\ \nu_n]$.
V_{mi}	Matrix of right eigenvectors for multirate closed loop matrix Φ_{mi}.
$W_c[t_0\ t_f]$	Periodic Controllability Gramain for time interval $[t_0\ t_f]$.
$W_o[t_0\ t_f]$	Periodic Observability Gramain for time interval $[t_0\ t_f]$.

$W=(sI-A)^{-1}B$	Open loop transfer function for system triple $\{A,B,C=I_n\}$.
W_L	Open loop transfer function for system triple $\{A,B,C=I_n\}$ subject to multiplicative perturbation Δ, i.e. $W_L = (I+\Delta)(sI-A)^{-1}B$.
x,u,y	State, input and output vectors.
x_e,u_e,y_e	Expanded state, input and output vectors.
$z = e^{sT}$	Discrete z operator.
$z_n = e^{sT/n}$	Discrete z_n operator.
$Z[F(z_n)]_{z_n \to z}$	Extraction of $F(z)$ from $F(z_n)$.

ACKNOWLEDGEMENTS

This research was funded by the Science and Engineering Research Council, British Aerospace (Brough) and Westland Helicopters plc. (Yeovil). Thanks are due especially to Dr Paul Taylor of Westland Helicopters plc. for his valued support of this work.

Special thanks are also due to Dr Ron Patton for his generous support and advice throughout the project. His enthusiastic supervision of this work has also been greatly valued.

DECLARATION

This thesis contains material from the following reports and papers which have been produced and previously used by the author:-

Patel Y. (1990), An Analysis of Multirate Control Applied to a Simplified Helicopter Model, Report for Westland Helicopters Limited, Yeovil, Somerset.

Patel Y, Patton R.J. (1990), A Robust Approach to Multirate Controller Design using Eigenstructure Assignment, *Proceedings of the American Control Conference*, San Diego, California, USA, pp 945-951.

Patel Y. (1991), State Space Techniques for Multirate Control Systems Analysis, Report for Westland Helicopters Limited, Yeovil, Somerset.

Patel Y., Patton R.J., Burrows S.P. (1991), Robust, Low Norm Multirate Control using Eigenstructure Assignment, *Proceedings of IEE Control 91 Conference*, Edinburgh, UK, pp 1165-1170.

Patel Y., Patton R.J. (1991), Design of Robust, Multirate Feedback Control using Eigenstructure Assignment, *Proceedings of the IMACS-IFACS Symposium on Modelling and Control of Technological Systems*, Lille, France, pp 309-315. Also to be published in *Mathematics of the Analysis and Design of Process Control*, Edited by Borne P. and Tzafestas S.G.

Patel Y., Patton R.J., Burrows S.P. (1991), The Design of Robust Multirate Aircraft Control Using Optimised Eigenstructure Assignment, *Proceedings of the AIAA Guidance, Navigation and Control Conference*, New Orleans, USA, pp 1805-1811. Also to appear in *AIAA Journal of Guidance, Control and Dynamics*.

Patel Y., Patton R.J. (1991), Deadbeat Control Algorithms for Multirate Control Systems, *Proceedings of the 1st European Control Conference*, Grenoble, pp 1598-1603.

Patel Y., Patton R.J. (1991), Insensitivity Properties of Multirate Feedback Control Systems, *Proceedings of the 30'th IEEE CDC Conference*, Brighton, UK, pp 2954-2959. Also to be published in *IEEE Transactions on Automatic Control*.

Patel Y., Patton R.J., Burrows S.P., Robust Eigenstructure Assignment for Multirate Control System Design, *To appear in the Proceedings of the 1st IEEE Conference on Control Applications*, Dayton, Ohio, USA, September 1992.

ABSTRACT

This thesis examines and develops design and analysis techniques for multirate control systems. The operation of a system can be defined as multirate if its inputs and outputs are updated at non-uniform rates. Many of the analytic problems posed by multirate systems are attributed to this time-varying nature. Two assumptions simplify the analysis of multirate system behaviour; all sampling operations are synchronised at periodic intervals and all sample rates are integer multiples of some common frequency. This work considers the modelling, analysis and design of multirate systems which meet both these requirements.

Many of the tools developed for multirate system analysis are based on frequency and switch decomposition techniques. The thesis begins with an investigation of the development, application and limitations of the classical implementations of the decomposition methods. The state variable formulation of the decomposition methods, which circumvent many problems associated with the early methods, is then described. The merits and application of the latter approach are examined.

The role of the periodic interval and the inter-relationship between input/output sample rates in determining the performance and (A,B) and (A,C) invariance properties of multirate systems is outlined. Different methods of selecting these sample parameters and their effect on the design of multirate control is investigated. In particular, the sample rate selection criterion which generates maximum design freedom for the solution of the multirate state feedback problem is generalised.

The remainder of the work is devoted to the development of state space design techniques. A new design method which can be used for the design of multirate compensators is introduced. The novel application of Eigenstructure Assignment design techniques to the design of multirate state feedback control is also investigated. Finally, the design of deadbeat multirate control systems is outlined.

1 DESCRIPTION AND PURPOSE OF RESEARCH

Multirate control has been investigated by many in the past motivated by the need to optimise the performance of systems with varying dynamic modes and to make efficient use of available hardware resources. The trend has been recently accelerated with the emergence of multiprocessor architectures. These require the decomposition of a control system into a number of functional subsystems which can then be handled as parallel processes. An efficient and natural method of rationalising the available processing power is to update and monitor the individual subsystems as according to their rate of change.

This philosophy is particularly suited to applications in the aerospace industry. The increasing demands on airborne computing, ranging from performance monitoring to control actuation, have created serious data throughput constraints on processors handling the tasks in a flight control system. In addition to this, the effective control of an aircraft demands a wide range of computation rates to cater for the disparate bandwidth requirements of its various subsystem components. Combined, these requirements have led to multirate, multiprocessor computation of digital flight laws.

Though the design and analysis of multirate systems emerged more than 30 years ago, no explicit and complete methodology which can exploit the advantages of multirate sampling for effective real time implementation exists. The contents of this thesis are the results of research to develop such a procedure.

2 HISTORICAL DEVELOPMENT OF MULTIRATE SYSTEM DESIGN AND ANALYSIS

2.1 System Models

Early analysis of sampled-data systems with multirate sampling was by means of the *switch* and *frequency decomposition* methods (Coffey and Williams, 1966; Kranc, 1957; Jury, 1967; Ragazzini and Franklin, 1958; Slansky and Ragazzini, 1955). These used Z-transform theory to develop highly complicated descriptions of the multirate closed loop system. The descriptions were normally simplified by assuming or approximating an integer relation between the sample rates and considering equivalent models with uniform sampling. The studies were confined to single input/ single output (SISO) systems and generally resulted in very unwieldy descriptions for a system with a number of sample rates.

The switch and frequency decomposition methods were primarily developed to analyse intersample behaviour of simple sampled data systems. Later, the use of multirate system design to significantly improve the performance of corresponding single rate designs was established (Ragazzini and Franklin, 1958). An improved time response and a reduction in intersample ripple was possible at the cost of increased computation and lower saturation limits. The designs were confined to synthesis of compensators in the forward path and as such were not applicable to open loop unstable systems.

The primary drawback of the decomposition methods is the inflexibility of the resulting closed loop system. Both frequency and switch decomposition methods satisfactorily address the fundamental requirements of the multirate control *analysis* tasks but are limited in their application to *design* techniques. In particular, the complexity of the multirate closed loop equations produced by the decomposition techniques severely impairs the ability of these methods to adopt an iterative design methodology (as is required for many classical design

methods based on a control synthesis approach). The modification of independent subsystem elements is a difficult task once the entire system description has been derived. This restricts the application of the decompostion techniques to systems of very low order and few loops.

Another drawback of the decomposition methods is that, for many multirate sampling configurations, the system transition equations derived by these techniques cannot be appropriately combined to produce a closed loop transfer function. This inability to derive the characteristic equation limits the assessment of system stability.

The introduction of a state space representation of discrete dynamics provided a turning point for the modelling of multirate system behaviour. The most notable contribution was that of Kalman and Bertram (1959) who, in their much cited work, *unified* the desciption of discrete systems with *any* sample and hold scheme in a state space form. In general, a linear, time-invariant continuous system sampled using a multirate scheme produces a time varying discrete system which is cumbersome to analyse for a high number of sample rates. Kalman and Bertram identified that, by confining multirate sampling schemes to integral sample period ratios, the resulting discrete system can be classed as a special type of periodic system. A time-invariant discrete model can then be used to describe the periodically time-varying system. The model thus derived can incorporate any number of input and output sample rates for a multi-input, multi-output, multirate system.

State space developments, based on the Kalman and Bertram approach, simplified the modelling of multirate systems (Albertos, 1990; Amit and Powell, 1981; Araki and Yamamoto, 1986; Berg et al, 1988; Boykin and Frazier, 1975; Chammas and Leondes, 1978; Francis and Gorgiou, 1988; Kargonekar et al, 1985; Kono, 1980; Meyer, 1990; Thompson, 1985). The application of these new state space methods enabled closed loop transfer functions to be derived and enhanced the mathematical tractability of the individual elements in the multirate system.

A number of different approaches were used in the development of the state space methods. A few methods simplified the *structure* of the overall multirate system by preliminary manipulation of system components into suitable multirate subsystems (Boykin and Frazier, 1975; Thompson, 1985). This approach deals with the intractability problems by decomposing the original multirate system into convenient (and simpler to analyse) multirate subsystems. Other methods formulated new and more flexible models of the actual switch and frequency decomposition processes (Albertos, 1990; Araki and Yamamoto, 1986; Chammas and Leondes, 1978; Francis and Gorgiou, 1988; Kono, 1980; Meyer, 1990). These techniques represented the multirate system equations derived by the decompostion methods in state space form to allow more complex multirate sampling configurations to be modelled with relative ease.

These and other state space modelling methods however, lead to non-minimal descriptions, which generate extraneous singularities that strictly do not exist.

2.2 Design Methods

The development of design methods for multirate systems has been slow. Early work concentrated on the discretisation of existing continuous compensators designed using classical synthesis techniques. This approach allowed single input, single output closed loop multirate systems to be designed satisfactorily, using classical analysis tools to determine the time responses and stability performance of the system.

The incorporation of a multirate sampling scheme into a prespecified controller structure is the most common approach adopted by current researchers for the design of multi-loop, multirate control systems (Berg et al, 1988; Glasson, 1980; Godbout et al, 1988; Rattan, 1984; Thompson, 1985). Many design techniques still rely on the classical synthesis (on a loop by loop basis) approach developed during the very

early stages of multirate research. The work of a few researchers (Glasson, 1980; Berg et al, 1988) has correlated the classical and the 'new' design methodologies to produce direct and more refined discrete system designs for multi-loop multirate systems. These use optimal strategies to achieve a desired performance, incorporating both the compensator gains and the loop sample rates as design parameters. This strategy is well suited to the problem due to the natural decomposition of the multirate system into subsystems of different sampling rates. In most cases, the objective of the multirate design is to match or improve the time domain performance of the corresponding single rate system.

Though the assignability of arbitary poles using multirate state feedback was established a number of years ago (Chammas and Leondes, 1978; 1979), suitable *state space* design techniques for multi-input, multi-output systems have been noticeably absent. Many of the state space methods that have been proposed have either been limited to single loop configurations or have not produced practically implementable solutions. The tendency to use the pre-specified controller approach has largely been due to the difficulty encountered in using established state space methods directly on multirate models. The direct application of state-space design methods, which do not use optimal policies, give impractical solutions.

There are two main problems associated the application of conventional design techniques; the adverse effects of intersample cross-coupling and the high amplitude, switched control signals that normally result from a multirate feedback structure. The optimal control approach (which primarily minimises the state and control input deviations) is the only suitable technique capable of addressing the requirements of the multirate design problem to emerge from recent developments. This dissertation considers the application of Eigenstructure Assignment techniques to alleviate the problems specific to the design of multirate control systems.

3 OUTLINE OF THESIS

Within the context of the recent research, the work contained in this thesis falls into the following three main topics of multirate control design and analysis:

(i) Multirate system modelling

(ii) The selection of input/output sample rates

(iii) The development of robust state space design methods for multi-input, multi-output multirate systems.

The first two chapters describe the modelling techniques used to represent the behaviour of multirate control systems with different sampling configurations. The suitability of the multirate system descriptions produced by these techniques for the application of established design and analysis methods is also examined. Chapter 3 outlines the factors which influence the selection of input/output sample rates. Chapters 4, 5, 6 and 7 concentrate on the design methods.

Chapter 1 contains a survey of the early frequency and switch decomposition modelling methods. The decompostion methods are best suited for the *analysis* of existing multirate control systems derived by the discretisation of existing classically designed continuous-time compensators. The switch decomposition technique is applied to analyse a multirate sampled, pitch attitude control loop of a helicopter. The difficulties encountered when analysing such configurations and an analytic technique which may be used to overcome these difficulties are outlined. The analytic technique is based on a spectral decomposition of specific blocks in the multirate closed loop system. The necessary underlying assumptions required for the application of this techniques are outlined and demonstrated.

Chapter 1 ends with a classical synthesis technique which can be

applied to design a compensator for a multirate system using the classical decomposition approach.

Chapter 2 is the state space parallel of Chapter 1. The first part of this chapter describes the state variable representation of discrete systems initiated by Kalman and Bertram and derives state space models for a number of different multirate sampling configurations. Though multirate system representations of this type are not new, this chapter does contain detail on the derivation of the state space models which is not found elsewhere. The reason for this is to provide a *complete* and clear understanding of the different approaches that may be used to model multirate system behaviour. The multirate state space models are complicated in their definition and take a tedious amount of decoding if simply presented in their final form. A lack of understanding of this derivation often leads to a (justified) reluctance to examine the subject further.

The different types of state space description are assessed for their suitability for state space design and analysis. More specifically, two features of the multirate state space descriptions are examined: the amount of information on the behaviour of the multirate system *during* the periodic interval (the *intersample* behaviour) and the accuracy of the characteristic singularities contained within the periodic description. Both features are essential. Information regarding the intersample behaviour is useful for *accurate* time and frequency domain analysis of the multirate systems; the singularities (which characterise multirate system performance) need to be correctly identified for the application of any pole assignment design techniques.

Many researchers have noted the non-minimal nature (i.e. a system description with eigenvalues which cancel) of multi-input, multi-output state space representations of multirate systems. This non-minimality aspect hinders the application of many established pole assignment

design techniques. This chapter introduces one class of multirate systems for which a minimal system description can be derived: the multirate input, fixed rate output (MIFO) system. Multirate systems which fall into this class are ideal candidates for the application of any pole assignment techniques. All the design techniques outlined in this thesis are developed for MIFO sampled multirate systems.

It is apparent that many aerospace establishments still rely (to a degree) on the wealth of knowledge accumulated over many years in classical control theory. For this reason, a digital approximation technique which preserves particular properties of a continuous time system and is comparatively easy to implement is described in the last part of Chapter 2. The method is new and is based on state space matching of the desired closed loop system dynamics to derive a multirate compensator which *approximates* the performance of its analogue counterpart. The technique is applied for the design of multirate sampled compensators for the pitch loop of an aircraft flight control system.

Chapter 3 examines the role of input, output sample rates in the design of a multirate control system. This chapter deals with two aspects of sample rate selection:-

The first aspect is concerned with the effect of sample parameters on the design of multirate control systems with a fixed (pre-specified) dynamic structure (e.g. the matched closed loop multirate system). The effect of varying the sample parameters on the performance of the multirate closed loop systems obtained by the compensator matching technique is examined. A means of determining the sample parameters required to maintain asymptotic stability and acceptable transient behaviour for the matched multirate closed loop system is also examined.

The second aspect is the influence of sample rates on the controllability, observability and internal structural properties of the multirate system. The ability of sample rates to determine the

controllability and observability conditions of a multirate sampled system has been noted by many researchers (Araki and Yamamoto, 1986; Bittani and Bolzern, 1985; Chammas and Leondes, 1978, 1979; Eckardt, 1989; Engwerda, 1988; Kono et al, 1991; Serrano and Ramadage, 1991). However, few have investigated in detail the factors which determine the choice of sample rates on the eigenvalue assignability problem (beyond a trial and error type of analysis). The work of Chapter 3 examines the *precise* influence of MIFO multirate system sample rates on the control design problem. This type of analysis is new; it seeks to establish the set of *minimum* sample rates required to satisfy the controllability conditions and more importantly, to produce unique (A,B) invariance conditions which generate extra design freedom for the feedback control problem. The different methods which may be used to derive these sets are examined. The link between these sample sets, MIFO canonical control structures and MIFO (A,B) invariance properties is, for the first time, clearly shown by the use of pencil equivalence relations.

The final part of Chapter 3 describes a MIFO pole assignment algorithm based on the canonical controllability forms (and (A,B) invariance properties) generated by the minimum sample rate sets. The application of the pole assignment algorithm is examined to assess its applicability for the design of MIFO feedback control. The algorithm is also used to examine the effect of the periodic interval on the gain margins of closed loop MIFO sampled systems. This analysis uses a very simple approach formulated entirely by the *form* of the canonical pole assignment algorithm.

The most significant contribution of the multirate work described in this thesis has been to use the unique MIFO (A,B) invariance properties to address the problem of impractical solutions arising from the direct use of established state variable techniques on multirate system descriptions. (Recall that the two main problems are the adverse intersample effects and high magnitude, switched control effort.) This

part of the work has been based on the application of the eigenstructure assignment technique to the MIFO system models. Chapter 4 describes the eigenstructure assignment technique.

Eigenstructure assignment techniques are used to design the eigenvalues and eigenvectors of a closed loop system. The application of these techniques for the design of continous-time and single rate discrete feedback control systems is well established. However, the use of eigenstructure assignment for the design of MIFO feedback control is new and has not been examined elsewhere. The eigenstructure assignment approach is particularly suited for the design of MIFO feedback control due to its *direct* use of the MIFO (A,B) invariance properties. Moreover, the extra MIFO system design freedom can be usefully applied for more accurate specification of eigenvectors in the MIFO system than in the equivalent continuous-time or single rate system.

Chapter 4 outlines the role of the eigenstructure in the closed loop system response. Eigenstructure assignment techniques are noted for their ability to design closed loop systems which are *insensitive* to variations or perturbations in the *nominal* system dynamics. This insensitivity is achieved by *decoupling* the modal interactions present in the closed loop system. Thus, the insensitivity properties contribute to the robustness of the closed loop system.

The benefits of closed loop system insensitivity can clearly be observed in the time domain. However, the link between closed loop system insensitivity and the more global frequency domain robustness properties which are desired from a feedback control system is not obvious and often omitted. One objective of Chapter 4 is to show the *precise* effect of the time domain criterion used for an insensitive solution to the eigenstructure assignment problem on the frequency domain robustness properties of the system.

The use of the extra design freedom offered by the MIFO system to assign a desired eigenstructure *precisely* is described. The way in which

the specification of a suitable eigenstructure will alleviate the problems of the MIFO sampled systems is also described.

The final section of Chapter 4 highlights the limited application of the insensitivity measures (which are used to solve the standard eigenproblem) for the assessment of MIFO multirate system behaviour. These established measures will only monitor the performance of the MIFO system at periodic intervals. The insensitivity measures are extended to cover the performance of the MIFO multirate system between periodic instants (i.e. the *intersample* instants). This extension provides a means of monitoring the intersample performance of MIFO sampled systems. It is, to the author's knowledge, the first analytic assessment of intersample behaviour.

The remaining chapters examine a number of different methods of solving the MIFO eigenstructure assignment problem.

Chapter 5 begins with a *generalisation* of the sample rate selection criterion which must be satisfied for *perfectly decoupled* solutions to the MIFO eigenproblem. The most direct method of assigning a set of desired eigenvectors is then described. This method is based on a least squares minimisation of the error between the desired and assigned eigenvectors.

The least squares method is applied to three examples (of varing complexity) to demonstrate, in a very simple way, the effective use of the MIFO (A,B) invariance properties by the eigenstructure assignment design methods to produce totally decoupled modes. The responses produced by the multirate and corresponding single rate systems are compared to illustrate the improvement in decoupling produced by the MIFO sampled systems. The cost of this improvement on the intersample behaviour of the multirate system is examined. The effect of using different sample sets generated by the generalised sample rate selection criterion is demonstrated with the use of examples. The effect of violating the generalised selection criterion is also investigated.

Chapter 5 finishes with a thorough examination of the *intersample* responses of the closed loop multirate systems produced by the least squares eigenstructure assignment procedure. Intersample behaviour is very rarely examined beyond a theoretical assessment and quite often totally ignored. However, the poor intersample behaviour of MIFO systems is the main factor which hinders the application of this otherwise appropriate method of monitoring system information. The reluctance to examine intersample performance stems from the difficulty encountered in analysing the behaviour of a multirate system at any instant other than the periodic instants. The periodic instants are the only point at which all dynamic changes within the multirate systems can be *uniformly* monitored. At all intersample instants there is a non-uniform update of the multirate system dynamics. The problem is exacerbated by the fact that, unless all modes within the closed loop system are decoupled, interactions between the various dynamic modes exist. Thus, it is difficult to isolate the specific effects caused by each new update of a system variable.

Chapter 5 makes use of the totally decoupled nature of the closed loop systems designed by the least squares eigenstructure assignment to conduct a clear and detailed analysis of the intersample effects.

The results of Chapter 5 show that the two desired qualities of the closed loop MIFO system present conflicting design criteria. Thus, a suitable solution must seek to achieve an acceptable compromise between the minimisation of control effort and the assignment of a prescribed modal structure.

Chapter 6 describes three techniques which may be used to provide such a solution. All three techniques attempt to minimise the elements of the gain matrix whilst maintaining the exceptionally good modal decoupling achievable by the MIFO sampled systems. The first technique is a new contribution in this work and adapts the least squares assignment problem to *constrain* the magnitude of the elements in the

multirate feedback matrix. The remaining two techniques are based on an optimised approach to the MIFO eigenproblem. The three techniques are applied to the examples of Chapter 5 to demonstrate their effectiveness.

Chapter 7 describes a deadbeat control design algorithm which may be applied to design a MIFO closed loop sytem which tracks a given reference input in a finite time. The deadbeat algorithm uses (A,C) invariance properties of the MIFO system to remove the undesired overshoot effects of transmission zeros. The application of this technique (which is new) is demonstrated with the use of two examples.

The contributions and limitations of this work are summarised in the final chapter. Suggestions on further work are also included.

CHAPTER ONE

CLASSICAL REPRESENTATION OF MULTIRATE SYSTEMS: FREQUENCY AND SWITCH DECOMPOSITION METHODS

1.1 INTRODUCTION

This Chapter examines the application of discrete Fourier transforms for multirate system analysis. Though the application of sampled data theory is well established for single rate discrete systems, its role in the analysis of multirate systems is less familiar and consequently difficult to apply. Section 1.2 summarises briefly the various methods of discrete data representation in the frequency, Laplace, Z and time domains. The notation used to describe the various multirate identities throughout the thesis is also introduced in this preliminary section.

To clarify the links between single rate and multirate discrete analytical techniques, Section 1.3 outlines the Fourier and Z transform principles which apply in the development of multirate operators based on the frequency and switch decomposition techniques (Boykin and Frazier, 1975; Coffey and Williams, 1966; Flowers and Hammond, 1972; Kranc, 1957; Jury, 1967; Patel, 1990; Ragazzini and Franklin, 1958; Slansky and Ragazzini, 1955; Thompson, 1986). The decomposition techniques were the earliest methods to address the analytic problems posed by multirate discrete systems; the combination of subsystems sampled at different rates unrelated by simple integer multiples of each other required lengthy and often intractable calculations. Furthermore, the derivation of input, output closed loop expressions was also impossible. The decomposition methods circumvent such problems by considering the system operation at a rate, the *base sample rate*, to which *all* other sample rates can be integrally related. Subsystems of

different rates can then be represented at a *uniform* sample rate.

The decomposition methods were realised by several independent researchers (Kranc, 1957; Ragazzini and Franklin, 1958; Slansky and Ragazzini, 1955;) each approaching the multirate system analysis in a different domain. Later, all were shown to be equivalent by Jury (1967). Slansky and Ragazzini (1955) developed the frequency domain approach. The switch decomposition method of Ragazzini and Franklin (1958) followed later; this technique was essentially developed from a time domain consideration of the frequency decomposition methods. At the same time, Kranc (1957) independently derived *vector* multirate operators based on advance and delay transformations using the switch decomposition approach.

Sections 1.3.1 and 1.3.2 review the frequency and switch decomposition methods and unifies the derivation of multirate discrete operators by considering discrete representations in *all* the relevant domains. The Z domain and Fourier identies for two basic type of multirate systems are examined; the slow rate input, fast rate output system and the fast rate input, slow rate output system. For these simple systems the fast rate is assumed to be an integer multiple of the slow sample rate. Section 1.3.3 then describes the switch decomposition operators for systems with multirate inputs and multirate outputs whose sample rates produce an rational ratio. The multirate behaviour of this type of system can be described in terms of a least commmon sample period which is related by integer multiples to both input and output sample periods. The vector decomposition operator is also introduced in Section 1.3.3. The identities of Sections 1.3.1, 1.3.2 and 1.3.2 form the elemental building blocks of *any* multirate system with integrally related sample rates.

The derivation of closed loop equations using the multirate identities of Section 1.3.1 to 1.3.3 are then examined in Section 1.3.4. Many single rate classical analysis methods are based on a system

description in a numerator denominator form, from which the system loop transfer can easily be isolated. For the multirate system descriptions formulated using the frequency and switch (vector) decomposition methods this is not a simple procedure. The functions of interest are usually inextricably embedded in the overall equations and for multiloop, multirate configurations the derivation of closed loop transfer functions may even be impossible. This clearly prevents the application of many classical analytic methods which are based on the characteristic equation of the open and closed loop transfer functions. Application of the switch decomposition method to a simple example in Section 1.3.4 demonstrates the difficulty encountered in manipulating the multirate system equations to form a closed loop system description.

To address these problems, a spectral decomposition technique (Boykin and Frazier, 1975) which facilitates the multirate modelling task by deriving equivalent single rate behaviour is presented in Section 1.3.4. For many multirate system modelling methods, some restriction is generally applied to simplify the derivation of a closed loop expression that is analytically useful. For the vector decompostion method considered here, an identifiable loop transfer and feedback function is produced only if the multirate samplers are located in strategic positions. Thus, the method is suited to a specific sampling configuration and therefore limited in its application. The application of this method is demonstrated with a simplified helicopter example. Closed loop transfer functions are derived for the multirate sampled helicopter system with a methodical development of the system equations. This is presented together with an outline of the conditions for which the representation is valid.

Section 1.3 is confined to the *analysis* of multirate systems. Section 1.4 examines a *design* method which uses a classical compensator synthesis approach (Ragazzini and Franklin, 1958).

1.2. DISCRETE-TIME SYSTEM REPRESENTATION

The operation of a sampled system can be described by discrete equivalents of the frequency domain identities used to represent analogue system behaviour (Franklin et al, 1990; Kuo, 1980). Consider a continuous signal f(t) which is sampled at a rate $\omega_s = 2\pi/T$ rads/sec. The Fourier transform of the continuous signal is given by,

$$F(j\omega) = \int_{-\infty}^{\infty} f^T(t)e^{j\omega s t}dt \qquad (1.2.1)$$

If the sampler is assumed to be ideal, (i.e. the sampling duration is insignificant compared with the sampling period T) the above equation can be represented in the s domain as:

$$F^T(s) = \frac{1}{T}\sum_{k=-\infty}^{\infty} F(s+jk\omega_s) \qquad (1.2.2)$$

Equation (1.2.2) encapulates the well known periodic nature of the sampled signal. For any singularity $s = s_p$ of a Laplace function F(s), the sampled description $F^T(s)$ has repeated singularities at $s = s_p+jkw$, for k = integers from $-\infty$ to ∞. This is the 'folding' effect of the singularities occurring at integral multiples of the frequency $\omega_s/2$. To enable an accurate recovery of the continuous signal F(s) from $F^T(s)$, the sample rate must be chosen to ensure that all poles of F(s) lie inside the primary strip $-\omega_s/2 \rightarrow \omega_s/2$ in the Laplace plane.

A time domain expression for $F^T(s)$ can be obtained by considering that the output $f^T(t)$ is a series of discrete values separated by intervals of period T, i.e.,

$$f^T(t) = \sum_{k=0}^{\infty} f(kT)\delta(t-kT) \qquad (1.2.3)$$

The bottom limit of the summation in (1.2.3) indicates that $f^T(t) = 0$ is assumed for all time $t<0$. Equation (1.2.3) simply represents the sampled signal as the value of the analogue signal superimposed onto an infinite series of impulses of unity magnitude, represented at each sample point by $\delta(t-kT)$. The Laplace transform of equation (1.2.3) gives the time domain equivalent of equation (1.2.2) as the discrete Fourier series,

$$F^T(s) = \sum_{k=0}^{\infty} f(kT)e^{-ksT} \qquad (1.2.4)$$

The discrete Z domain representation then simply corresponds to a change of variable $z = \exp(sT)$ in the above equation. This gives an infinite time domain series,

$$Z[F^T(s)] = F^T(z) = \sum_{k=0}^{\infty} f(kT)z^{-k} \qquad (1.2.5)$$

which is the z transform of f(t). Equation (1.2.5) represents discrete values of a continuous signal sampled at a rate 1/T, placed at the correct instants within an infinite time frame by powers of z^{-1}. For a *periodic* time function which repeats itself every p instants, ie $f(kT) = f(kT+pT)$, a finite discrete Fourier transform can be defined for the period pT (Franklin et al, 1990) as,

$$F_p^T(s_p) = \sum_{k=0}^{p-1} f(kT)e^{-j2\pi k/p} \qquad (1.2.6)$$

where $s_p = j2\pi/pT$. The sum of equation (1.2.6) is clearly periodic with

period p.

2.2.1 Inverse Identities

The function of the inverse identities are to recover the sampled data signal f(kT) from the time and frequency domain expressions of equations (1.2.1) to (1.2.6). Unlike its analogue counterpart where the inverse of F(s) uniquely defines f(t), the inverse of F(z) will not necessarily yield the correct time function f(t). From the definition of the sampled signal, it is clear that the discrete inverse function will accurately represent f(t) only at the instants (kT).

One simple method of obtaining f(kT) from F(z) is to expand the infinite series of equation (1.2.5). Though accurate, this method is not as useful as the partial fraction or contour integration methods. For the partial fraction technique, the function zF(z) is expanded into terms of the form $Az/(z-e^{-aT})$ (A=constant) and inverted (Katz, 1981) to give f(kT). Alternatively, contour integration extracts f(kT) from F(z) using the follow formula,

$$f(kT) = \frac{1}{2\pi j}\int_{C}^{\infty} F^{T}(z)z^{k-1}dz \qquad (1.2.7)$$
$$-\infty$$

where F(z) is assumed to be analytic in the closed path C (i.e. C encloses all singularities of $F(z)z^{k-1}$). The above inverse transform can be calculated using Cauchy's residue theorem which states that:

$$f(kT) = \sum_{i=1}^{n} \mathrm{Res}[F^{T}(z)z^{k-1}]_{\lambda_i} \qquad (1.2.8)$$

where $\text{Res}[\cdot]_{\lambda i}$ denotes residues of the function $[\cdot]$ at the poles of $F^T(z)$, $\{\lambda_i\}$, i=1,..,n. For the discrete periodic series of equation (1.2.6), the inverse function is given by (Franklin et al 1990):

$$f(kT) = \frac{1}{p} \sum_{k=0}^{p-1} F^T(z_p) e^{j2\pi k/p} \qquad (1.2.9)$$

1.3 CLASSICAL OPERATORS

This section relates the frequency and z domain single rate identities of Section 1.2 to their multirate counterparts and develops multirate operators arising from the application of the decomposition methods. The purpose of the decomposition method is to represent multirate system behaviour at uniform intervals common to all sample rates. This interval is termed the *base sample period* and is denoted T_b. To ensure compatibility of multirate subsystems, all subsystem transition equations are defined for the largest time interval commmon to all sample rates. This interval is the *main interval of sampling* and is denoted T.

Sections 1.3.1 and 1.3.2 examine the basic fast rate input/ slow rate output and slow rate input/ fast rate output multirate configurations of Figure 1.3.1 using *switch* decomposition methods (the switch decomposed systems are shown in Figures 1.3.2). These multirate schemes have a simple integer relation between the input and output sample rates. In all cases the slow/fast sample rate ratio ($1/T:1/T_b$) is assumed to be 1:4. The discrete operator associated with the slow signal is defined $z = \exp(sT)$, while that of the fast signal is similarly defined as $z_n = \exp(sT_b)$. Multirate identities for the subsystems of Figure 1.3.1 form the building blocks of all integer related multirate

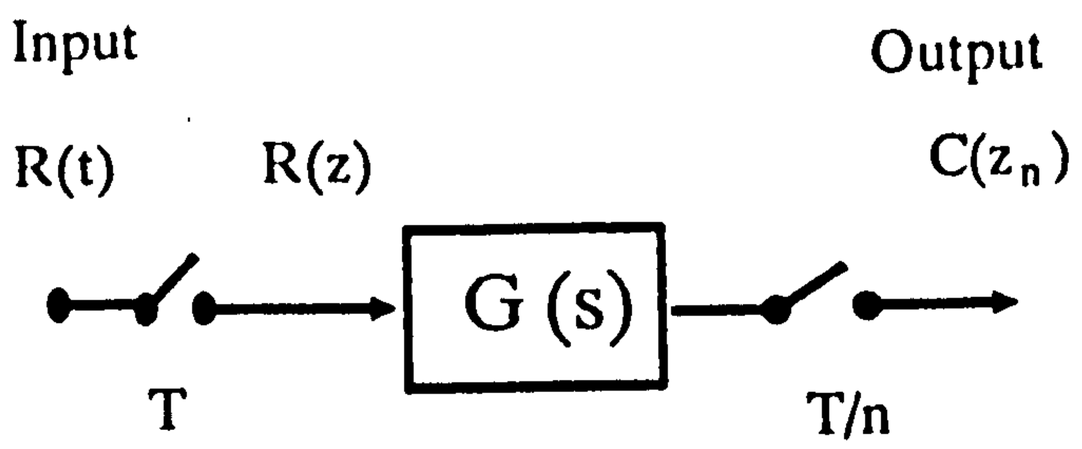

a)

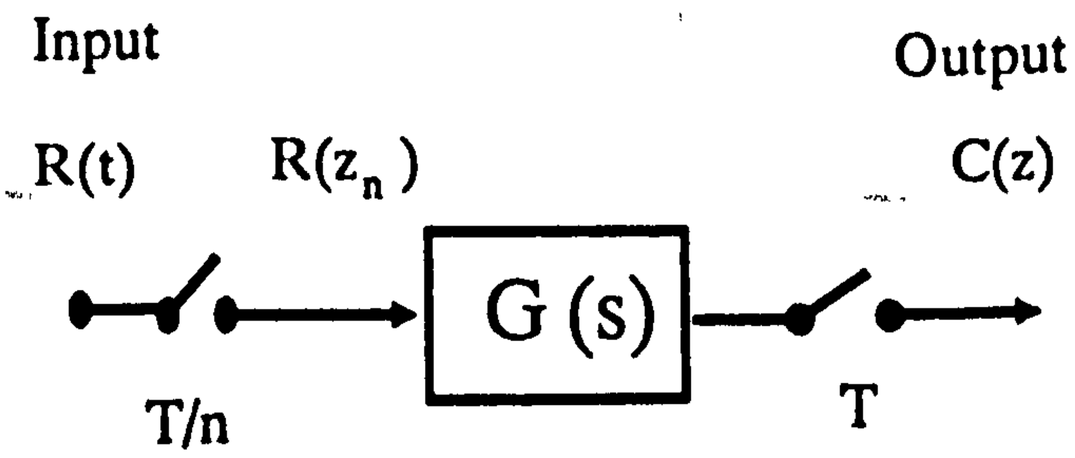

b)

Figure 1.3.1 Multirate sampled data system with

a) slow rate input / fast rate output

b) fast rate input / slow rate output

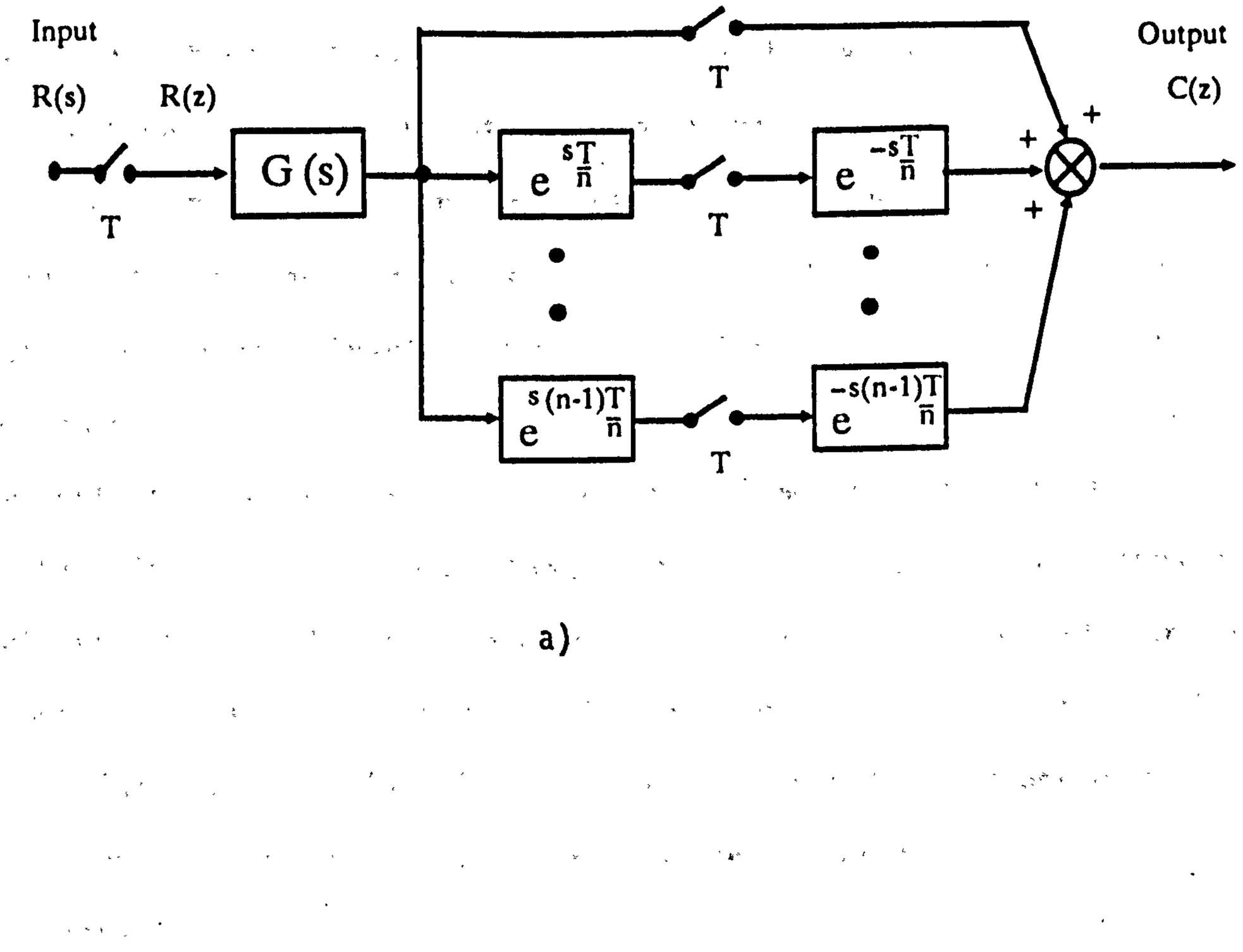

a)

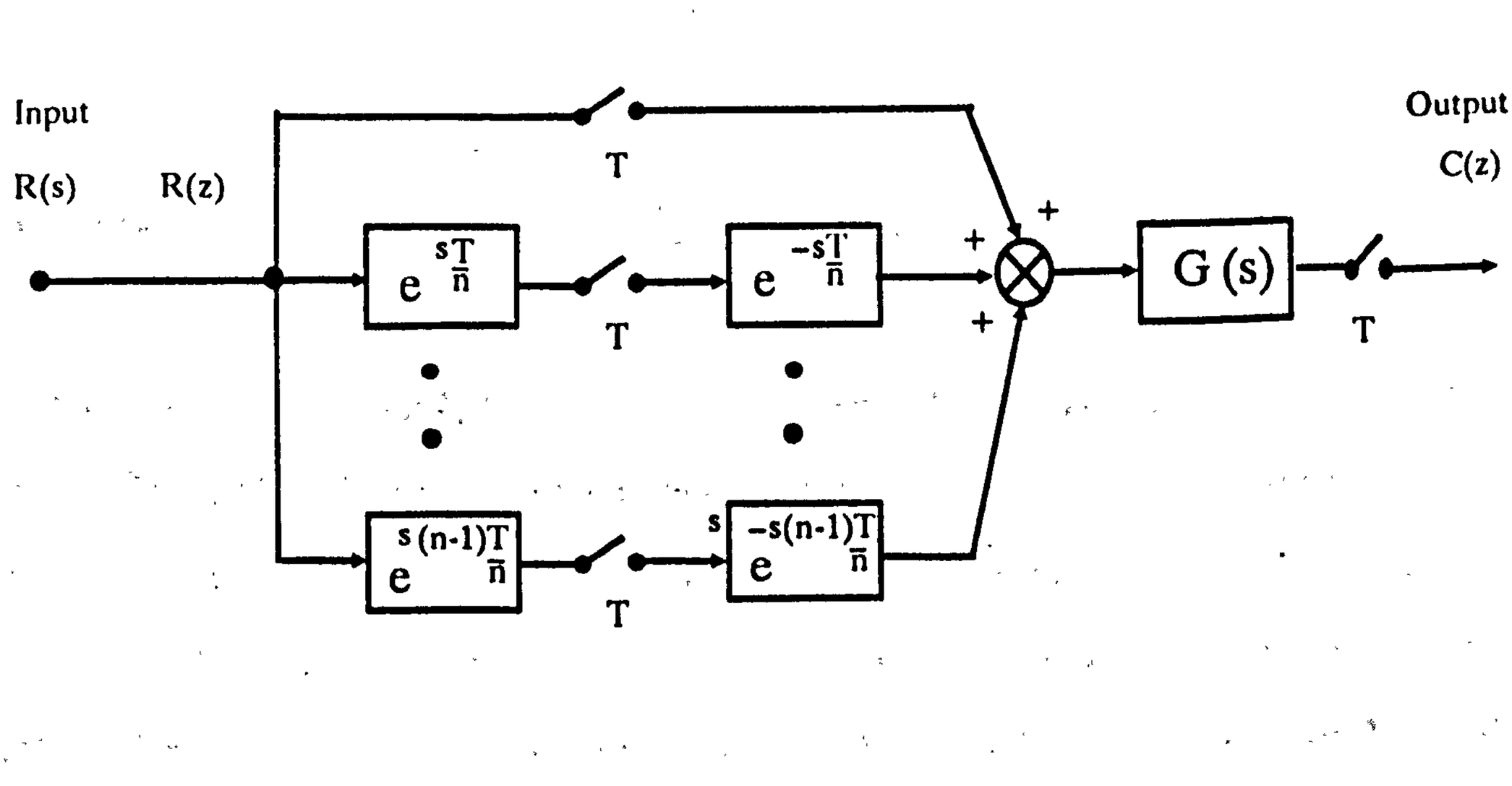

b)

Figure 1.3.2 Multirate sampled data system with

a) decomposed slow rate / fast rate system

b) decomposed fast rate /slow rate system

sampled data systems.

Section 1.3.3 examines multirate configurations with sample rates that do not have a *direct* integer relationship with each other, but can be represented in terms of a *common* highest frequency. For these subsystems, multirate operators are derived using *vector* decomposition methods; the correspondence between the switch and vector decomposition techniques being clearly identified. The derivation also gives an indication of the complexity that is encountered in examining even the simplest of multirate systems using the decompostion techniques.

Finally, a note about the terminology used. In all subsequent sections of this thesis, references to intersample instants are with respect to the main interval of sampling. That is, time $t=(kT+T_b)$, $t=(kT+2T_b)$,.., $t=(kT+(n-1)T_b)$ k=integer, are all intersample instants. Also, the Laplace and z transform notation of Section 1.2 is used unless otherwise stated.

1.3.1 Slow rate input/fast rate output system

For the slow input/fast output system of Figure 1.3.1a) the input signal is updated once during every four output sample instants. To simplify the analysis, it is assumed that all input/output transitions are synchronised at the main sample instant (Figure 1.3.3a); i.e. the fast output response is determined by the combined main sample and intersample responses to an input which is updated at the main sample instants. An example of input/output transitions which are not synchronised at common main sample instants is shown in Figure 1.3.3b. The fast sampled output of this system is registered two base sample periods after the main sample instant, i.e. delayed by $2T_b$. Though this timing distinction is trivial when considering the configuration of Figure 1.3.1a in isolation; its purpose is to ensure that no 'hidden'

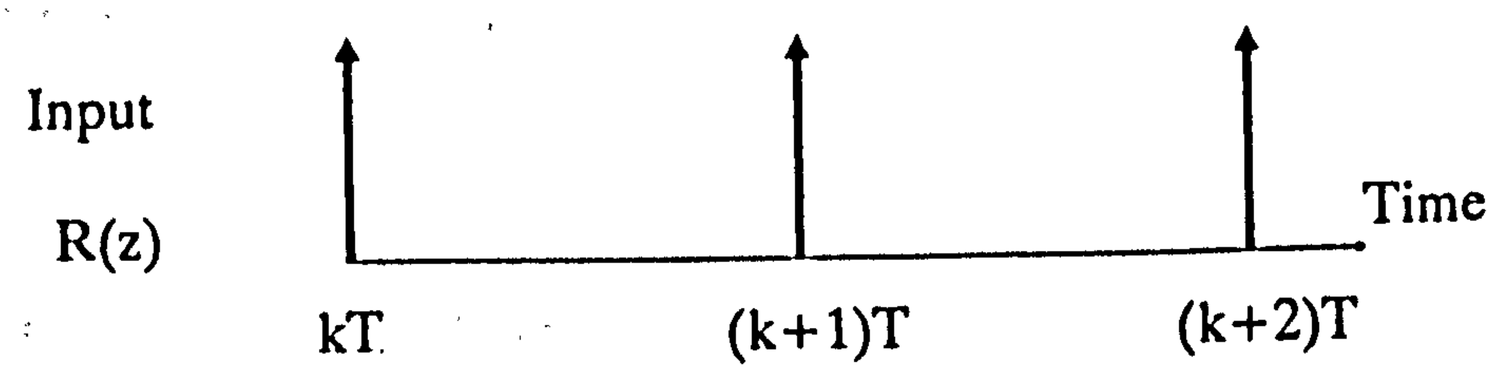

a)

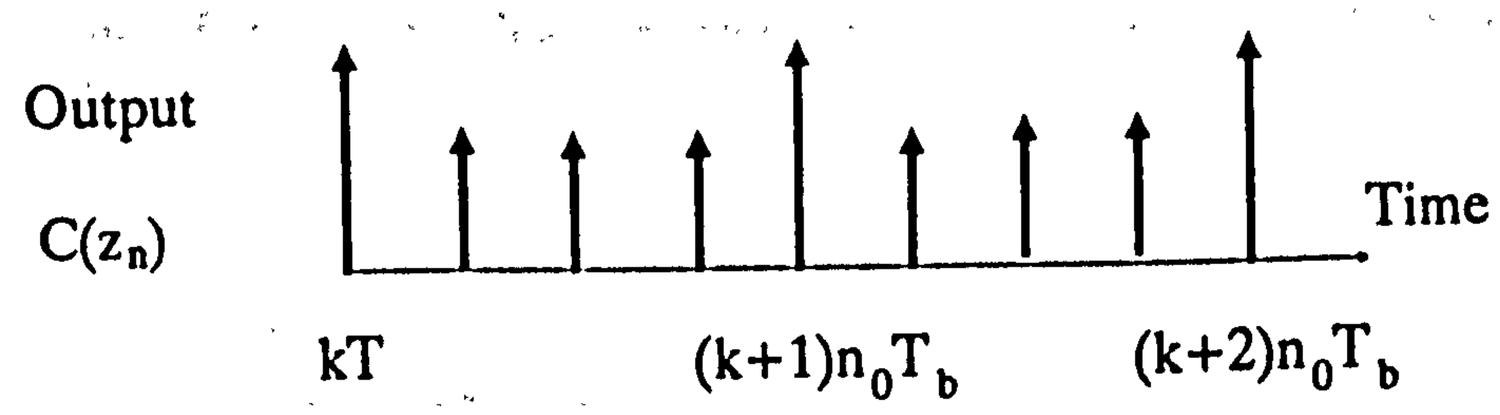

b)

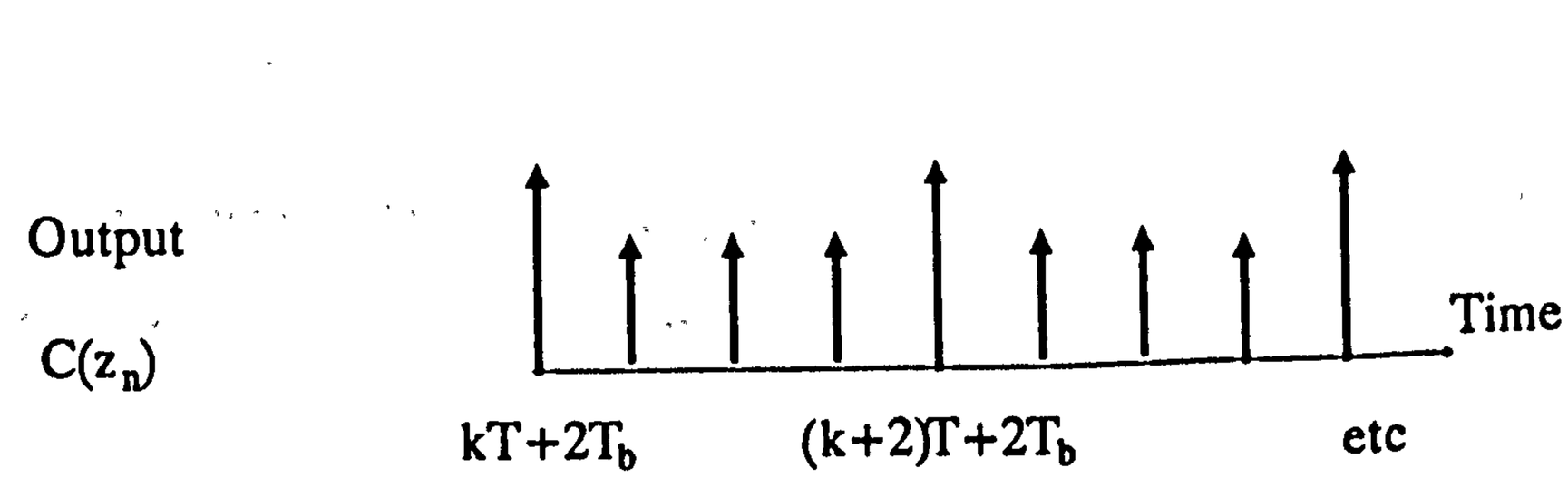

Figure 1.3.3 Timing diagrams for slow/fast multirate system with input/output transitions synchronised at

a) main sample instants

b) base sample instants

time delays become incorporated into the overall equations when connecting several multirate subsystems together. Such delays can cause closed loop system instability (El-Sakkary, 1990; Feng, 1984).

The fast output of the system in Figure 1.3.1b is given by,

$$C^{T}/n(s) = G^{T}/n(s)R^{T}(s) \tag{1.3.1}$$

where, from equation (1.2.2),

$$G^{T}/n(s) = \frac{n}{T} \sum_{k=-\infty}^{\infty} G(s+j\frac{2\pi kn}{T}) \tag{1.3.2}$$

The equivalent frequency domain representation of the fast output signal is,

$$C^{T}/n(s) = \frac{n}{T} \sum_{k=-\infty}^{\infty} C(s+j\frac{2\pi kn}{T}) \tag{1.3.3}$$

A time domain expression, $C^{T}/n(z_n)$, can be obtained by considering that the output discrete series of interest is,

$$c^{T}/n(t) = \sum_{k=0}^{\infty} c(kT/n)\delta(t-kT/n) \tag{1.3.4}$$

which gives the output values at any instant t=kT/n as:

$$c(kT/n) = \sum_{\ell=0}^{\infty} r(\ell T)g(kT/n-\ell T) \tag{1.3.5}$$

In accordance with the development of equations (1.2.3) to (1.2.5), equation (1.3.4) gives the infinite z domain time series,

$$C^{T/n}(z_n) = \sum_{k=0}^{\infty} c(kT/n)z_n^{-k} \qquad (1.3.6)$$

Equation (1.3.6) can be expressed in terms of the discrete input signal and plant z transfer function by substitution of (1.3.5) to give,

$$C^{T/n}(z_n) = \sum_{k=0}^{\infty}\sum_{\ell=0}^{\infty} r(\ell T)g(kT/n-\ell T)z_n^{-k} \qquad (1.3.7)$$

If an integer m is defined such that $\ell T+mT_b = kT_b$ (i.e. the fast sample rate instants kT_b are defined as the sum of the slow sample rate instants ℓT and intersample instants mT_b) then,

$$C^{T/n}(z_n) = \sum_{\ell=0}^{\infty} r(\ell T) \sum_{m=-\ell n}^{\infty} g(mT/n)z_n^{-(n\ell+m)} \qquad (1.3.7)$$

If the system action is assumed to be causal then,

$$C^{T/n}(z_n) = \sum_{\ell=0}^{\infty} r(\ell T)z_n^{-n\ell}\sum_{m=0}^{\infty} g(mT/n)z_n^{-m} \qquad (1.3.8)$$

$$= R(z_n^n)G(z_n) \qquad (1.3.9)$$

For subsystems with a ZOH preceding G(s), the above equations apply with all z transforms of the plant transfer function being determined by,

$$G_h^T(z_n) = (1-z^{-1})Z[G(s)/s] \qquad (1.3.10)$$

(The ZOH element is of period T since this determines the duration of input signal persistence.)

All multirate expressions have, thus far, been formulated for the smallest time interval, T_b. Multirate system transitions over the main interval of sampling can be defined by considering the switch decomposed subsystem of Figure 1.3.2a, where the fast output path is represented as a series of appropriately advanced and delayed slow rate paths. The overall response is determined by the sum of the decomposed paths. This sampling scheme now offers a means of describing disparate sample rate components within a system in a *uniform* manner. The principles of operation are simple; the intersample values of the output signal are determined by advancing the system response by a multiple of the base interval (appropriate to the intersample instant) and delaying the corresponding output by the same interval. In this way, the response of the system is 'shifted' backwards and forwards in time to arrive at the correct overall response at the main sample instants.

Application of this decomposition technique to the subsystem of Figure 1.3.2a gives the following fast sampled output,

$$C^T(z) = \sum_{k=0}^{n-1} Z[\,G(s)\exp(ksT/n)\,]R^T(z)\; z^{-k/n} \tag{1.3.11}$$

which can be expressed as,

$$C^T(z) = R^T(z)\sum_{k=0}^{n-1} G^T(z,k/n)\; z^{1-k/n} \tag{1.3.12}$$

where $G^T(z,k/n)$ is the modified z transform defined by,

$$G^T(z,m) = z^{-1}\sum_{k=0}^{\infty} g(kT+mT)z^{-k} \tag{1.3.13}$$

Equations (1.3.11) to (1.3.13) show that, in contrast to all previous

multirate expressions for the slow/fast multirate system, the switch decomposition technique produces only main sample rate terms. Thus, the switch decomposition approach possesses the vital quality of sample rate uniformity.

1.3.2 Fast rate input/slow rate output system

For the fast input/slow output system of Figure 1.3.1b the input signal is updated four times during every single output sample interval. As for the slow/fast system, it is assumed that all input/output transitions are synchronised at main sample instants. The *fast* rate output of this system is given by,

$$C^{T/n}(s) = G^{T/n}(s)R^{T/n}(s) \tag{1.3.14}$$

To obtain a slow signal from the fast output of equation (1.3.14) a method of representing the system output at intervals T must be applied. That is, in the Laplace domain, $C^T(s)$ must be extracted from $C^{T/n}(s)$. The desired slow output is given by,

$$C^T(s) = \frac{1}{T}\sum_{k=-\infty}^{\infty} C(s+j\frac{2\pi k}{T}) \tag{1.3.15}$$

If an integer m is defined such that $k = \ell n+m$, $-\infty<\ell<\infty$ and $m = 0, 1,.., (n-1)$ then,

$$C^T(s) = \frac{1}{T}\sum_{\ell n+m=-\infty}^{\infty} C(s+j\frac{2\pi\ell n}{T} +j\frac{2\pi m}{T}) \tag{1.3.16}$$

which can be written as,

$$C^T(s) = \frac{1}{T}\sum_{m=0}^{n-1}\sum_{\ell=-\infty}^{\infty} C(s+j\frac{2\pi\ell n}{T}+j\frac{2\pi m}{T}) \qquad (1.3.17)$$

From the frequency domain definition of equation (1.2.2) it is evident that the inner sum is simply the fast rate identity $C^{T/n}(s)$ frequency shifted by $\omega_m=2\pi m/T$ and multiplied by T/n, i.e.

$$C^T(s) = \frac{1}{T}\sum_{m=0}^{n-1}\frac{T}{n} C^{T/n}(s+\omega_m) \qquad (1.3.18)$$

The corresponding time domain description is given by,

$$C^T(s) = \sum_{m=0}^{n-1} c(mT/n)e^{-j2\pi m/n} \qquad (1.3.19)$$

which will be recognised as the periodic identity of (1.2.6) (Franklin et al, 1990). This is to be expected since the operation of the multirate system is periodic with interval $T = nT_b$.

On substituting the fast rate expression of equation (1.3.14) into (1.3.18), the frequency domain description of the fast/slow system is determined to be:

$$C^T(s) = \frac{1}{n}\sum_{m=0}^{n-1} G^{T/n}(s+\omega_m)\ R^{T/n}(s+\omega_m) \qquad (1.3.20)$$

which if z transformed, gives the z domain description,

$$C^T(z) = \frac{1}{n}\sum_{m=0}^{n-1} G^{T/n}(z_n e^{-j2\pi m/n})\ R^{T/n}(z_n e^{-j2\pi m/n}) \qquad (1.3.21)$$

Expressions (1.3.18) to (1.3.21) all represent the fast/slow system of Figure 1.3.1b. The switch decomposition identity corresponding to Figure 1.3.2b is obtained (as before) by considering the advanced and delayed signals flanking the samplers. The z-transform of the slow output is given by:

$$C^T(z) = \sum_{k=0}^{n-1} Z[R(s)\exp(ksT/n)]\, Z[G(s)\exp(-ksT/n)] \qquad (1.3.22)$$

which (by use of the modified z-transform) simplifies to,

$$F^T(z) = R^T(z)G^T(z) + \sum_{k=1}^{n-1} zG^T(z,1-(k/n))\, R^T(z,k/n) \qquad (1.3.23)$$

Equation (1.3.23) shows clearly that the slow output includes the effects of all fast input signals. An alternative expression for a slow output from a fast system can be obtained by picking out the n'th sample from a fast output signal. This is known as *skip sampling*. One method of achieving a skip sampled expression is by isolating the slow output $C^T(z)$ from the fast output expression $C^{T/n}(z_n)$ where,

$$C^T(z) = \sum_{v=0}^{\infty} c(vT)z^{-v} \qquad (1.3.24)$$

$$C^{T/n}(z_n) = \sum_{k=0}^{\infty} c(kT/n)z^{-k} \qquad (1.3.25)$$

Since $C^T(z)$ is essentially a subset of $C^{T/n}(z_n)$ it is possible to separate the main interval values from the fast rate description by means of the inverse relationships of Section 1.2 (which are used to

derive z transforms from discrete time functions). By definition, values of the discrete output time series are determined by the inverse of the z_n transform in closed form, i.e.

$$C(kT/n) = \frac{1}{2\pi J} \int_{\Gamma} C^{T/n}(z_n) z_n^{k-1} \, dz_n \tag{1.3.26}$$

The contour Γ is required to encapsulate all singularities of $C^{T/n}(z_n)$. If (1.3.26) is substituted into equation (1.3.24) with $k = vn$ then,

$$C^T(z) = \sum_{v=0}^{\infty} \left[\frac{1}{2\pi J} \int_{\Gamma} C^{T/n}(z_n) z_n^{vn-1} \, dz_n \right] z^{-v} \tag{1.3.27}$$

$$= \sum_{v=0}^{\infty} \left[\frac{1}{2\pi J} \int_{\Gamma} C^{T/n}(z_n) z_n^{vn-1} z^{-v} \, dz_n \right] \tag{1.3.28}$$

$$= \sum_{v=0}^{\infty} \left[\frac{1}{2\pi J} \int_{\Gamma} C^{T/n}(z_n) z_n^{vn} z^{-v} \, dz_n (z_n^{-1}) \right] \tag{1.3.29}$$

If $z_n z^{-1} < 1$ then,

$$\sum_{v=0}^{\infty} z_n^{vn} z^{-v} = \frac{1}{1 - z_n z^{-1}} \tag{1.3.30}$$

and the integral and summation of equation (1.3.29) can be interchanged to give,

$$C^T(z) = \frac{1}{2\pi J} \int_{\Gamma} \frac{C^{T/n}(z_n)}{1 - z_n z^{-1}} \frac{dz_n}{z_n} \tag{1.3.31}$$

which can be calulated by the sum of residues of $C^{T/n}(z_n)/z_n$ at the

singularities of $C^{T/n}(z_n)$, $\{\lambda_i\}$, i=1,..,n ie,

$$C^T(z) = \sum_{i=1}^{n} \text{Res}[\, C^{T/n}(z_n) z_n^{-1} \,]_{\lambda_i} \qquad (1.3.32)$$

1.3.3 Multirate input, multirate output system with rational sample rate ratios

Sections 1.3.1 and 1.3.2 examined multirate systems with a simple integer relation between the fast and slow sample rates using the fundamental discrete identities of Section 1.2. The same approach can be applied to develop multirate operators for multirate systems with rational sample rate ratios (Boykin and Frazier, 1975; Coffey and Williams, 1966; Kranc, 1957). An example of this type of system is shown in Figure 1.3.4.

An equivalent single rate model can be derived for the system of Figure 1.3.4 by using appropriate advance and delay operations on the different sample rate paths. For this system, the input is sampled at rate $1/T_m$ and the output at rate $1/T_p$, where T_m and T_n are integrally related to a least common sample period T_b by,

$$T_p = \frac{n_o}{p} T_b \qquad T_m = \frac{n_o}{m} T_b \qquad T_b = \frac{T}{n_o} \qquad (1.3.33)$$

where n_o/m and n_o/p are integers and T is the main interval of sampling. The input, output samplers are decomposed into m and p parallel slow rate samplers synchronised to operate at a single rate 1/T. This produces the system of Figure 1.3.5a.

If E^{n+} and E^{n-} are defined as vector time advance and delay operations given by,

$$E^{n+} = [\ 1 \quad e^{sT/n} \quad e^{2sT/n} \quad ..... \quad e^{(n-1)sT/n}\ ]^T$$

$$E^{n-} = [\ 1 \quad e^{-sT/n} \quad e^{-2sT/n} \quad ..... \quad e^{-(n-1)sT/n}\ ] \quad . \qquad (1.3.34)$$

then Figure 1.3.5a can be represented by the block diagram of Figure 1.3.5b. E^{n+} and E^{n-} are the *vector decomposition operators* or the *Kranc operators*, suitably named after their inventor Kranc (1957).

The uniformly sampled system description may now be derived by extending the identities of Sections 1.3.1 and 1.3.2. The equations for the system of 1.3.5b are:

$$R^*(z) = Z[\ E^{m+}R(s)\ ] \qquad (1.3.35)$$

$$C_a^*(z) = R^*(z)Z[\ E^{p+}G(s)E^{m-}\ ] \qquad (1.3.36)$$

$$C(z) = C_a^*(z)Z[\ E^{p-}\ ] \qquad (1.3.37)$$

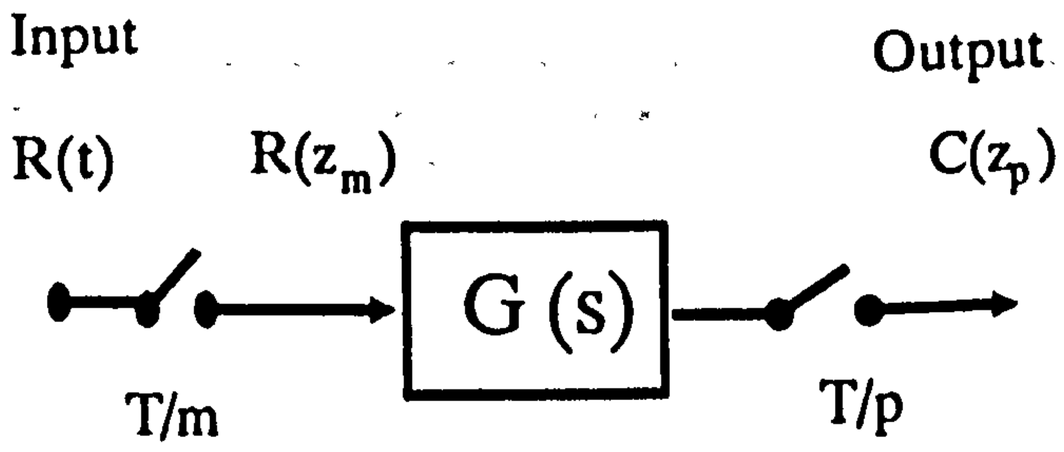

$$T/m \neq T/p$$

$$m/p = \text{irrational}$$

Figure 1.3.4 A multirate system with rational sample rates

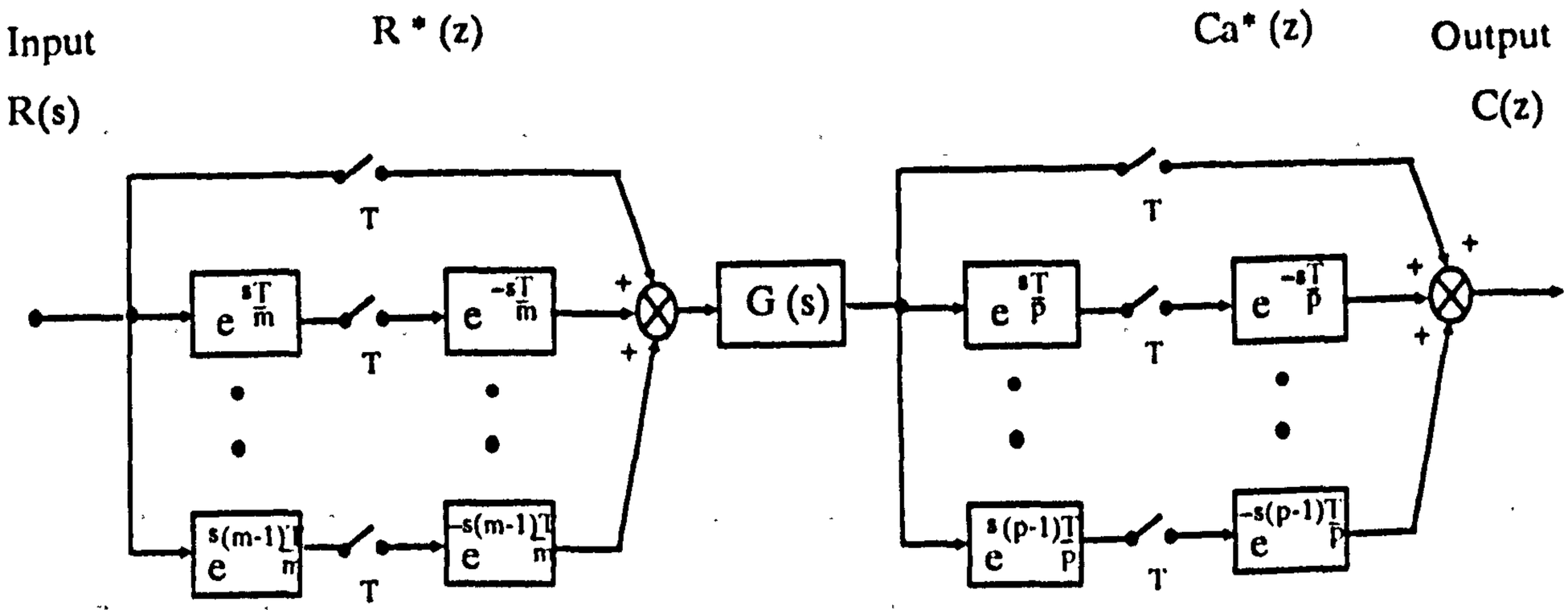

a)

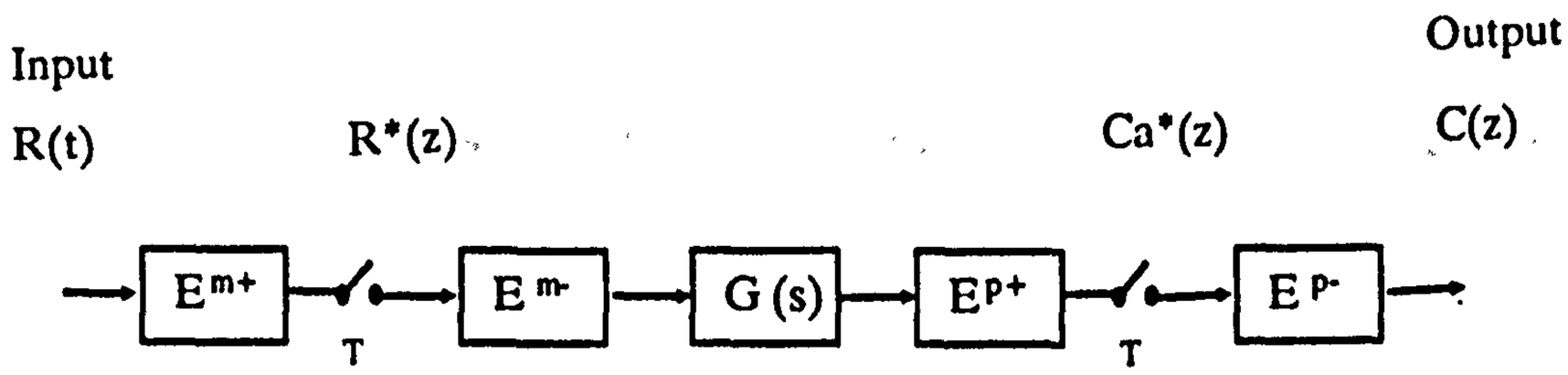

b)

Figure 1.3.5 The multirate system of Figure 1.4 in

a)switch decomposed form

b)vector decomposed form

Multirate operators $Z[E^{m+}R(s)]$, $Z[E^{p-}]$ correspond to the advanced input and delayed output signals which can be represented as follows:

$$Z[E^{m+}R(s)]^T = [R(z) \quad Z[R(s)e^{sT/m}] \quad Z[R(s)e^{2sT/m}] \;..\; Z[R(s)e^{(m-1)sT/m}]]$$

$$Z[E^{p-}] = [1 \quad z^{-kT/p} \quad z^{-2kT/p} \quad ..... \quad z^{-(p-1)kT/p}] \qquad (1.3.38)$$

The remaining term $Z[E^{p+}G(s)E^{m-}]$ can be similarly defined. The multirate operator will be a n_o/m input, n_o/p output identity determined by,

$$Z[E^{p+}G(s)E^{m-}] = \begin{bmatrix} 1 \\ e^{sT/p} \\ e^{2sT/p} \\ \vdots \\ e^{(p-1)sT/p} \end{bmatrix} G(s) \; [1 \quad e^{-sT/m} \quad e^{-2sT/m} \;..\; e^{-s(m-1)T/m}] \qquad (1.3.39)$$

which can be represented as:

$$Z[E^{p+}G(s)E^{m-}] = \begin{bmatrix} G^T(z) & G^T(z,\Delta_1) & \dots & G^T(z,\Delta_{m-1}) \\ G^T(z,1+1/p) & G^T(z,\Delta_1+1/p) & \dots & G^T(z,\Delta_1+1/p) \\ \vdots & \vdots & . & \vdots \\ G^T(z,1+(p-1)/p) & G^T(z,\Delta_1+1+(p-1)/p) & & G^T(z,\Delta_{m-1}+1+(p-1)/p) \end{bmatrix} \qquad (1.3.40)$$

where $\Delta_k = 1-k/m$ and $z = e^{-sT}$. The vector representation of (1.3.40) encapsulates all intersample behaviour of the multirate system but is not in a form useful for classical analysis. It does not for example, yield an analytic characteristic equation. However, the Kranc operator method does ensure that the transmission of all paths affected by the multirate sampling is in terms of vector advance and delay blocks. Thus, this representation allows the multirate system to be manipulated using standard signal flow diagram and block reduction techniques to simplify the analysis. The following example demonstrates this approach.

1.3.4 Vector decomposition of a simplified multirate helicopter

This section applies the switch decomposition operators of Sections 1.3.1 to 1.3.3 to examine the closed loop behaviour of a multirate controlled pitch attitude loop of a helicopter. A reduced order model of the helicopter system (Taylor, 1991) is used. The reasons for this are two-fold; to portray clearly the growth in dimension that is generally produced by multirate system analysis and, to simplify the manipulations required to derive a closed loop transfer functions.

For multirate control, attitude and rate information is fed back at different rates. The helicopter pitch rate dynamics are typically much faster than those of pitch attitude. Thus, rate information should ideally be monitored faster than the attitude signal, as shown in Figure 1.3.6.

The system equations for the helicopter are derived (Patel, 1990) by considering the accumulated effect of all fast signal within a slower sample period, T. Inserting vector decompostions on the faster rate feedback loop leads, via the block diagram of Figure 1.3.7a, to the signal flow diagram of Figure 1.3.7b. Signal flow diagram reduction techniques can be applied to Figure 1.3.7b to derive a transfer function. This transfer function will describe the T-periodic behaviour of the closed loop multirate system.

A set of transition equations for the vector decomposed system of Figure 1.3.7b are formulated first. The output equations for all non-input nodes are:

$$\theta^T(z) = (D_1G_1G_2)^T(z)(R-\theta)^T(z) - (D_2G_1G_2E^{n-})^T(z)x^T(z) \qquad (1.3.41)$$

$$x^T(z) = (E^n+D_1G_1)^T(z)(R-\theta)^T(z) - (E^n+D_2G_1E^{n-})^T(z)x^T(z) \qquad (1.3.42)$$

A combination of (1.3.41) and (1.3.42), to eliminate the intermediate

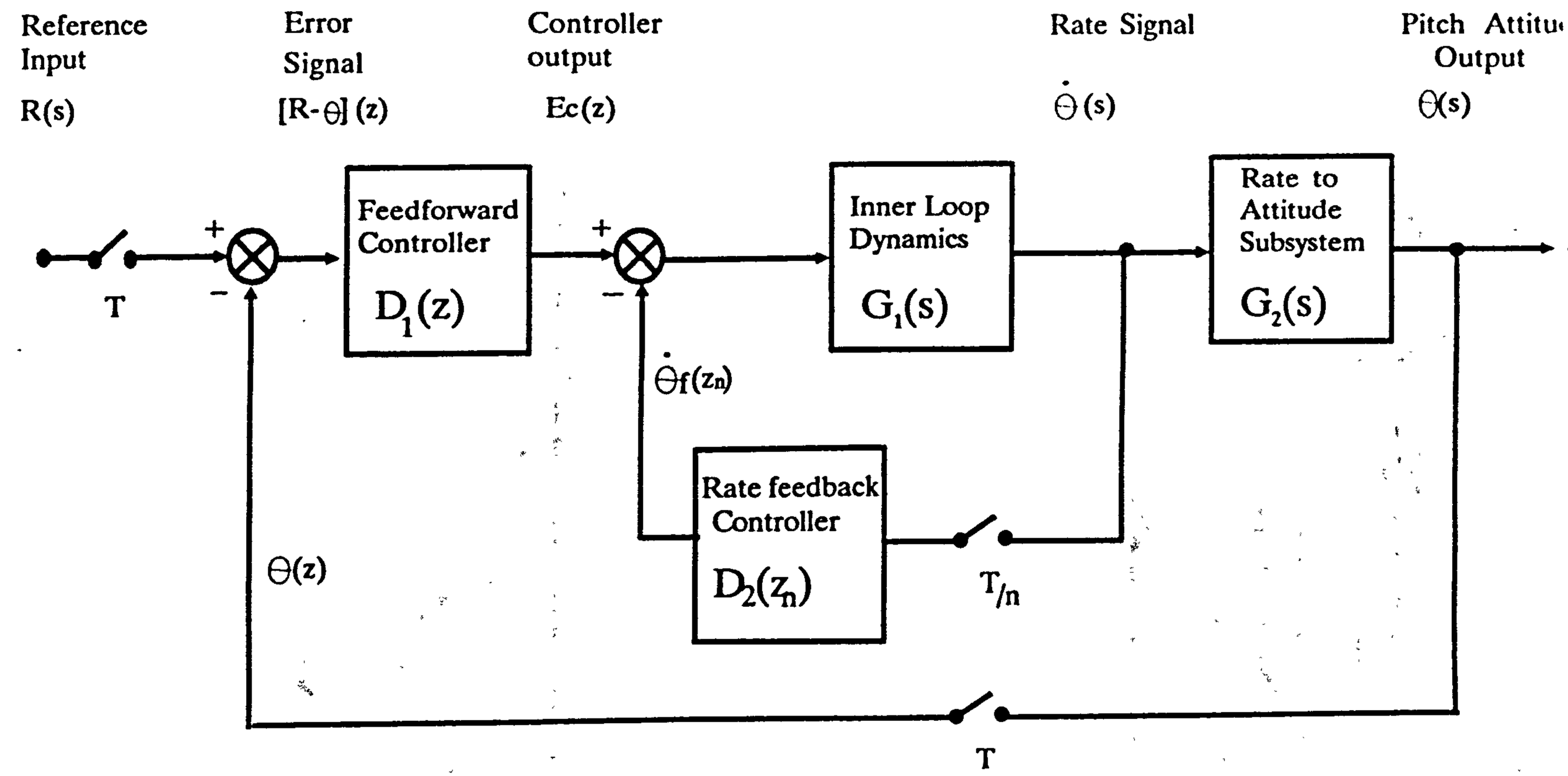

Figure 1.3.6 Multirate pitch attitude control of a simplified helicopter

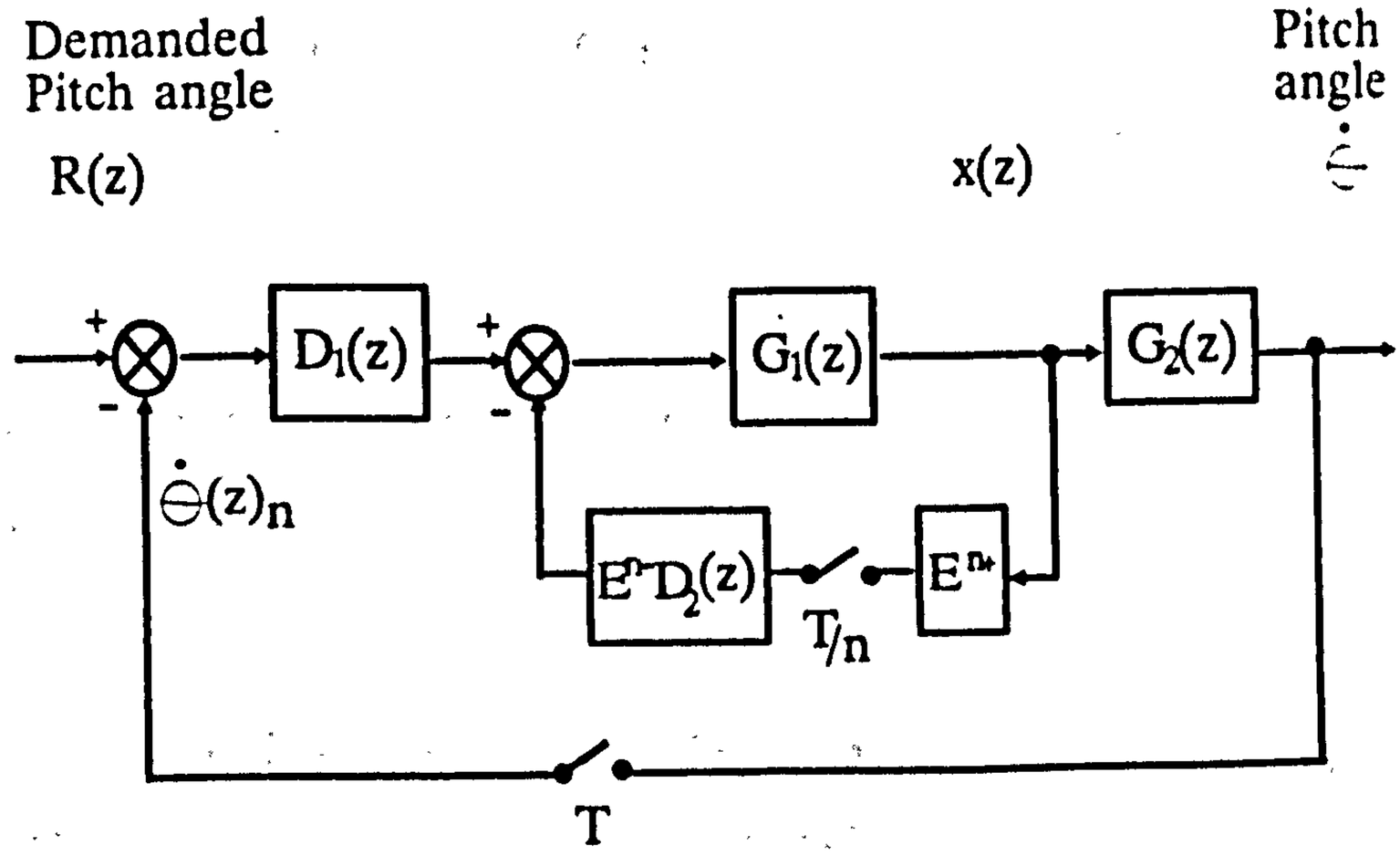

a)

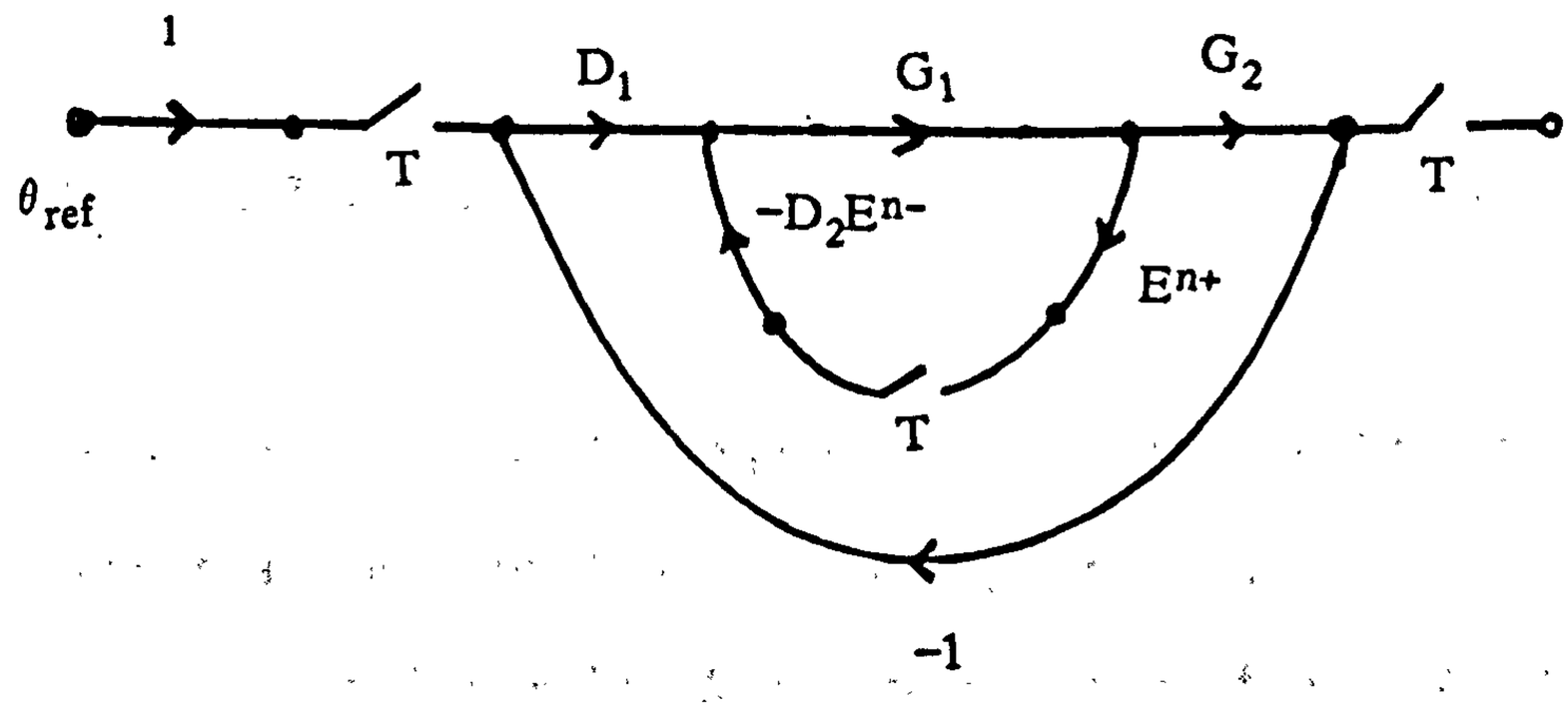

b)

Figure 1.3.7 Multirate helicopter:

a)vector decomposed block diagram

b)signal flow diagram

variable $x^T(z)$, gives the following closed loop equation,

$$\theta^T(z) = [D_1G_1G_2]^T(z)\,[R-\theta]^T(z) - \frac{[D_2G_1G_2E^{n-}]^T(z)\,[E^{n+}D_1G_1]^T(z)\,[R-\theta]^T(z)}{I + [E^{n+}D_2G_1E^{n-}]^T(z)} \tag{1.3.43}$$

Let $F = D_2G_1$. In transfer function form $[E^{n+}FE^{n-}]^T$ can be expressed by the (n x n) block matrix,

$$\begin{bmatrix} F^T(z) & F(^T(z,n-1/n) & F^T(z,n-2/n) & .. & F^T(z,1/n) \\ zF^T(z,1/n) & F^T(z) & F^T(z,n-1/n) & .. & F^T(z,n-2/n) \\ \vdots & \vdots & \vdots & & \vdots \\ zF^T(z,n-1/n) & zF^T(z,n-2/n) & zF^T(z,1/n) & & F^T(z) \end{bmatrix} \tag{1.3.44}$$

where the following notation is used for the modified z transforms,

$$Z[F(s)e^{-sTk/n}] = F^T(z,1-k/n) \tag{1.3.45}$$

$$Z[F(s)e^{sTk/n}] = zF^T(z,k/n) \tag{1.3.46}$$

The multirate operator of (1.3.44) requires inversion for the derivation of a closed loop transfer function. However, the inverse of function $[E^{n+}FE^{n-}](z)$ is clearly not simple. A method which unifies the multirate sampling process to produce equations which can be easily manipulated and thus address this inversion problems is the spectral decomposition technique of Boykin and Frazier (1975). With the use of this technique, (1.3.44) can be represented spectrally as,

$$(E^{n+}FE^{n-})^T = \sum_{i=0}^{n-1} \left[(e_iv_i) \sum_{k=0}^{n-1} F^T(z,n-k/n)\,\lambda_i{}^k \right] \tag{1.3.47}$$

where,

$$e_i = n^{-1/2} \left[\lambda_i 0 \quad \lambda_i \quad \ldots\ldots \quad \lambda_i n-1 \right]^T \tag{1.3.48}$$

$$v_i = n^{-1/2} \left[\lambda_i 0 \quad \lambda_i -1 \quad \ldots\ldots \quad \lambda_i -(n-1) \right] \tag{1.3.49}$$

$$\lambda_i = z^{1/n} \exp(j2\pi i/n) \tag{1.3.50}$$

and $e_i v_j = \delta_{ij}$, the Kroneker delta. Using the slow to fast transform, the advanced/delayed identity of (1.3.47) can be expressed as,

$$(E^{n+} F E^{n-})^T = \sum_{i=0}^{n-1} (e_i v_i)\ F^{T/n}(\lambda_i) \tag{1.4.11}$$

The advance operation $(E^{n+}F)^T$ is the first column of the matrix given in (1.3.44) and is defined as:

$$(E^{n+}F)^T = n^{-1/2} \sum_{i=0}^{n-1} (e_i) F^{T/n}(\lambda_i) \tag{1.3.52}$$

Similarly, the delay operation is the first row of the (n x n) block matrix in (1.3.44) and can be defined as:

$$(F E^{n-})^T = n^{-1/2} \sum_{i=0}^{n-1} (v_i) F^{T/n}(\lambda_i) \tag{1.3.53}$$

The simplification of equation (1.3.53) is examined. Let

$$Y^{T/n}(z) = (D_2 G_1 G_2 E^{n-})^T\ \Psi^T(z)\ (E^{n+} D_1 G_1)^T (R-\theta)^T \tag{1.3.54}$$

where,

$$\Psi^T(z) = [I + (E^{n+}D_2G_1E^{n-})^T]^{-1} \tag{1.3.55}$$

From the definitions of equation (1.3.41), it follows that:

$$\Psi^T(z) = \sum_{i=0}^{n-1} (e_i v_i)[1+(D_2G_1{}^{T/n})(\lambda_i)]^{-1} \tag{1.3.56}$$

$$Y^{T/n}(z) = \frac{1}{n} \sum_{i=0}^{n-1} (v_i)D_1G_2G_1{}^{T/n}(\lambda_i) \sum_{i=0}^{n-1} (e_i v_i)[1+D_2G_1{}^{T/n}(\lambda_i)]^{-1} \sum_{i=0}^{n-1} (e_i)D_1G_1{}^{T/n}(\lambda_i) \tag{1.3.57}$$

$$= \frac{1}{n} \sum_{i=0}^{n-1} \frac{(D_1G_2G_1)^{T/n}(\lambda_i)\ (D_1G_1)^{T/n}(\lambda_i)}{[1+(D_2G_1)^{T/n}(\lambda_i)]} \tag{1.3.58}$$

This fast rate description can be skip-sampled (using the identity of (1.3.32)) to produce $Y^T(z)$. The closed loop transfer function then becomes,

$$\frac{\theta^T(z)}{R(z)} = \frac{(D_1G_2G_1)^T(z) - Y^T(z)}{1 + (D_1G_1G_2)^T(z) - Y^T(z)} \tag{1.3.59}$$

1.4 MULTIRATE COMPENSATOR SYNTHESIS

Section 1.3 examined the *analysis* of multirate control systems. This section outlines a classical *design* method of Ragazzini and Franklin (1958). More recent examples of classical multirate design techniques include the work of Felui et al (1990) and Eckardt (1990). Felui et al apply the Ragazzini and Franklin synthesis techniques to design a mixed single rate and multirate control scheme for deadbeat control; Eckardt similarly uses the classical synthesis approach but formulates the

problem in state-space.

The synthesis method outlined in this section can be used to design multirate control systems of the type shown in Figure 1.4.1. For this control scheme, the open loop system to be controlled has a transfer function G(s) and the multirate compensator to be designed is denoted by $D(z_n)$. The compensator dynamics are to be determined according to some desired design criterion.

Using the notation of Section 1.2, the equations for Figure 1.4.1 are:

$$E(z) = R(z) - \dot{\theta}(z) \tag{1.4.1}$$

$$u(z_n) = D(z_n)E(z_n^n) \tag{1.4.2}$$

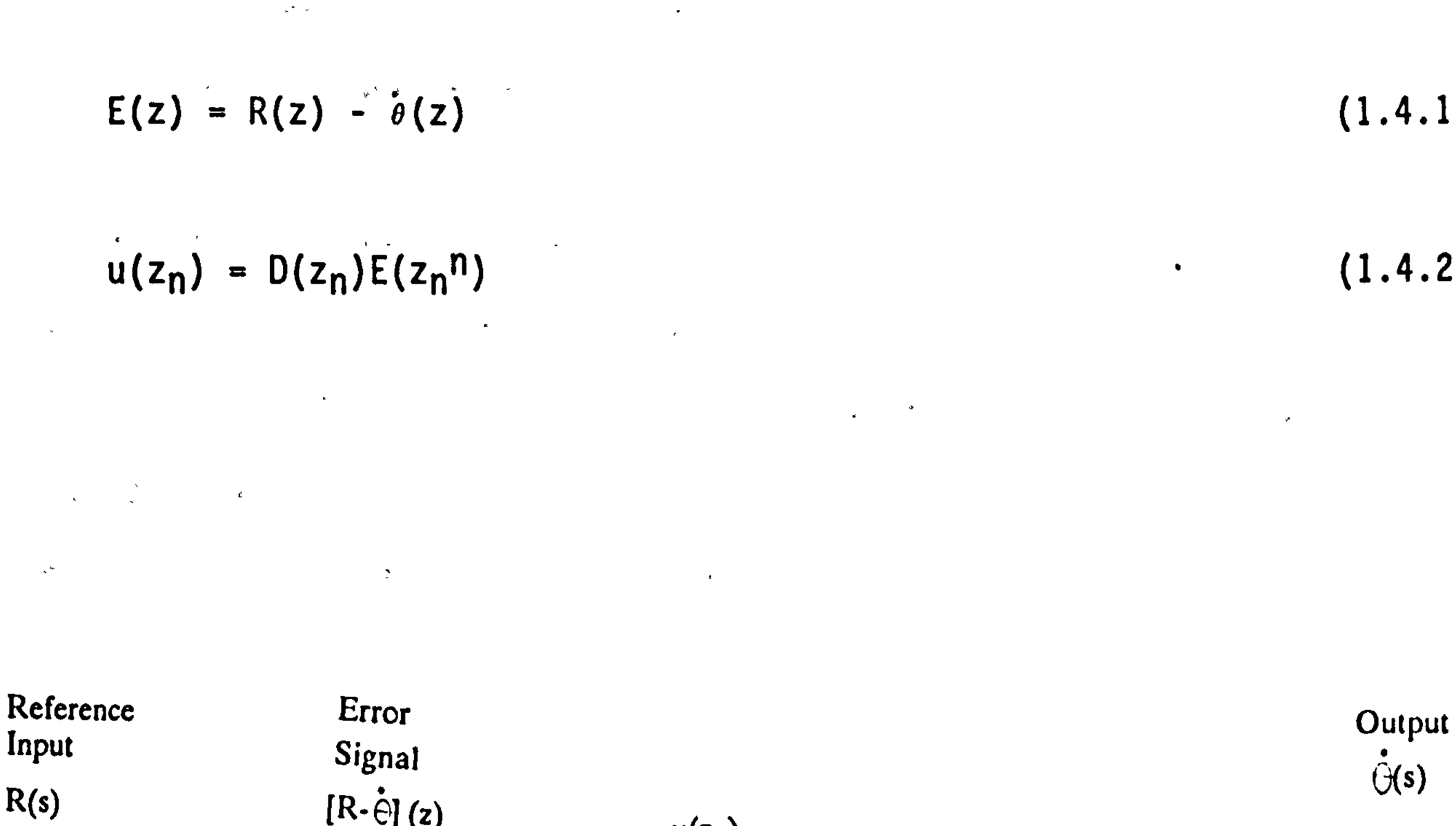

Figure 1.4.1 Classical multirate control loop

$$\dot{\theta}(z_n) = G(z_n)u(z_n) \tag{1.4.3}$$

The design requirements are to determine a multirate compensator such that the resulting closed loop system exhibits the desired behaviour and in addition, fulfils the following objectives:

i) Closed loop system performance is causal.

ii) Any open loop singularities which lie outside the z domain unit circle remain uncancelled.

The first condition ensures physical realisability of the closed loop system whilst the second requirement prevents imperfect cancellation of unstable singularities (which may induce further instability) in the closed loop design. Thus, if the open loop system dynamics can be split into an unstable subsystem $G_u(s)$ and a stable subsystem $G_s(s)$ i.e.,

$$G(s)= G_u(s)G_s(s) \tag{1.4.4}$$

then, the controller must be of the form,

$$D(z_n)= F(z_n)[\,G_u(z_n)\,]^{-1} \tag{1.4.5}$$

where $F(z_n)$ is, as yet, an unspecified part of the compensator. If the desired closed loop system is specified by a transfer function $H(z)$ i.e.,

$$\dot{\theta}(z) = H(z)R(z) \tag{1.4.6}$$

then a combination of equation (1.4.6) with equations (1.4.2) to (1.4.5)

will give an expression for the desired controller $D(z_n)$. From equations (1.4.1) to (1.4.3),

$$u(z_n) = D(z_n)\,[R(z_n^n) - \dot{\theta}(z_n^n)] \tag{1.4.7}$$

$$\dot{\theta}(z_n) = G(z_n)\,D(z_n)\,[R(z_n^n) - \dot{\theta}(z_n^n)] \tag{1.4.8}$$

To resolve the sampling incompatibility of the two output terms in equation (1.4.8), $\dot{\theta}(z)$ must be extracted from $\dot{\theta}(z_n)$ using any of the methods described in Section 1.3. If this extraction operation is denoted by $Z[\cdot]_{zn\to z}$ i.e.,

$$\dot{\theta}(z) = Z[\dot{\theta}(z_n)]_{zn\to z} \tag{1.4.9}$$

then,

$$\dot{\theta}(z) = [R(z) - \dot{\theta}(z)]\,Z[G(z_n)D(z_n)]_{zn\to z} \tag{1.4.10}$$

Thus,

$$\dot{\theta}(z) = \frac{Z[G(z_n)D(z_n)]_{zn\to z}}{1 + Z[G(z_n)D(z_n)]_{zn\to z}}\,R(z) \tag{1.4.11}$$

To determine the compensator dynamics, equations (1.4.11) and (1.4.6) are combined to give,

$$Z[G(z_n)D(z_n)]_{zn\to z} = \frac{H(z)}{1 - H(z)} \tag{1.4.12}$$

$$1 + Z[G(z_n)D(z_n)]_{zn\to z} = \frac{1}{1 - H(z)} \tag{1.4.13}$$

Equations (1.4.12) and (1.4.13) specify the desired (compensated) open loop dynamics in terms of the slow discrete operator. A desired closed loop transfer function in z_n, $H(z_n)$, is required to obtain an expression for $F(z_n)$. From equation (1.4.5), this is provided by,

$$H(z_n) = \frac{G(z_n)D(z_n)}{1 + Z[G(z_n)D(z_n)]_{zn\to z}} \tag{1.4.14}$$

The required compensator is then determined from the substitution of equation (1.4.13) into (1.4.14) to give:

$$F(z_n) = \frac{G_u(z_n)H(z_n)}{G(z_n)[1-H(z_n^n)]} \tag{1.4.15}$$

Example 1.4 Design of multirate control for the simplified helicopter

Reconsider, the multirate attitude control loop of the helicopter of Example 1.3. This example uses the synthesis technique described above to design a multirate compensator such that the resulting (closed loop) pitch attitude system tracks a given reference signal in a finite time. To cast the pitch attitude control problem into the configuration of Figure 1.4.1, assume that the whole of the inner rate loop operates as a continuous subsystem represented by transfer function G(s).

The desired closed loop transfer function may be determined from the final value theorem which states that,

$$\lim_{k\to\infty} E(kT) = \lim_{zn\to 1} (1-z_n^{-1})E(z_n) \tag{1.4.16}$$

$$= \lim_{zn\to 1} (1-z_n^{-1})[R(z_n)-R(z_n^n)H(z_n)] \tag{1.4.17}$$

Thus, for the error $E(kT/n)$ to become zero, $[R(z_n)-R(z_n^n)H(z_n)]$ must not contain any infinite z_n series terms. For example, if the helicopter reference input is a ramp signal described by $R(s) = A/s^2$ then,

$$R(z_n^n) = \frac{Tz_n^{-n}}{(1-z_n^{-n})^2}$$

$$R(z_n) = \frac{Tz_n^{-1}}{n(1-z_n^{-1})^2} \tag{1.4.18}$$

and,

$$\lim_{k\to\infty} E(kT/n) = \lim_{zn\to 1} (1-z_n^{-1})T \left[\frac{z_n^{-1}}{(1-z_n^{-1})^2} - \frac{z_n^{-n}H(z_n)}{(1-z_n^{-n})^2}\right] \tag{1.4.19}$$

$$= \lim_{zn\to 1} T(1-z_n^{-1})^{-1} [L(z_n)] \tag{1.4.20}$$

In this case, $H(z_n)$ must be chosen to nullify the effects of infinite series terms $(1-z_n^{-1})^2$ and $(1-z_n^{-n})^2$ to ensure that $E(kT/n)$ will go to zero in finite time. This condition is satisfied by an $L(z_n)$,

$$L(z_n) = (1-z_n^{-1})^r \tag{1.4.21}$$

If a choice of $r = 0$ is selected then $H(z_n)$ is determined to be,

$$H(z_n) = \frac{(1-z_n^{-n})^2}{z_n^{-n}} \left[\frac{-1}{1-z_n^{-1}}\right] \tag{1.4.22}$$

The multirate feedforward control design is complete with $H(z_n)$ as given above together with equation (1.4.15). The remaining unknown terms of

equation (1.4.15) are $G_u(z_n)$ and $H(z_n^n)$. The former can be determined from noting that the open loop helicopter is stable, thus $G_u(s) = 1$ and $D(z_n) = F(z_n)$. Furthermore, $H(z_n^n) = Z[H(z_n)]_{zn \to z}$. Inserting all this information into (1.4.15) then gives,

$$D(z_n) = \frac{H(z_n)}{G(z_n)[1-Z[H(z_n)]_{zn \to n}]} \qquad (1.4.23)$$

For this example, the isolation of $H(z_z^n) = Z[H(z_n)]_{zn \to z}$ from $H(z_n)$ can be determined by inspection. This is determined to be:

$$H(z_n^n) = \frac{-(1-z_n^{-n})^2}{z_n^{-n}(1-z_n^{-n})} \qquad (1.5.24)$$

The derivation of $H(z_n^n)$ from $H(z_n)$ is not always so simple; for more complex $H(z_n)$ the inversion formula given by equation (1.3.31) may be applied. This gives,

$$H(z_n^n) = \frac{1}{2\pi J} \int_{\Gamma} \frac{H(z_n)}{1-z_n z^{-1}} \frac{dz_n}{z_n} \qquad (1.5.25)$$

Since the closed loop system produced by compensator $D(z_n)$ of (1.4.23) is designed to track ramp signals, the system will also track step inputs.

1.6 SUMMARY

This chapter has described s, Z and time domain identities (or operators) for elemental multirate configurations and applied them for the design and analysis of simple multirate systems. The main objective of this chapter has been to unify the two classical approaches used to

represent multirate system behaviour; the frequency decomposition method of Slansky and the switch (and vector) decomposition methods of Ragazzini and Franklin (and Kranc).

Section 1.2 outlined the preliminaries of discrete system representation in the Laplace, Discrete and time domains to clarify the links between the different domains.

Sections 1.3.1 and 1.3.2 have derived the identities for slow/fast and fast/slow multirate systems with simple integer (rational) relations between the fast and slow sample rates. These identities were obtained by incorporating time advance and delay units before and after every multirate sampler to produce an equivalent single rate system. Section 1.3.3 has considered a system with both multirate inputs and multirate outputs with sample rates which do not have a rational relationship. In this case, the derivation of a multirate operator was made possible by identifying the lowest fast sample rate ($1/T_b$) and the lowest slow sample rate ($1/T$) common to both the input and output sample rates. This operator was derived by using the vector representation of the switch decomposed system, i.e. the vector decompostion method of Kranc.

The vector decomposition method was observed to be a simple replacement of advance and delay operations in a number of (parallel) switch decomposed paths by vector operators. The vector operators can then be represented by block functions. An advantage of this approach is that the resulting multirate system description is in a form which can be manipulated and simpified using block reduction techniques (which is not possible with the switch decomposition approach). However, it must be noted that for many cases, the block reduction techniques only apply when the sampling operations occur at 'convenient' locations within the loop. This is a common drawback of all the classical decomposition methods which generally results in an inability to derive a closed loop multirate system description.

The vector decomposition operators were applied in Section 1.3.4 to formulate equations for an example based on a helicopter pitch loop. The controllers for the pitch motion use rate and attitude information which is updated at different rates. This example highlights another drawback which hinders the derivation of a closed loop transfer function for a multirate system: the inversion of matrices whose elements are tranfer functions with few common factors. These matrices are the vector decomposition multirate operators. An inversion is required if a matrix of transfer functions is embedded in the denominator of the closed loop system expression.

Section 1.3.4 outlines the spectral decomposition method of Boykin and Frazier which may be used to simplify the inversion of the vector decomposition operator. The example demonstrated that once the un-invertable expression was spectrally decomposed, standard block manipulation and synthesis methods could be applied to obtain a closed loop expression for the helicopter pitch loop.

The last section of this chapter, Section 1.4, outlined a design technique which can be applied to synthesise multirate compensators. The method is based on the early work of Ragazzini and Franklin and is demonstrated with the design of a tracking compensator for the helicopter pitch loop of Section 1.3.4.

CHAPTER TWO

STATE SPACE REPRESENTATION OF MULTIVARIABLE MULTIRATE SYSTEMS

2.1. INTRODUCTION

Chapter 1 has outlined the manipulation and analytic problems encountered when using classical operators to form multirate closed loop system transfer functions. Many of these problems can be circumvented by the use of state space techniques to describe multirate system behaviour. State space models can also provide vital intersample information and allow more flexible combinations of multirate subsystems. In general, a linear, time-invariant continuous system sampled using a multirate scheme produces a time varying discrete system which is cumbersome to analyse for a high number of sample rates. Kalman and Bertram (1959) identified that if *all* input, output and control sample periods are confined to integer multiples of a common smallest time interval (the base period), the discrete system can be classed as a special type of periodic system. A time-invariant discrete model can then be used to describe the periodically time-varying multirate system.

The (frequently cited) work of Kalman and Bertram is the earliest unification of sampled data system representation in state space. It has provided a platform for the subsequent development of many state space modelling techniques for multirate systems (Albertos, 1990; Al Rhamani and Franklin, 1990; Amit and Powell, 1981; Araki and Yamamoto, 1986; Berg et al, 1988; Chammas and Leondes, 1978, 1979; Eckardt, 1989; Francis and Gorgiou, 1988; Glasson, 1980; Godbout et al, 1988; Kargonekar et al, 1985; Kono, 1980; Kono et al, 1990; Litkouhi and Khalil, 1985; Luse, 1988; Mahmoud, 1982; Meyer, 1990; Meyer and Burrus, 1975; Patel, 1991; Thompson, 1986). This chapter derives state space

models for the basic fast/slow, slow/fast SISO multirate systems of Chaper 1. In addition, a *general* state space system model which can be applied to any MIMO multirate system with input/output sample rates that can be integrally related to a base period is also derived.

As for the classical vector and switch decomposition methods, state space multirate system analysis requires that all independent subsystem dynamics be defined for a largest common time period (the main interval of sampling) within which integer multiples of all other sample periods can be represented. This ensures that different multirate subsystems can be combined in a compatible manner. Multirate sampling relationships and other preliminaries of multirate state space modelling are outlined in Section 2.2. For completeness, the derivation of *single rate* discrete, state space equations is also detailed in Appendix A. Section 2.3 develops state space equivalents of the classical operators used to describe the multirate sampling configurations of Chapter 1. This section is organised in accordance with the classical developments in Chapter 1; Sections 2.3.1 and 2.3.2 examine state space modelling of simple, integrally related, slow/fast, fast/slow sampled SISO systems, followed by state space modelling of multirate input, multirate output systems with rational sample rate ratios in Section 2.3.3.

The general MIMO multirate system model, which can represent *any* multirate sampling scheme which satisfies the neccessary sampling inter-relationships, is then described in Section 2.4. This model is fairly complex in its description. The task is addressed with the use of an example; beginning with equations for a simple 2 input, single output multirate system and building up to the general MIMO configuration.

The difference in multirate state-space operators which contain main sample and intersample information and operators which provide only main sample data is important. Intersample behaviour is useful for the accurate determination of multirate frequency domain performance. For this reason, the objective of Sections 2.3 and 2.4 is to formulate

multirate state-space representations which encapsulate all intersample effects accurately. In comparison, Section 2.5 examines state space models for a class of slow/fast, fast/slow systems which contain only main sample information. The different capabilities offered by each type of model for system design and analysis is clearly outlined.

Section 2.6 applies the multirate operators developed in the preceding sections to analyse a variation of the helicopter pitch attitude control example of Chapter 1. The example is different in that samplers are placed in different locations. The analysis is repeated with a clear, step by step formulation of the required state space closed loop equations. This example demonstrates the use of the state space operators and indicates the merits of using this approach.

Section 2.7 outlines a state space technique for the design of multirate compensators. This technique is based on *matching* the desired closed loop performance of an existing (compensated) continuous-time system. An important feature of this method is that the closed loop *structure* of the original continuous-time system is maintained. The technique assumes that the multirate system has identical compensator dynamics to that of the continuous system. The objective of the design method is to determine the multirate compensator gains required to match continuous-time system performance.

Though this method can be applied to single rate discrete systems, it is better suited for the design of multirate compensators. The reason for this is entirely due to the different amount of design freedom (which is determined by the number of input/output updates within one main sample period) made available by the two sampling schemes. In the single rate case, a good match of the desired system performance is not always possible due to the limited design opportunity offered by the uniform, single rate update mechanism. However, multirate sampling can be used to increase the number of updates within one sample period and thus generate extra design freedom for the matching technique. Thus an

accurate match of the desired closed loop dynamics can be obtained with multirate sampling. An example based on the design of a multirate proportional plus integral (P+I) compensator for an aircraft pitch rate loop demonstrates this procedure. The performance of the multirate system and the corresponding single rate closed loop system is compared to highlight the effectiveness of the multirate sampling scheme.

2.2 PRELIMINARIES OF MULTIRATE STATE SPACE REPRESENTATION

It is common practice in the formulation of discrete state space equations to assume that all D/A converters preceding analogue system components are modelled by zero-order holds (ZOHs). Furthermore, all A/D and D/A elements present in the system are assumed to operate synchronously at a *single uniform rate*. State space equations derived using this approach (see Appendix A) produce discrete models which are equivalent to discrete transfer functions obtained by,

$$G_h(z) = \frac{z-1}{z} Z\left[\frac{G(s)}{s}\right]_T = \left[\begin{array}{c|c} \Phi(T) & \Gamma(T) \\ \hline C & D \end{array}\right] \qquad (2.2.1)$$

where G(s) is the continuous function of interest. Equation (2.2.1) is the standard Z transform of a continuous component preceded by a ZOH.

To describe a multirate system where the input, output samplers operate periodically but with different periods (see Figure 2.2.1), a complete set of transition equations must be determined for an interval equal to the least common multiple of all the sample periods (T in Figure 2.2.1). This interval was defined as the main interval of sampling in Chapter 1. Since the sampling sequence is T-periodic this set of transition equations will describe the multirate state system at any time.

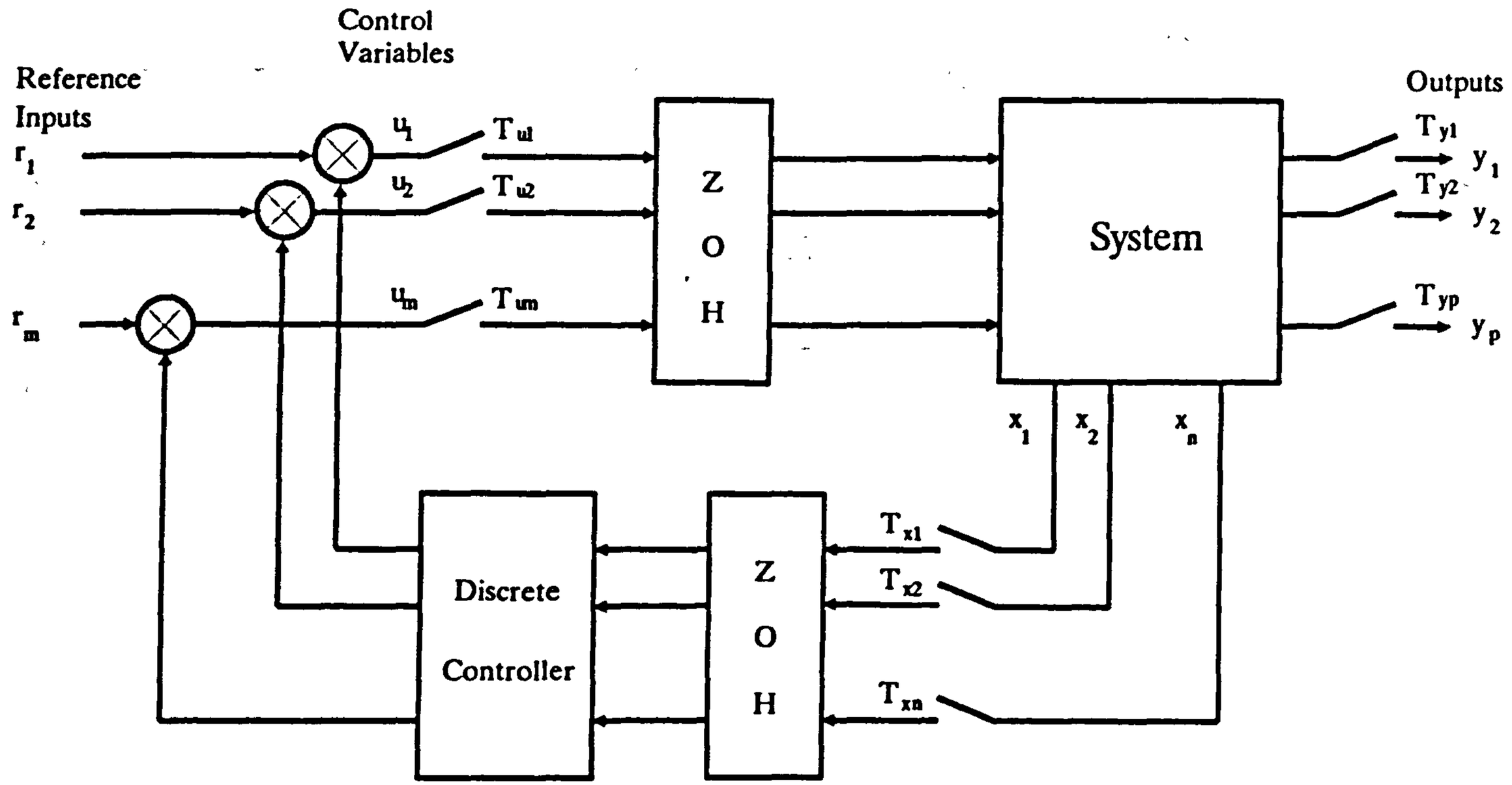

Figure 2.2.1 State space discrete system with multirate inputs and multirate outputs.

Consider a simple multirate system with only two sample periods T_1 and T_2. If the sample period ratios are rational then,

$$\frac{T1}{T_2} = \frac{n_1}{n_2} \qquad (2.2.2a)$$

(where n_1, n_2 have no common factor). There exists a lowest common multiple n_o and a lowest common sample period T such that,

$$T_1 = n_1 \frac{T}{n_o} \qquad \text{and} \qquad T_2 = n_2 \frac{T}{n_o} \qquad (2.2.2b)$$

(Recall from Chapter 1 that the ratio $T_b=T/n_o$ defines the base sample period). The behaviour of the system sampled at intervals T_b is termed the *base dynamics*. The periodic nature of the time varying system implies that the discrete state equation parameters have the property,

$$\begin{aligned} \Phi[kT+iT_b,kT] &= \Phi[iT_b,0] \qquad i = 0,..,(n_o-1) \\ \Gamma[kT+iT_b,kT] &= \Gamma[iT_b,0] \\ C[kT+iT_b,kT] &= C[iT_b,0] \end{aligned} \qquad (2.2.3)$$

To extend the sampling inter-relationships of (2.2.2) to a system with n sample rates define,

$$\begin{aligned} \ell_i &= \frac{n_o}{n_i} \qquad i = 1,..,n \\ T_i &= \frac{T}{n_i} = \ell_i T_b \\ N &= n_1 + n_2 +..+ n_m \end{aligned} \qquad (2.2.4)$$

For the multirate system equations the state, control and output vectors are defined for intersample points as well as for the main interval sample instants. The intersample points for each vector are determined by its particular update rates. These expanded vectors are of the form,

$$x_e[(k+1)T] = \begin{bmatrix} x[kT+T_b] \\ x[kT+2T_b] \\ \vdots \\ x[kT+(n_0-1)T_b] \\ x[(k+1)T] \end{bmatrix} \tag{2.2.5}$$

$$u_e(kT) = \begin{bmatrix} u_{1e}(kT) \\ u_{2e}(kT) \\ \vdots \\ u_{me}(kT) \end{bmatrix} \tag{2.2.6}$$

where,

$$u_{ie}(kT) = \begin{bmatrix} u_i[kT] \\ u_i[kT+T_i] \\ \vdots \\ u_i[kT+(n_i-1)T_i] \end{bmatrix} \tag{2.2.7}$$

The expanded output vector $y_e(kT)$ is defined similarly to $u_e(kT)$. Also used is matrix $I_{n,i}$ which is defined as a (n x n) zero matrix with diagonal unit entries starting on the (i+1)th element, eg,

$$I_{5,2} = \begin{bmatrix} 0 & 0 & 0 & 0 & 0 \\ 0 & 0 & 0 & 0 & 0 \\ 0 & 0 & 1 & 0 & 0 \\ 0 & 0 & 0 & 1 & 0 \\ 0 & 0 & 0 & 0 & 1 \end{bmatrix} \tag{2.2.8}$$

and $(n_0 x n_0)$ block matrices M_1 and M_2 which are defined as,

$$M_1 = \begin{bmatrix} 0 & . & 0 & I_{n_0} \\ 0 & . & . & 0 \\ . & . & . & . \\ . & . & . & . \\ 0 & . & . & 0 \end{bmatrix} \qquad M_2 = \begin{bmatrix} 0 & . & . & . & 0 \\ I_{n_0} & 0 & . & . & 0 \\ 0 & I_{n_0} & . & . & 0 \\ . & . & . & . & . \\ 0 & . & . & I_{n_0} & 0 \end{bmatrix} \tag{2.2.9}$$

where the 0 and I_{n_0} blocks are null and identity matrices respectively, both of dimension (n_0 x n_0).

Time-invariant equations for multirate systems can be derived in several forms of varying complexity. The equations are determined either

by the particular multirate sampling scheme they describe or by the amount of information necessary for the application of design and analysis techniques. For each form, the amount of information available in the equations determines the ease of sampling reconfigurabilty. These forms can be categoried as follows:

1) A concise description for systems with varying input (output) and fixed output (input) sampling. The equations represent state and output (input) parameters only at main interval sample instants and the control (ouput) matrix at points where the inputs (outputs) change.

2) A low dimensional description for a system with different input and output sample rates with a constraint on the input/output sampling inter-relationships. This leads to a set of coefficients representing control and output parameters at the instants indicated by their respective sample rates. In this case, the state vector is defined for some base sample rate common to all the sampling rates.

3) A high dimensional description for a system with different input/output sample rates but with no constraints on the sampling configuration. The equations consist of simple coefficients representing all the parameters at some base sample instants common to all sampling rates.

The SISO decomposition operators of Chapter 1 fall into category (2) only. In correspondence with the developments of Chapter 1, Sections 2.3.1 to 2.3.3 formulate transition equations for slow/fast, fast/slow, SISO systems of category (2). Section 2.3.4 develops state equations for multirate systems of category (1). The usefulness of each type of description is also outlined.

2.3 STATE SPACE OPERATORS FOR SISO MULTIRATE SYSTEMS

This section derives multirate state space operators for the slow input/fast output and fast input/slow output sampled systems of Figure 1.3.1. These systems have a main interval of sampling T and a single input u and a single output y uniformly sampled at either T or at the base rate T_b. Since T_b defines the *smallest* common interval of all sample rates present in the multirate systems, the multirate state space operators are composed from discrete system dynamics defined for this period (the *base rate dynamics*) given by:

$$G_1(z_n) = Z[G_1(s)]Tb = \left[\begin{array}{c|c} \Phi(Tb) & \Gamma(Tb) \\ \hline C & D \end{array}\right] \qquad (2.3.1)$$

To ensure that subsystems of different rates can be combined in a compatible manner each multirate operator must incorporate the correct number of input/output transitions that occur during the main sample interval. Furthermore, each output must correspond to the value expected from the multirate system *at the correct time instant within the main interval timeframe*. This corresponds to the requirement that every state equation contained within the multirate operators must only describe system transition during the intersample period associated with that state equation, and not contain 'accumulated' responses from any other time interval. This may model the occurence of some sample and hold operations faster than they physically occur, but is necessary in order to represent time domain behaviour of the system accurately. This 'oversampling' produces the characteristic non-minimal feature of multirate state space representations (Araki and Yamamoto, 1986).

For classical multirate operators, the incorporation of ZOH elements in the discrete system was effected simply by including the hold dynamics at the z transform stage. For the state space developments of

Sections 2.3.1 and 2.3.2, a clear distinction is made between systems with and without ZOHs, since different models arise for the two cases.

2.3.1 Slow rate input, fast rate output system.

For this system the output is sampled at instants $t = kT_b$ while the input is updated at instants t=kT. Thus, the sampling relations of equation (2.2.4) give,

$$\begin{aligned} &n_0=4 \\ &n_u=1 \qquad \ell_u=4 \qquad T_u=4T_b \\ &n_y=4 \qquad \ell_y=1 \qquad T_y=T_b \end{aligned} \tag{2.3.3}$$

where subscripts u and y denote input and output, respectively. The transition equations for this system are calculated by determining how $y[kT+T_b]$, $y[kT+2T_b]$, $y[kT+3T_b]$ and y[(k+1)T] may be calculated from x(kT) and control input u[kT].

Slow input, fast output rate system without ZOH

The base rate dynamics for the slow input, fast output multirate system without a ZOH are given by the quadruplet of equation (2.3.1). The state space description which describes the performance of this system over the period T must have one input and four outputs. Since there is no hold element the system will respond to an input only at main instants. All subsequent intersample values will be determined by the system unforced or natural reponse to the 'intial conditions' produced by the system response to the main sample step input. This would indicate that only the main sample instant transition equation has forced system dynamic elements (i.e. Γ terms). Thus, the state equations

for the slow input, fast output multirate system are:

$$x_e[(k+1)T] = A_{sf1}x_e[kT] + A_{sf2}x_e[(k+1)T] + B_{sf}u_e[kT] \qquad (2.3.4)$$

$$y_e[(k+1)T] = C_{sf1}x_e[kT] + C_{sf2}x_e[(k+1)T] + D_{sf}u_e[(k+1)T] \qquad (2.3.5)$$

where A_{sf1}, A_{sf2} and B_{sf1} are defined,

$$A_{sf1}=\begin{bmatrix} 0 & 0 & 0 & \Phi(Tb) \\ 0 & 0 & 0 & 0 \\ 0 & 0 & 0 & 0 \\ 0 & 0 & 0 & 0 \end{bmatrix} \quad A_{sf2}=\begin{bmatrix} 0 & 0 & 0 & 0 \\ \Phi(Tb) & 0 & 0 & 0 \\ 0 & \Phi(Tb) & 0 & 0 \\ 0 & 0 & \Phi(Tb) & 0 \end{bmatrix}$$

$$B_{sf}=\begin{bmatrix} \Gamma(Tb) \\ 0 \\ 0 \\ 0 \end{bmatrix} \qquad (2.3.6)$$

Similarly,

$$C_{sf1}=\begin{bmatrix} 0 & 0 & 0 & C \\ 0 & 0 & 0 & 0 \\ 0 & 0 & 0 & 0 \\ 0 & 0 & 0 & 0 \end{bmatrix} \quad C_{sf2}=\begin{bmatrix} 0 & 0 & 0 & 0 \\ C & 0 & 0 & 0 \\ 0 & C & 0 & 0 \\ 0 & 0 & C & 0 \end{bmatrix} \quad D_{sf}\begin{bmatrix} D \\ 0 \\ 0 \\ 0 \end{bmatrix} \qquad (2.3.7)$$

Rearranging equations (2.3.4) and (2.3.5) to combine similar state vectors gives,

$$x_e[(k+1)T] = [I_n-A_{sf2}]^{-1}A_{sf1}x_e[kT] + [I_n-A_{sf2}]^{-1}B_{sf}u_e[kT] \qquad (2.3.8)$$

$$y_e[(k+1)T] = [I_n-C_{sf2}]^{-1}C_{sf1}x_e[kT] \qquad (2.3.9)$$

When the impulse responses of the above state space model and its switch decomposition counterpart (given by equations (1.3.9) and (1.3.12)) are compared, only values of the z_n^{-4} and higher terms correspond. Thus state equations (2.3.8) and (2.3.9) give an accurate output signal *after*

n intial zero values.

Slow input, Fast output rate system with ZOH

The base rate dynamics with a ZOH are given by the discrete system quadruplet,

$$G_{1h}(z_n) = \left[\begin{array}{c|c} \Phi_h(T_b) & \Gamma_h(T_b) \\ \hline C & D \end{array}\right] \qquad (2.3.10)$$

The ZOH ensures that the step input persists for all main sample *and* intersample instants. Thus, the state equation for the slow input/fast output multirate system are given by:

$$x_e[(k+1)T] = A_{sfh1}x_e[kT] + A_{sfh2}x_e[(k+1)T] + B_{sfh}u_e[kT] \qquad (2.3.11)$$

$$y_e[(k+1)T] = C_{sf1}x_e[kT] + C_{sf2}x_e[(k+1)T] + D_{sfh}u_e[(k+1)T] \qquad (2.3.12)$$

where A_{sfh1} and A_{sfh2} have the same form as A_{sf1}, A_{sf2} of equation (2.3.7) with $\Phi(Tb)$ replaced by $\Phi_h(Tb)$ and B_{sfh}, D_{sfh} are defined,

$$B_{sfh} = \begin{bmatrix} \Gamma_h(T_b) \\ \Gamma_h(T_b) \\ \Gamma_h(T_b) \\ \Gamma_h(T_b) \end{bmatrix} \qquad D_{sfh} = \begin{bmatrix} D \\ D \\ D \\ D \end{bmatrix} \qquad (2.3.13)$$

Equations (2.3.11) and (2.3.12) rearranged gives,

$$x_e[(k+1)T]=[I_n-A_{sfh2}]^{-1}A_{sfh1}x_e[kT] + [I_n-A_{sfh2}]^{-1}B_{sfh}u_e[kT] \qquad (2.3.14)$$

$$y_e[(k+1)T]=[I_n-C_{sf2}]^{-1}C_{sf1}x_e[kT] + [I_n-C_{sf2}]^{-1}D_{sfh}u_e[(k+1)T \qquad (2.3.15)$$

The impulse response of (2.3.15) matches that of the corresponding classical operator of equation (1.3.23) after n=4 initial zero terms.

2.3.2 Fast rate input, slow rate output system.

For this system the output is sampled at instants t = kT while the input is updated at instants t = kT_b. Thus, the sampling relations of equation (2.2.4) give,

$$n_0=4$$

$$n_u=4 \qquad \ell_u=1 \qquad T_u=T_b$$

$$n_y=1 \qquad \ell_y=4 \qquad T_y=4T_b \tag{2.3.16}$$

The transition equations for this system are calculated by determining how y[(k+1)T] may be calculated from x(kT) and the series of control inputs u[kT], u[kT+T_b], u[kT+$2T_b$] and u[kT+$3T_b$].

<u>Fast input, slow output rate system without ZOH</u>

The multirate operator which describes state transitions of this system over the period T must have four inputs and one output. The system will respond to an input at every base sample instant. The output signal at main interval instants will thus be determined by the system response to an input at the preceding intersample point within the main sample period timeframe. Hence, the input/output relations for this system are described by the following state equations:

$$x_e[(k+1)T] = A_{fs1}x_e[kT] + A_{fs2}x_e[(k+1)T] + B_{fs}u_e[kT] \tag{2.3.17}$$

$$y[(k+1)T] = C_{fs}x_e[(k+1)T] + D_{fs}u_e[(k+1)T] \tag{2.3.18}$$

where $A_{sf1} = A_{fs1}$, $A_{sf2} = A_{fs2}$ and B_{fs}, D_{fs} are defined,

$$B_{fs} = \begin{bmatrix} \Gamma(T_b) & 0 & 0 & 0 \\ 0 & \Gamma(T_b) & 0 & 0 \\ 0 & 0 & \Gamma(T_b) & 0 \\ 0 & 0 & 0 & \Gamma(T_b) \end{bmatrix} \quad D_{fs} = \begin{bmatrix} D & 0 & 0 & 0 \\ 0 & D & 0 & 0 \\ 0 & 0 & D & 0 \\ 0 & 0 & 0 & D \end{bmatrix} \tag{2.3.19}$$

The multirate output matrix of equation (2.3.18) is defined,

$$C_{fs} = \begin{bmatrix} 0 & 0 & C & 0 \end{bmatrix} \tag{2.3.20}$$

Rearranging equation (2.3.17) to combine state vectors $x_e[(k+1)T]$ gives,

$$x_e[(k+1)T] = [I_n - A_{fs2}]^{-1} A_{fs} x_e[kT] + [I_n - A_{fs2}]^{-1} B_{fs} u_e[kT] \tag{2.3.21}$$

Fast input, slow output rate system with ZOH

The principles of operation of this multirate system are identical to those of the fast input, slow output rate multirate system of Section 2.2, the only difference being the presence of ZOHs. Thus, the state equation for the slow input, fast output multirate system with ZOHs are:

$$x_e[(k+1)T] = A_{fsh1} x_e[kT] + A_{fsh2} x_e[(k+1)T] + B_{fsh} u_e[kT] \tag{2.3.22}$$

$$y[(k+1)T] = C_{fs} x_e[(k+1)T] + D_{fs} u_e[(k+1)T] \tag{2.3.23}$$

where A_{fsh1} and A_{fsh2} have the same form as A_{fs1}, A_{fs2} of equation (2.3.17) with $\Phi(Tb)$ replaced by $\Phi_h(Tb)$ and B_{fsh} has the same form of B_{fs} with $\Gamma(T_b)$ replaced by $\Gamma_h(T_b)$. C_{fs} is unaffected by the hold dynamics and thus given by equation (2.3.20). Equation (2.3.22)

rearranged gives,

$$x_e[(k+1)T]=[I_n-A_{fsh2}]^{-1}A_{fsh1}x_e[kT] + [I_n-A_{fsh2}]^{-1}B_{fsh}u_e[kT] \quad (2.3.24)$$

The equations of Sections 2.3.1 and 2.3.2 all define the T-periodic behaviour of simple multirate systems and thus codify the invariant nature of the system. Appropriately modified equations of this form can be combined to describe the behaviour of the MIMO multirate sampled system. This is addressed in the following section.

2.3.3 Multirate input, multirate output system with rational sample rate ratios.

The multirate operator which describes the action of this system must allow multiple sample rates for both inputs *and* outputs. One input/output sampling inter-relationship constraint applies for the development of this operator: only rates which can be expressed as integer multiples of the input base sample rate T_b are allowed for the output signals. The SISO system of Figure 1.3.4 falls into this category of multirate systems, i.e. category (2) of the multirate system types mentioned in the introduction of Section 2.3. It is different from the high dimensional model of category (3) where the output sample periods can take *any* value related by integer multiples of an output base sample period which is not necessarily the same as the input base sample period. It is in fact, a special form of the high dimensional description where the output sample rates are related by the same base sample period as the input sample rates. Hence the reduced dimensionality of the model.

This model uses the expanded system vectors, $x_e(kT)$, $u_e(kT)$ and $y_e(kT)$, to calculate all the necessary intersample parameter values. The

control vector $u_e(kT)$ and output vector $y_e(kT)$ are defined only for sample points at which they change. The state vector $x_e(kT)$ is in the maximally expanded form which defines the states at every base sample instant. This is necessary in order to accomodate the coupled nature of the multivariable system when forming the output equation.

As for the development of classical Kranc operators in Section 1.3.3, the equations for this system are derived by considering a SISO system with an input sample rate $1/T_m$ and output sample rate $1/T_p$. For this system, the sample parameters of (1.3.33) apply. Two cases are examined. The first considers the multirate operator for a system where the presence and duration of a ZOH can be decided. The second model assumes that a ZOH of duration T_b precedes the continuous system.

<u>System with/without ZOH of varying selectable duration</u>

Assume that the base rate dynamics (which defines the states of this system at the instants kT_b) are represented by the quadruple,

$$G(z_n) = Z[\,G_{(s)}\,]_{Tb} = \left[\begin{array}{c|c} \Phi & \Gamma \\ \hline C & D \end{array}\right] \qquad (2.3.25)$$

The state space Kranc operator for the MIMO multirate system of Figure 1.3.4 is given by the following non-minimal multirate quadruple:

$$Z[\,E^{p+}G(s)E^{m-}\,] = \left[\begin{array}{c|ccccc} \Phi^n & \Phi^{n-1}\Gamma & \Phi^{n-1-n/m} & \cdots & \Phi^{n-1-(m-1)n/m} \\ \hline C & D_{11} & D_{12} & \cdots & D_{1m} \\ C\Phi^{n/p} & D_{21} & D_{22} & \cdots & D_{2m} \\ \vdots & \vdots & \ddots & & \vdots \\ C\Phi^{(p-1)n/p} & D_{p1} & \cdots & & D_{pm} \end{array}\right] \qquad (2.3.26)$$

where,

$$D_{ij} = C\Psi\left[\frac{(i-1)n}{p} - \frac{(j-1)n}{m} - 1\right] B + \Omega_{ij} \tag{2.3.27}$$

$$\Psi(k) = \begin{cases} \Phi^k & \text{if } k > 0 \\ 0 & \text{otherwise} \end{cases} \tag{2.3.28}$$

$$\Omega_{ij} = \begin{cases} D & \text{if } \frac{(i-1)n}{p} - \frac{(j-1)n}{m} = 0 \\ 0 & \text{otherwise} \end{cases} \tag{2.3.29}$$

System with ZOH of duration T_b

Assume the base rate dynamics of the system preceded by a ZOH are given by the quadruple,

$$G_h(z_n) = Z[G_{ho}(s)G(s)] = \left[\begin{array}{c|c} \Phi_h & \Gamma_h \\ \hline C & D \end{array}\right] \tag{2.3.30}$$

$$G_{ho}(s) = \frac{1-\exp(sT/n)}{s}$$

The following multirate quadruple defines the Kranc operator:

$$Z[E^{p+}G_{ho}(s)G(s)E^{m-}]$$

$$= \left[\begin{array}{c|ccc} \Phi_h^n & \Phi_h^{n-1}X\Gamma & \Phi_h^{n-1-n/m}X\Gamma \ldots & \Phi_h^{n-1-(m-1)n/m}X\Gamma \\ \hline C & D_{11} & D_{12} & \ldots D_{1m} \\ C\Phi_h^{n/p} & D_{21} & D_{22} & \ldots D_{2m} \\ \vdots & \vdots & \ddots & \vdots \\ C\Phi_h^{(p-1)n/p} & D_{p1} & \ldots & D_{pm} \end{array}\right] \tag{2.3.31}$$

where,

$$X = \sum_{k=0}^{n/m\ -1} \Phi^k \tag{2.3.32}$$

$$D_{ij} = C\left[\sum_{k=0}^{n/m\ -1} \Psi\left[k + \frac{(i-1)n}{p} - \frac{(j-1)n}{m} - \frac{n}{m} \right] \right] B + \Omega_{ij} \qquad (2.3.33)$$

$$\Psi(k) = \begin{cases} \Phi^k & \text{if } k > 0 \\ 0 & \text{otherwise} \end{cases} \qquad (2.3.34)$$

$$\Omega_{ij} = \begin{cases} D & \text{if } 0 < \frac{(i-1)n}{p} - \frac{(j-1)n}{m} < \frac{n}{m} \\ 0 & \text{otherwise} \end{cases} \qquad (2.3.35)$$

The two state space Kranc operators differ in the ZOHs assumed. The first (defined by (2.3.26)) can be used for systems with or without a hold. The hold, if included, can be of any duration between T = 0 and t = T/m. The Kranc operator of (2.3.31) assumes a 'short' ZOH of period T_b. Since the ZOH dynamics have a significant effect on the sampled data system response the distinction between the two is of importance. (The function of the hold is to filter out unwanted harmonic frequencies from the sampled signal. It introduces phase lags and so adversly affects the stability of the system.)

The Kranc operators only describe the states at the instants defined by a particular combination of input and output sample rates. Thus, it is necessary to translate the system to the lowest sample rate ($1/T_b$) to ensure correct convolutions. This is performed by the following expansion,

$$G^T(z^n) = \left[\begin{array}{ccc|c} 0 & \ldots. & 0 \ \Phi & \Gamma \\ I & \ldots. & 0 \ 0 & 0 \\ & \ddots & \vdots & 0 \\ 0 & \ldots. & 0 \ 0 & 0 \\ \hline 0 & \ldots. & 0 \ C & D \end{array}\right] \qquad (2.3.36)$$

which is, in effect, a slow rate to fast rate transformation. Another useful state space operator is the matrix representation of the skip

sampling transform of Chapter 1 defined:

$$G^T(z) = \left[\begin{array}{c|c} \Phi^n & \Phi^{n-1}\Gamma \\ \hline C & D \end{array}\right] \qquad (2.3.37)$$

2.4 MIMO MULTIRATE SYSTEM MODELLING

Thus far, the multirate state space operators described have all been applied to SISO systems only. This section derives a state space model for the general MIMO multirate system of Figure 2.2.1. To clarify the derivation, equations for the 2 input, 1 output example system shown in Figure 2.3.1 are described first.

2.4.1 Two input/ single output system equations

For this system the input sample rates are $\{1/T_{mi}\}=\{m/T\}$ while the single output sample rate is $1/T_p = p/T$. Furthermore, all rates are integer multiples of $1/T_b = n_0/T$. Appropriate time-invariant equations can be determined by considering the effect of the series of inputs (generated by the two inputs) over the main sample interval at each base sample interval. If $T_{mi} > T_b$, the ith input signal is updated only every $\ell_{mi} = (n_0/mi)$ base sample periods. Thus, for $(\ell_{mi}-1)$ base sample periods subsequent to an input update at instant kT, system behaviour is determined by the unforced or natural response to the 'initial conditions' generated by the system response to the kT input update.

Consider the MIMO system quadruplet {A,B,C,D} of Figure 2.3.1 with input sample rates 3/T, 2/T (m_1=3, m_2=2), and an output sample rate 2/T (p=2). The fastest common sample rate is 6/T (n_0=6). The expanded state, control and output vectors for this system are:

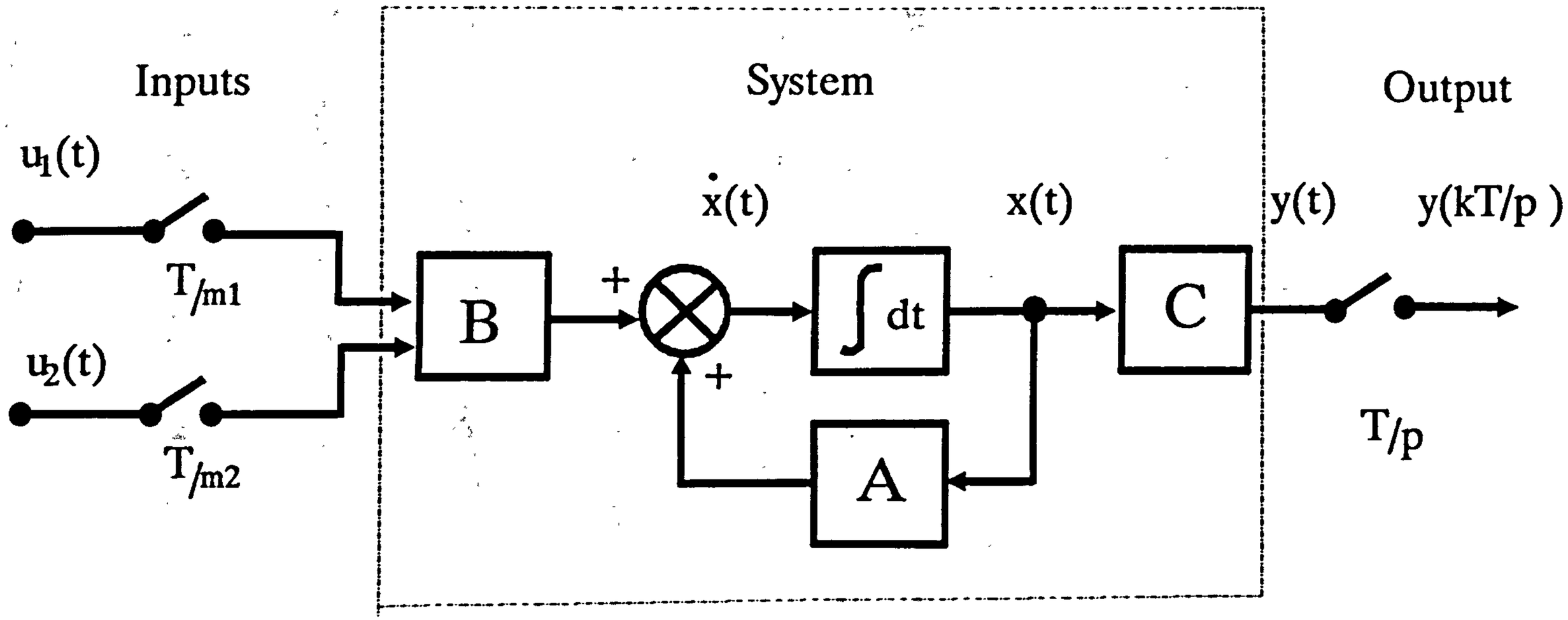

Figure 2.3.1 State space multirate system with rational input/output sample rates

$$x_e(kT) = \begin{bmatrix} x[kT+T_b] \\ x[kT+2T_b] \\ \vdots \\ x[kT+5T_b] \\ x[(k+1)T] \end{bmatrix} \tag{2.4.1}$$

$$u_e(kT) = \begin{bmatrix} u_1[kT] \\ u_1[kT+T_{m1}] \\ u_1[kT+2T_{m1}] \\ u_2[kT] \\ u_1[kT+T_{m2}] \end{bmatrix} \tag{2.4.2}$$

$$y_e(kT) = \begin{bmatrix} y_1[kT] \\ y_1[kT+T_p] \end{bmatrix} \tag{2.4.3}$$

The state space model which describes system performance over the period T must have three inputs and two outputs. Thus, using the base rate dynamics of equation (2.3.1) the multirate state equations for the system of Figure 2.3.1 are given by:

$$x_e[(k+1)T] = A_{m1}x_e[kT] + A_{m2}x_e[(k+1)T] + B_m u_{1e}[kT] \tag{2.4.4}$$

$$y_{1e}[(k+1)T] = C_{m1}x_e[kT] + C_{m2}x_e[(k+1)T] + D_m u_{1e}[(k+1)T] \tag{2.4.5}$$

Matrices A_{m1}, A_{m2} and B_m are defined,

$$A_{m1} = M_1\Phi_{Tb}[1,0] \qquad A_{m2} = M_2\Phi_{Tb}[1,0] \tag{2.4.6}$$

$$B_m = \begin{bmatrix} \Gamma_{1,Tb}[1,0] & 0 & 0 & \Gamma_{2,Tb}[1,0] & 0 \\ \Gamma_{1,Tb}[1,0] & 0 & 0 & \Gamma_{2,Tb}[1,0] & 0 \\ 0 & \Gamma_{1,Tb}[1,0] & 0 & \Gamma_{2,Tb}[1,0] & 0 \\ 0 & \Gamma_{1,Tb}[1,0] & 0 & 0 & \Gamma_{2,Tb}[1,0] \\ 0 & 0 & \Gamma_{1,Tb}[1,0] & 0 & \Gamma_{2,Tb}[1,0] \\ 0 & 0 & \Gamma_{1,Tb}[1,0] & 0 & \Gamma_{2,Tb}[1,0] \end{bmatrix} \tag{2.4.7}$$

$\Phi[1,0]$, $\Gamma[1,0]$ are defined in Appendix A. Matrices M_1, M_2 are defined in (2.2.9) and $\Gamma_{i,Tb}[1,0]$ denotes $\Gamma_{Tb}[1,0]$ formed using the ith column of the original continuous time control matrix. Similarly,

$$C_{m1}=M_1C \qquad C_{m2}=M_2C \tag{2.4.8}$$

$$D_m = \begin{bmatrix} D & 0 & 0 & 0 & 0 & 0 \\ 0 & D & 0 & 0 & 0 & 0 \\ 0 & 0 & D & 0 & 0 & 0 \\ 0 & 0 & 0 & D & 0 & 0 \\ 0 & 0 & 0 & 0 & D & 0 \\ 0 & 0 & 0 & 0 & 0 & D \end{bmatrix} \tag{2.4.9}$$

Rearranging equations (2.4.4) and (2.4.5) to combine similar state vectors gives,

$$x_e[(k+1)T] = \Phi_{MR2}x_e[kT] + \Gamma_{MR2}u_e[kT] \tag{2.4.10}$$

$$y_e[(k+1)T] = C_{MR2}x_e[kT] + D_{MR2}u_e[kT] \tag{2.4.11}$$

where,

$$\Phi_{MR2} = [I_n-A_{m2}]^{-1}A_{m1} \qquad \Gamma_{MR2} = [I_n-A_{m2}]^{-1}B_m \tag{2.4.12}$$

$$C_{MR2} = [I_n-C_{m2}]^{-1}C_{m1} \qquad D_{MR2}[I_n-C_{m2}]^{-1}D_m \tag{2.4.13}$$

2.4.2 The General MIMO Multirate System Model

The equations for any MIMO multirate system with rational rates are now defined. State equations (2.4.10), (2.4.11) of the above example effectively contain two subsystems of the form described in Section (2.3.1) and (2.3.2). The combined response of the two subsystems

defines the overall system response at every base sample instant within the interval [kT, (k+1)T]. For the general MIMO multirate system model, m such subsystems are appropriately modified and combined to produce the complete time invariant state equations. Recall that the input and output vectors are only defined at those instants indicated by their respective sample rates. Hence, the control and output matrices of the general MIMO multirate model must reflect this. With this in mind, the general state equations are defined:

$$x_e[(k+1)T]=[0\ 0..\hat{\Phi}_{Tb}]x_e(kT)+[\hat{\Gamma}_{1,1}..\ \hat{\Gamma}_{1,n1},..,\hat{\Gamma}_{m,1}..\ \hat{\Gamma}_{m,nm}]u_e(kT) \quad (2.4.14)$$

A comparison of equations (2.4.10) and (2.4.14) defines the (nn_0) x (nn_0) transition matrix Φ_{MR2} as:

$$\Phi_{MR2} = [0\ 0..\hat{\Phi}_{Tb}] \quad (2.4.15)$$

Matrix Φ_{MR2} consists of $(n_0\text{-}1)$ zero matrices of dimension $(nn_0 \times n)$. Matrix $\hat{\Phi}_{Tb}$ is defined,

$$\hat{\Phi}_{Tb} = [\Phi_{Tb}[1,0]^T\ \ \Phi_{Tb}[2,0]^T\ \ldots\ \Phi_{Tb}[n_0,0]^T]^T \quad (2.4.16)$$

The formulation of the control matrix in equation (2.4.14) is more involved. During the time interval [kT,(k+1)T] the inputs are updated at a maximum of m different rates. The contribution of each input to a particular state, $x_i[t]$ at any instant t, $kT < t \leq (k+1)T$, must consequently be calculated from different sample points. This leads to a (1 x m) block control matrix,

$$\Gamma_{MR2} = [\tilde{\Gamma}_1\ \tilde{\Gamma}_2\ ..\ \tilde{\Gamma}_m] \quad (2.4.17)$$

whose block matrices $\tilde{\Gamma}_k$ are defined as:

$$\tilde{\Gamma}_k = \{\hat{\Gamma}_{k,i}\} \qquad i=1,..,n_k \tag{2.4.18}$$

Subscript k of expression (2.4.18) is used to indicate that *all* Γ terms are with respect to the kth column of the original system control matrix, Γ. Subscript i denotes the column index of the multirate control matrix. Each $(n_0 \times 1)$ block matrix element, $\hat{\Gamma}_{k,i}$, is defined by considering whether the kth input is updated or not at each base sample instant. This gives the description,

$$\hat{\Gamma}_{k,i}(j) = \begin{cases} 0 & j < (i-1)\ell_k \\ \Gamma[j,(i-1)\ell_k] & (i-1)\ell_k < j < i\ell_k \\ \Phi[j,i\ell_k]\Gamma[i\ell_k,(i+1)\ell_k] & j > i\ell_k \end{cases} \tag{2.4.19}$$

The output equation for the general multirate system is similarly defined; Equation (2.4.11) can also be expressed as,

$$y_e(kT)=[\Psi[n_1,1,0],..,\Psi[n_m,1,0]]x_e(kT)+[\tilde{D}_1\ \tilde{D}_2\ ..\ \tilde{D}_m]u_e(kT) \tag{2.4.20}$$

$$\Psi[k,j,i] = \begin{bmatrix} C_{Tb}[1,j-1] \\ C_{Tb}[2,j]\Phi_{Tb}[j,i] \\ C_{Tb}[3,j]\Phi_{Tb}[j+1,i] \\ \vdots \\ C_{Tb}[k,j]\Phi_{Tb}[j+k+2,i] \end{bmatrix} \qquad k > j > i \tag{2.4.21}$$

$\tilde{D}_k$ is the $(n_k \times n_k)$ matrix,

$$\tilde{D}_k = \{\tilde{D}_{k,i}\} \qquad i=1,..,n_k \tag{2.4.22}$$

whose ith $(n_k x 1)$ column vector is defined:

$$\tilde{D}_{k,i} = I_{n1,i}\ \Psi[n_k+1,i,i]\ \Gamma_{Tb}[i,i-1] \tag{2.4.23}$$

The transition equations of all the multirate systems considered so far are derived by considering how the *expanded* state vector $x_e[(k+1)T]$ may be calculated from $x_e(kT)$ and the series of control inputs over the interval [kT (k+1)T]. These equations determine the state at every base sample instant. For some intersample instants, a change in neither the inputs or outputs occurs. At these instants, the multirate system matrices have terms which represent the system 'free' or natural response to the last input/output transition. Thus, these matrices necessarily include many terms which serve no input/output characterisation purpose.

This approach to multirate system modelling, as highlighted by Araki et al (1985), leads to *non-minimal* descriptions. The non-minimality feature is clearly evident from the multirate system transition matrix of equation (2.4.15), which defines the multirate system as having $(n-1)n_0$ poles at the origin and n non-zero poles. In reality, only the n non zero poles accurately characterise system input, output behaviour. The rest result from the 'over-sampling' necessary to codify the invariant periodic transitions of the system.

In general, the transition equations of a system are required to represent dynamical information in a form amenable for system design and analysis. The state space formulations of Sections 2.3 and 2.4 accurately model time domain behaviour and are thus useful for analysis using time response data. The models also provide the necessary intersample information lacking in the classical operators of Chapter 1. However, due to the non-minimal nature of the state space descriptions, the state space models are not suitable for the application of many established state space design techniques. The following section derives the more useful minimal descriptions for a class of multirate systems.

2.5 MINIMAL STATE SPACE MODELS

Minimal state space equations can be derived for MIMO multirate systems which fall into two classes of periodicity. These are the systems of category (1) mentioned in the main introduction of this section. The behaviour of category (1) systems is characterised by input (output) signals which all undergo an integer number of transitions during a single output (input) transition. These systems can either have *multiple input* rates and a *fixed output* rate (MIFO) or a *fixed input* rate and *multiple output* rates (FIMO). The design techniques outlined in this thesis all apply to the MIFO multirate system. The typical input, output transitions of a MIFO system are illustrated in Figure 2.5.1.

Transistion equations for a SISO, MIFO system are derived first by considering how state vector x[(k+1)T] may be calculated from x(kT) and the multiple control signals provided by a single input u_1 over interval [kT (k+1)T]. For this system, the input signal is sampled at intervals $T_1 = T/n_1$ whilst the output is monitored every main sample instant. Thus, the transition equation which determines the main instant state vector is given by,

$$x[(k+1)T] = \Phi_{Tb}[t,t_0]x[t_0] + \Gamma_{Tb}[t,t_0]u_1[t_0] \qquad (2.5.1)$$

where $t = (k+1)T$, $t_0 = (k+1)T-T_b$ and Γ, Φ relate to the SISO subsystem only. The periodicity condition of (2.2.4) combined with the sampling relation $T = n_1T_b$ allows this to be written as,

$$x[(k+1)T] = \Phi[n_1T_b,(n_1-1)T_b]x[t_0] + \Gamma[n_1T_b,(n_1-1)T_b]u_1[t_0] \qquad (2.5.2)$$

If $x[(k+1)T - T_b]$ is then written in terms of $x[(k+1)T - 2T_b]$ and $u_1[(k+1) - 2T_b]$ and the recursive procedure continued until x[kT] is reached, the following system transition equation for the periodic

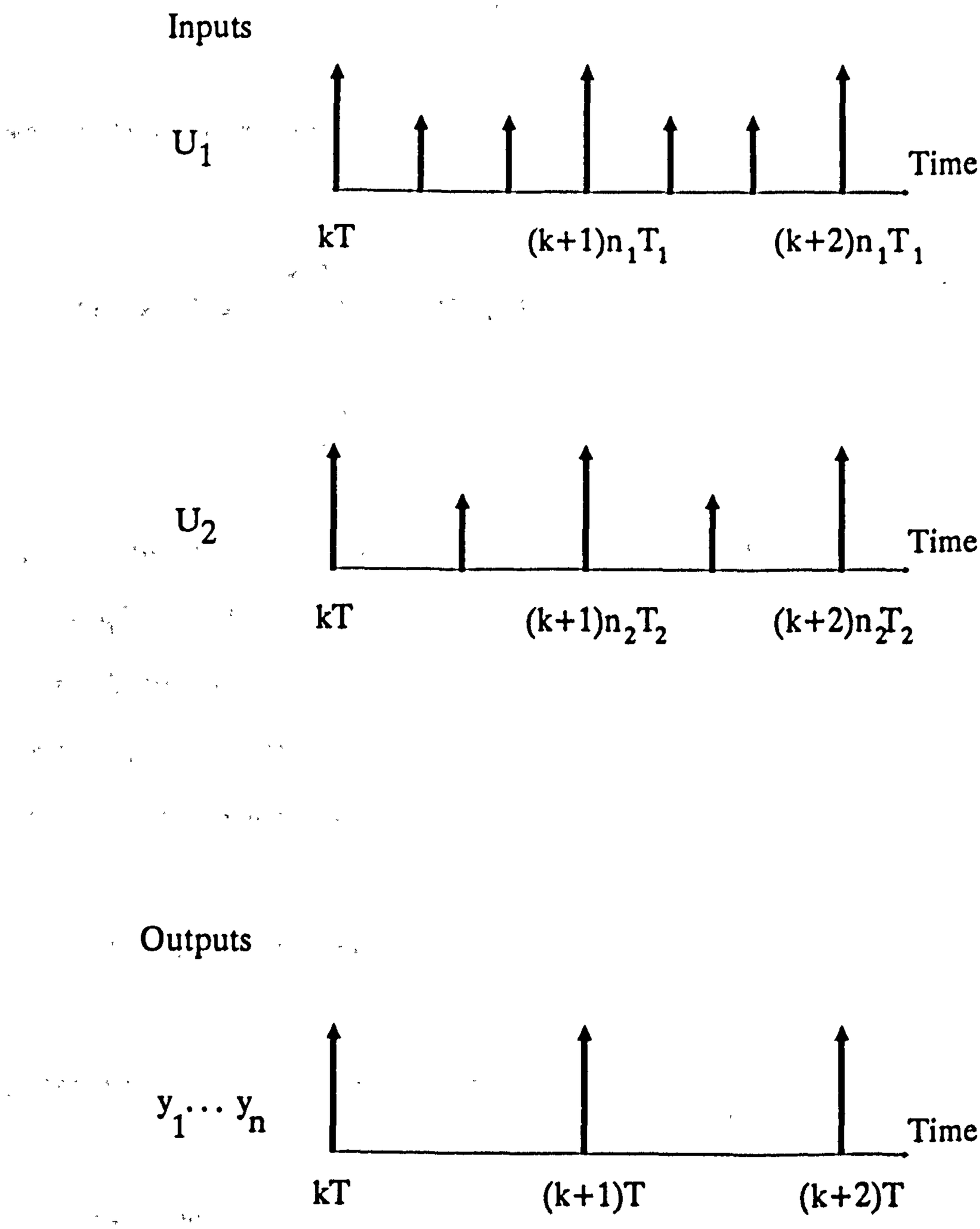

Figure 2.5.1 Input, output transitions of a MIFO sampled system

interval T can be easily arrived at,

$$x[(k+1)T] = \Phi_{Tb}[n_1,0]x(kT) + \sum_{i=0}^{n_1-1} \Phi_{Tb}[n_1,(i+1)\ell_1]\Gamma_{Tb}[(i+1)\ell_1,i\ell_1]u_1(kT+iT_b) \quad (2.5.3)$$

where $\ell_1 = n_0/n_1$ and,

$$\Phi_{Tb}[k,j] = \begin{cases} \prod_{i=j}^{k-1} \Phi[(i+1)T_b,iT_b] & k>j \\ I_n & k=j \\ 0 & k<j \end{cases} \quad (2.5.4)$$

I_n is the (n x n) identity matrix. It must be noted that the definition of $\Phi_{Tb}[k,j]$ for k<j is not strictly true since the discrete state transitions can occur both forwards and backwards in time. It will however, apply to state equations for $kT < t \leq (k+1)T$. Equation (2.5.3) can also be expressed in matrix form,

$$x[(k+1)T] = \Phi_{Tb}[n_0,0]x(kT) + \bar{\Gamma}_{Tb,1}(n_0)\, u_{1e}(kT) \quad (2.5.5)$$

where $u_{1e}(kT)$ is in the expanded form of (2.2.6) with m=1 and,

$$\bar{\Gamma}_{Tb,1}(n_0) = [\Phi_{Tb}[n_0,\ell_1]\Gamma_{Tb}[\ell_1,0],\ \Phi_{Tb}[n_0,2\ell_1]\Gamma_{Tb}[2\ell_1,\ell_1], \ldots,\Gamma_{Tb}[n_0,(n_1-1)\ell_1]] \quad (2.5.6)$$

Here $\bar{\Gamma}_{Tb,i}(n_0)$ denotes Γ_{Tb} formed using the ith column of the original system control matrix. For this single input system i=1. Since the state and output vectors are only defined at the main interval instants, the output equation is given by ,

$$y(kT) = C_{Tb}[n_0,0]x(kT) \quad (2.5.7)$$

To develop state equations for systems with multiple inputs of varying sample rates, equations of the form (2.5.5) are combined to produce the full description,

$$x[(k+1)T] = \Phi_{MR1}x(kT) + \Gamma_{MR1}u_e(kT) \qquad (2.5.8)$$

where,

$$\Phi_{MR1} = \Phi_{Tb}[n_0,0] \qquad \Gamma_{MR1} = [\bar{\Gamma}_{Tb,1}(n_0) \;..\; \bar{\Gamma}_{Tb,m}(n_0)] \qquad (2.5.9)$$

The multirate system matrices of equation (2.5.8) use the MIMO state and control matrices. Vector $u_e(kT)$ is the full expanded control vector of the MIMO system. Equation (2.5.9) shows that the multirate control matrix is in a block partioned form corresponding to a maximum of m different input update rates during the interval [kT, (k+1)T]).

2.6 STATE SPACE ANALYSIS OF THE MULTIRATE HELICOPTER SYSTEM

The helicopter system of Figure 2.6.1 (where the transmission of all paths affected by the multirate sampling is in terms of advance and delay operations) is examined using the state space Kranc operators of Section 2.3. A block diagram reduction technique is applied first to simplify the multirate system analysis. The signal flow diagram of the decomposed helicopter system of Figure 2.6.1 can be manipulated using standard reduction formulae to give the configuration of Figure 2.6.2.

Using the signal flow diagram of Figure 2.6.2, the following stages develop the full closed loop multirate system description in state space using the definitions of Section 2.3.3. Define $K_1(z)$ and $K_2(z)$ as follows,

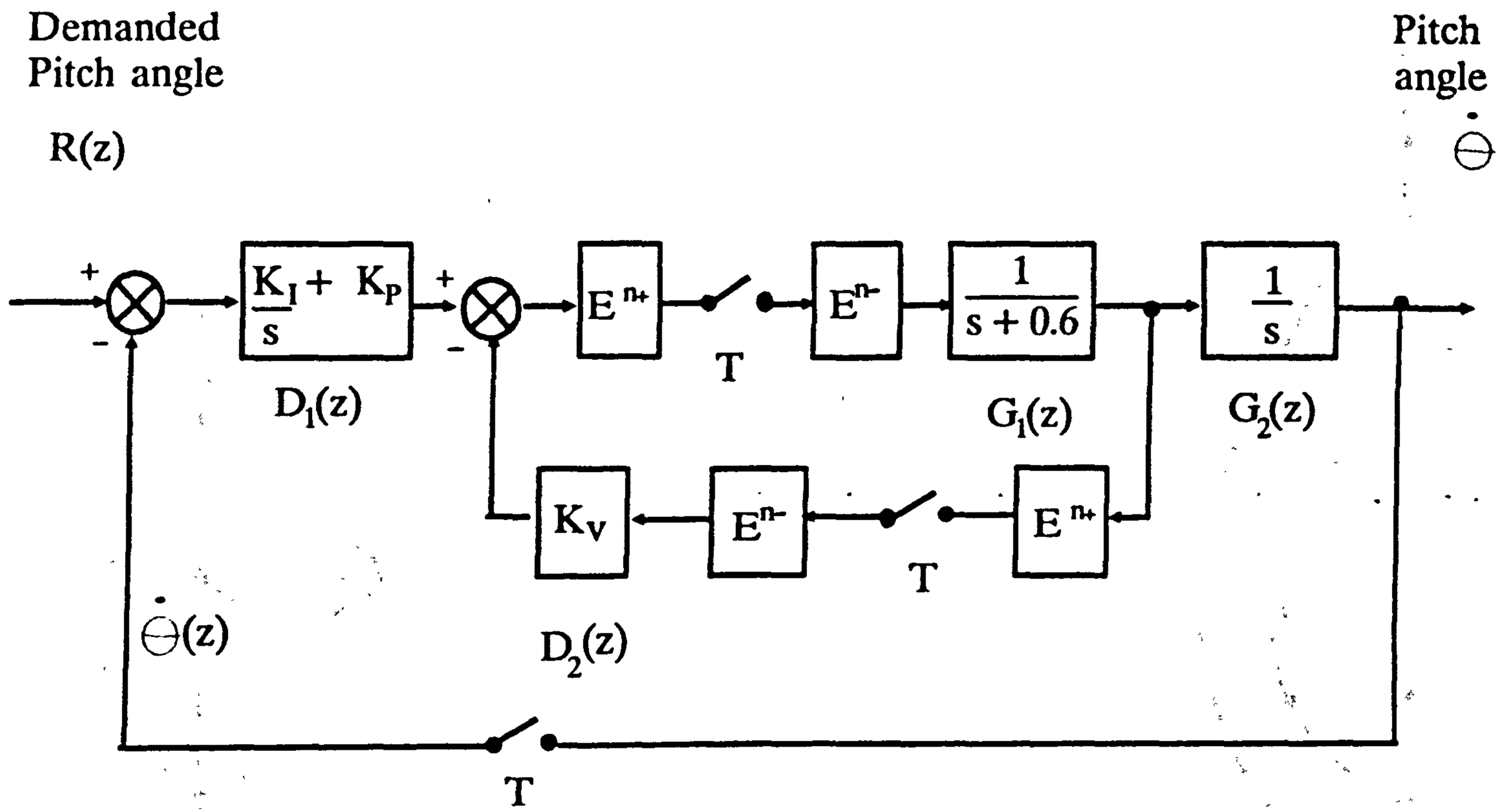

Figure 2.6.1 Switch decomposed multirate helicopter system

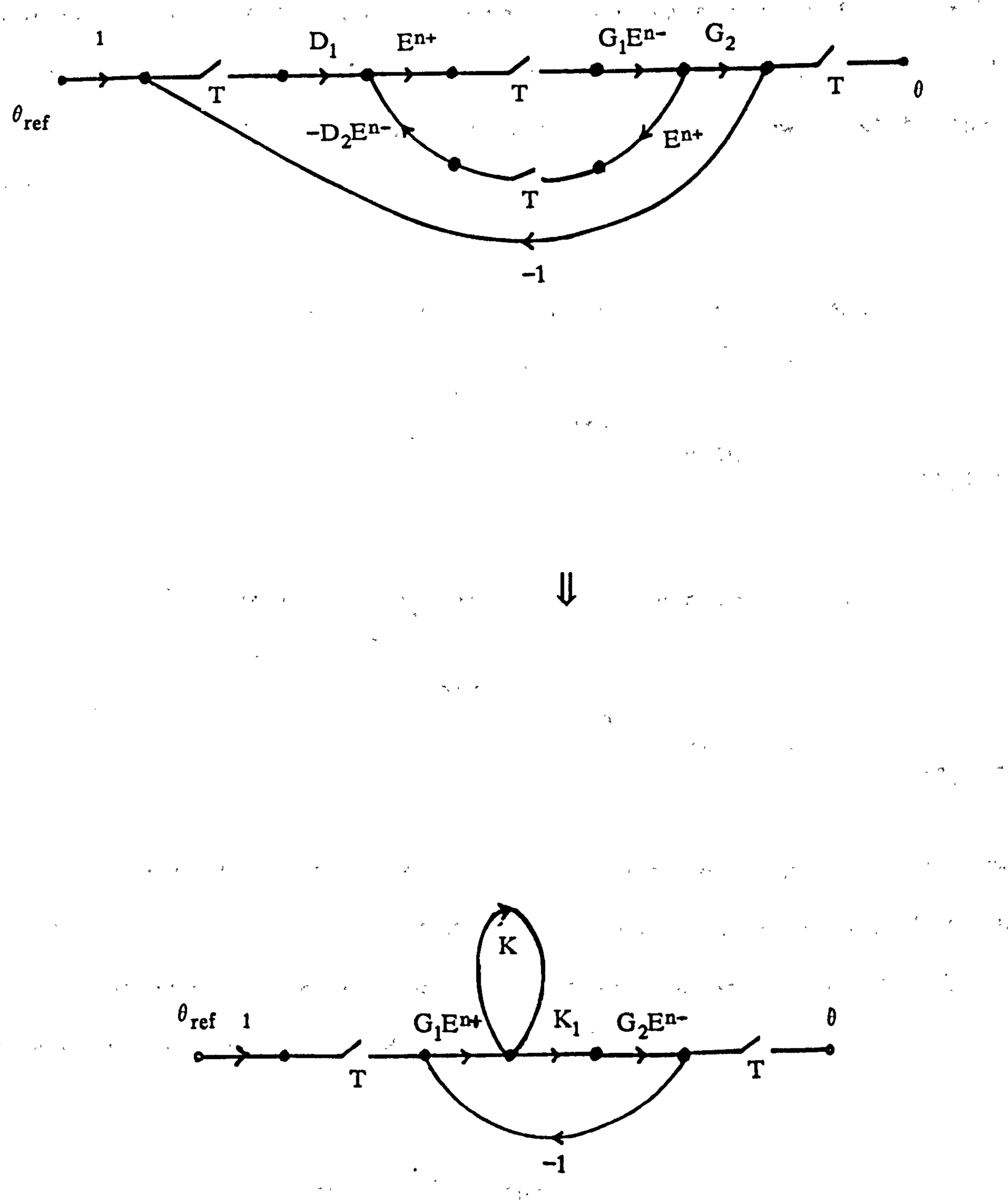

Figure 2.6.2 Signal flow diagram of switch decomposed multirate helicopter system

$$K_1(z) = (E^{p+}G_{ho}G_1E^{p-})^T$$

$$K_2(z) = K_1(z)[1 + (E^{p+}G_{ho}G_1E^{p-})^T(E^{m+}G_{ho}D_2E^{m-})^T(z)]^{-1} \qquad (2.6.1)$$

Using equation (2.3.31) and assuming a main sample period of T = 0.1 secs and a ZOH of period T/n (since both G_1 and D_2 are preceded by the fast sampler), $K_1(z)$ and $K_2(z)$ are given by the following state space quadruplets,

$$K_{1(z)} = \left[\begin{array}{c|cccc} (0.9851)^4 & 0.0237 & 0.0241 & 0.0244 & 0.0248 \\ \hline 1.0000 & 0 & 0 & 0 & 0 \\ 0.9851 & 0.0248 & 0 & 0 & 0 \\ 0.9705 & 0.0244 & 0.0248 & 0 & 0 \\ 0.9560 & 0.0241 & 0.0244 & 0.0248 & 0 \end{array}\right] \qquad (2.6.2)$$

$$K_{2(z)} = \left[\begin{array}{c|cccc} 0.8504 & 0.0022 & 0.0229 & 0.0238 & 0.0248 \\ \hline 1.0000 & 0 & 0 & 0 & 0 \\ 0.9603 & 0.0248 & 0 & 0 & 0 \\ 0.9222 & 0.0238 & 0.0248 & 0 & 0 \\ 0.8856 & 0.0229 & 0.0238 & 0.0248 & 0 \end{array}\right] \qquad (2.6.3)$$

K_2 is the transfer function of the inner rate loop running four times faster than the (outer) attitude loop, hence the 4 input, 4 output description over the sample period T. This can be convolved with the advanced error signals provided by $(E^{m+}D_1)^T$ where,

$$(E^{m+}G_{ho}D_1) = \left[\begin{array}{c|c} 1.0000 & 1.0000 \\ \hline 0.0100 & 1.0000 \\ 0.0100 & 1.00025 \\ 0.0100 & 1.00050 \\ 0.0100 & 1.00075 \end{array}\right] \qquad (2.6.4)$$

to give,

$$K_3 = K_2*(E^{m+}G_{ho}D_1) = \left[\begin{array}{cc|c} 0.8504 & 0.0009 & 0.0935 \\ 0 & 1.0000 & 1.0000 \\ \hline 1.0000 & 0 & 0 \\ 0.9603 & 0.0002 & 0.0248 \\ 0.9222 & 0.0005 & 0.0487 \\ 0.8856 & 0.0007 & 0.0715 \end{array}\right] \qquad (2.6.5)$$

where * denotes convolution. The feedforward path transmission is obtained by convolving K_3 with $(G_{ho}G_2E^{P-})^T$ as follows,

$$(G_{ho}G_2E^{P-})^T = \left[\begin{array}{cc|c} 1.0000 & 0 & 1.0000 \\ 1.0000 & 0 & 0 \\ \hline 0.1000 & 0 & 0 \\ 0.0975 & 0.0025 & 0 \\ 0.0950 & 0.0050 & 0 \\ 0.0925 & 0.0075 & 0 \end{array}\right] \qquad (2.6.6)$$

$$K_4 = K_3*(G_{ho}G_2E^{P-})^T$$

$$= \left[\begin{array}{cc|cccc} 1.0000 & 1.0000 & 0.1000 & 0.0975 & 0.0950 & 0.0925 \\ 0 & 1.0000 & 0 & 0.0025 & 0.0050 & 0.0075 \\ \hline 1.0000 & 0 & 0 & 0 & 0 & 0 \end{array}\right] \qquad (2.6.7)$$

Forming the feedback loop using K_4 gives the following closed loop multirate system quadruplet,

$$K_{5(z)} = \left[\begin{array}{c|cccc} 0.8504 & 0.0022 & 0.0229 & 0.0238 & 0.0248 \\ \hline 1.0000 & 0 & 0 & 0 & 0 \\ 0.9603 & 0.0248 & 0 & 0 & 0 \\ 0.9222 & 0.0238 & 0.0248 & 0 & 0 \\ 0.8856 & 0.0229 & 0.0238 & 0.0248 & 0 \end{array}\right] \qquad (2.6.8)$$

The state space quadruplet of equation (2.6.8) has four inputs and four outputs, indicating that *all* intersample input/output transitions are contained within the closed loop description.

2.7 MULTIRATE SYSTEM DESIGN USING MATCHING TECHNIQUE

A common requirement in many control fields is the translation of continuous designs to the discrete plane to enable digital implementation of established control laws. This is especially true of digital flight control applications which traditionally rely on generic analogue control schemes that have passed rigorous certification and validation procedures. Many digital Automatic Flight Control systems (AFCS) are, as a result, based on the simulation of analogue compensators with fast discrete components (Tischler, 1989) on the assumption that a fast enough discrete system will accurately represent its continuous counterpart. In practice, a sample frequency approximately 10 times the highest frequency component in the continuous system is recommended. The discrete controllers are therefore not designed directly in the dicrete plane, but *mapped* from the continuous plane to the discrete plane. In this way, the re-certification and validation requirements are minimised. A serious drawback of this approach is that a much higher sample rate than is strictly necessary may be imposed on the digital AFCS to match the time domain performance of its analogue equivalent. This has many detrimental effects on the overall AFCS design. The high frequency components impose greater bandwidth requirements on notch filters, present a much more difficult noise attenuation task and most importantly, severely degrade an already critical phase margin. The fast computation facilities offered by the digital computer have, thus, created many problems for the design of digital AFCS, which have a primary task of simulating their continuous counterpart.

Many s-plane to z-plane mapping techniques are available for the design of single rate discrete systems from an existing continuous design (Houpis, 1985; Katz, 1981; Rattan, 1984; Whitbeck and Hofmann, 1978). These include established methods which use Z transforms, Tustin

transforms, pole/zero matching, etc. However, these techniques are only useful in cases where the entire *closed loop* system can be discretised. In general, the *structure* of the continuous system is lost in the translation to the discrete plane. The problems arise from the fact that a closed loop discrete system formed from the combination of independently discretised components does not give the same response as a discrete system obtained by discretising the *entire* closed loop description. (In general, the former yields a degraded response compared to the response of the latter.) Thus, theoretically, an existing continuous design can, by mapping the closed loop system from the s-plane to z-plane, produce a closed loop discrete system with equivalent performance. However, this generally does not yield a digital system with the same independent components as the continuous system, (i.e. a phase advance filter in the continuous design may not translate as a phase advance filter in the digital system). AFCS typically comprise a large number of independent filters, each performing a specific control task and *fixed* in location within the overall system. Application of established mapping techniques for the derivation of digital AFCS which *exactly* match the performance of its analogue counterpart and which are practically useful is at best complex but more realistically impossible.

Methods which use the discrete equivalent of the desired closed loop continuous system as the design criteria can be used to produce suitable discrete systems. Ragazzini and Franklin (1958) produced the earliest discrete system examples using this type of design procedure. Though this technique may produce a closed loop discrete system which matches the performance of its continuous counterpart it does not always lend itself to physical realisability and often requires laborious manipulations. The latter problem is encountered when isolating independent discrete compensator and plant dynamics from the overall closed loop system description. The physical limitations arise from

large order or non-causal compensator dynamics. Thus the early design methods, though sound in their approach, do suffer from inherent computational and practical drawbacks which limit their application.

The problems presented by these methods can be circumvented by a discrete matching design approach which is based on a *fixed* compensator structure. The objective of the model matching method is to obtain a discrete system whose control, state and output trajectories correspond *exactly* with those of a desired continuous closed loop system. The method ensures that the plant and controller dynamics are kept strictly isolated from each other during the design procedure, thus obviating the need for any manipulation to extract independent controller components subsequent to the design process.

Single rate discrete systems can be designed using this method, but their limited design freedom dictates an *approximation* of the desired closed loop response. The resulting approximated design does not necessarily yield a good correspondence with the continuous system responses. However, multirate sampled systems can give an *exact* match in desired system response. This is demonstrated below with the design of compensators for the pitch rate control of an aircraft.

2.7.1 Pitch Rate Control Design Example

The aircraft to be controlled is a remotely piloted vehicle (rpv), called the Machan, developed for research purposes by GEC Avionics, Rochester. The flight dynamics of this aircraft, as determined from wind tunnel tests and other identification means, are well documented (Aslin, 1985) and will not be detailed in full here.

Pitch attitude control by elevator (with the engine thrust being maintained constantly zero) is considered. The longitudinal pitch motions of an aircraft are characterised by the pitch rate (q) to elevator deflection angle (η) transfer function. The pitch dynamics

comprise two modes: the *short period pitching oscillation* and the *phugoid oscillation*. The open loop pitch dynamics of the Machan aircraft for a stick-fixed operation at an airspeed of $33ms^{-1}$ are given by,

$$\frac{(q-q_a)}{\eta} = \frac{-13.58s(s+3.0729)(s+0.079)}{(s+1.18104\pm j3.4698)(s+0.0066\pm j0.6618)} \qquad (2.7.1)$$

where, q_a is the pitch rate signal demanded by the autopilot. The short period and phugoid modes, as characterised by the complex pole pairs, are determined to have the following frequency and damping:

short period: frequency ω_n=3.52
damping ζ = 0.44

s=phugoid: frequncy ω_n=0.16
damping ζ = 0.74

The zero at the origin in (2.7.1) differentiates pitch attitude to derive pitch rate. The pitch rate autostabiliser would typically comprise the P+I control configuration of Figure 2.7.1. Note from this diagram that a ratio 1:10 is maintained between the proportional and integral gains, K_p:K_i. This is an acceptable assumption used to simplify the design procedure. Figure 2.7.2 shows the root locus plot of the compensated system which is used to determine appropriate gains for the closed loop pitch rate loop. This plot shows that a choice of gains K_i = 2.5, K_p = 0.25 will give an adequately damped response for the short period and phugoid modes. The unit step response of the pitch rate loop with this choice of compensator gains is shown in Figure 2.7.3.

The effect of both the short period and phugoid oscillations is clearly visible in this closed loop pitch system response. The short

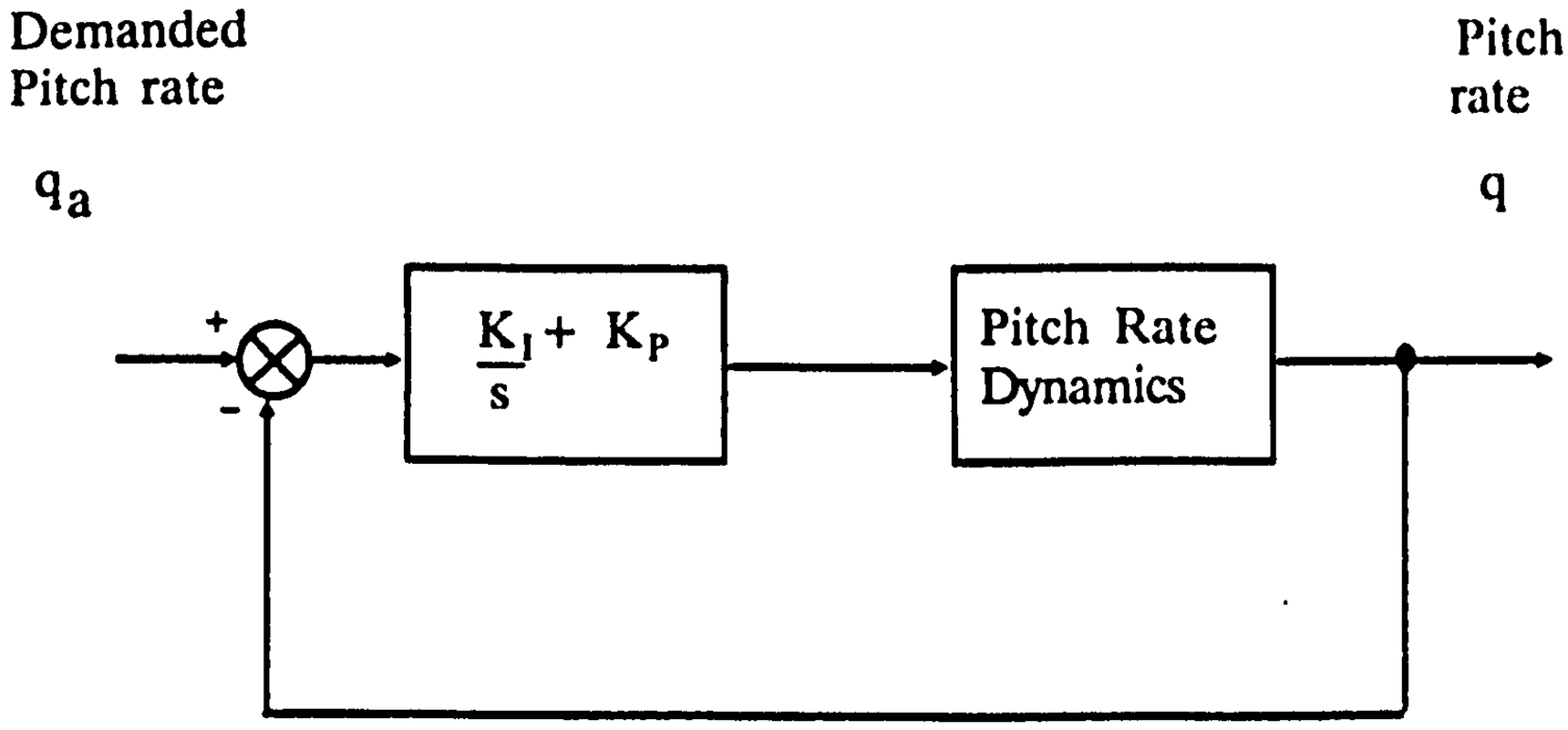

Figure 2.7.1 P+I compensated pitch rate loop

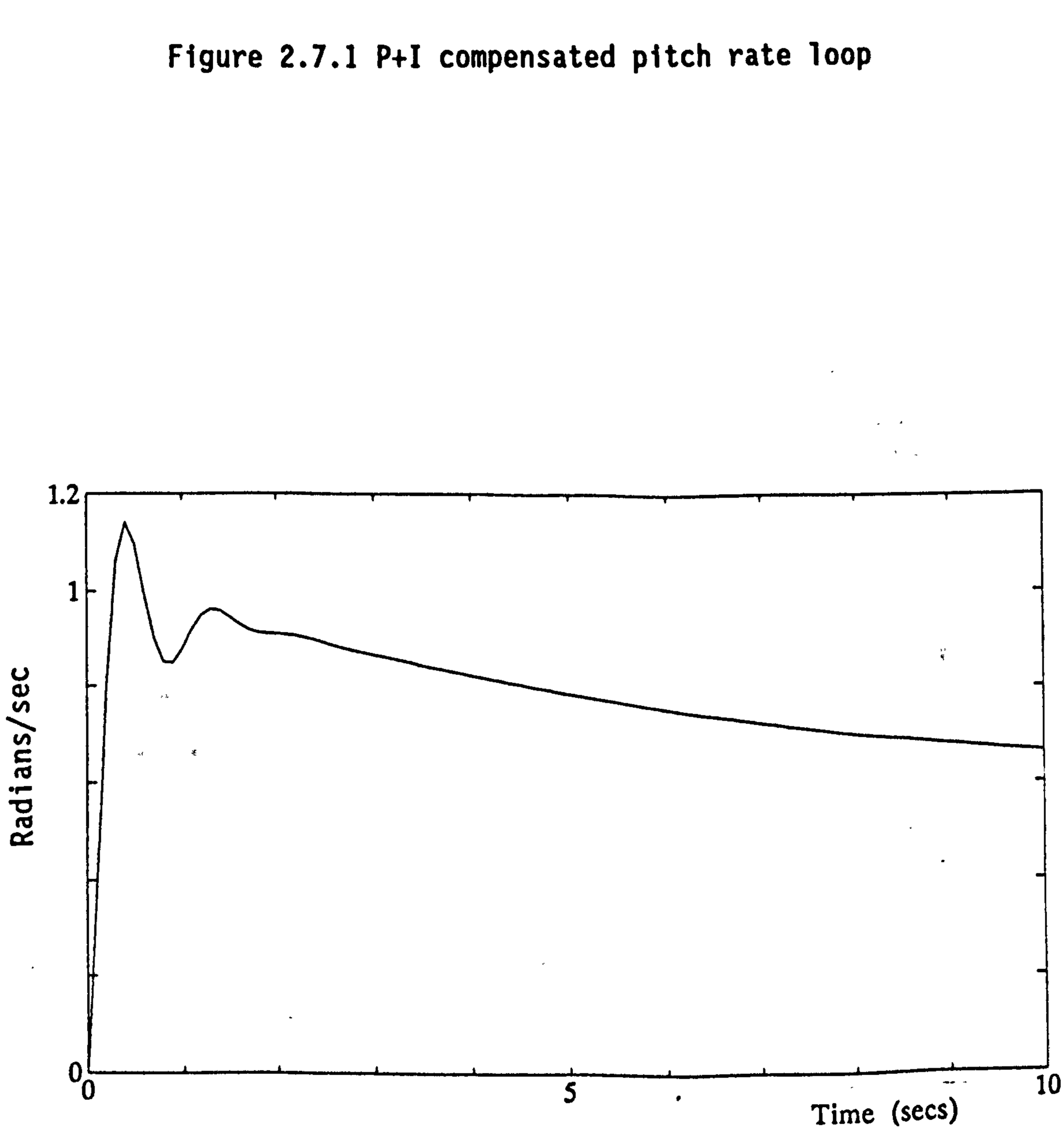

Figure 2.7.3 Unit step response of compensated pitch rate loop with compensator gains K_I=2.5, K_p=0.25

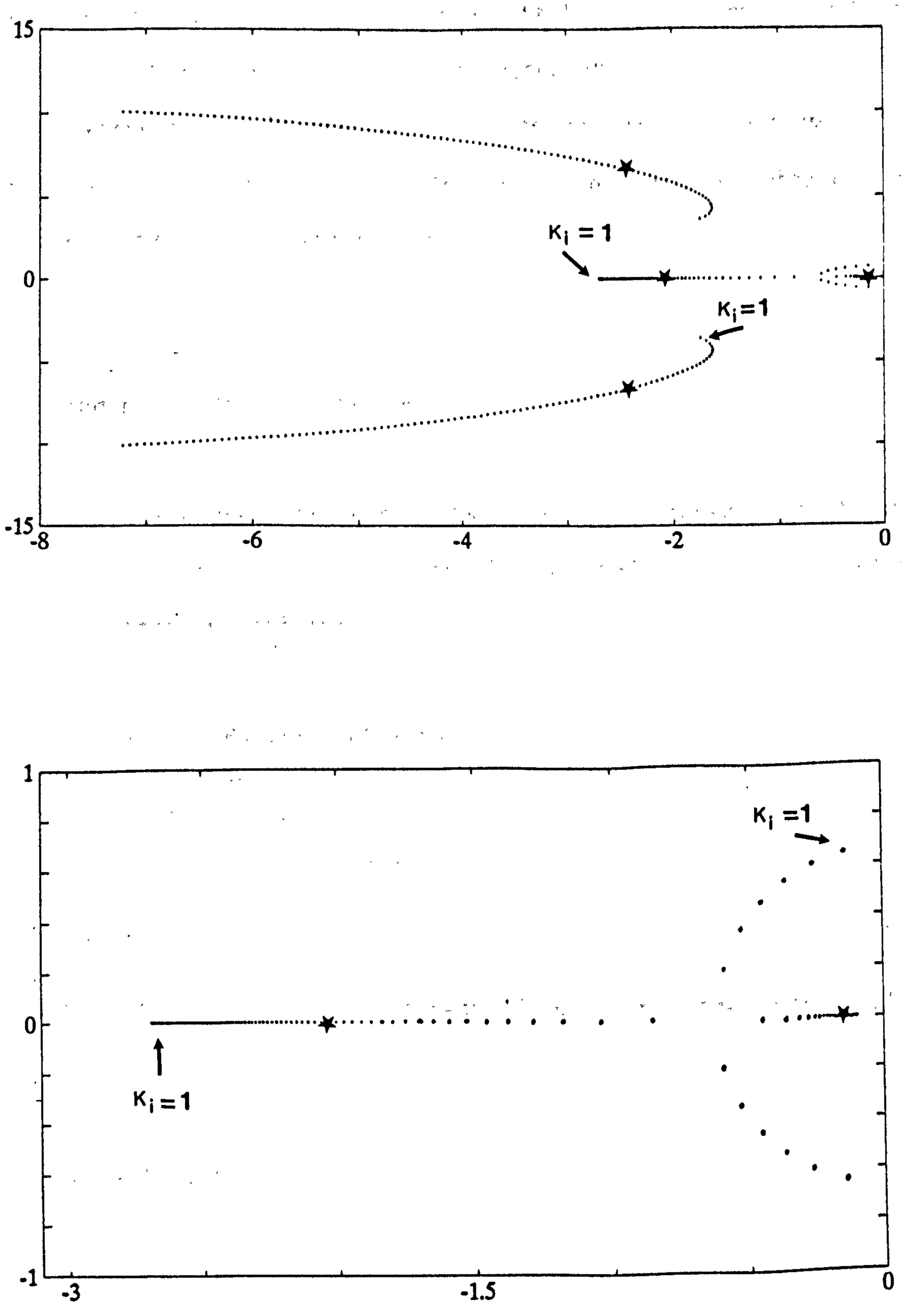

Figure 2.7.2 Root locus of compensated system

period mode rapidly dies away while the phugoid mode manifests itself as a long term oscillation about the desired steady state value. The corresponding oscillation in pitch attitude is slow enough to be corrected by the pilot and thus quite acceptable.

The response of Figure 2.7.3 is the continuous performance to be matched by the discrete system. The degree of matching obtained by the single rate system is examined first.

2.7.2 Single Rate Matched Design

First, the closed continuous system whose response is to be matched is represented in state space form. The aircraft longitudinal state and control vectors are defined:

$$x_p = \begin{bmatrix} u \\ w \\ q \\ \theta \end{bmatrix} = \begin{bmatrix} \text{forward velocity} \\ \text{vertical velocity} \\ \text{pitch rate} \\ \text{pitch attitude} \end{bmatrix}$$

$$u_p = [\eta] \qquad (2.7.2)$$

The state space description corresponding to the transfer function of (2.7.1) is:

$$\dot{x}_p(t) = A_p x_p(t) + B_p u_p(t)$$

$$y_p(t) = C_p x_p(t) + D_p u_p(t)$$

where,

$$A_p = \begin{bmatrix} -0.059 & 0.147 & 0 & -9.81 \\ -0.475 & -2.930 & 32.77 & 0 \\ 0.166 & -0.416 & -0.645 & 0 \\ 0 & 0 & 1 & 0 \end{bmatrix} \qquad B_p = \begin{bmatrix} 0 \\ 5.318 \\ -13.58 \\ 0 \end{bmatrix}$$

$$C_p=[0\ 0\ 1\ 0] \qquad D_p=[0] \tag{2.7.3}$$

Define the P+I compensator dynamics in state space as:

$$\dot{x}_c(t) = A_c x_c(t) + B_c u_c(t)$$

$$y_c(t) = C_c x_c(t) + D_c u_c(t)$$

where,

$$A_c = [0] \quad B_c = [1] \quad C_c = [K_i] \quad D_c = [K_p] \tag{2.7.4}$$

and x_c, u_c and y_c denote compensator vectors. Cascading the controller and pitch rate dynamics of (2.7.3) and (2.7.4) gives the compensated open loop system description:

$$\dot{x}(t) = A_{OL} x(t) + B_{OL} u(t)$$

$$y(t) = C_{OL} x(t) + D_{OL} u(t)$$

where,

$$A_{OL} = \begin{bmatrix} A_c & 0 \\ B_p C_c & A_p \end{bmatrix} \quad B_{OL} = \begin{bmatrix} B_c \\ B_p D_c \end{bmatrix}$$

$$C_{OL} = [\ D_p C_c \quad C_2\ ] \quad D_{OL} = [D_c D_p] \tag{2.7.5}$$

The open loop transfer function is determined from,

$$G_{OL}(s) = C_{OL}[sI - A_{OL}]^{-1} B_{OL} + D_{OL} = \left[\begin{array}{c|c} A_{OL} & B_{OL} \\ \hline C_{OL} & D_{OL} \end{array}\right] \tag{2.7.6}$$

The augmented state, control and output vectors are defined:

$$x = \begin{bmatrix} x_c \\ x_p \end{bmatrix} \quad u = \begin{bmatrix} u_c \\ u_p \end{bmatrix} \quad y = \begin{bmatrix} y_c \\ y_p \end{bmatrix}$$

Closure of the pitch rate loop using negative feedback gives the state space quadruplet,

$$G_{CL}(s) = \left[\begin{array}{c|c} A_{CL} & B_{CL} \\ \hline C_{CL} & D_{CL} \end{array}\right] \tag{2.7.7}$$

where,

$$A_{CL} = \begin{bmatrix} A_c & B_c C_p \\ B_p C_c & A_p + B_p D_c C_p \end{bmatrix} \quad B_{CL} = \begin{bmatrix} B_c \\ B_p D_c \end{bmatrix}$$

$$C_{CL} = [D_p C_c \quad C_p] \quad D_{CL} = [D_c D_p] \tag{2.7.8}$$

Inserting numerical values into equation (2.7.7) with K_I=2.5, K_p=0.25 determines the closed loop pitch rate transfer function as,

$$\frac{q(s)}{q_a(s)} = \frac{-13.58(s+3.0729)(s+0.079)}{(s+2.4237 \pm j6.6108)(s+2.033 \pm j0.1483)} \tag{2.7.9}$$

The first step of the matching design procedure requires a discrete equivalent of the desired closed loop continuous system. A system description obtained by a direct discretisation of the closed loop continuous system does not yield the same response as a system obtained by closing the discretised open loop system, i.e.

$$G_{CL}(z) \neq \frac{G_{OL}(z)}{I + G_{OL}(z)} \tag{2.7.10}$$

Thus, it is more appropriate to define the desired *open loop* discrete

system than to determine a closed loop discrete system. The reason for this is simply that the closure of the compensated system using *discrete* negative feedback loop is likely to introduce destabilising effects which may make a reasonable match impossible. To ensure that a stable discrete system match is always possible, an open loop discrete equivalent of the desired closed loop system is selected as the starting point. This modification does not result in a strict match of the closed loop system performance, but does provide a realistic (and necessary) indication of the achievable discrete system response.

The desired open loop discrete system G_{DOL} is selected to be that obtained by z-transforming (2.7.5) with a period T=0.1, i.e.,

$$G_{DOL}(s) = C_{DOL}[sI-\Phi_{DOL}]^{-1}\Gamma_{DOL} + D_{DOL} \qquad (2.7.11)$$

The closed loop discrete system response for this choice of sample rate is shown in Figure 2.7.4, together with the response of the original continuous design that the discrete system is attempting to match. This response shows that the achievable closed loop discrete response has a slightly larger overshoot than its analogue counterpart.

Before proceeding with the single rate matched design, the feasibility of deriving a suitable closed loop discrete system from a combination of the discrete open loop pitch dynamics and discrete compensator (obtained by z transformation) is examined. The performance of the single rate system obtained in this manner is shown in Figure 2.7.5. This reponse clearly suffers from an unacceptable oscillation (demonstrating the drawbacks outlined in the introductory paragraph of this section).

The single rate, open loop discrete system that is to be designed (such that its closed loop response matches the response produced by the desired system of (2.7.11) is defined,

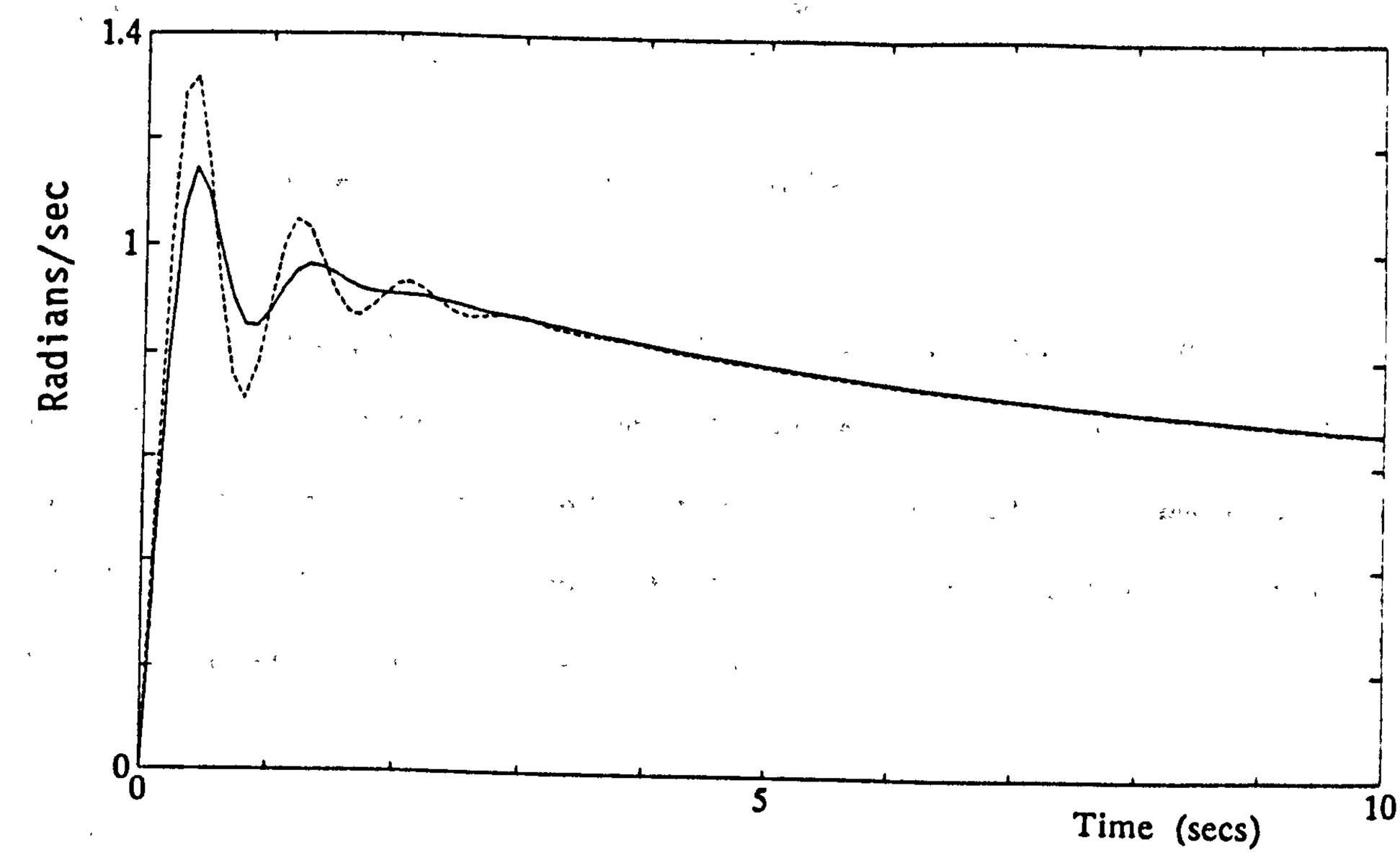

Figure 2.7.4 Desired discrete pitch rate loop response (compared with desired analogue closed loop response).

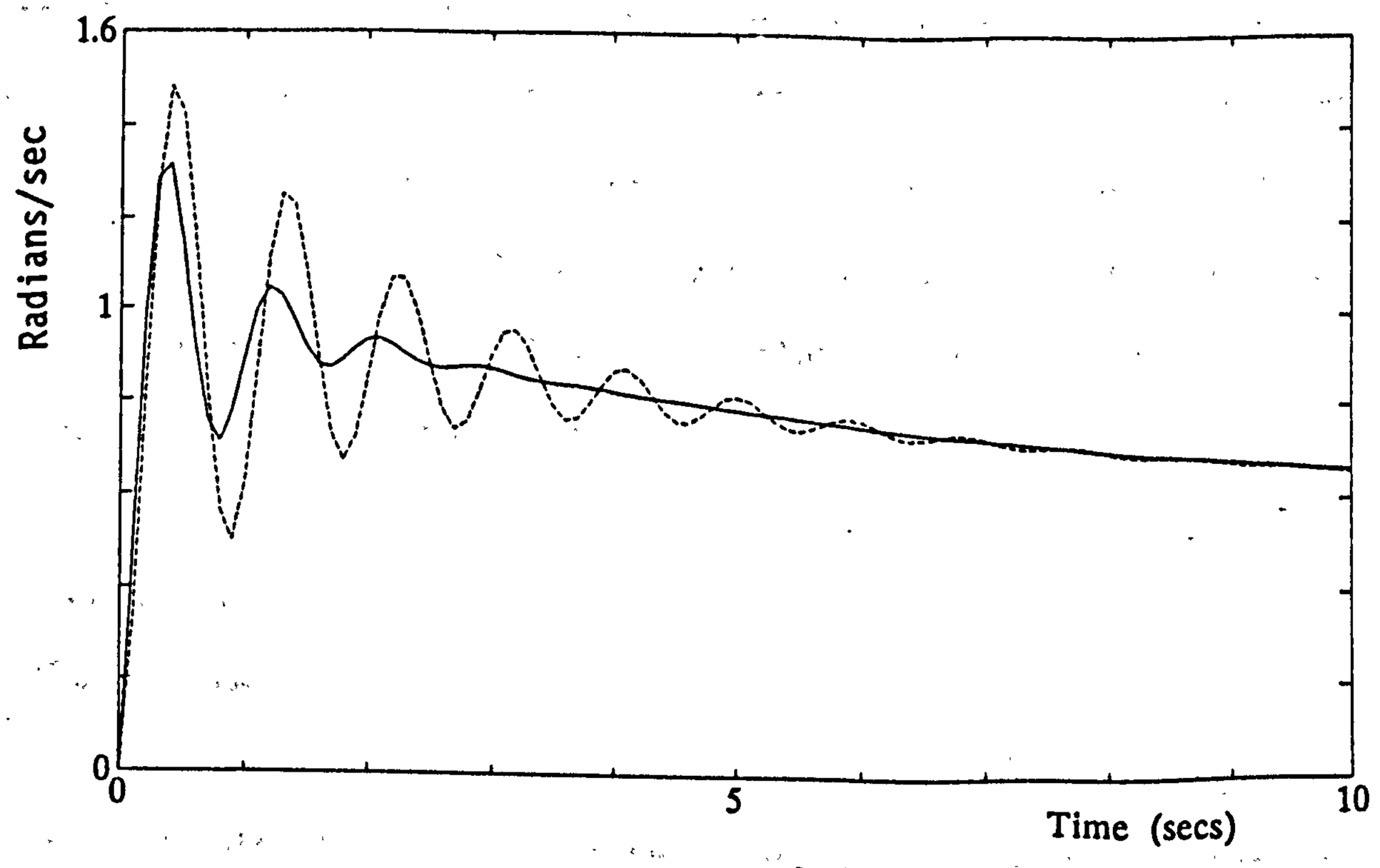

Figure 2.7.5 Unit step response of single rate pitch rate system obtained by direct discretisation of individual components (compared with desired discrete closed loop response).

$$\Phi_{MOL} = \begin{bmatrix} \Phi_{mc} & 0 \\ \Gamma_{mp}C_{mc} & \Phi_{mp} \end{bmatrix} \quad \Gamma_{MOL} = \begin{bmatrix} \Gamma_{mc} \\ \Gamma_{mp}D_{mc} \end{bmatrix} \tag{2.7.12}$$

$$C_{MOL} = [\, D_{mp}C_{mc} \quad C_{mp} \,] \quad D_{MOL} = [D_{mc}D_{mp}] \tag{2.7.13}$$

where $\{\Phi_{mc}, \Gamma_{mc}, C_{mc}, D_{mc}\}$, $\{\Phi_{mp}, \Gamma_{mp}, C_{mp}, D_{mp}\}$ represent the discretised compensator and aircraft dynamics for a sample period T=0.1. An examination of the desired and matched discrete system equations of (2.7.12) and (2.7.13) shows that for *exact* system matching, the following relations must be satisfied:

$$A_{mc} = A_c$$

$$B_{mc} = B_c \tag{2.7.14a}$$

$$\Gamma_{mp}C_{mc} = \Gamma_p C_c$$

$$\Gamma_{mp}D_{mc} = \Gamma_p D_c \tag{2.7.14b}$$

The right hand side terms of (2.7.14) are determined from (2.7.12). The first two matching conditions have a direct relationship and require no solution. Since $\Gamma_{mp} \in R^{nxm}$, $\Gamma_p C_c \in R^{nxr}$, $\Gamma_p D_c \in R^{nxm}$ the last two matching conditions both present an overdetermined problem. Hence, the single rate system will only yield an approximate solution for compensator matrices C_{mc}, D_{mc}. The solution of the latter is clearly dependent on Γ_{mp}. The compensator gains,

$$C_{mc} = (\Gamma_{mp})^{\dagger}\Gamma_p C_c$$

$$D_{mc} = (\Gamma_{mp})^{\dagger}\Gamma_p D_c \tag{2.7.15}$$

(where $\dagger$ denotes the Moore-Penrose inverse, i.e. the pseudoinverse) will define the achievable open loop single rate system G_{MOL},

$$G_{MOL}(z) = C_{MOL}[sI-\Phi_{MOL}]^{-1}\Gamma_{MOL} + D_{MOL} \tag{2.7.16}$$

which *approximates* the desired single rate system, G_{DOL}. Applying this matching method determines the single rate P+I compensator gains for the pitch rate loop to be:

$$K_p = 0.3457 \qquad K_i = 2.5 \tag{2.7.17}$$

The closed loop response of the compensated single rate system with these gains is shown in Figure 2.7.6. (The desired discrete system response is included to provide a comparison.) Figure 2.7.6 shows that the effect of inaccurate matching in open loop system dynamics is a slightly less damped response. A much closer single rate match with the desired continuous system response *may* be obtained by suitable adjustment of P+I gains but a direct one step match is not possible.

MULTIRATE MATCHED DESIGN

This section examines pitch rate control using the MIFO multirate sampling schemes of Figure 2.7.7. (Section 2.5 derives the relevant open loop system equations for the MIFO sampled system.). For this multirate configuration much more design freedom is made avilable for the matching algorithms by increasing the control updates within one main sample timeframe. The first sampling scheme (Figure 2.7.7a) incurs no extra cost on sensor equipment by monitoring the system output only once during a main sample interval. Control signals are injected into the aircraft pitch dynamics at the faster rate n/T. The sampling configuration of Figure 2.7.7b requires both error $(q-q_a)$ and control signals to be updated at the fast rate n/T. Both sampling schemes effectively require gain scheduling of compensator gains.

The compensated multirate open loop pitch rate loop is considered first. If the input sampling multiplicity is selected to be n_1=4, using

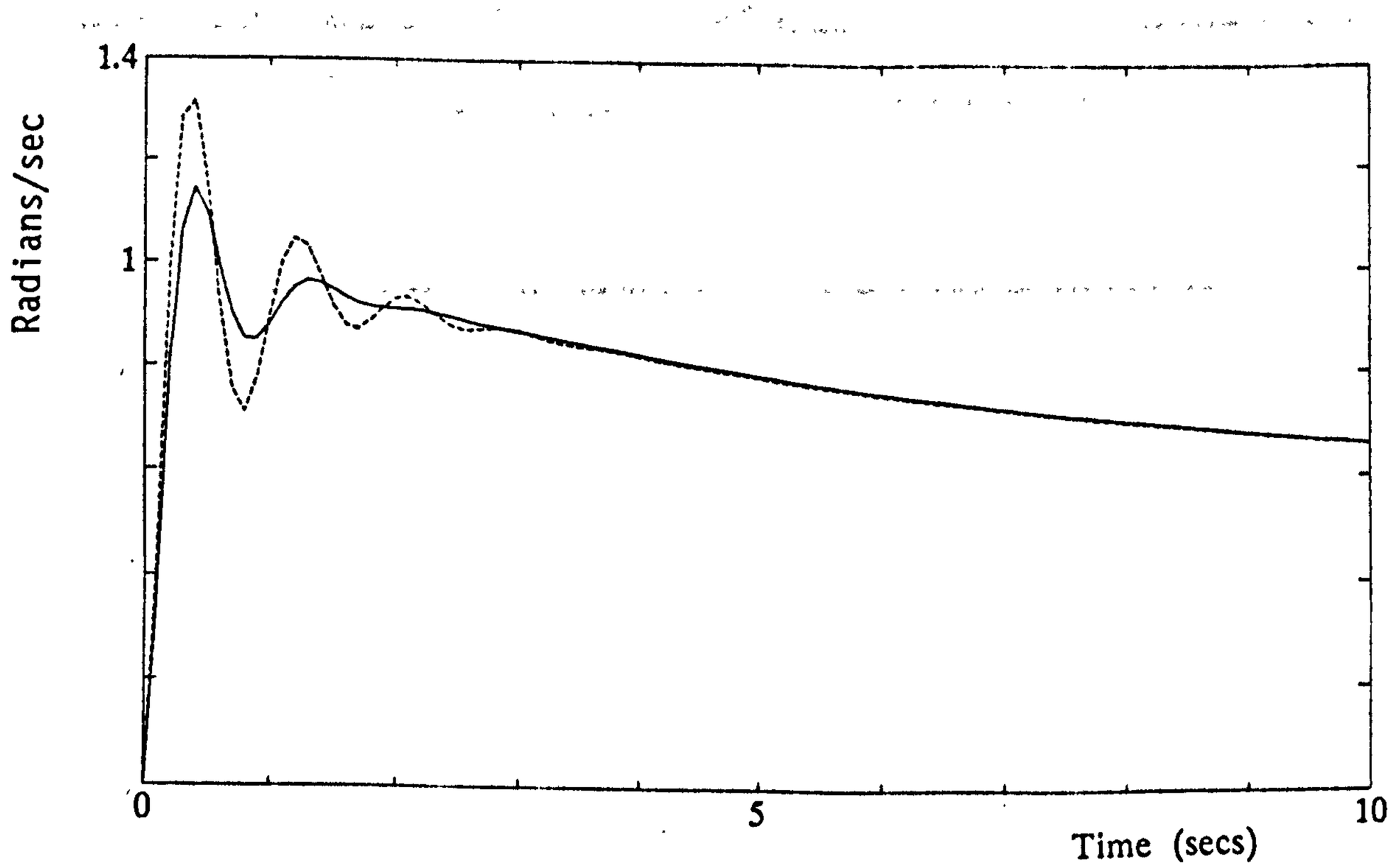

Figure 2.7.6 Unit step response of achievable single rate pitch rate system (compared with desired discrete closed loop response).

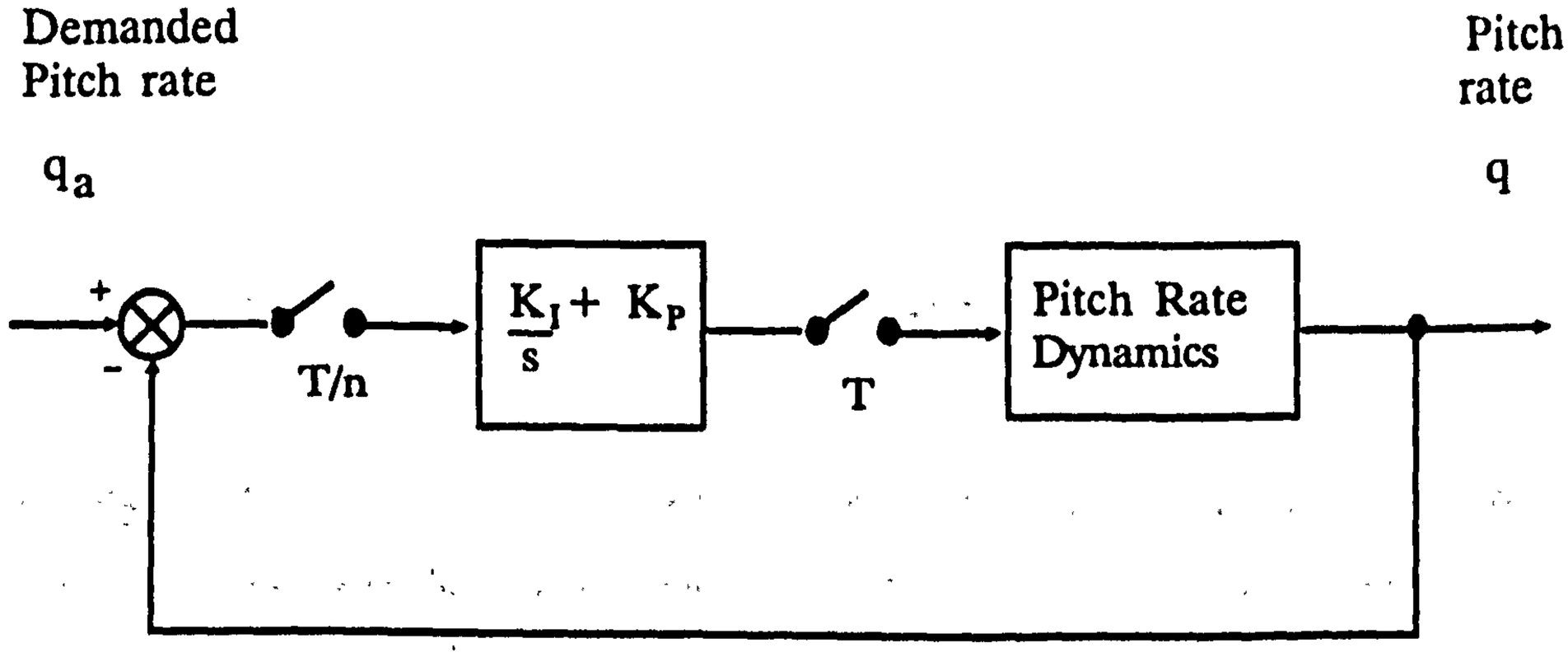

a)

b)

Figure 2.7.7 Multirate P+I control schemes of pitch rate loop.

equations (2.5.8) to (2.5.10), the pitch rate loop transfer is defined by multirate state equations:

$$x_p[(k+1)T] = \Phi_{MRp}x_p(kT) + \Gamma_{MRp}u_{pe}(kT)$$
$$y_p[(k+1)T] = C_p x_p[(k+1)T] + D_p u_{pe}[(k+1)T] \qquad (2.7.17)$$

where,

$$\Phi_{MRp} = \Phi_{Tb}[n_0;0] \qquad \Gamma_{MRp} = [\bar{\Gamma}_{Tb}(n_0)] \qquad (2.7.18)$$

Vector $u_{pe}(kT)$ is in the expanded form of (2.2.6). Control matrix $\bar{\Gamma}_{Tb}(n_0)$ is determined for the single input error signal from equation (2.5.17) with sample parameters $\{n_1=n_0=4,\ \ell_i=1\}$.

For the multirate case, an underdetermined problem will arise for the two matching conditions of equations (2.7.14b) if $n_0<r$ or $n_0<m$ (as for the single rate case). Since $\Gamma_{MROL} \in R^{nxn0}$, where $n_0 > r$, $n_0 > m$, for the multirate systems of Figure 2.7.7, an overdetermined problem is now generated by the matching condition. Thus, an exact match is guaranteed by the solutions provided by (2.7.15).

The design procedure outlined for the single rate case with Φ_{MRp}, Γ_{MRp} replacing Φ_{mp}, Γ_{mp}, and $\{\Phi_{mc}, \Gamma_{mc}, C_{mc}, D_{mc}\}$ representing discrete compensator dynamics for period T/n_1 is repeated for the multirate case. This gives the following set of gains for the P+I compensator:

K_p=0.2694 K_i=2.5
K_p=0.3583 K_i=2.5
K_p=0.3917 K_i=2.5
K_p=0.4806 K_i=2.5 (2.7.19)

Note that only the proportional gain requires scheduling over main interval T.

The closed loop multirate systems of Figure 2.7.7 formed with this set of gains gives the unit step responses of Figure 2.7.8. Figure 2.7.8a shows the match of the first multirate system (error signal update rate=1/T) with the desired discrete system response, while Figure 2.7.8b shows the match of the second multirate system (error signal update rate=n/T) with the desired *continuous* system response. The latter response is seen to almost *exactly* match the desired system response of Figure 2.7.3. Control signal and state trajectories also correspond with the same degree of accuracy.

The above design has demonstrated how the extra design freedom generated by the multirate sampling schemes of Figure 2.7.7 can be usefully applied for the design of discrete compensators. Increasing both input and output sample rates of the compensator on the final discrete system has been clearly illustrated to produce very close correspondence with the original continuous design. This is achieved using a direct mapping technique with no requirement for any 're-tuning' of gains to produce the desired response, as may be necessary for the single rate case.

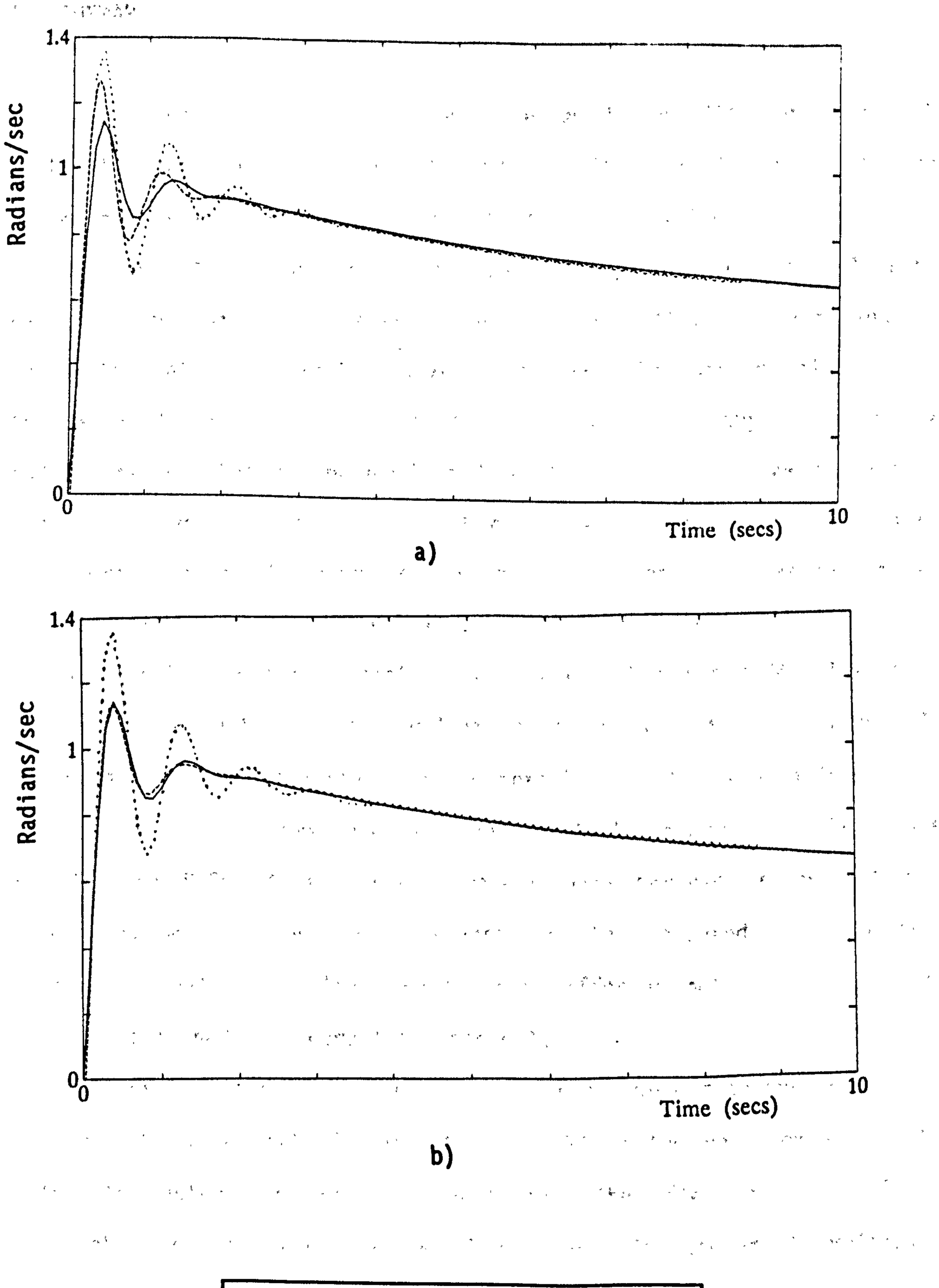

Figure 2.7.8 Unit step responses of achievable multirate rate pitch rate system (compared with desired discrete closed loop response).

2.8 SUMMARY

This chapter has derived state space models for different types of multirate sampling schemes and described a design method used for the design of compensators for one class of multirate systems.

Section 2.2 introduced state space representation of multirate systems. The sampling inter-relationships and other preliminaries of multirate state space modelling were outlined. This section also listed the three (different) types of state space models, of varying complexity and dimension, that may be used to describe multirate system behaviour. Each model type was determined either by the multirate sampling scheme it described or by the amount of information it contained (as influenced by the design and analysis techniques applied to the model).

Section 2.3 described state space models for the SISO slow/fast, fast/slow and multirate input/multirate output systems of Section 1.3. The objective of this section was to formulate state space models which encapsulate all intersample and hold effects accurately. For this reason, the SISO state space operators were derived to reflect the precise number of input/output transitions that occured during a main sample interval (this also ensured that different multirate subsystems could be combined in a compatible manner).

SISO systems with and without a ZOH element were examined separately in order to show that the effect of a ZOH in the development of the multirate system equations is significant. The effect is particularly noticeable in the state space model for the multirate input/ multirate output system (with rational sample rate ratio) of Section 2.3.3. (Note that this model is the state space equivelent of the Kranc vector decomposition operator of Section 1.3.3). The derivation of all the state space models of Section 2.3 was quite straightforward.

Secion 2.4 derived a state space model for MIMO multirate systems. One restriction was applied for the development of this model; the

multirate inputs and outputs must be related by a common base period. As a result of this sampling constraint the invariant, multivariable, multirate sampled-data system state equations naturally adopt a block form. The equation parameters and vectors consist of partioned block matrices of varying dimension. Each block dimension is specific to a sample rate and is determined by the associated multiple of the base sample period T_b. This restriction also ensured that the dimension of the MIMO model remained as low as possible.

Intersample behaviour is useful for the accurate determination of time and frequency domain performance. Section 2.4 shows that the intersample information is gained at the cost of a high dimensional, *non-minimal* state space description (the former is obtained despite the restriction on input/output sample inter-relationships of the MIMO model). Minimality in this sense, is with respect to the closed loop system singularities. The MIMO model of Section 2.4 generates $(n-1)n_0$ extraneous poles and zeros at the origin which strictly, do not exist.

Many state space design and analysis techniques require the characteristics of both minimal and non-minimal multirate models. The difference is of particular importance when considering the *design* of multirate control systems. A minimal description is better suited for the application of state space control design techniques. Section 2.5 outlines the derivation of a minimal state space model for a class of systems which have fast, multirate input updates within a slow, fixed rate output timeframe: the MIFO system. The design methods outlined in the remainder of this thesis are all applied to MIFO systems.

The minimality of the MIFO state space model is achieved by considering the system response only at instants where the input signal is updated. The MIFO system model also has the advantage of being a low dimensional multirate state space description.

One particular point that is noted from Sections 2.3, 2.4 and 2.5 is that the state space models do (despite their individual limitations)

minimise the tractability problems presented by the early classical methods.

Section 2.6 demonstrated the use of the multirate state space operators for the derivation of closed loop equations. This section repeats the analysis of the helicopter pitch rate control example of Section 1.4.

Section 2.7 outlines a method which may be used to design multirate compensators for a MIFO sampled system from a (given) continuous closed loop system design. The objective of the method is to retain the *controller structure* within the closed system (i.e. a lead/lag filter in the continous-time system will remain a lead/lag filter in the multirate system). Thus, this method is particularly suitable for cases where a multirate discrete design is to be derived with minimal effort from an existing continuous design.

The design method is based on matching the multirate system (minimal) closed loop description to a single rate discrete design obtained from the specified continuous-time closed loop system. The performance of the multirate compensated system was compared to that produced by a single rate discrete system (designed using the same technique). The multirate system was shown to produce a much closer match to the desired closed loop performance, thus demonstrating the advantages offered by MIFO sampling.

CHAPTER THREE

SAMPLE RATE SELECTION

3.1 INTRODUCTION

The ability of the sample rate of a system to govern performance measures such as speed of response, gain margins and asymptotic stability is well known for single rate discrete systems (Diduch and Doraiswami, 1987; Houpis, 1985; Mita, 1980; Powell and Katz, 1975). In general, trade-offs exist between the different system qualities. For example, a high sample rate will usually yield a faster response time at the cost of larger control signals whilst low sample rates will decrease the control signal magnitude but increase instability. Thus, the designer is often required to make a judicious choice of input/output sample rates. The correct choice of sample rate for a single rate discrete system will provide an acceptable compromise between such performance qualities.

Many factors influence the choice of input, output and control sample rates for a multirate control system. The choice may be imposed by physical constraints (e.g. computation throughput, hardware limitations) or by a combination of subsystems operating at pre-specified varying rates (e.g. systems with remote transmission links, distributed systems). For multirate systems whose sample rates can be chosen by the designer, an obvious selection criterion is the improvement of system performance or operation within acceptable stabilty limits. For the multirate systems described in Chapters 1 and 2, sample rate selection is classified by two parameters: the main sample interval T and input/output sampling multiplicities $\{n_i\}$.

Multirate systems fall into two categories; those with a *fixed*

dynamic control structure (eg P+I, lag/lead type compensation) and those for which the control structure is to be designed (using either classical or state/ouput feedback configurations). The former class of multirate systems offer limited scope for improvement in system performance by sample rate variation. For these systems, update rates of subystem elements are determined largely by heuristic adjustment of input/output sampling multiplicities until a specific performance criterion is adequately met. Examples of this approach include the work of Glasson (1982), Rattan (1984) and Godbout et al (1988). Glasson uses an optimisation procedure to select compensator gains and loop sample rates such that disturbance rejection properties of the closed loop system are enhanced. The work of Rattan is based on transformation of existing analogue designs to multirate sampled schemes. Loop sample rate selection, in this case, is determined by matching the multirate system frequency response to that of its corresponding analogue design. The techniques of Glasson and Rattan both require iterative adjustment of loop sample rates using an inner to outer loop closure approach. The closure of each successive loop is such that the desired performance criteria of that particular loop is met whilst maintaining a good overall closed loop response. The conclusion to be drawn from these studies is that an improvement in the performance of fixed-structure, dynamically controlled multirate systems by the choice of input/output sample rates presents a difficult challenge to the designer.

A greater opportunity for improvement in system performance accompanies the development of multirate systems with no pre-determined controller structure. For such cases, controller sample rates and dynamics can be selected either to fulfil subsystem bandwidth requirements or to enhance specific system qualities. Control design methods for these systems can be divided into classical (SISO) and modern MIMO categories. The work of Felui et al (1990) and Ragazzini and Franklin (1958) falls into the first category. Felui et al (1990) use a

mixed single rate feedback, multirate series dynamic compensator configuration to design a closed loop system with a finite impulse response. They demonstrate the effect of varying the error signal update rates (ie error signal multiplicity) of a multirate series compensator (in the forward path) on the transient reponse and the speed of attainment of desired steady state values. Faster error sampling within one feedback signal update was, for their example, shown to reduce the settling time at the cost of increased transient overshoots and control effort. In general, the application of such classical design methods is restricted to fairly simple, SISO multirate control configurations.

The design requirements of MIMO multirate control schemes are more adequately addressed by state space techniques (Al-Rahmani and Franklin, 1990; Glasson, 1980; Hagiwara and Araki, 1988; Hagiwara et al, 1990). The most important criteria for the selection of system sample rates, in this case, are the achievement of multirate controllability and observability conditions. These are prerequisite conditions for the application of *all* state space design techniques and thus a crucial requirement in the multirate control design procedure.

This chapter investigates the key issues relating to sample rate selection for multirate systems and is organised as follows: Section 3.2 examines the influence of sample rate choice on the stability and general performance of fixed structure multirate control systems. The pitch rate control example of Chapter 2 showed that the continuous-time system matching design method requires a choice of input sample rate multiplicities to guarantee an accurate match of relevant compensator dynamics. This example is repeated to demonstrate the effect of varying the main sample instant T on closed loop multirate discrete behaviour. Pre-determined dynamic controllers for the pitch rate loop of the remote pilotly vehicle are cast into a multirate sampled environment and the effects of varying sample rates on the matching design procedure investigated. Absolute stability (as distinct from *aymptotic* stability)

often provides the *limiting* condition for sample rate selection for this type of multirate system. Analytical techniques to determine this critical sample parameter are investigated using a root locus approach.

Section 3.3 establishes the *minimum* input/output sample rate multiplicity necessary to ensure controllability and observability of multirate systems. The role of this choice of sample rates in the multirate control problem is examined with respect to related (A,B), (A,C) invariance properties. These properties are characterised by the *Kronecker Invariants* and can be determined from pencil representations of the internal system. They are also used to generate particular canonical forms. Sections 3.3 and 3.4 examine the role of a subset of the Kronecker invariants in the pole placement problem for analogue, single rate and multirate systems using canonical forms. This examination establishes the fundamental link between the three system types and neatly encapsulates (A,B) invariance concepts in an application-oriented manner. This analysis provides the core design criteria for *all* control problems and is thus examined in some detail. In particular, Section 3.4 demonstrates the effect of the controllability criteria on MIFO multirate pole assignability using a canonical pole placement algorithm, the *Popov algorithm* (Kailath, 1980).

Many researchers have reported the ability of sample rate selection in MIMO systems to influence system *robustness* (Albertos, 1990; Araki and Yamamoto, 1986; Francis and Gorgiou 1988; Hagiwara and Araki, 1988; Kargonekar et al, 1985; Mita et al, 1980; Zhu and Skelton, 1991). The relation between sample rate selection and the achievability of performance and stability robustness is examined in detail in Chapters 4 and 5. This Chapter closes with a discussion of the general results to be expected from such an analysis. Section 3.5 presents an analytic method to determine the scalar gain margins for a class of multirate closed loop systems designed using the Popov algorithm. The margins provide accurate figures for the maximum and minimum perturbations

allowed in the MIFO system control matrix to ensure closed loop asymptotic stability. The effect of the main sample interval and input/ouput multiplicities on asymptotic stability performance measure is outlined and analysed with the use of an example.

3.2 IMPACT OF SAMPLE RATES ON FIXED-COMPENSATOR STRUCTURE SYSTEMS

The pitch rate loop of Section 2.7 is re-examined briefly to demonstrate the effect of the sample parameter T in discrete system performance. For the P+I control scheme of Figure 2.7.1, the matched discrete designs were produced for a choice of gains K_i=2.5, K_p=0.25, as selected from the root locus plot of Figure 2.7.2. The unit step response of the corresponding closed loop pitch rate dynamics (Figure 2.7.3) was shown to exhibit a relatively large overshoot in the short period mode and quite a significant phugoid oscillation. Both can be reduced by a choice of gains, K_i=7, K_p=0.7. The corresponding closed pitch rate loop gives the unit step reponse of Figure 3.2.1. This response demonstrates clearly the superior compensator design.

The first stage of the matching technique of Section 2.7 requires a desired open loop discrete system to be determined from the compensated analogue design. The choice of the main sampling period T at this stage of the design procedure plays an important role; it effectively determines the degree of analogue performance matching that is likely to be achieved by the multirate system. The lower and upper bounds on the choice of 1/T will be dictated by the critical Nyquist frequency and any computation throughput constraints (such as those imposed by hardware). The former will ensure that the system will be sampled sufficiently fast enough to ensure accurate representation of data. Within this limit, T is ideally chosen to be as large as possible without compromising discrete system performance.

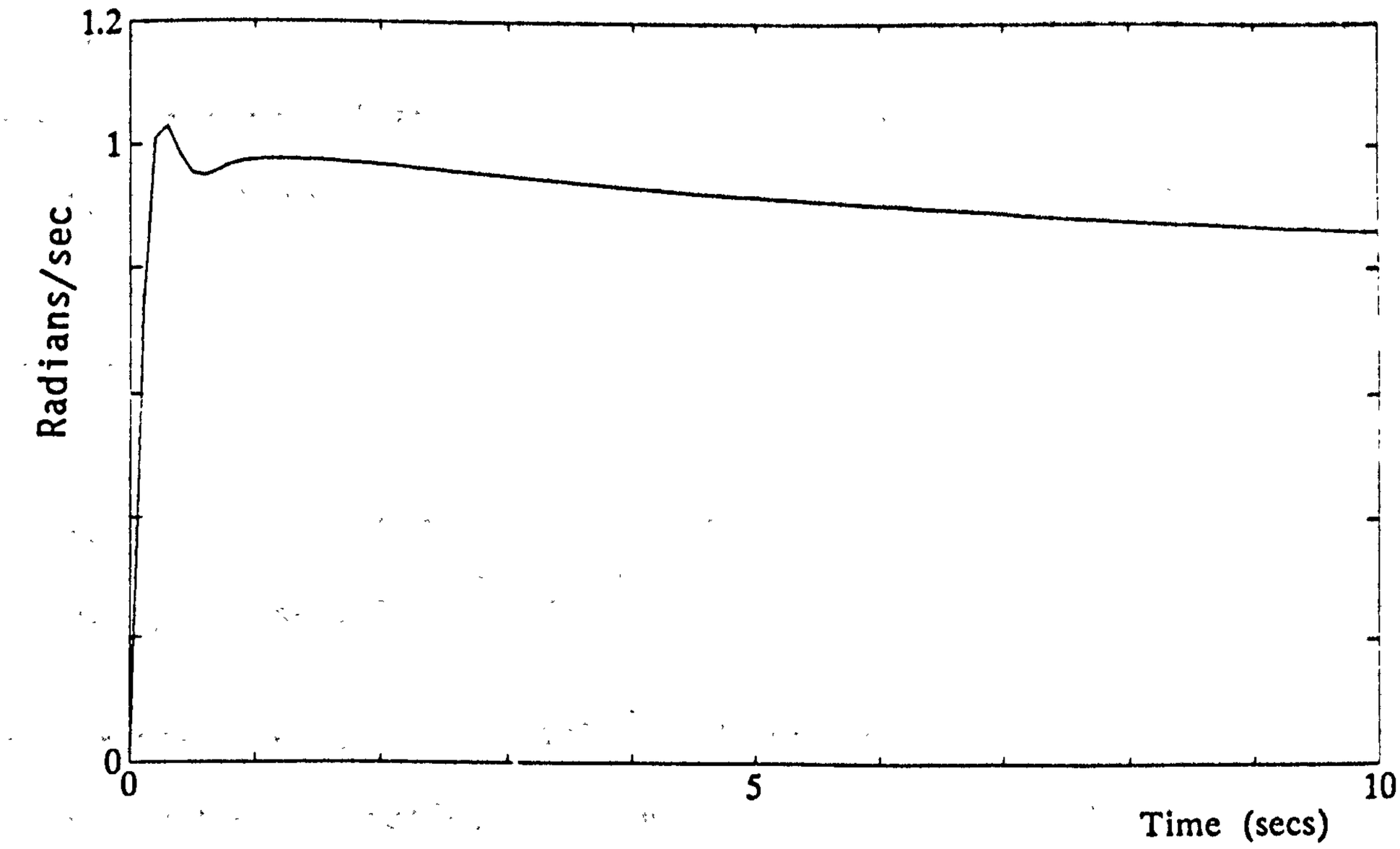

Figure 3.2.1 Step response of analogue pitch rate loop for P+I gains K_j=7, K_p=0.7

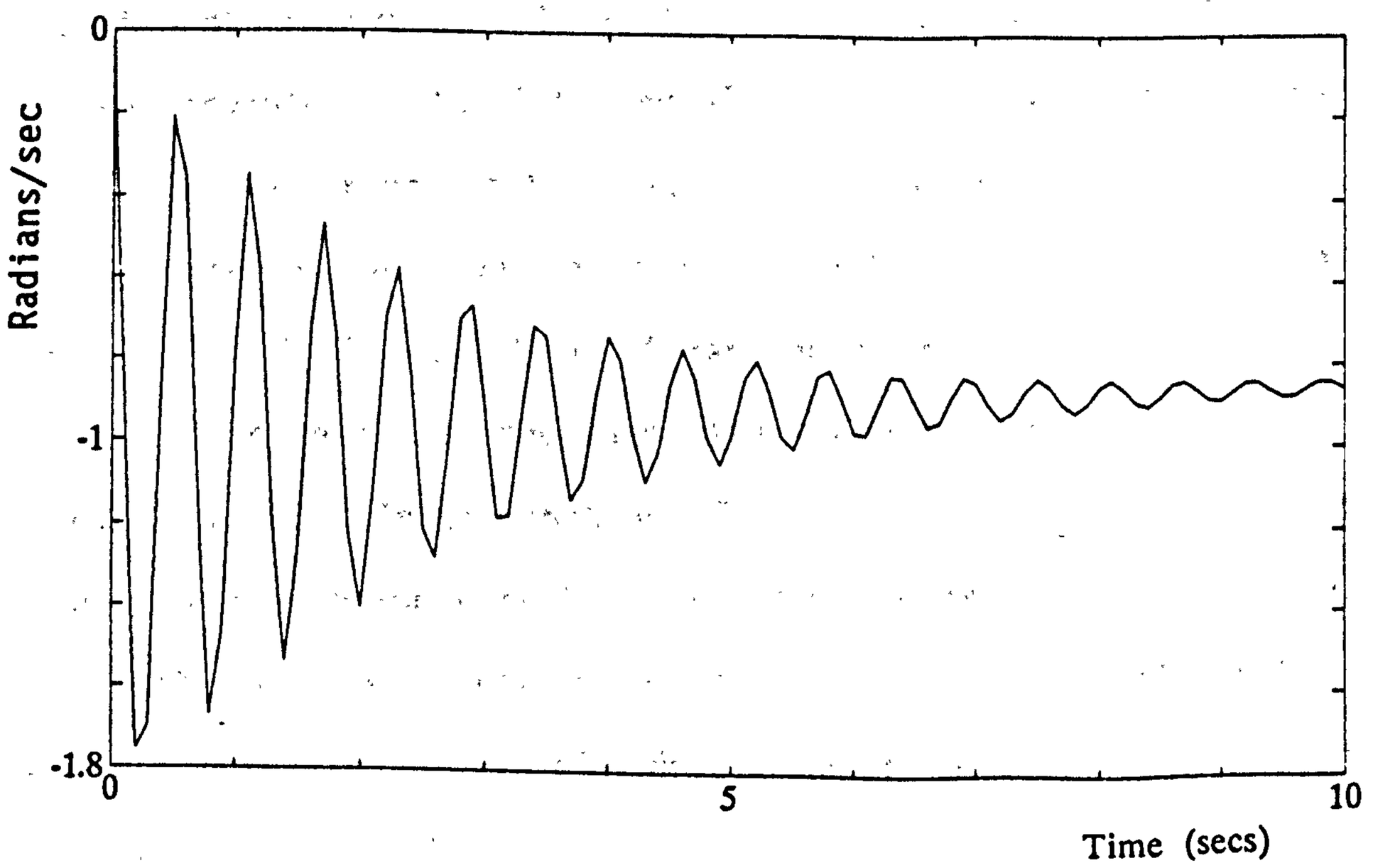

Figure 3.2.2 Step response of discrete pitch rate loop with K_j=7, K_p=0.7, T=0.1

The improved design (illustrated in Figure 3.2.1) is considered to demonstrate the effect of T on discrete system performance. If the gains K_i=7, K_p=0.7 are inserted into the discrete system with T=0.1 secs (as in Section 2.7), the following closed loop transfer function is obtained:

$$\frac{q(s)}{q_a(s)} = \frac{135.8(s+10)(s+3.0729)(s+0.079)}{(s+5.2334\pm j9.2300)(s+2.5702)(s+0.1029)} \qquad (3.2.1)$$

An examination of the resulting discrete singularities shows that the above system is stable, but the discrete system response to a unit step input is a highly oscillatory. This is shown in Figure 3.2.2.

A root locus plot of the closed loop system pole positions with varying T can provide useful information at this stage of the design procedure. The plot can be used to establish the achievability of an acceptable closed loop discrete system from a specified continuous-time design and a given choice of sample instant T. This root locus plot will have two other purposes. It will indicate the limiting value of T which ensures asymptotic stability and also provide a means of monitoring the effect of T on transient behaviour as assessed by pole positions.

A discrete root locus plot of the poles for the closed loop system formed with K_i=7, K_p=0.7 for T ranging from 0.001 secs to 0.2 secs is shown in Figure 3.2.3, together with the limiting stability boundary of the unit circle. An examination of this plot reveals that an acceptable discrete-time design cannot be produced for *any* choice of T. Decreasing T accentuates the clustering of poles at the +1 point on the z-plane whilst increasing T rapidly draws the complex pair to the unstable region.

The poles for the maximum and minimum sample periods, T=0.001secs and T=0.2secs, demonstrates this effect. These are as follows:

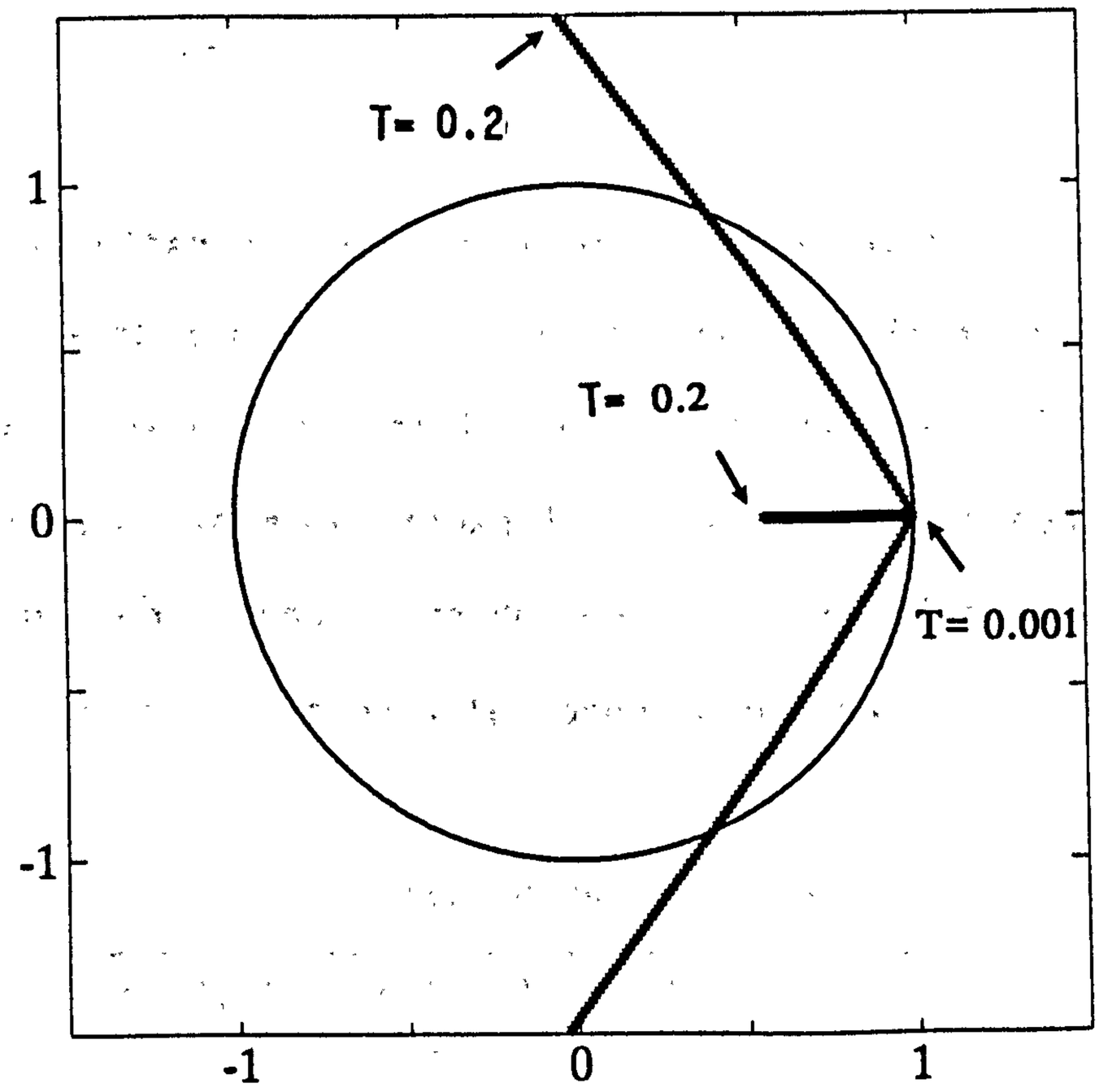

Figure 3.2.3 Root locus for discrete pitch rate loop for T=[0.001, 0.2]

T=0.001 0.9948±j0.0092

0.9974

0.9999

1.0000

T=0.2 0.0753±j1.5561

0.5620

0.9813

1.0000 (3.2.2)

Clearly, a suitable starting point for the matching procedure cannot be realised for this continuous-time design specification.

A modification such that local velocity feedback is applied around the pitch rate dynamics (shown in Figure 3.2.4) is considered to improve the original continuous-time design. A choice of gains K_r=1, K_i=2, K_p=20 gives the following compensated open loop dynamics:

$$\frac{q(s)}{q_a(s)} = \frac{(s+10)(s+3.0729)(s+0.079)}{(s+32.3462)(s+9.1214)(s+2.8191)(s+0.0873)} \qquad (3.2.3)$$

The above system produces the well damped response shown in Figure 3.2.5 to a unit step input.

A suitable main sample period for the design can be determined from the root locus plot for varying T. This is given in Figure 3.2.6. From this plot, it can be seen that as T→0, the poles cluster around the +1 point whilst for T→0.5 the complex pole pair are attracted to the unstable region. An acceptable discrete response for this closed loop analogue system is produced by T=0.02secs.

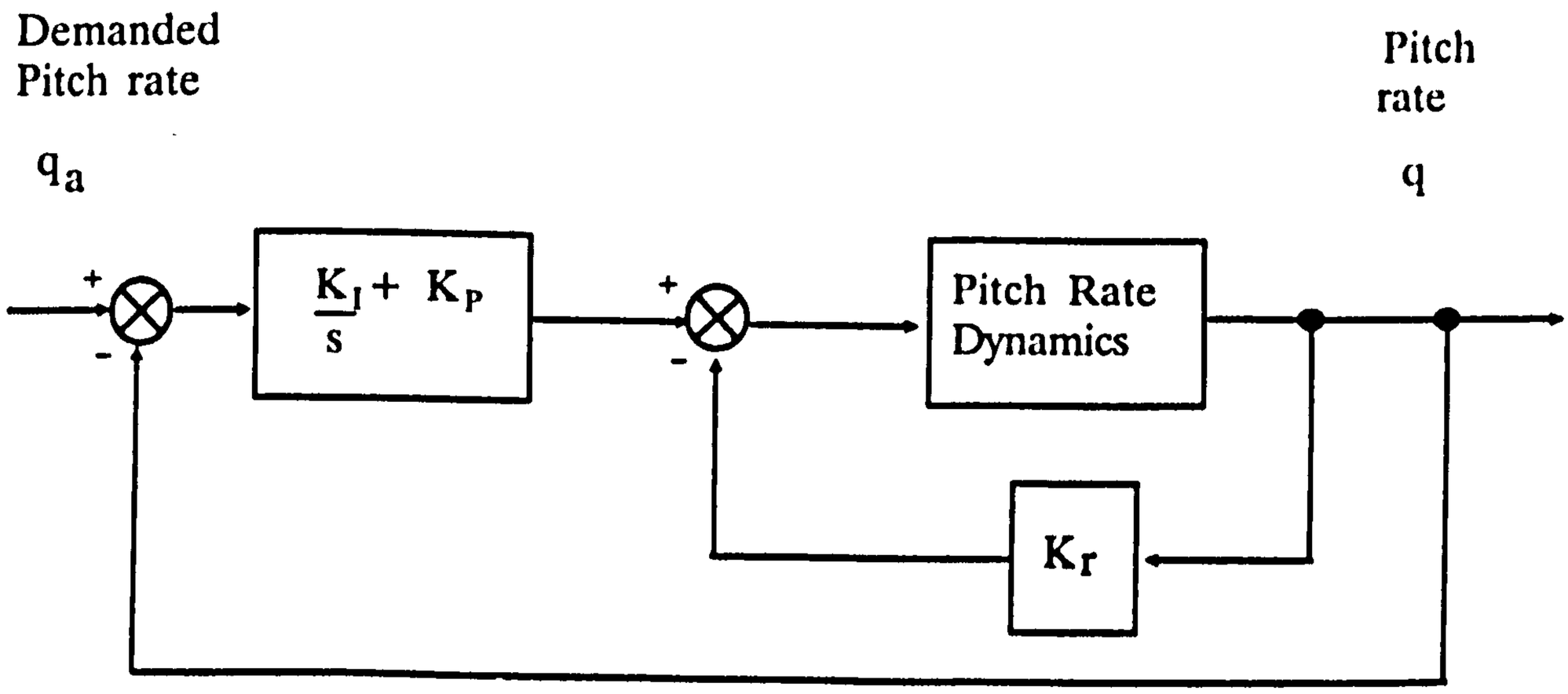

Figure 3.2.4 Analogue pitch rate loop with local velocity feedback and P+I compensator

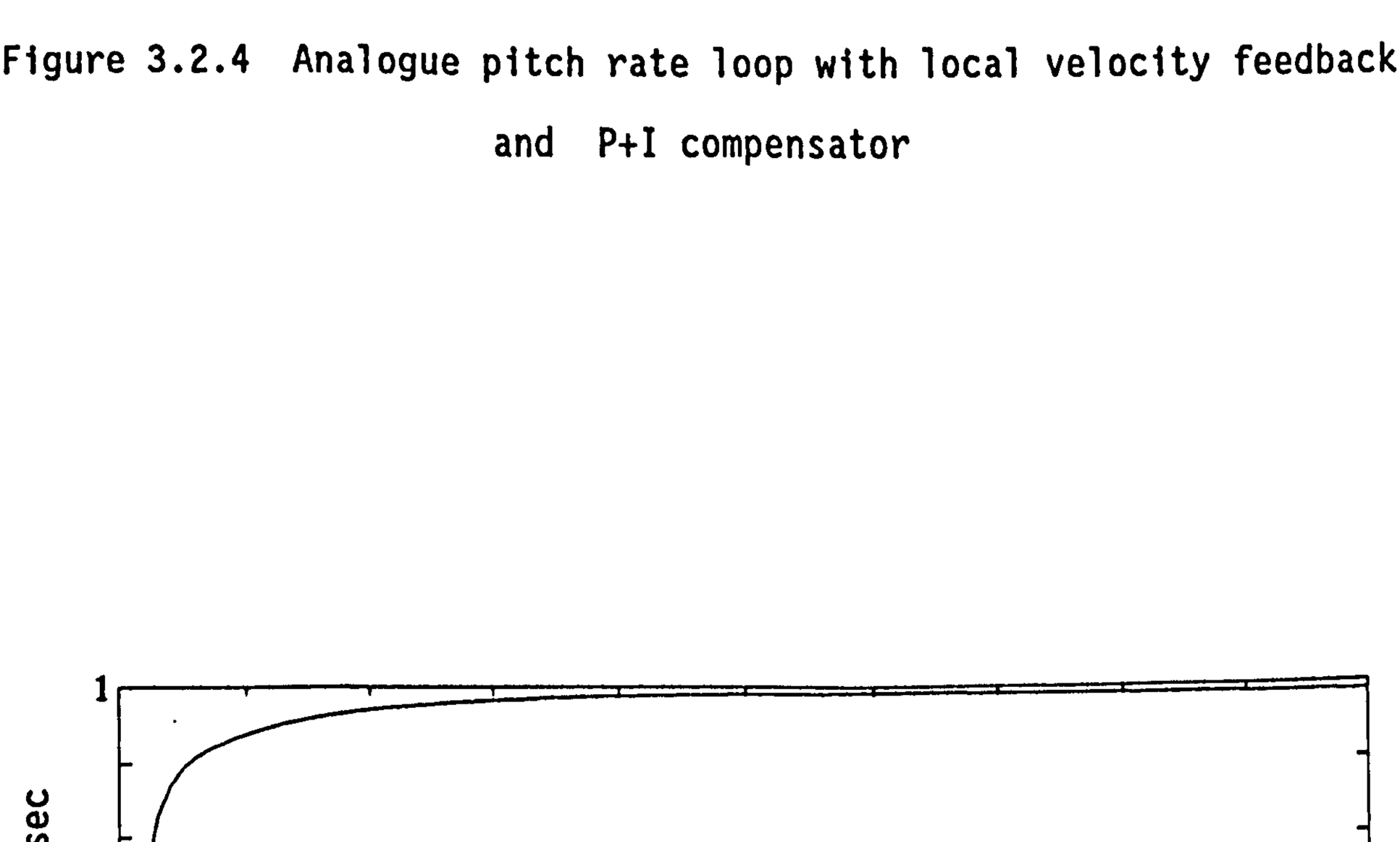

Figure 3.2.5 Step response of analogue pitch rate loop with local velocity feedback K_r=1 and P+I gains K_i=20, K_p=2

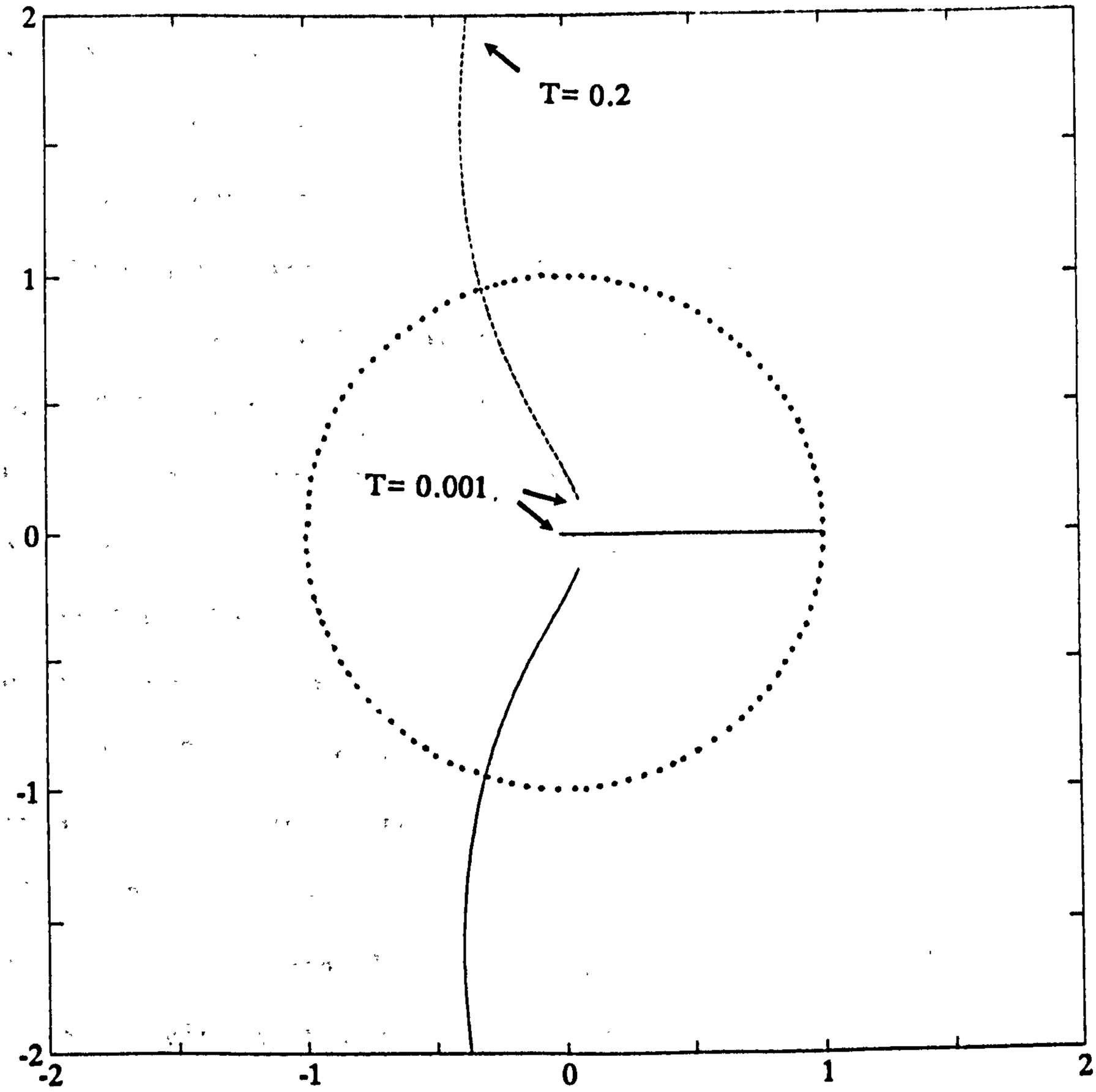

Figure 3.2.6 Root locus for discrete pitch rate loop with local velocity feedback K_r=1 and P+I gains K_I=20, K_p=2.

T=[0.001, 0.2]

3.3 MULTIRATE CONTROLLABILITY AND OBSERVABILITY

Controllability and observability properties of multirate and general periodic systems have been examined by many in the past (Al-Rahmani and Franklin, 1990; Bittani et al, 1984; Bittani and Bolzern, 1985; Chammas and Leondes, 1978, 1979; Engwerda, 1988; Graselli and Longhi, 1986; Kano and Nishimura, 1985; Kono, 1980; Kono and Suzuki, 1991; Kuo, 1980, Lennartson, 1988, 1989). The achievement of these fundamental properties is important when applying multivariable control techniques. The concepts which apply to the continuous time case can, in fact, be extended to the general periodic system. Some distinctions arise for the general periodic case (Al-Rahmani and Franklin, 1990; Bittani et al, 1984, Kano and Nishimura, 1985), requiring a clear specification of the time interval over which the controllability and observability conditions apply. This section outlines the conditions for controllability of the general periodic system.

If a time varying system can be described by continuous T-periodical system matrices {A(t), B(t)} (where A(·) is assumed analytic) an associated transition matrix $\Phi(t,\tau)$ can be derived to describe the periodicity of {A(t), B(t)}, i.e.

$$\Phi(t+T,\tau+T)=\Phi(t,\tau)$$

This can be obtained using the Floquet method (Kailath, 1980). The eigenvalues of the corresponding monodromy matrix $\Phi(T,0)$ will characterise the periodic behaviour of the time-varying system. The system is said to be controllable iff the controllability gramian,

$$W[t_0,t_f] = \int_{t_0}^{t_f} \Phi(t_0,\tau)B(\tau)B^T(\tau)\Phi^T(t_0,\tau)d\tau$$

is non-singular. The case where $t_f=T$, $t_0=0$ will satisfy periodic controllability.

A summary of the controllability and observability aspects which apply to the MIFO multirate system are outlined in the next two sections.

3.3.1 Controllability

A discrete system is said to be controllable over a time interval $[t_0,t_f]$ if, for any initial time stage $t_0=kT$ there exists a set of controls $u[(k+i)T]$, $i=0,1,..,(q-1)$, which drives the system state from the initial state $x(kT)$ to any final state $x[t_f]=x[(k+q)T]$ for $(k+q)T > kT$. This is less strict than *complete* controllability which requires that *every* element of the initial state vector $x_i[kT]$ be driven to a final value $x_i[(k+q)T]$. *This distinction is not trivial for the multirate system since the (1 x nxN) expanded vector $x_e[kT]$ comprises n subsets (corresponding to $A \in R^{nxn}$) of time delayed/advanced components of system states.* Uncontrollability of any element of $x_e[kT]$ thus has different implications than in the general single rate discrete case.

If $\Phi[t_0,t_f]$ is the periodic state transition matrix for the MIFO system and $W_c[t_0,t_f]$ is the periodic controllability Gramian matrix defined as,

$$W_c[t_0,t_f] \triangleq w_c w_c^T \qquad (3.3.1)$$

where w_c is the q-block matrix (for any set of multirate sample parameters n_0, n, ℓ, T_b) given by,

$$w_c = \{w_{cj}\} \qquad j = 0,..,(q-1)$$

$$w_{cj} = \sum_{i=0}^{n-1} \Phi_{Tb}[n_0,(i+1)\ell]\Gamma_{Tb}[(i+1)\ell,i\ell] \qquad (3.3.2)$$

then x(kT) is controllable over $[t_0,t_f]$ iff it belongs to the range space of $W_c[t_0,t_f]$. That is, $x(kT) \in R(W_c[t_0,t_f])$. The necessary and sufficient condition for complete controllability is that $R(W_c[t_0,t_f]) = n$. This requirement can be demonstrated by considering the simplest of the periodic state equations developed for the SISO MIFO system in Chapter 2. From state equation (2.5.5) it follows that the periodic transition equation determining the states over q steps each of period T is,

$$x[(k+q)T] = \Phi^q[n_0,0]x(kT) + [w_{c1}\ w_{c2}\ ..\ w_{c(q-1)}][u_{1e}(kT)..u_{1e}[(k+q-1)T]^T \qquad (3.3.3)$$

which can be rearranged to form the linear equation,

$$X[(k+q),k] = w_c U \qquad (3.3.4)$$

where,

$$X[(k+q),k] = x[(k+q)T] - (\Phi_{Tb}[n_0,0])^q x(kT) \qquad (3.3.5)$$

incorporates the natural response. The forced response components w_c, U of (3.3.4) are compatibly dimensioned. Equation (3.3.5) has a solution for each $X[(k+q),k] \in R^n$ iff $R[w_c] = R^n$. Since $R[w_c] = R[w_c w_c^T]$ then the condition for complete controllability must hold.

3.3.2 Observability

The properties of observability are similarly arrived at and will

simply be stated here: A system is said to be observable over time interval $[t_0,t_f]$ if any state $x(t_0)$ can be determined from any $x[t_f]=x[(k+i)T]$, $i=0,1,..,(q-1)$ for $(k+q)T>kT$. As with controllability, this is less stringent than complete observability which requires *every* state $x_i[kT]$ be observable over the specified time interval.

Observability is the dual concept of controllability. Thus, from the controllability conditions outlined above it follows that a state $x_i(kT)$ is unobservable over the period $[t_0,t_f]$ (it is assumed that $t_0=kT$ and $t_f=(k+q)T$)) iff $x_i(kT)$ lies in the nullspace of $W_o[t_0,t_f]$. That is, $x_i(kT) \epsilon N(W_o[t_0,t_f])$ where,

$$W_o[t_0,t_f] = w_o w_o^T \tag{3.3.6}$$

whose q-block matrix w_o is given by,

$$w_o = \{w_{oq}\} \qquad j = 1,..,q$$

$$w_{oq} = \sum_{i=(0)\ell}^{(n-1)\ell} \sum_{j=0}^{(i-1)} C_{Tb}[i+1,j+1]\ \Phi_{Tb}[i,j+1]\ \Gamma[j+1,j] \tag{3.3.7}$$

$W_o[t_0,t_f]$ is the periodic observability Gramian for any set of multirate sample parameters. Consequently, for unobservable states $N(W_o[t_0,t_f])=R^n$. The necessary and sufficient condition for complete observability is that $N(W_o[t_0,t_f]) = \{0\}$.

From the above definitions it is clear that the choice of sample period affects the conditions of controllability and observability. The controllability Gramian becomes rank deficient if for any $i\neq j$ and $T\neq 0$,

$$w_{cj} = w_{ci} \qquad i,j = 1,..,n-1 \tag{3.3.8}$$

and similarly, the observability conditions are not satisfied if for any $i \neq j$ and $T \neq 0$,

$$W_{oj} = W_{oi} \qquad i,j=1,..,n-1 \qquad (3.3.9)$$

The sample parameters for a multirate system must therefore be carefully selected to ensure that no modes of the sampled-data system become either uncontrollable or unobservable.

3.4 THE ROLE OF INPUT SAMPLE RATES IN MULTIRATE FEEDBACK PROBLEMS

The controllability and observability properties outlined in Section 3.3 are satisfied by an appropriate choice of input/output sample rate multiplicities for the multirate system. The early multirate pole placement techniques of Chammas and Leondes (1978, 1979) were based on SISO systems. These authors recommended a choice of input/output sample rate multiplicities $\{n_i\} > \{n\}$. This choice is imposed by the limited number of inputs/outputs available for the achievement of multirate controllability properties in a SISO system. An examination of equations (3.2.2) and (3.2.5) which derive the necessary controllability condition $R(W_C[t_0,t_f]) = R^n$ reveals that this property can be achieved iff $\sum n_i > n$. Thus, an input sample rate multiplicity $n_i > n$ is required for a SISO system.

Later MIMO multirate techniques continued to support the use of multirate input/ouput multiplicities $\{n_i\} > \{n\}$. However, for MIMO systems these multiplicities result in a much higher input/ouput sampling than is strictly necessary in order to satisfy periodic controllability and observability conditions. Hagiwara and Araki (1986) recognised the ability to lower sample rate multiplicities for the pole placement problem, but provided no indication of the impact of sample rate

multiplicities on the design. This section examines the selection of input samples rates in order to achieve exactly MIFO multirate controllability for the general pole placement problem. Since this work concentrates principally on the state feedback problem, only the controllability conditions are examined in detail. Equivalent conditions can be derived for the observability properties by use of duality relations.

Equations (3.3.2) to (3.3.7) contain control and output matrix terms that look very much like an intermediate step in the development of canonical forms. This would indicate that the multirate controllability conditions are strongly linked to *canonical* forms. Many state-space canonical forms may exist for a given system (Fahmy and O'Reilly, 1983; Kailath, 1980; Luenberger, 1967). Luenberger (1967) identified some general canonical forms useful for MIMO control applications. Section 3.4.1 reviews two types of canonical forms and Section 3.4.2 outlines their role in the development of state feedback pole placement algorithms. The (A,B) invariance properties associated with these canonical forms can be usefully employed to generate appropriate multirate control input sample rates for the multirate pole placement problem. Section 3.4.3 outlines this procedure with the use of pencil equivalence relations (Gantmacher, 1959; Kailath, 1980).

3.4.1 Canonical forms and input sample rates

A continuous-time pair {A,B}, $A \epsilon R^n$, $B \epsilon R^m$ is said to be controllable iff no left eigenvector p of A is orthogonal to all the columns of B, i.e.,

$$p^T A = \lambda p^T \qquad p^T B = 0 \text{ iff } p \equiv 0 \tag{3.4.1}$$

Equivalently, the discrete pair $\{\Phi,\Gamma\}$ is controllable iff,

$$\text{rank}\,[zI-\Phi \quad \Gamma] = n \qquad \text{for all } z \tag{3.4.2}$$

which can alternatively be stated as,

$$\text{rank}\,[\Gamma \quad \Phi\Gamma, \ldots, \Phi^{n-1}\Gamma] = n \tag{3.4.3}$$

Non-singularity of the controllability matrix is sufficient to ensure that any initial state x[kT] can be transferred to an arbitary state x[(k+n)T].

Canonical forms are generated by applying a similarity transformation T_c to $\{\Phi,\Gamma\}$. T_c is obtained by appropriate arrangement of the linearly independent columns of the *controllability* (or reachability) matrix $[\Gamma_1\ \Phi\Gamma_1\ ,\ldots,\ \Phi^{n-1}\Gamma_1]$. Two particular arrangements (which influence the internal operation of the system in different ways) are examined. Both are termed controller canonical forms (Kailath, 1980). A controllable discrete-time triple (Φ,Γ,C) with n=9, m=3 is assumed for both cases.

The transformation matrix for the first canonical form is determined by the following procedure:

(i) Select the first column of discrete control matrix Γ, say Γ_1. Collect the maximum number of linearly independent columns from $[\Gamma_1\ \Phi\Gamma_1\ ,\ldots,\ \Phi^{n-1}\Gamma_1]$. The power of Φ for the last independent vector is denoted l_1-1. The process is continued for all columns $\{\Gamma_i\}$, i=1,..,m until n independent vectors have been collected. That is, $\sum l_i = n$, i=1,..,m. The combined vectors will form matrix M_{c1}:

$$M_{c1} = [\Gamma_1\ ..\ \Phi^{l1-1}\Gamma_1,\ \Gamma_2\ ..\ \Phi^{l2-1}\Gamma_2,\ldots,\ \Gamma_m\ ..\ \Phi^{lm-1}\Gamma_m] \tag{3.4.4a}$$

Assume for this example that $\{l_i\}=[4\ 3\ 2]$. Define,

$$m_i = \sum_{j=1}^{i} l_j \qquad i=1,..,\hbar \quad \hbar<m \tag{3.4.4b}$$

and M_{ci} as the m_i'th row of M_c^{-1}. Transformation T_{c1} is defined:

$$T_{c1} = \begin{bmatrix} M_{c1} \\ M_{c1}\Phi \\ M_{c1}\Phi^2 \\ M_{c1}\Phi^{l1-1} \\ - - - - - \\ M_{c2} \\ M_{c2}\Phi \\ M_{c2}\Phi^{l2-1} \\ - - - - - \\ M_{c3} \\ M_{c3}\Phi^{l3-1} \end{bmatrix} \tag{3.4.4c}$$

(ii) Perform a change of basis, $x=T_{c1}^{-1}z$ such that,

$$z[(k+1)T] = T_{c1}\Phi T_{c1}^{-1}z[kT]) + T_{c1}\Gamma u[kT]$$

$$y[(k+1)T] = CT_{c1}^{-1}x[(k+1)T] \tag{3.4.4d}$$

This produces $\Phi_{c1}=T_{c1}\Phi T_{c1}^{-1}$, $\Gamma_{c1}=T_{c1}\Gamma$, which are of the form,

$$\Phi_{c1} = \left[\begin{array}{cccc|ccc|cc} 0 & 1 & 0 & 0 & 0 & 0 & 0 & 0 & 0 \\ 0 & 0 & 1 & 0 & 0 & 0 & 0 & 0 & 0 \\ 0 & 0 & 0 & 1 & 0 & 0 & 0 & 0 & 0 \\ x & x & x & x & x & x & x & x & x \\ - & - & - & - & - & - & - & - & - \\ 0 & 0 & 0 & 0 & 0 & 1 & 0 & 0 & 0 \\ 0 & 0 & 0 & 0 & 0 & 0 & 1 & 0 & 0 \\ x & x & x & x & x & x & x & x & x \\ - & - & - & - & - & - & - & - & - \\ 0 & 0 & 0 & 0 & 0 & 0 & 0 & 0 & 1 \\ x & x & x & x & x & x & x & x & x \end{array}\right] \qquad \Gamma_{c1} = \left[\begin{array}{ccc} 0 & x & x \\ 0 & x & x \\ 0 & x & x \\ 1 & x & x \\ - & - & - \\ 0 & 0 & x \\ 0 & 0 & x \\ 0 & 1 & x \\ - & - & - \\ 0 & 0 & 0 \\ 0 & 0 & 1 \end{array}\right] \tag{3.4.4e}$$

where 'x' denotes an element that may or may not by 0.

The effect of transformation T_{c1} on $\{\Phi,\Gamma\}$ is to create partial subsystems (the diagonal blocks of Φ_{c1}) interacting with each other by the 'x' rows of the Φ_{c1} matrix. The partial systems are of dimension $(l_i x l_i)$ and are in a lower companion form. The 'x' rows of the Γ_{c1} matrix indicate that the partial decoupling between subsystems intially requires possibly all m inputs. The number of control inputs participating in setting up this interaction decreases by 1 at each stage of decoupling and finally the system is reduced to a single input task at the last diagonal block (as indicated by the single 1 in the last control matrix block).

The second canonical form is produced by a different method of selecting n linearly independent column vectors from the controllability matrix. This is outlined below:

(i) Select the first n linearly independent column vectors from controllability matrix $[\Gamma\ \Phi\Gamma\ ,\ldots,\ \Phi^{n-1}\Gamma]$ and rearrange them to form:

$$M_{c2} = [\Gamma_1\ \Phi\Gamma_1\ ,..,\ \Phi\mu 1-1\Gamma_1\ \Gamma_2,..,\ \Phi\mu 2-1\Gamma_2\ \Gamma_m,..,\ \Phi\mu m-1\Gamma_m] \quad (3.4.5a)$$

Proceed with the formulation of transformation matrix T_{c2} as indicated for (3.4.4) above with the following exception:

$$m_i = \sum_{j=1}^{i} \mu_j \qquad i=1,..,m \qquad (3.4.5b)$$

(ii) Perform change of basis, $z=T_{c2}^{-1}x$ as before. If $\{\mu_i\}=[4,3,2]$ is assumed, this will generate the system $\{\Phi_{c2},\Gamma_{c2},C_{c2}\}$ with,

$$\Phi_{c2} = \left[\begin{array}{cccc|ccc|cc} 0 & 1 & 0 & 0 & 0 & 0 & 0 & 0 & 0 \\ 0 & 0 & 1 & 0 & 0 & 0 & 0 & 0 & 0 \\ 0 & 0 & 0 & 1 & 0 & 0 & 0 & 0 & 0 \\ x & x & x & x & 0 & 0 & 0 & 0 & 0 \\ - & - & - & - & - & - & - & - & - \\ 0 & 0 & 0 & 0 & 0 & 1 & 0 & 0 & 0 \\ 0 & 0 & 0 & 0 & 0 & 0 & 1 & 0 & 0 \\ x & x & x & x & x & x & x & 0 & 0 \\ - & - & - & - & - & - & - & - & - \\ 0 & 0 & 0 & 0 & 0 & 0 & 0 & 0 & 1 \\ x & x & x & x & x & x & x & x & x \end{array}\right] \qquad \Gamma_{c2} = \left[\begin{array}{ccc} 0 & 0 & 0 \\ 0 & 0 & 0 \\ 0 & 0 & 0 \\ 1 & x & x \\ - & - & - \\ 0 & 0 & 0 \\ 0 & 0 & 0 \\ 0 & 1 & x \\ - & - & - \\ 0 & 0 & 0 \\ 0 & 0 & 1 \end{array}\right] \qquad (3.4.5e)$$

In contrast to Φ_{c1}, the coupling between the diagonal blocks of Φ_{c2} is strictly one way. *Furthermore, a fixed number of inputs are assigned to a particular subsystem.* This form of interaction and control input allocation is represented diagramatically in Figure 3.4.1. If,

$$\Phi_{c2} = \left[\begin{array}{ccc} \Phi_{11} & \Phi_{12} & \Phi_{13} \\ \Phi_{21} & \Phi_{22} & \Phi_{23} \\ \Phi_{31} & \Phi_{32} & \Phi_{33} \end{array}\right]$$

then in Figure 3.4.1 S_1, S_2, S_3 represent the partial systems formed by the $(\mu_i x \mu_i)$ digonal blocks Φ_{11}, Φ_{22}, Φ_{33}, while the intersection of (S_i) denote the couplings between the different subsystems. Control inputs u_1, u_2 and u_3 are assigned to subsystem S_1, and inputs u_2, u_3 are assigned to S_2 etc. Thus the intersection $S_1 \cap S_2$ corresponds to Φ_{21}, whilst $S_1 \cap S_3$ corresponds to Φ_{31}, $S_2 \cap S_3$ to Φ_{32} etc.

Clearly, the controller canonical forms are convenient ways of enforcing particular relationships between control inputs and state vectors. In particular, the transformations T_{c1} and T_{c2} provide different means of *distributing* control effort to the system as a whole and also to specific subsystems. The first method of selecting a suitable canonical basis tends to allocate the greatest control task to the first partial subsystem Φ_{11} and the least to subsystem Φ_{33}. This is due to the priority given to Γ_1 in selecting the basis vectors. This method of prioritising control inputs may result in some control inputs not participating in setting up the canonical form at all. A further

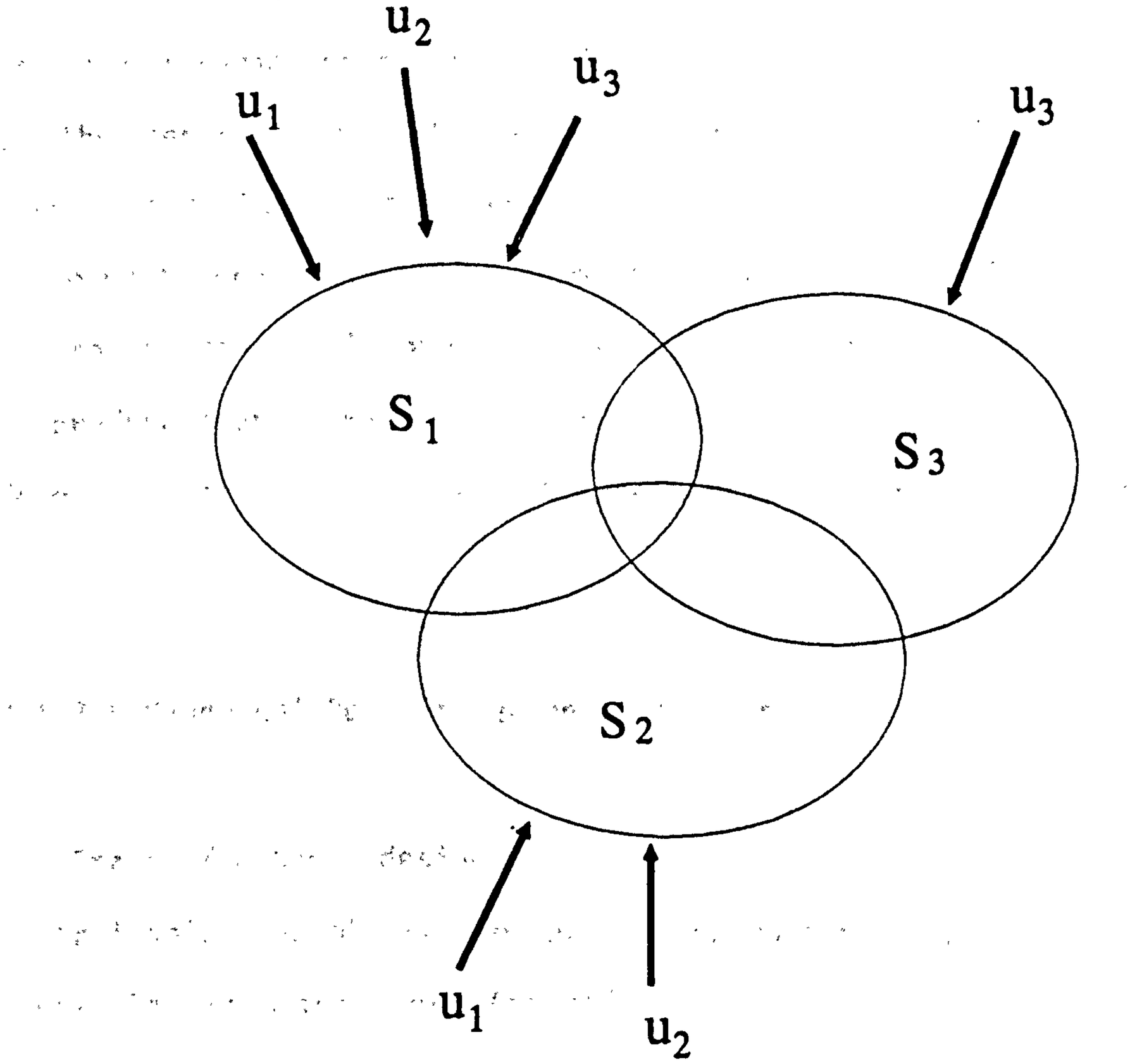

Figure 3.4.1 The allocation of inputs and subsystem interaction in the canonical system of (3.2.5)

point worth noting is that dimensions of the diagonal blocks of Φ_{c1} vary dependending on the ordering of the control matrix columns. In this respect, Φ_{c1} cannot strictly be termed canonical since canonical implies the existence of unique cyclic blocks (Gantmacher, 1959) but is commonly referred to as such in many texts.

A more evenly distributed control input effort is generated by the second canonical form of Φ_{c2}, Γ_{c2}. This form generally utilises all available control inputs in a well defined manner to set up a much stricter interaction between different subsystems. The special structure of the second canonical form was identified by Popov, (1972) to be useful in certain control applications (in particular, the general pole assignment problem). This form is thus referred to as the Popov controller canonical form. Of particular interest is the set (μ_i) used to produce transformation T_{c2}. Unlike the indices of the first canonical form, the set (μ_i) is invariant irrespective of control input ordering.

3.4.2 A Canonical Pole Assignment Algorithm

State feedback design using a preliminary transformation of a controllable and observable continuous system triplet (A,B,C) to the controller canonical form (as defined by Popov) requires the following design stages:

(i) Perform a change of basis $x=T^{-1}z$,

$$\dot{z}(t) = TAT^{-1}z(t) + TBu(t) \qquad (3.4.6a)$$

where $A_{c2} = TAT^{-1}$, $B_{c2} = TB$ are in the Popov controller canonical form.

(ii) Apply change of basis to control inputs u. i.e.,

$$u(t) = Gw(t) \tag{3.4.6b}$$

such that each transformed control input component of w acts only on one subsystem of A_{c2}. If the associated minimal column indices are $\{\mu_i\}$, this gives an open loop description:

$$\dot{z}(t) = A_{c2}z(t) + B_{c2}Gw(t) \tag{3.4.6c}$$

where $B_{c2}G$ is a (nxm) matrix with all zero elements except for 1's in the $(\mu_i+1,\ i)$'th, i=1,..,m positions.

(iii) Introduce state feedback,

$$w(t) = Kz(t) \tag{3.4.6d}$$

such that desired closed poles are assigned to the transformed system $\{A_{c2},\ B_{c2}G\}$.

For the single input case, a direct calculation of the feedback gain matrix K based on the above procedure is provided by the Bass–Gura algorithm (Kailath, 1980):

$$K = [P_{CL}(s)-P(s)](\Theta^{-1})^T M_{c2}^{-1} \tag{3.4.6e}$$

where P(s) is the open loop polynomial,

$$P(s) = \det(sI-A) = s^n + a_1s^{n-1} + a_2s^{n-1} + a_3s^{n-1} + .. + a_n$$

and P_{CL} is an arbitary closed loop polynomial:

$$P_{CL}(s) = \det(sI-A+BK)$$

The matrix Θ is a lower triangle Toeplitz matrix with first column $[1\ a_1\ a_2\ \ldots\ a_n]^T$.

A direct formula for the multi-input case is more involved. Stages (i) and (ii) facilitate the pole shifting task by isolating the μ_i'th or γ_i'th rows which are to be changed to produce the desired closed loop characteristics. If the open loop and desired closed loop μ_i'th (or γ_i'th) rows are denoted $P_{\mu i}$, $P_{CL\mu i}$ (or $P_{\gamma i}$, $P_{CL\gamma i}$) respectively and polynomial $k_{T\mu i}$ ($k_{T\gamma i}$) is defined as the difference $k_{T\mu i}=P_{\mu i}-P_{CL\mu i}$ ($k_{T\gamma i} = P_{\gamma i}-P_{CL\gamma i}$) then a multi-input feedback matrix can be determined from:

$$K=G^{-1}(N-M)T_{c2} \qquad (3.4.6f)$$

$$N = \begin{bmatrix} P_{\mu 1} \\ \vdots \\ P_{\mu m} \end{bmatrix} \qquad M = \begin{bmatrix} k_{T\mu 1} \\ \vdots \\ k_{T\mu m} \end{bmatrix}$$

(Details of this design procedure are contained in D'Azzo and Houpis, 1981). Closed loop system behaviour, in the original system co-ordinates is then described by,

$$\dot{x}(t) = [A+BGKT]x(t) \qquad (3.4.7)$$

An interesting feature of the closed loop system is that it maintains its open loop internal block coupling (as indicated by equations (3.4.4e), (3.4.5e) or Figure 3.4.1). The invariance of $\{\mu_i\}$ under feedback was first recognised by Kalman (1972) and Popov (1972). The following section represents this property by pencil equivalence

relations of the open loop and closed loop systems. The link between the necessary MIFO mulitrate controllability conditions and $\{\mu_i\}$ can be established by considering the *internal* multirate system description in relation to the single rate feedback control problem.

3.4.3 Pencil Equivalence Relations

Now, consider the singular matrix pencils of the single rate and multirate systems. Further, define the strictly proper equations of an open loop single rate system by the (n+p) x (n+m) singular pencil,

$$H(z) = \begin{bmatrix} zI-\Phi & \Gamma \\ C & 0 \end{bmatrix} = \begin{bmatrix} H_1(z) \\ H_2(z) \end{bmatrix} \tag{3.4.8}$$

and define,

$$H_c(z) = \begin{bmatrix} zI-\Phi_c & \Gamma_c \\ C_c & \end{bmatrix} = \begin{bmatrix} H_{c1}(z) \\ H_{c2}(z) \end{bmatrix} \tag{3.4.9}$$

as the singular matrix pencil of the desired closed-loop single rate system. Then, $H(z)$ and $H_c(z)$ are said to be *strictly equivalent* (Gantmacher, 1959; Kailath, 1981; Kalman, 1972) iff,

$$H(z) = L\, H_c(z)\, R \tag{3.4.10}$$

where L, R are constant, non-singular matrices of the form,

$$L = \begin{bmatrix} L_{11} & L_{12} \\ 0 & L_{22} \end{bmatrix} \qquad R = \begin{bmatrix} R_{11} & 0 \\ R_{21} & R_{22} \end{bmatrix} \tag{3.4.11}$$

This equivalence is characterised by a set of invariants known as the

Kronecker invariants (Kalman, 1972). For an examination of state feedback control only $H_1(s)$ and $H_{c1}(s)$ are of interest for which a subset of the Kronecker invariants, the minimal column indices denoted μ_i, are pertinent. Considering the relevant feedback system elements only, equation (3.4.11) reduces to,

$$H_1(z) = L_{11}\, H_{c1}(z) \begin{bmatrix} R_{11} & 0 \\ R_{21} & R_{22} \end{bmatrix} \tag{3.4.12}$$

For state feedback, a suitable form for L and R (as defined by the Popov controller canonical pole placement algorithm of Section 3.4.2) is,

$$L_{11} = T_c \qquad R = \begin{bmatrix} T_c^{-1} & 0 \\ KT_c^{-1} & G \end{bmatrix} \tag{3.4.13}$$

with det $G \neq 0$ and an arbitary feedback matrix K. If now, the singular matrix pencil of the desired closed-loop multirate system is defined as,

$$H_m(z) = \begin{bmatrix} zI-\Phi_m & \Gamma_m \\ C_m & 0 \end{bmatrix} = \begin{bmatrix} H_{m1}(z) \\ H_{m2}(z) \end{bmatrix} \tag{3.4.14}$$

then $H(z)$ and $H_m(z)$ are related by,

$$H(z) = S_L\, H_m(z)\, S_R \tag{3.4.15}$$

S_L and S_R can be further decomposed,

$$S_L = LP \qquad S_R = QR \tag{3.4.16}$$

The L, R matrices are concerned with the feedback properties and matrices P, Q encapsulate the multirate properties. A distinctive feature of these matrices is that controllability is invariant under R

and observability is invariant under L. Thus for (3.4.15) to hold with feedback in the multirate case, the controllability and observability properties must be maintained by a suitable choice of open-loop multirate system matrices. P and Q will reflect this suitability.

For state feedback applied to a MIFO multirate system described by Section 2.5, P and Q are of the form,

$$P = \begin{bmatrix} I & 0 \\ I & I \end{bmatrix} \qquad Q = \begin{bmatrix} I & 0 \\ 0 & Q_{22} \end{bmatrix} \tag{3.4.17}$$

P obviously does not affect any properties. A suitable Q can be produced by a choice of input sample rates such that $n_i > \mu_i$. Scalars μ_i are the minimal column indices of the single rate system (Section 3.4.1 has outlined a method for the determination of μ_i).

The minimal column indices $[\mu_1\ \mu_2\ ..\ \mu_m]$ of a controllable pair $[\Phi\ \Gamma]$ are defined such that,

$$\det [\ \Gamma_1\ ..\ \Phi^{\mu 1-1}\Gamma_1,\ \Gamma_2\ ..\ \Phi^{\mu 2-1}\Gamma_2\ ,...,\ \Gamma_m\ ..\ \Phi^{\mu m-1}\ ] \neq 0 \tag{3.4.18a}$$

$$n = \sum_{i=1}^{m} \mu_i \qquad \text{where } \Phi\ \epsilon\ R^n \tag{3.4.18b}$$

are satisfied. They are, in fact, equivalent to the minimal column indices related to the continuous system pencil [sI-A B] for almost all T (main interval of sampling). An examination of the controllability condition shows that this correspondence fails when,

$$T = \frac{2k\pi}{Im[w_i - w_j]} \qquad k=\pm 1,\ \pm 2,\ \pm 3,.... \tag{3.4.19}$$

where $\{z_i\} = \exp(jw_iT)$, i=1,..n are the discrete system poles. Likewise, multirate controllability and observability is not ensured if any sample

rate T/n_i satisfies (3.4.19) (Al-Rahmani and Franklin, 1990). These conditions simply ensure that the rate of monitoring the input/ouput behaviour does not correspond to the characteristic frequency of any mode. A correspondence would clearly render that particular mode 'invisible' at the input/output.

The role of the minimal column indices in the determination of MIFO multirate (Φ_{MRI},Γ_{MRI}) invariant subspaces is now defined:

Consider the controllable discrete system triple $\{\Phi,\Gamma,C\}$. The system can be transformed to a controller canonical form by a change of basis T_{c2} such that the vector $z=T_{c2}^{-1}x$ lies in the controllable vector space $S_c \epsilon R^n$. S_c can be further decomposed into a set of invariant subspaces, $\{S_i \epsilon R^{\eta i}\}$, which have no vector in common except the null vector and,

$$S_c = \{S_i\} \qquad i=1,..,m \qquad (3.4.20)$$

S_i are defined as the (Φ,Γ) invariant subspaces since, by definition of the similarity transformation T_{c2},

$$\Phi\Gamma_i \epsilon S_i \qquad \text{for all } \Gamma_i \epsilon S_i \qquad (3.4.21)$$

(Γ_i is the ith input column of the discrete input matrix). The dimension of the single rate (Φ,Γ) subspaces are determined by the minimal column indices of the triple $\{\Phi,\Gamma,C\}$, i.e. $\eta_i=\mu_i$. Indices $\{\mu_i\}$ clearly define fundamental structural properties of the system which are invariant irrespective of the choice of basis. These structural properties can be usefully exploited when assigning poles by MIFO sampled feedback control.

The multirate controllability selection criterion of (3.4.18b) matches that of (3.4.4b) and (3.4.5b) in the development of single rate canonical forms. A selection of input sample rates $n_i = \mu_i$, $n_i = l_i$ will thus ensure MIFO controllability. Furthermore, this choice of input

sample rates will produce $(S_i \in R^{\eta i})$ with $(\eta_i)=(1)$ for $i=1,..,\sum n_i=n$. In this way, a maximum number of S_i are produced from a decomposition of the single rate (Φ,Γ) invariant subspaces. Multirate systems with this choice of input sample rate are said to possess *maximal* $(\Phi_{MR1},\Gamma_{MR1})$ *invariant subspaces* (Fessas, 1979; Gantmacher, 1956; Kono et al, 1991).

One use of this unique feature in the MIFO multirate state feedback pole assignment problem is outlined in the following section.

3.5 A Multirate Pole Assignment Algorithm

The equivalence relations of the open and closed loop system detailed in Section 3.4.3 can be extended to formulate a simple MIFO multirate pole assignment algorithm. This section derives this pole assignment algorithm. The algorithm is based on the multirate controller canonical form generated using input sample multiplicities (μ_i) or (l_i). The applicability of this algorithm to design MIFO feedback control systems is investigated by two examples.

Consider the application of the pole assignment procedure of Section (3.4.2) to a MIFO system whose input sample rates are chosen to be the set (μ_i/T) or (l_i/T). For this class of MIFO systems, a change of basis $T_{c2}=\Gamma_{MR1}^{-1}$ presents itself as an appropriate candidate for the achievement of stage (i). This is to be expected since a suitable transformation is selected from n independent vectors of matrix $[\Gamma_{MR1}\ \Phi_{MR1}\Gamma_{MR1}\ ..\ \Phi_{MR1}^{n-1}\Gamma_{MR1}]$ and $\Gamma_{MR1} \in R^n$.

If Γ_{MR1} is selected as the basis of the controllable subspace then the need for G, (the change of basis that is normally required on the control vector in stage(ii)) is obviated. A choice of transformation $T_{c2}=\Gamma_{MR1}^{-1}$ automatically produces the necessary input decoupling effect. This would indicate that the MIFO system with input rates (μ_i/T) possesses an internal structure akin to the Popov controller canonical form. Thus, the MIFO pole placement problem is expected to be a more

direct formulation than that outlined in (3.4.6) above. This is confirmed below.

State feedback pole assignment of a multirate controllable MIFO system using the Popov controller canonical form ($T_{C2} = \Gamma_{MR1}^{-1}$, G=I) can be summarised by the internal relationship between the open loop and closed loop multirate systems as follows.

If H_M is the singular matrix pencil of the desired closed loop system (as given in Section 3.3) which is to be obtained from the open loop system H_{MOL} then the two satisfy:

$$H_{MOL1}(z) = \Gamma_{MR1}\, H_{M1}(z) \begin{bmatrix} \Gamma_{MR1}^{-1} & 0 \\ K\Gamma_{MR1}^{-1} & I \end{bmatrix} \qquad (3.5.1)$$

where,

$$H_{MOL1}(z) = [zI - \Phi_{MR1} \quad \Gamma_{MR1}] \qquad H_{M1}(z) = [zI - \Phi_M \quad \Gamma_M] \qquad (3.5.2)$$

are the upper portions of the open and closed loop singular pencils respectively, and K is the required feedback matrix. This equivalence relation yields the expression for K as:

$$K = \Gamma_{MR1}^{-1}(\Phi_M - \Phi_{MR1}) \qquad (3.5.3)$$

which is much simpler than the corresponding single rate formula (given in Section 3.4.2).

Thus far, the difference in MIFO system performance produced from selecting $\{\mu_i/T\}$ or $\{l_i/T\}$ has not been mentioned. Chapter 5 will examine the details of this issue. For the present study it will suffice to say that both choices of input sample rate multiplicities will satisfy multirate controllability conditions and also yield simpler canonical pole placement algorithms. The applicability of the feedback

design algorithm of (3.5.3) is examined below with two examples.

Example 3.5.1

The system to be examined (D'Azzo and Houpis, 1981) is described by the continuous-time state matrices:

$$A = \begin{bmatrix} 0 & 1 & 0 \\ 0 & 0 & 1 \\ -6 & -11 & -6 \end{bmatrix} \quad B = \begin{bmatrix} 1 & 1 \\ 0 & 1 \\ 1 & 1 \end{bmatrix} \quad C = I_n \tag{3.5.4}$$

The open loop poles of this system are {-1 -2 -3}. A multirate feedback matrix is to be designed such that closed loop poles {-0.5 -0.6 -0.7} are assigned. The main interval of sampling is selected to be T=0.1 secs (this does not render any of the modes uncontrollable). The MIFO controllability criterion indicates the input sample rates $T_1=T/2$, $T_2=T$.

Applying the pole placement algorithm of (3.5.3) with this choice of sample rates determines the feedback matrix as (the derivation of this gain matrix is detailed in Appendix B):

$$K = \begin{bmatrix} -90.9383 & 142.5186 & -133.8662 \\ 67.8615 & -100.5865 & 111.0562 \\ 1.5504 & -11.4956 & 10.9277 \end{bmatrix} \tag{3.5.5}$$

Example 3.5.2

The system to be examined (Hagiwara and Araki, 1988) is described by the continuous system triple,

$$A = \begin{bmatrix} 2 & 0 & 0 & 0 \\ 2 & -1 & 0 & 0 \\ -1 & 0 & -3 & 0 \\ 1 & 0 & 0 & -2 \end{bmatrix} \quad B = \begin{bmatrix} 0 & 0.5 \\ 1 & 0 \\ 1 & 0 \\ 0 & 1 \end{bmatrix} \quad C = I_3 \tag{3.5.6}$$

The eigenvalues of A are {-2 -1 -3 -2}. The open loop poles are to be moved by feedback to {-2.5 -1.5 -2.1 -0.5}. The main sample period is chosen to be t=0.4 secs. The input sample rates are determined to be $T_1=T_2=T/2$ (from the multirate controllability criterion). Applying the pole assignment design algorithm of (3.5.3) to the MIFO system produced by this choice of sample parameters determines the following feedback matrix:

$$K = \begin{bmatrix} 7.9792 & -27.6307 & 10.9033 & -7.5180 \\ -5.0800 & 16.3543 & -6.6323 & 9.4079 \\ -22.3789 & 7.1449 & 14.3609 & -14.4975 \\ 15.2851 & -2.5259 & -21.4240 & 21.4277 \end{bmatrix} \qquad (3.5.7)$$

The above design examples show that a drawback (and a characteristic) of this canonical pole assignment algorithm is that the feedback matrices have very high gain elements. This feature is clearly undesirable. The large magnitude of the first feedback matrices would be highly impractical to implement. The elements of the second gain matrix are not very large. This is due to the fairly decoupled open loop system selected by Hagiwara and Araki, (1988) to demonstrate the application of their multirate feedback design technique. Such well decoupled open loop modes are not often encountered in real systems but does simplify the multirate feedback control design task considerably. This point will be demonstrated further by Example 5.4.2 in Chapter 5.

A suitable measure for the overall magnitude of a feedback matrices is its associated 2-norm, $\|K\|_2$. $\|K\|_2$ is defined as the maximum positive value of $(K^{*T}K)^{1/2}$ (Golub and Van Loan, 1973). The $\|K\|_2$ of the feedback matrices of (3.5.5) and (3.5.7) are 271.4602 and 45.7873, respectively.

3.6 STABILITY ANALYSIS OF MULTIRATE CLOSED LOOP SYSTEMS

This section examines the effect of T on the stability of MIFO sampled closed loop systems designed using a canonical pole assignment algorithm based on equation (3.5.3) (Albertos, 1990). In order to derive an analytic expression for the closed loop system gain margins $\gamma = [\gamma_{min}\ \gamma_{max}]$, the allowable closed loop system is confined to be a scalar contraction of the open loop system. This effectively restricts the assignment of closed loop poles to specific regions in the z-plane and may not be suited to all applications. The scalar contraction assumption does however, allow the role of T in determining closed loop system stability to be demonstrated with relative ease.

A feature of multirate control systems that is frequently observed by researchers is the flexibility in performance and stability robustness offered by the variation of input/ouput sample rates (Albertos, 1990; Francis and Gorgiou, 1988; Hagiwara and Araki, 1988; Kargonekar et al, 1985; Serrano and Ramadage, 1991). Stability robustness is demonstrated in Section 3.6.2 by observing the effect of a variation in T on gain margins γ for an example system.

3.6.1 GAIN MARGIN BOUNDS

For robustness analysis it is common practice to consider the effect of perturbations or uncertainty in open loop dynamics on the closed loop system. A source of uncertainty that needs particular attention in the MIFO feedback problem is that contained in control matrix Γ_{MR1}, since this *predicts* forthcoming intersample state values during interval T. If inaccuracies of this predictive matrix are represented by a scalar γ, i.e. the true plant behaviour is described by,

$$x[(k+1)T] = \Phi_{MR1}x[kT] + \gamma\Gamma_{MR1}u_e[kT] \qquad (3.6.1)$$

then applying feedback $u_e[kT] = Kx[kT]$, where K is determined from the algorithm of equation (3.5.3), gives the closed loop expression,

$$x[(k+1)T] = [\Phi_{MR1} + \gamma\{\Phi_M - \Phi_{MR1}\}]\, x[kT] \qquad (3.6.2)$$

If the choice of closed loop dynamics is restricted such that $\Phi_M=\alpha\Phi_{MR1}$ then (3.6.2) can be written as:

$$\begin{aligned} x[(k+1)T] &= [1+\gamma(\alpha-1)]\Phi_{MR1}x[kT] \\ &= \Phi_{CL}x[kT] \end{aligned} \qquad (3.6.3)$$

For asymptotic stability, the eigenvalues of the closed loop system $\{\lambda_i[\Phi_{CL}]\}$ must lie within the unit circle, i.e.,

$$|\lambda_i[\Phi_{CL}]| < 1 \qquad (3.6.4)$$

Since the closed loop dynamics are constrained to a scalar contraction α of the open loop system, the closed loop eigenvalues are defined $\{\lambda_i[\Phi_{CL}]\} = \alpha\{\lambda_i[\Phi_{MR1}]\}$. Condition (3.6.4) can thus be stated as:

$$[1+\gamma(\alpha-1)]\ |\lambda_i[\Phi_{MR1}]| < 1 \qquad i=1,..,n \qquad (3.6.5)$$

If $\lambda_{MAX} = [\max_i\ |\lambda_i[\Phi_{MR1}]|\ ]^{-1}$ then a rearrangment of (3.6.5) determines the uncertainty bounds for closed loop stability as,

$$\gamma MIN = \frac{1-\lambda MAX}{1-\alpha} < \gamma < \frac{1+\lambda MAX}{1-\alpha} = \gamma MAX \qquad (3.6.6)$$

A closed loop system satisfying the above conditions is said to be

stable for all $\gamma \in [\gamma_{MIN}\ \gamma_{MAX}]$. For a given open loop system λ_{MAX} is fixed (since this is a function of the maximum open loop eigenvalue), thus a means of varying γ for a given system can only be provided by α. A low α will yield increased gain margins. This effectively implies a lower value of T which in turn, demands greater control effort. The reason for the increased control demand can be attributed to the fact that $K \propto (1-\alpha)\Phi_{MR1}$. A more detailed analysis of the role of T in determining gain margins given by (3.6.6) is demonstrated in the following section.

Note that similar scalar gain margin relations cannot be derived for perturbations (say β) in the open loop transition matrix by simply replacing Φ_{MR1} with $\beta\Phi_{MR1}$ in equation (3.6.7). The reason for this is that Γ_{MR1} incoporates $(\Phi_{MR1})^{1/n_0}$ in its formulation. Thus, perturbations in Φ_{MR1} cause corresponding perturbations in Γ_{MR1} which cannot be represented in a simple manner to derive scalar gain margins. In this case, it is more appropriate to consider the effect of *matrix* perturbations (which are bounded by matrix norms) to provide a more realistic interpretation of multirate stability robustness. The work of Owens and Raya (1982) provides an analysis of this type. This approach considers the effect of *simultaneous* perturbations in the state transition and control matrices on closed loop system stability.

3.6.2 EXAMPLE TO DEMONSTRATE THE EFFECT OF T ON STABILITY

The system to be examined is described by the continuous matrices:

$$A = \begin{bmatrix} 0.4093 & 0.2390 & 0.0659 & 0.5617 \\ 0.5955 & 0.1428 & 0.3004 & 0.4278 \\ 0.9427 & 0.6714 & 0.5768 & 0.4559 \\ 0.0087 & 0.6131 & 0.7263 & 0.3327 \end{bmatrix} \quad B = \begin{bmatrix} 0.0580 \\ 0.6908 \\ 0.6767 \\ 0.9687 \end{bmatrix} \quad C = I_3 \qquad (3.6.7)$$

The eigenvalues of A are {1.7466 -0.2026 -0.0412±j0.04769}, indicating an unstable open loop system. The effect of the main sample interval T on stability robustness can be demonstrated by examining the corresponding variation in gain margins $\gamma = [\gamma_{MIN}\ \gamma_{MAX}]$. The variation cannot be examined for a consistent set of desired closed loop poles due to the contracted closed loop dynamics enforced by the parameter α. However, a useful consistent case for comparison can be presented by examining the scalar gain margin bounds for the *maximum* value of α which produces a stable closed loop system. Plots of α vs T and γ vs T for MIFO state feedback designs will then illustrate the general stability robustness properties.

For this example, the input sample rate multiplicity is required to be 4 to satisfy the multirate controllabity criteria of Section 3.3. The range of main sample intervals $T \in [0.01\ 1]$is examined. Proceeding with the design method outlined in Section 3.6.1 and determining γ, α and $\|K\|$ for each choice of T gives the plots of Figures 3.6.1 and 3.6.2. The following points are noted from these results:

i) The α vs T plot shows that the maximum allowable open loop system contraction α increases with decreasing T (as expected).

ii) The corresponding effect on stability margins γ (Figure 3.6.1b) is a rapid increase in the allowable maximum and minimum gain margins as T approaches 0.01secs. This plot confirms the relation of equation (3.6.6) which indicates increasing gain margins for $T \to 0$.

iii) The $\|K\|$ vs T plot (Figure 3.6.2a) shows that larger gain margins translate as an increase in the demanded control effort.

iv) $\|K\|$ drops away rapidly from its maximum value at T=0.01. A sample interval $T \in [0.01\ 0.075]$ yields an impractical design; no realistic

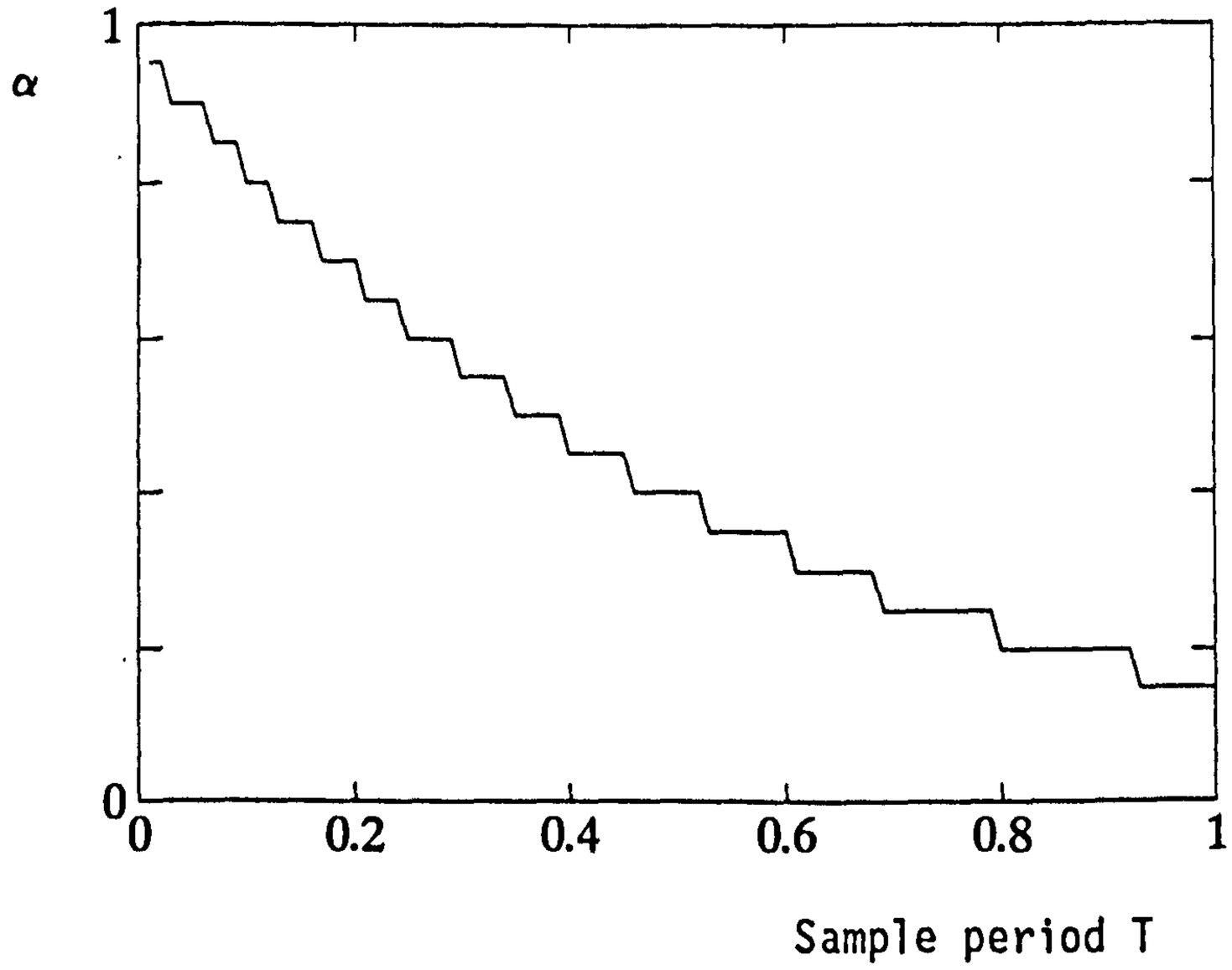

Figure 3.5.1a) α vs T (Scalar contraction vs main sample period vs)

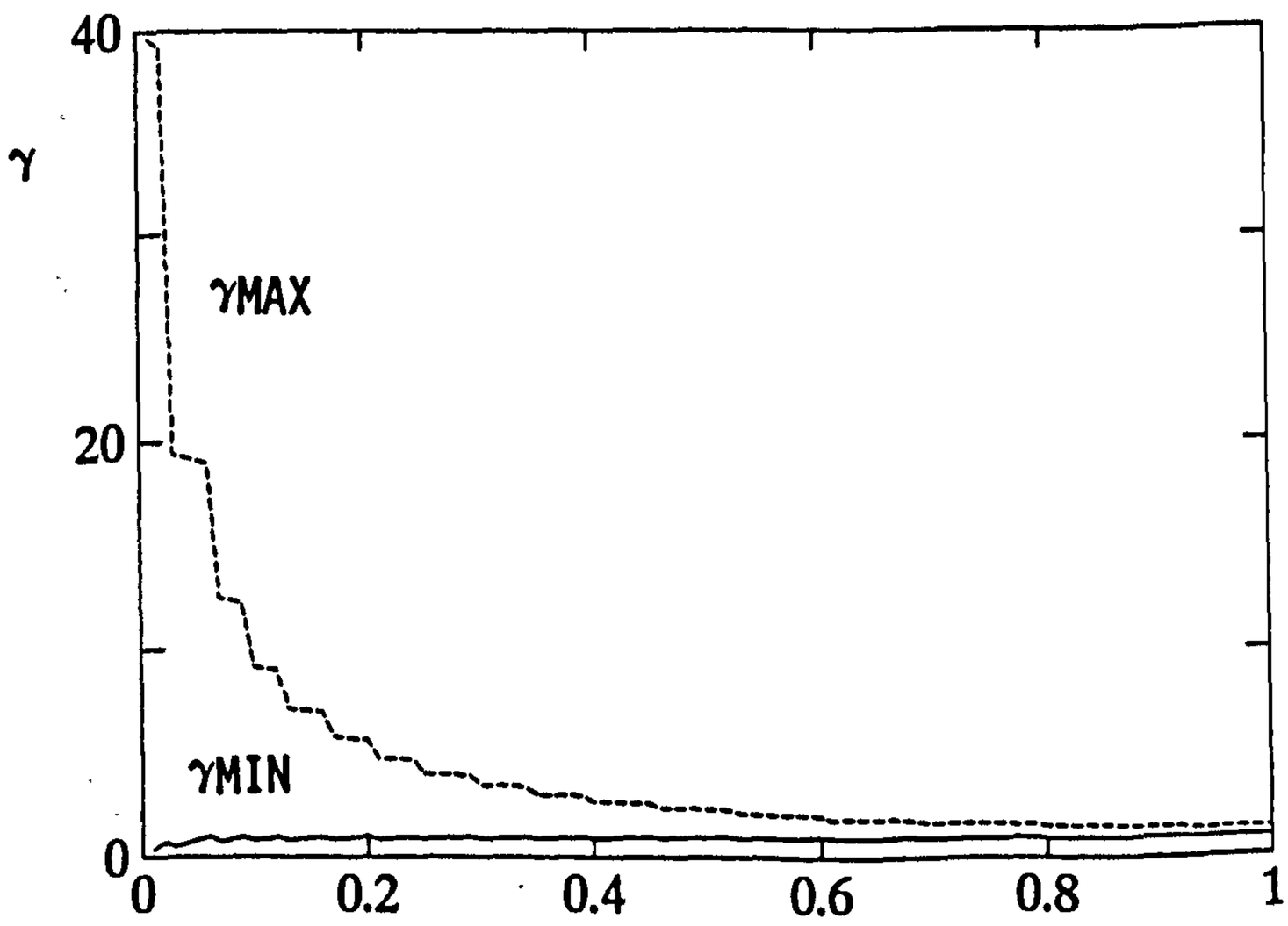

Figure 3.5.1b) γ vs T=[γMIN γMAX] (Gain margins vs main sample period)

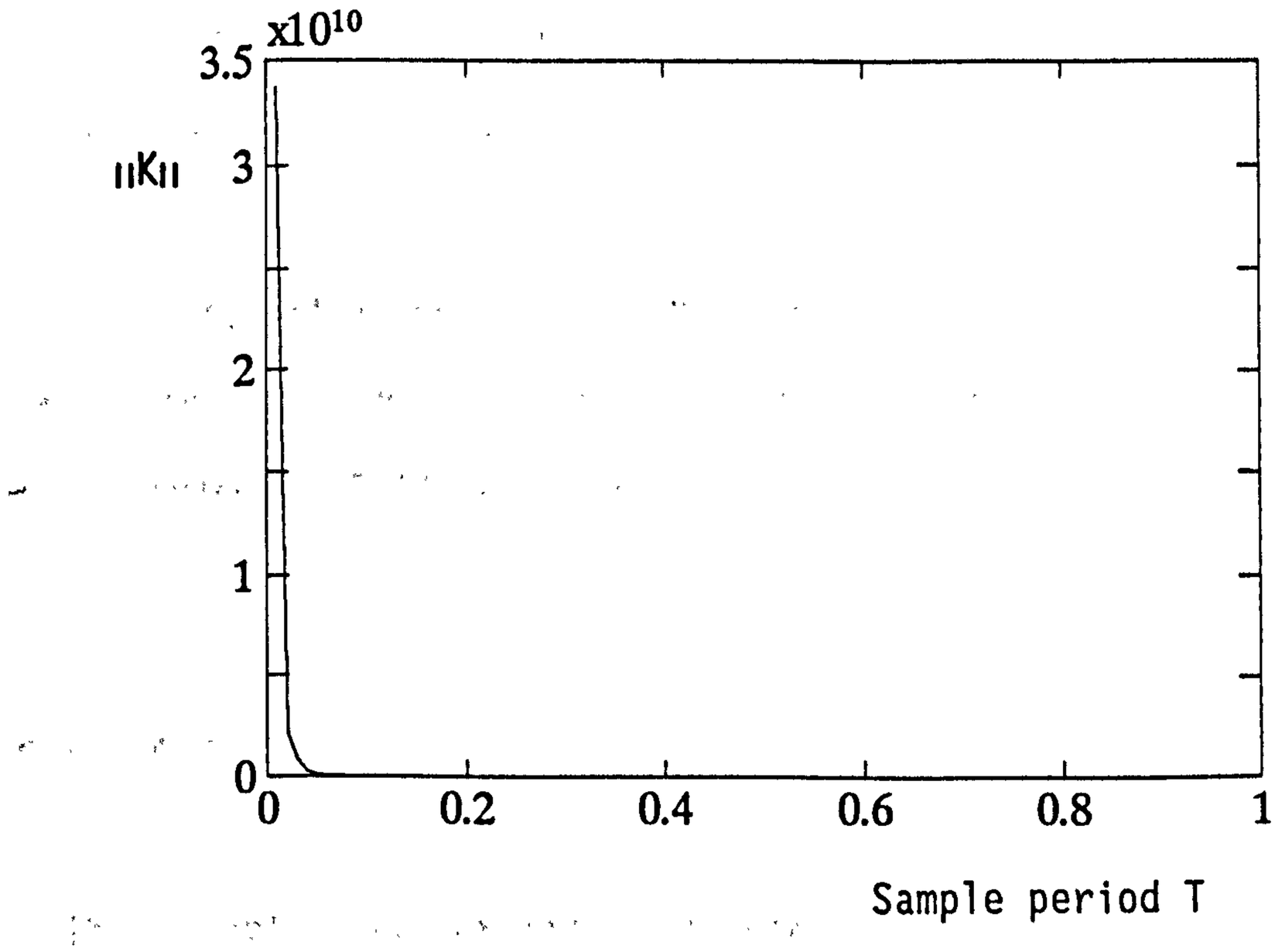

Figure 3.5.2a) ||K|| vs T (Feedback gain norm vs main sample period vs)

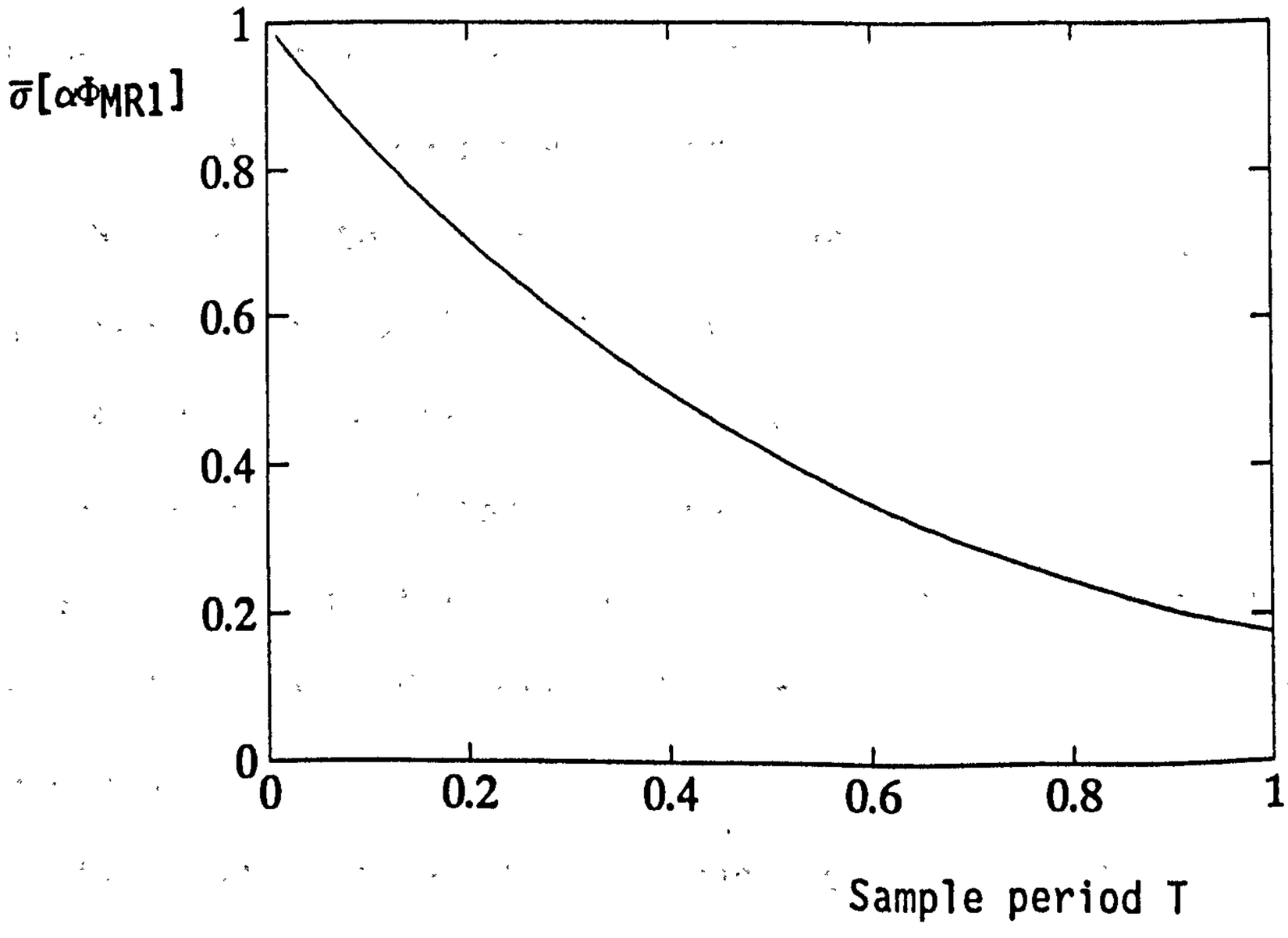

Figure 3.5.2b) $\bar{\sigma}[\alpha\Phi_{MR1}]$ vs T (Maximum singular value of closed loop system transition matrix vs main sample period vs)

control system would be able to generate such large input signals.

v) The $\bar{\sigma}[\Phi_{MR1}]$ vs T plot (Figure 3.6.2b) shows that for this system, $\bar{\sigma}[\Phi_{MR1}] \rightarrow$large as $T \rightarrow 0$. This factor contributes to the increased control demand trend for $T \rightarrow 0$.

When used together the γ and $\|K\|$ plots provide a useful assessment of closed loop system performance. For this particular example, a main sample period $T \epsilon [0.075\ 0.5]$ produces acceptable regions of γ and $\|K\|$.

3.6 SUMMARY

This chapter has examined performance and stablility issues related to the choice of input/output sample rates in MIFO multirate systems.

Section 3.2 examined the role of T in the design of classical feedback discrete control systems. Values of T for which closed loop system stability was guaranteed were determined by the position of discrete system roots with respect to the unit circle in the z-plane. A root locus for varying T was shown to be useful for this purpose.

The multirate controllability and observability conditions were outlined in Section 3.3. The choice of input multirate sample rates to satisfy these properties was shown to be connected to single rate controller canonical forms by use of internal system descriptions. Links between output multirate sample rates and observer canonical forms can be similary derived using duality relations between controllability and observability.

Two particular controller canonical representations were examined, each relating the inputs and states to a different internal structure, characterised by indices sets $\{\mu_i\}$, $\{l_i\}$. In particular, the (A,B) invariance properties of the Popov controller canonical form were shown

to be uniquely defined by the dimension of the diagonal subsystem blocks, $\{\mu_i\}$. The set $\{\mu_i\}$ for a given system is invariant irrespective of the ordering of the system inputs and outputs and relates directly to the controllable subspaces of the system. The set $\{l_i\}$ is dependent on the ordering of system inputs. A choice of input sample rates $\{\mu_i/T\}$, $\{l_i/T\}$ were shown to generate maximal MIFO $(\Phi_{MR1},\Gamma_{MR1})$ *invariance* and was demonstrated to produce a much simpler Popov feedback control algorithm than for the single rate case.

Section 3.5 used the Popov feedback algorithm to design MIFO feedback control for two example systems. Both feedback matrices contained very high gain elements (as monitored by high $\|K\|_2$ figures) which results in high magnitude, switched state and control performance in the closed loop system. Thus, the Popov feedback design algorithm cannot (usefully) be applied to MIFO systems. This observation does in fact, apply to the application of all standard state space feedback design algorithms.

Section 3.6 used the Popov algorithm to investigate the influence of main sample interval on the level of uncertainty allowable in Γ_{MR1} to maintain closed loop stability. The limitations posed by the assumptions used in this analytical formulation are recognised. The technique does, however, provide an idea of the general stability *robustness* to be expected by varying the basic sample rate, T in a very simple manner. (Note that the simplicity and form of the MIFO Popov feedback algorithm is a major contributing factor in the development of this technique.) The general conclusion drawn from this investigation is that stability robustness can be varied by T selection, but at the risk of incurring increased control effort. This confirms the general result voiced by many researchers and furthermore, highlights the practical drawbacks attached to this flexibiliity.

CHAPTER FOUR

EIGENSTRUCTURE ASSIGNMENT

4.1 INTRODUCTION

Chapter 3 highlighted the unique canonical properties of the MIFO sampled system and demonstrated the limited applicability of established state space methods for multirate feedback control design using these properties. One technique that makes direct use of (A,B) and (A,C) invariant subspaces to tailor the closed loop performance of a system is Eigenstructure Assignment. The objective of eigenstructure assignment techniques is to design a state or output feedback matrix which assigns desired closed loop eigenvalues and which simultaneously satisfies other design criteria. The technique is thus capable of making *full* use of the maximal (A,B) invariance conditions generated by the multirate system models.

One useful quality that may be simultaneously designed is the *insensitivity* of the closed loop system to perturbations in the nominal system dynamics (Andry et al, 1983; Burrows, 1990; Byers and Nash, 1989; Cruz et al, 1981; Garg, 1989; Golub and Wilkinson, 1976; Kantor and Andres, 1983; Kautsky et al, 1985; Moore, 1976; Owens and O'Reilly, 1989; Paduano and Downing, 1989; Porter, 1969; Raman and Calise, 1987; Sinswat and Fallside, 1977; Sobel and Shapiro, 1987; Sogaard-Anderson et al, 1986; Srinathkumar and Jategaonkar, 1985; Wilkinson, 1965, 1984). Insensitivity properties contribute to the overall *robustness* of the closed loop system. Another useful quality is the design of low magnitude feedback gains (Burrows, 1990; Owens and Mielke, 1982; Rew et al, 1989; Roppenecker, 1986) to reduce the control effort demanded by the closed loop system. The insensitivity and low feedback gain

properties are particularly useful for the MIFO pole placement problem. A feedback design which incorporates these two qualities will directly minimise the characteristic large magnitude and switched control and state responses of a MIFO system.

This chapter outlines the *robust* eigenstructure assignment problem and defines the performance qualities to be gained from this design approach. The application of robust eigenstructure assignment for the design of continuous-time and single rate discrete control is well established. However, the use of this method to address the multirate pole placement problem is new and, to the author's knowledge, has not been examined elsewhere.

Numerous techniques have been developed to provide solutions to the basic eigenproblem. The unified objective of all *robust* eigenstructure assignment methods is to provide an insensitive feedback control design. Literature on this subject characterises closed loop system robustness in terms of many (different) time and frequency domain performance measures. To provide a distinction between the various robustness characteristics, Section 4.2 outlines some global robustness measures derived from a frequency domain perspective (Cruz et al, 1981; Doyle and Stein, 1981; Lekhtomaki, 1981; Ly, 1983; Safonov, 1981). Singular value plots of appropriate system functions which provide bounding conditions for frequency domain robustness properties are also introduced in Section 4.2.

Section 4.3 describes the output feedback eigenstructure assignment problem. The use of design freedom made available by (A,B), (A,C) invariant subspaces is outlined together with some general rules regarding the robustness properties achievable by a given (A,B,C) triple. The robustness quality obtained using this design technique is the *insensitivity* of the closed loop system eigenstructure to variations in the nominal system dynamics. The variations (or perturbations) may arise from inaccurate identification or modelling, disturbances and

measurement errors. Insensitivity is monitored by the *conditioning* of the closed-loop system right eigenvectors (Kautsky et al, 1985; Wilkinson, 1965, 1984). The vector and matrix conditioning measures which provide suitable design criteria for a robust solution to the general eigenproblem are introduced in Section 4.3.

The appropriateness of using eigenvector conditioning as a measure of system robustness is then examined. Kautsky et al (1985) summarised the relationship between mathematical conditioning measures and general robustness properties. Section 4.4 outlines in some detail, the *precise* effect of the closed loop eigenstructure on system performance robustness as monitored by singular value plots in the frequency domain. This examination is confined to *global* robustness properties of insensitive eigenstructures. The correspondence between the closed loop eigenstructure and MIMO system stability robustness is also examined in some detail in Section 4.4.

The design freedom offered by discrete control structures is reviewed in Section 4.5. The influence of the main sample period on the MIMO performance and stability bounds of the preceding section is also briefly examined.

The MIFO pole placement problem uses the minimal state space descriptions of Chapter 3. This results in a closed loop transition matrix which contains *only* main sample information. The following quote from Francis and Gorgiou (1988) highlights the problems associated with this limitation in the design of general periodic feedback control structures:

" the performance of digital feedback controllers and possible limitations of periodic feedback control, in general, remain important subjects for further research. For instance, it is not known how to compare quantitatively, the improvement in the sensitivity with respect to a certain parameter against a potential deterioration in intersample

behaviour, disturbance attenuation, or even possible increase in the sensitivity to other parameters".

A means of monitoring the sensitivity of multirate intersample behaviour to changes in the nominal system matrices is outlined in Section 4.6. The single rate and continuous time sensitivity measures are extended to cover MIFO multirate intersample performance. This extended analysis is new and, to the author's knowledge, is the first (quantitative) assessment of multirate intersample behaviour. The analysis is based on an expansion of the minimal state space description (which is used for pole placement algorithms) to a non-minimal model once the system is expressed in a closed loop form. The new measures thus derived can be used to monitor the sensitivity of MIFO feedback designs at relevant intersample instants. In particular, the multirate sensitivity measures will enable the design trade-offs between the achievement of right eigenvector conditioning and the reduction in magnitude and switching of control and state responses to be assessed.

Section 4.6 is confined to a theoretical assessment of these effects. The examples of Chapter 5 and 6 will demonstrate clearly the effect of trading off different closed loop system properties.

4.2. FREQUENCY DOMAIN ROBUSTNESS PROPERTIES

For a SISO system whose open loop transfer function is given by G(s), the variation of the system gain $\|G(j\omega)\|$ with frequency ω is a fundamental method of monitoring closed loop system performance. For MIMO systems *vector* gain is used to provide an equivalent measure of system gain. The upper and lower bounds of the vector gain of a MIMO system described by a transfer function matrix G(s) (at any frequency ω) are given by the maximum and minimum singular values $\bar{\sigma}[G(j\omega)]$ and

$\underline{\sigma}[G(j\omega)]$, respectively. These are defined as:

$$\|G(j\omega)\| = \bar{\sigma}[G(j\omega)]$$

$$\|G^{-1}(j\omega)\| = \underline{\sigma}[G(j\omega)]^{-1} \qquad (4.2.1)$$

Since, by the above definition,

$$\underline{\sigma}[G(j\omega)] < \|G(j\omega)\| < \bar{\sigma}[G(j\omega)] \qquad (4.2.2)$$

all possible input/output frequency responses of the MIMO transfer function G(s) are confined to lie in a bounded region.

The *ideal* frequency response of a closed loop system (as bounded by its singular value plots) is shaped according to the different (and conflicting) control problems that the system has to deal with over the low, crossover and high frequency regions. The feedback control problems can generally be classified as uncertainties, disturbances and sensor noise. By considering the impact of these effects on system inputs, outputs and controls, the design requirements to produce a closed loop system with ideal singular value plots can be formulated (Doyle and Stein, 1981; Lekhtomki, 1981; Ly, 1983; Safonov, 1981).

Consider the feedback configuration of Figure 4.2.1. The system has a loop transfer function G(s) and multiplicative uncertainty L(s). Thus the effective (perturbed) loop transfer function is given by,

$$G_L(s) = G(s)[L(s)+1] \qquad (4.2.3)$$

The system is also subjected to noise and disturbance; a disturbance with transfer function D(s) is acting within the loop and sensor noise N(s) is injected into the feedback path. Hence, the system output is given by:

$$Y(s) = \frac{R(s)-N(s)}{1 + G_L^{-1}(s)} + \frac{D(s)}{1 + G_L(s)} \qquad (4.2.4a)$$

where the input error $E(s) = R(s)-Y(s)$ is:

$$E(s) = \frac{R(s)-D(s)}{1 + G_L(s)} + \frac{N(s)}{1 + G_L^{-1}(s)} \qquad (4.2.4b)$$

Control activity U(s) is determined to be,

$$U(s) = \frac{R(s)-N(s)-D(s)}{1 + G_L(s)} \qquad (4.2.4c)$$

The influence of the return difference $[1+G_L(s)]$ and complementary sensitivity (or inverse return difference) $[1+G_L^{-1}(s)]^{-1}$ functions on the disturbance and sensor noise components is examined. From equations (4.2.4), it can be seen that for good sensor noise reduction, disturbance rejection and acceptable control activity, the desired gain response requires,

$$\left.\begin{aligned} [1 + G_L(s)]^{-1} &\ll 1 \\ [1 + G_L^{-1}(s)]^{-1} &\simeq 1 \end{aligned}\right\} \quad \text{at low frequencies} \qquad (4.2.5a)$$

and,

$$\left.\begin{aligned} [1 + G_L(s)]^{-1} &\simeq 1 \\ [1 + G_L^{-1}(s)]^{-1} &\ll 1 \end{aligned}\right\} \quad \text{at high frequencies} \qquad (4.2.5b)$$

Clearly, it is not possible to have both disturbance and sensor noise attenuation at either high or low frequencies since,

$$[1 + G_L(s)]^{-1}[1 + G_L^{-1}(s)]^{-1} = I \qquad (4.2.6)$$

A suitable tradeoff between the two qualities and control activity is thus necessary for "good" overall robustness over the entire frequency range. Singular value plots of the return difference and complementary sensitivity operators can provide the bounding conditions for this trade-off in MIMO feedback control design (Doyle and Stein, 1981; Ly, 1983).

Singular value plots of the *ideal* system are shown in Figure 4.2.2. Large gains at low frequencies ($[1+G_L]>1$) correspond to good command following and disturbance rejection properties while small gains ($[1+G_L]\simeq 1$) at high frequencies denote good sensor noise attenuation.

The specification of a frequency dependent performance curve, which governs the characteristics of system response to commands and disturbance, is not difficult for SISO systems. Stability, input/output response and loop performance can readily be translated into frequency dependent design criteria. However, the specification of frequency dependent robustness bounds for the MIMO system is not so simple; frequency curves for individual loops cannot easily be lumped together to shape a bounding region, as given by equation (4.4.2), for the *whole* system. Many unknown 'disturbance' factors affect the overall response of a MIMO system, the majority of which cannot be either *quantified* as components of bounded magnitude or accurately specified to occur at a given frequency.

To address this overall uncertainty, the robust eigenstructure assignment design methods assume design criteria which *globally* minimise the effect of *unstructured* perturbations occuring in all loops. The unified objective of the robust eigenstructure assignment technique is to design a closed loop system which has defined transient reponses for each mode (as determined by the position of closed loop eigenvalues (λ_i)) and an *internal* system operation that is capable of producing the desired response in the most efficient manner. The internal system operation is characterised by the closed loop system right and left

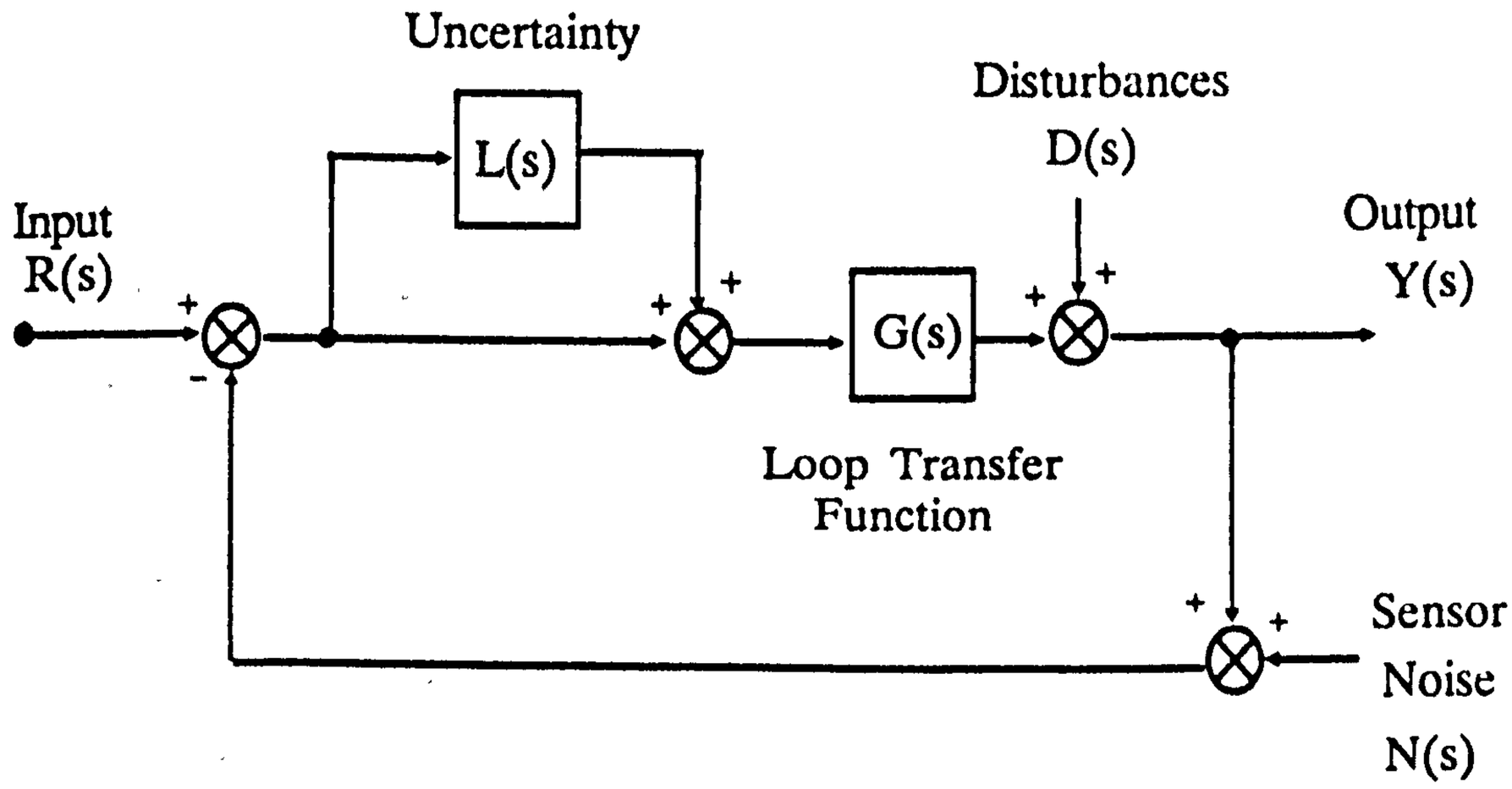

Figure 4.2.1 Typical feedback system configuration with noise, disturbance and uncertainty effects.

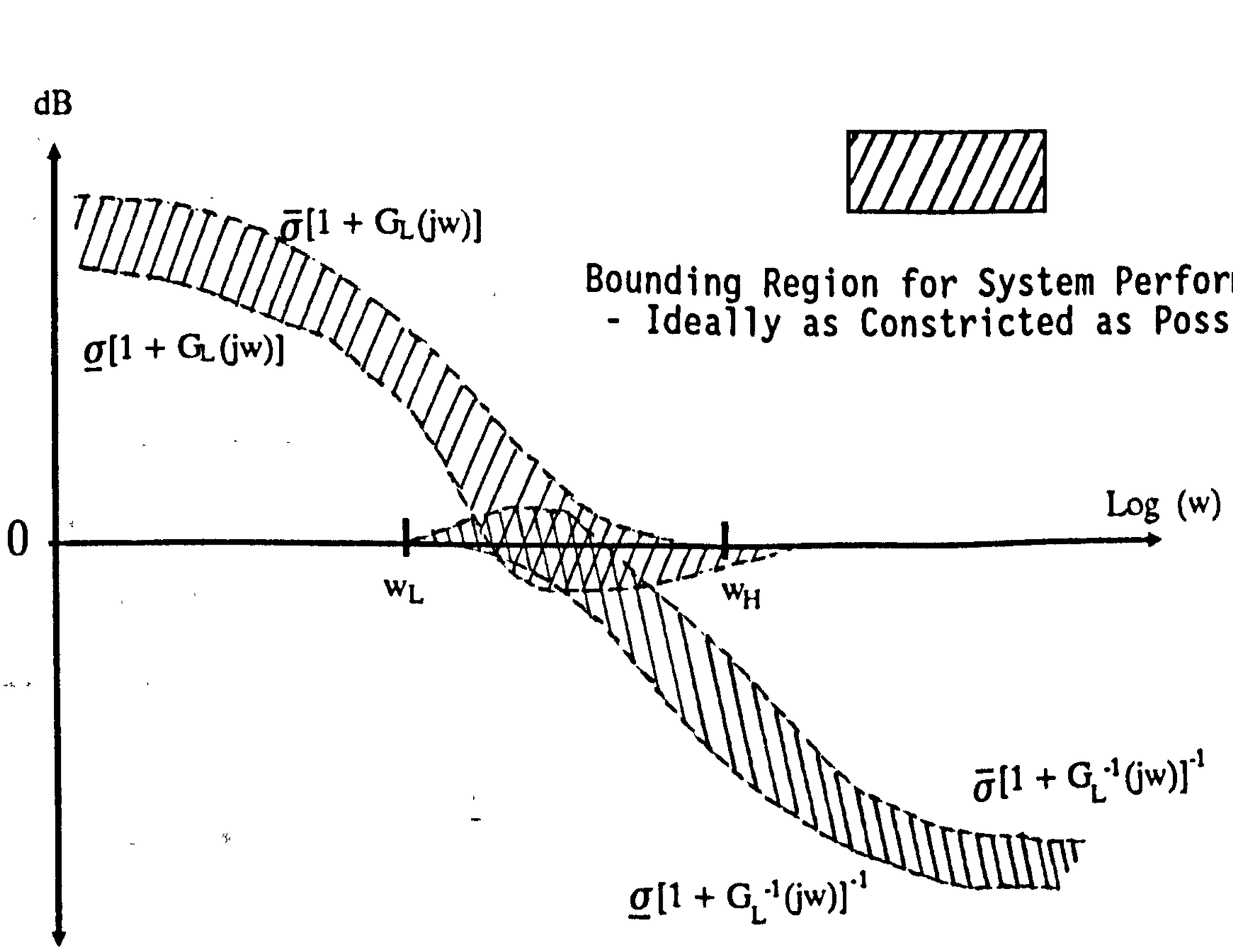

Figure 4.2.2 Frequency response of a feedback system contaminated with noise, disturbance and uncertainty.

eigenvectors, $\{\nu_i, l_i\}$. The eigenvalues and corresponding eigenvectors combined form the system eigenstructure. (The relationship between the eigenstructure of a closed loop system and its output time response is detailed in the Section 4.3).

For a given system, the desired closed loop internal structure can be determined from the control tasks it is expected to fulfil. For many systems the anticipated control tasks dictate that the transient response of every closed loop mode is maximally decoupled from the transient response of every other mode. That is, the internal structure maintains maximal insensitivity of every mode to perturbations in any other mode. When total modal decoupling is achieved the closed loop system is said to be *perfectly* decoupled.

In contrast, some systems are ideally required to maintain specific modal couplings which support their closed loop performance. Examples of modally interactive closed loop systems include flight control systems, chemical processing plants, water flow systems and economic systems (Andry et al, 1983; Garg, 1989; Kautsky et al, 1985; Moore, 1976; Paduano and Downing, 1989; Smith, 1991; Shapiro and Chung, 1981; Sobel and Shapiro, 1987; Srinathkumar and Jategaonkar, 1985; Mielke and Tung, 1985; White, 1991). For these cases the modal couplings are chosen either to retain natural inter-dependencies of open-loop modes in closed loop or to prescribe specific modal interactions that will ensure efficient operation. (The examples of Chapters 5 and 6 will examine flight control applications where the modal structure is selected to enhance aircraft maneouvreability.)

The required modal structure is translated into the desired set of right eigenvectors to be assigned by the eigenstructure assignment procedure. A solution which assigns a robust modal structure will produce a closed loop system that has minimum control action conflict within the *whole* system. The closed loop system eigenstructure is said to be *well-conditioned*. Efficient control and state transient behaviour

is thus guaranteed by reducing undesired deviations from the neccessary interaction of dynamic modes.

This design of a well conditioned eigenstructure effectively decreases the amount of *gain* present in the system. In the frequency domain this translates as a constriction of the bounded performance region of equation (4.2.2). That is, the amount of uncertainty the system can tolerate to maintain the specified system behaviour is increased. Thus, right eigenvector specification can intuitively be observed to have a *global* beneficial effect on closed loop system performance and stability robustness in the frequency domain.

4.3 ROBUST EIGENSTRUCTURE ASSIGNMENT

For MIMO systems the design criterion that may be specified, using state space design methods that do not consider robustness, is limited to the assignment of a desired set of eigenvalues. Eigenvalues with large negative real parts will ensure that the nominal system is well within the stable performance region. Eigenvalues can also be placed to cancel the effect of undesired zero modes or to modify the speed and damping of nominal open loop responses. For these "non-robust" methods the closed loop performance is designed for the *nominal* system. The performance of the closed loop system is therefore, not guaranteed to hold over operating regions which cause a deviation in the system dynamics from its nominal description. As a worst case, this lack of robustness can result in a destabilising variation in closed loop performance. A highly "sensitive" closed loop system may, for example, have its nominally designed far left eigenvalues rapidly converge on the unstable boundary for some operating points. Clearly, some "insensitivity" of the closed loop eigenvalues to perturbations in the system dynamics will provide robust performance.

This section describes the eigenstructure assignment problem and outlines how insensitivity qualities can be incorporated into a multivariable closed loop design using feedback control. The general output feedback control problem is outlined first:

4.3.1 The output feedback eigenproblem

The output feedback eigenvalue assignment problem of a MIMO continuous system {A,B,C}, $x \epsilon R^n$, $u \epsilon R^m$, $y \epsilon R^r$, requires control of the form,

$$u(t) = K(y(t)-r(t)) \qquad K \epsilon R^{mxr} \qquad (4.3.1)$$

to be applied such that the closed-loop system matrix (A+BKC) has a desired set of eigenvalues $\{\lambda_i\}$ (r(t) is some input reference signal). Assuming (A,B) (A,C) are completely controllable and observable a range of feedback matrices K will provide the solution. The extra degrees of freedom in the underdetermined solution can be used to specify other desirable properties. Moore (1976) characterised this freedom in terms of the assignability of the closed-loop eigenvectors, $\{\nu_1\ \nu_2\ ..\ \nu_n\}$, $\nu_i \epsilon \mathbb{C}$ corresponding to the desired self-conjugate set of poles $\{\lambda_1\ \lambda_2\ ..\ \lambda_n\}$, $\lambda_i \epsilon \mathbb{C}$. The role of the eigenvectors in shaping the closed loop system response is examined:

The feedback of equation (4.3.1) will produce a closed loop description,

$$\begin{aligned} \dot{x}(t) &= (A+BKC)x(t) + BKr(t) \\ &= A_{CL}x(t) + B_{CL}r(t) \end{aligned} \qquad (4.3.2)$$

The solution of (4.3.2) is given by,

$$x(t) = \exp(A_{CL}t)x_0 + \int_0^t \exp(A_{CL}\tau)B_{CL}r(t-\tau)d\tau \qquad (4.3.3)$$

The closed loop properties of interest for the eigenstructure assignment procedure are isolated by a modal decomposition. Assume $\{\lambda_i\}$ are distinct and $\lambda_i \in R$, then a transformation $x = Vz$ will produce:

$$\Lambda = L^T A_{CL} V \qquad \Lambda=\text{diag}\{\lambda_1\ \lambda_2\ ..\ \lambda_n\} \qquad (4.3.4a)$$

Matrices $V = [\nu_1\ \nu_2..\nu_n]$ and $L^T = [l_1\ l_2..l_n]$ are the right and left eigenvector sets corresponding to the pole spectrum $\{\lambda_1\ \lambda_2\ ..\ \lambda_n\}$. That is,

$$A_{CL}\nu_i = \nu_i\lambda_i \qquad l_i^T A_{CL} = \lambda_i l_i^T \qquad i=1,..,n \qquad (4.3.4b)$$

In general $\lambda_i \in \mathbb{C}$, in which case Λ is of Jordan form (D'Azzo and Houpis, 1981). With the use of transformation (4.3.4a), the state transition matrix $\exp(A_{CL}t)$ can be represented as:

$$\exp(A_{CL}t) = \sum_{i=1}^{n} \nu_i \exp(\lambda_i t) l_i^T \qquad (4.3.5)$$

A substitution of equation (4.3.5) into (4.3.3) defines the system output response to be:

$$y(t)=\sum_{i=1}^{n} C[\nu_i \exp(\lambda_i t)](l_i x_0) + \sum_{i=1}^{n}\sum_{j=1}^{m} C\nu_i l_i b_j \int_0^t \exp(\lambda_i \tau) r_j(t-\tau)\, d\tau \qquad (4.3.6)$$

The unforced component (i.e. the natural response) of the closed loop system output comprises n products of the form $\nu_i \exp(\lambda_i t)$ and $l_i^T x_0$. The ability to select $\{\nu_i\}$, $\{l_i^T\}$ in addition to $\{\lambda_i\}$ forms the basis of

eigenstructure assignment. For the autonomous system, these three design parameters completely characterise the output transient response: The eigenvalues $\{\lambda_i\}$ determine the rate of decay ($\lambda_i<0$) or growth ($\lambda_i>0$) of each mode $\exp(\lambda_i t)$; The right eigenvectors $\{\nu_i\}$ determine the amount each mode contributes to every output transient whilst the left eigenvectors determine the influence of inital conditions in the natural response. The closed loop eigenvectors thus govern the 'shape' and initial 'perturbation' of the system transient response.

The effect of $\{\nu_i\}$, $\{l_i^T\}$ on the forced component of equation (4.3.6) is very important. Terms $(l_i^T b_i)$ determine the degree to which elements of the input signal r influence the system output response. Thus, the left eigenvectors can be designed to decouple the effect of input command signals. This is termed *control decoupling* and is of particular use in the design of input precompensators, input disturbance decoupling and command following systems (Burrows, 1990; Fahmy and O'Reilly, 1988; Garrard et al, 1989; Patton and Chen, 1991; Smith, 1991; White, 1991).

The general eigenstructure assignment problem for transient response design is now described. Consider the natural response part of equation (4.3.2). A rearrangment of decomposition (4.3.4) allows this to be written as (White, 1991):

$$\begin{bmatrix} \lambda_i I-A & -B \\ KC & -I \end{bmatrix}\begin{bmatrix} N_{\lambda i} \\ M_{\lambda i} \end{bmatrix} = 0 \qquad (4.3.7a)$$

$$M_{\lambda i} = KC\nu_i \qquad (4.3.7b)$$

The columns of $N_{\lambda i}$ span the right eigenvector subspace, termed the "admissible" subspace. Similarly, the dual left eigenvector relations can be written as (White, 1991):

$$\begin{bmatrix} \lambda_i I - A^T & -C^T \\ K^T B^T & -I \end{bmatrix} \begin{bmatrix} L_{\lambda i} \\ H_{\lambda i} \end{bmatrix} = 0 \tag{4.3.8a}$$

$$H_{\lambda i} = K^T B^T l_i \tag{4.3.8b}$$

$L_{\lambda i}$ is a basis for the left eigenvectors.

The majority of eigenstructure assignment techniques emphasise the design of right eigenvectors, $\{v_i\}$, (Andry et al, 1983; Garg, 1989; Kautsky et al, 1985; Moore, 1976), since their specification is seen to prescribe very powerful modal decoupling properties of benefit to many applications. The left eigenvectors are intrinsically linked to the right eigenvector set, and thus $\{v_i\}$ design methods would appear to offer little scope for the specification of $\{l_i\}$. Techniques which re-adjust right eigenvectors subsequent to the first iteration of the design procedure can, however, provide some means of assigning desired left eigenvectors (Fahmy and O'Reilly, 1988, Patton and Chen, 1991). The assignment of the *entire* desired eigenstructure at the first pass is based on a parameterisation of the eigenproblem in terms of *both* right and left eigenvector assignability.

The assignment of desired eigenvalues $\{\lambda_i\}$ and right eigenvectors $\{v_i\}$ requires the solution of,

$$\begin{bmatrix} \lambda_i I - A & -B \end{bmatrix} \begin{bmatrix} N_{\lambda i} \\ M_{\lambda i} \end{bmatrix} = 0 \tag{4.3.9}$$

For the autonomous system, the achievability of desired $\{\lambda_i\}$ and $\{v_i\}$ using output feedback u(t)=Ky(t) is determined by the degrees of freedom made available by the C,B matrices in (4.3.7a). This freedom allows max(m,r) eigenvalues to be placed with min(m,r) elements of each corresponding eigenvector being precisely assigned (Davison, 1976; Kimura, 1975; Roppenecker and O'Reilly, 1989; Shapiro and Chung, 1981; Smith, 1991). Thus, for r=n (e.g. $C=I_n$ which converts the output

feedback control problem to that of *state* feedback) all n poles λ_i may be assigned with a maximum of m elements in each associated right eigenvector being achieved *exactly*. However, the majority of systems have r<n, indicating that the design freedom available for eigenstructure assignment using output feedback is very limited. For many systems m<n also hence, in general, it is not possible to assign *precisely* the *whole* closed loop eigenstructure.

Many techniques exist to provide a solution to the eigenproblem of equation (4.3.7a). The assignability condition is seen to be determined by design parameters $\{\lambda_i\}$ $\{\nu_i\}$. The limited design freedom dictates that some compromise on the choice of either λ_i, ν_i or both is necessary, with an appropriate solution satisfying suitable design criteria. Solutions which involve the adjustment of both λ_i, ν_i require optimisation techniques to determine the direction of movement of the two free parameters to satisfy given design criteria (Burrows, 1990; Muchopadhyay and Newson, 1985; Roppenecker, 1986; Roppenecker and O'Reilly, 1989; Sogaard-Anderson et al, 1986; the work of Burrows (1990) provides an excellent up-to-date examination of these methods).

However, for many control problems there is little opportunity to vary λ_i. Also, generic feedback design techniques are based on *a priori* selection of $\{\lambda_i\}$, determined by some loop-shaping criteria. For this general setting, the eigenproblem solution requires the search of an acceptable set of right eigenvectors $\{\nu_{ai}\}$ corresponding to a given (fixed) set of desired eigenvalues $\{\lambda_i\}$. The following chapters concentrate on the solution of this category of eigenproblem.

4.3.2 The State Feedback Eigenproblem

This section examines the solution of (4.3.7a) using state feedback (Kimura, 1975; Moore, 1976). For every desired eigenvalue $\lambda_i \epsilon R$, define

(Mielke and Tung, 1985),

$$S_{\lambda i} = [\lambda_i I - A \; : \; -B] \tag{4.3.10}$$

and a compatibly dimensioned matrix,

$$R_{\lambda i} = \begin{bmatrix} N_{\lambda i} \\ M_{\lambda i} \end{bmatrix} \tag{4.3.11}$$

whose columns form the basis for the nullspace of $S_{\lambda i}$, $N(S_{\lambda i})$. For a given system pair (A,B) and a given set of $\{\lambda_i\}$, the assignable right eigenvector is selected by an appropriate combination of columns from the admissible subspace. The design parameter which determines this combination (and thus provides a solution to equation (4.3.9)) is any (mx1) column vector k_i which satisfies,

$$[\lambda_i I - A \; : \; -B] R_{\lambda i} k_i = 0 \tag{4.3.12}$$

Let the desired right eigenvectors be denoted $\{\nu_{di}\}$. A set of right eigenvectors can be selected such that $\nu_{ai} \in N(S_{\lambda i})$. That is:

$$\nu_{ai} = N_{\lambda i} \, k_i \tag{4.3.13}$$

Hence,

$$(\lambda_i I - A) N_{\lambda i} k_i - B M_{\lambda i} k_i = 0 \tag{4.3.14}$$

The eigenvector set $\{\nu_{ai}\}$ determined by (4.3.13) are termed the *assignable* or *admissible* right eigenvectors. The admissible right eigenvectors are selected to be as close as possible to the desired set $\{\nu_{di}\}$.

Gain matrix K is determined from the combination of n terms of the form given in equation (4.3.7b). A real feedback matrix K will exist if the admissible right eigenvectors $\{\nu_{ai}\}$ form a linearly independent set, V. In this case,

$$K = MV^{-1}$$

$$M = [M_{\lambda 1}k_1 \; M_{\lambda 2}k_2 \; .. \; M_{\lambda n}k_n] \tag{4.3.15}$$

A modified approach is required for the calculation of the nullspace for $\lambda_j \in \mathbb{C}$ (Mielke and Tung, 1985; Silverthorn and Reid, 1980). Assume $\lambda_{d1}=\lambda_{d2}^*$. The real and imaginary parts of the right eigenvector must satisfy:

$$(A+BK)(\nu_{Re}+j\nu_{Im}) = (\nu_{Re}+j\nu_{Im})(\lambda_{Re}+j\lambda_{Im}) \tag{4.3.16}$$

Equating real and imaginary parts gives the equation

$$\begin{bmatrix} \lambda_{Re}I-A & : & -\lambda_{Im} & : & -B & : & 0 \\ \lambda_{Im} & : & \lambda_{Re}I-A & : & 0 & : & -B \end{bmatrix} \begin{bmatrix} \nu_{Re} \\ \nu_{Im} \\ K\nu_{Re} \\ K\nu_{Im} \end{bmatrix} = 0 \tag{4.3.17}$$

The basis for the nullspace of the 2nx2(n+m) matrix of equation (4.3.17) is given by,

$$R_{C\lambda i} = \begin{bmatrix} N_{\lambda i} \\ P_{\lambda i} \\ M_{\lambda i} \\ Q_{\lambda i} \end{bmatrix} \tag{4.3.18}$$

The real and imaginary parts of the (admissible) complex right eigenvectors are determined in a similar manner to the assignment of

real eigenvectors. Parameters k_i are designed to select an appropriate combination of vectors from the real and imaginary admissible subspaces so that:

$$\begin{bmatrix} \nu a\mathrm{Re} \\ \nu a\mathrm{Im} \end{bmatrix} = \begin{bmatrix} N_{\lambda i} \\ P_{\lambda i} \end{bmatrix} k_i \qquad (4.3.19)$$

Calculation of the gain matrix real valued K then proceeds as before except ν_{Re} and ν_{Im} occupy two columns of the right eigenvector matrix V, with associated M matrix columns being $[M_{\lambda i}k_i \; Q_{\lambda i}k_i]$.

4.3.3 Insensitivity criteria

Sections 4.3.1 and 4.3.2 have highlighted that the open loop system whose eigenstructure is to be designed, generally has a fewer number of inputs and outputs than the number of closed loop modes to be assigned (i.e. m<n, r<n). This indicates that an overdetermined eigenproblem is posed by equation (4.3.7). Thus, the solution can only produce admissible right eigenvectors $\{\nu_{ai}\}$ which *approximate* the desired vectors $\{\nu_{di}\}$. A suitable design criterion must, therefore, be applied to select a feedback matrix which yields an acceptable set $\{\nu_{ai}\}$ for the general eigenproblem. This section presents the established insensitivity criterion (Kautsky et al, 1985; Wilkinson, 1965, 1984) used for the complete solution of the eigenstructure assignment problem.

Assume for simplicity that $\{\lambda_i\} \in R$. The closed loop system matrix can then be decomposed as:

$$V\Lambda V^{-1} = A + BK \qquad (4.3.20)$$

where $\Lambda = \mathrm{diag}\{\lambda_1 \; \lambda_2 \; .. \; \lambda_n\}$ and V is the matrix whose columns are the

right eigenvectors of the closed-loop system. A measure of the insensitivity of the solution is the right eigenvector conditioning,

$$\kappa(V) = \|V\|_2 \|V^{-1}\|_2 \tag{4.3.21}$$

$\|V\|_2$ is defined as the maximum positive eigenvalue of $(V^{*T}V)^{1/2}$. The measure $\kappa(V)$ provides an upper bound on the eigenvalue variations $\delta\lambda$ due to an arbitary perturbation Δ in the system matrix, i.e.,

$$|\delta\lambda| \leq \kappa(V)\|\Delta\| \tag{4.3.22}$$

Another measure of conditioning is provided by worst case analysis (Wilkinson, 1965). If all components of the closed loop system matrix are subject to *unstructured* perturbations, the maximum perturbation in any λ_i is related to the condition number,

$$c_i = \frac{\|v_i\|_2 \|\ell_i\|_2}{|\ell_i^T v_i|} \geq 1 \tag{4.3.23}$$

where v_i and l_i are the right and left eigenvectors corresponding to the i'th eigenvalue λ_i. (For $\lambda_i \in R$, $1/c_i$ is the cosine of the angle between v_i and l_i). The specific effect of c_i on the closed loop eigenvalues is as follows: if a perturbation of order $O(\epsilon)$ in the coefficients of closed loop matrix (A+BK) generates perturbed eigenvalues λ_{ip}, then the difference in the nominal and perturbed eigenvalues (Kautsky et al, 1985) satisfies,

$$|\lambda_i - \lambda_{ip}| = O(nc_i\epsilon) + O(\epsilon^2) \tag{4.3.24}$$

Thus, the first order perturbation in λ_i is proportional to c_i. More

precisely, the variation in any closed loop eigenvalue $\delta\lambda_i$ due to a perturbation Δ (Wilkinson, 1965) is given by,

$$\delta\lambda_i \leq l_i^T \Delta v_i \tag{4.3.25}$$

Clearly, minimising c_i will increase the insensitivity of the closed loop eigenvalues. A value of $c_i=1$ is said to give a *perfectly* conditioned λ_i, (i.e. a *maximally* insensitive eigenvalue). The measures of (4.3.21) and (4.3.23) are related: If the columns of $V = [v_1\ v_2\ ,..,\ v_n]$ are normalised, ie $\|v_i\|=1$ then,

$$\max_i c_i \leq \kappa(V) \tag{4.3.26}$$

Clearly, the minimisation of $\kappa(V)$ (which provides an upper bound on the sensitivities of the individual closed loop poles to system perturbations) is a suitable design criterion for an overall well conditioned solution to the eigenproblem.

Thus, the robust eigenstructure assignment problem can be summarised as the selection of matrices K and V such that $\kappa(V)$ is minimised, subject to the constraint

$$(A + BK)V = V\Lambda \tag{4.3.27}$$

For a well-conditioned or robust solution, the right eigenvectors are chosen to be as mutually orthogonal as possible or to have a specific modal structure which prescribes the correct interaction of closed loop dynamics.

4.4 IMPACT OF $\kappa(V)$ ON CLOSED LOOP SYSTEM ROBUSTNESS

Section 4.2 outlined the general frequency domain properties desired of MIMO feedback systems. The theoretical confirmation of enhancing closed system robustness via right eigenvector assignment can easily be developed. Consider the matrix conditioning $\kappa(F(s))$ of a given matrix F(s) (which is a function of frequency s) and the maximum and minimum singular values of F(s). The two are related by,

$$\kappa(F(s)) = \frac{\bar{\sigma}[F(s)]}{\underline{\sigma}[F(s)]} \qquad (4.4.1)$$

showing that $\kappa(F(s))$ is a measure of gain 'spread' of F(s) at frequency s. The correspondence between $\kappa(V)$ and the bounded desired performance curves of Figure 4.4.2 is clarified in the following sections. The desired feedback control properties to be examined are summarised below:

Figure 4.4.2 shows that good command following and disturbance attenuation requires large loop gains at low frequencies, ie,

$$[I + G(jw)] \simeq G(jw) \qquad \omega < \omega_L \qquad (4.4.2)$$

and low gains at high frequencies for noise rejection, ie,

$$[I + G(jw)] \simeq I \qquad \omega > \omega_H \qquad (4.4.3)$$

In the crossover region $\omega_L < \omega < \omega_H$, good stability margins are produced (Safonov, 1981) if,

$$[I + G(jw)] > 1 \qquad (4.4.4a)$$

$$[I + G(jw)^{-1}] > 1 \qquad (4.4.4b)$$

The above system robustness properties are examined for each region of the frequency scale (Sogaard-Anderson, 1985). Unless otherwise stated it is assumed that, for a given pair (K,V) satisfying equation (4.3.23), the nominal and perturbed loop transfer operators are defined as:

$$G(s) = KW \tag{4.4.5a}$$

$$G_L(s) = KW_L \tag{4.4.5b}$$

where $W = -(sI-A)^{-1}B$, $W_L = -(I+\Delta)(sI-A)^{-1}B$.

4.4.1 Low frequency robustness

Using norm relations, for large loop gains equation (4.4.2) can be written as:

$$\underline{\sigma}[I+KW] \simeq \underline{\sigma}[KW]$$

$$I+[KW]^{-1} \simeq I$$

$$\underline{\sigma}[I+KW] \simeq 1 \tag{4.4.6}$$

Thus, for good performance robustness, $\underline{\sigma}[KW]$ is required to be large for $\omega_L < \omega$. Using Schwartz inequality relations, a lower bound for $\underline{\sigma}[KW]$ can be found:

$$\underline{\sigma}[KW] > \underline{\sigma}[K] \cdot \underline{\sigma}[W]$$

Since, $K = MV^{-1}$ (equation (4.3.15)),

$$\underline{\sigma}[K] > \underline{\sigma}[M] \cdot \underline{\sigma}[V^{-1}]$$

$$> \frac{\underline{\sigma}[M]}{\bar{\sigma}[V]}$$

$$\Rightarrow \quad \underline{\sigma}[KW] > \frac{\underline{\sigma}[M]\ \underline{\sigma}[W]}{\bar{\sigma}[V]} \qquad (4.4.7)$$

$\underline{\sigma}[W]$ is determined by the open loop continuous system and perturbation dynamics thus, $\underline{\sigma}[KW]$ can be maxmised if $\bar{\sigma}[V]$ is minimised and $\underline{\sigma}[M]$, $\underline{\sigma}[W]$ maximised.

4.4.2 High frequency robustness

Equation (4.4.3) can be written as:

$$[I+KW] \simeq I$$

$$\underline{\sigma}[I+KW] \simeq 1$$

$$\underline{\sigma}[I+(KW)^{-1}] \simeq \underline{\sigma}[(KW)^{-1}] \qquad (4.4.8)$$

Thus, for good stability robustness $\underline{\sigma}[(KW)^{-1}]$ is required to be large for $\omega < \omega_H$. The lower bound for $\underline{\sigma}[(KW)^{-1}]$ can be found, using the inequality relations, to be:

$$\underline{\sigma}[(KW)^{-1}] > \frac{\underline{\sigma}[V]}{\bar{\sigma}[M]\ \bar{\sigma}[W]} \qquad (4.4.9)$$

Thus, $\underline{\sigma}[(KW)^{-1}]$ can be maximised if $\underline{\sigma}[V]$ is maximised and $\bar{\sigma}[M]$, $\bar{\sigma}[W]$ minimised.

4.4.3 Crossover Robustness and Stability Margins

Lower bounds for the left hand side functions of equations (4.4.4) are required in order to determine MIMO stability margins (Cruz et al, 1981; Lehtomaki et al, 1981; Safonov, 1981). The relationship between the open loop and closed loop feedback system, $W_C = [sI-(A+BK)]^{-1}B$, can be written (Macfarlane, 1970):

$$W[I + KW]^{-1} = W_C \tag{4.4.10a}$$

$$[I + KW] = (W)^{\dagger}W_C \tag{4.4.10b}$$

where $()^{\dagger}$ denotes the Moore–Penrose inverse (Golub and Van Loan, 1983). This can be recognised as an equivalent expression for (4.4.4a). A corresponding expression for equation (4.4.4b) can be found by noting that,

$$KW[I + KW]^{-1} = [I + (KW)^{-1}]^{-1}$$
$$= KW_C \tag{4.4.11}$$

Since,

$$W_C = V(sI-\Lambda)^{-1}V^{-1}B \tag{4.4.12}$$

the lower bounds of equations (4.4.10) and (4.4.11) are determined as:

$$\underline{\sigma}[I + KW] > \underline{\sigma}[B^{\dagger}].\underline{\sigma}[V^{-1}].\underline{\sigma}[j\omega I - \Lambda].\underline{\sigma}[V].\underline{\sigma}[W]$$

$$> \frac{\underline{\sigma}[j\omega I - \Lambda] \; . \; \underline{\sigma}[W]}{\overline{\sigma}[B] \; \kappa(V)} \tag{4.4.13a}$$

$$\underline{\sigma}[I + (KW)^{-1}] > \frac{\underline{\sigma}[j\omega I - \Lambda] \cdot \underline{\sigma}[V]}{\bar{\sigma}[M].\bar{\sigma}[B]} \qquad (4.4.13b)$$

Thus, good stability margins require that $\underline{\sigma}[V]$, $\underline{\sigma}[j\omega I-\Lambda]$ are maximised and $\bar{\sigma}[M]$, $\bar{\sigma}[B]$ minimised.

From the concluding remarks of Sections 4.4.1, 4.4.2 and 4.4.3 it is clear that maximising $\underline{\sigma}[V]$ and minimising $\bar{\sigma}[V]$ over *all* frequency ranges (and thus effectively minimising k(V)) has a *direct* beneficial effect on closed loop system robustness. Kautsky et al (1985) outlined how minimising $\kappa(V)$ maximised a lower bound on closed loop stability margins over *all* feedback matrices which assign given stable eigenvalues. Bounding conditions for the gain matrix (which are of particular importance in the MIFO control eigenproblem) can be found using this analysis. The following section develops the relevant norm relations for the feedback gain matrix.

4.4.4 Gain Matrix Bounds for Stability Robustness

If a closed-loop system remains stable for multiplicative perturbations Δ then the perturbed return difference matrix will satisfy (Lehtomaki, 1981),

$$\det[sI - (A+BK+BK\Delta)] \neq 0 \qquad s=j\omega \qquad \forall\omega \qquad (4.4.14)$$

which can be written:

$$\begin{aligned}\det[sI - (A+BK+BK\Delta)] &= \det[sI-A]\ \det[I-(sI-A)^{-1}BK(I+\Delta)] \\ &= \det[[sI-A]\ \det[I+W_L K] \qquad (4.4.15)\end{aligned}$$

If $\det[sI-(A+BK)]\neq 0$, then clearly $\det[sI-(A+BK+BK\Delta)]\neq 0$ and the following relation is also satisfied,

$$\bar{\sigma}[BK\Delta] < \min_{s=j\omega} \underline{\sigma}(sI - (A+BK)) \equiv \delta(F) \tag{4.4.16}$$

Equation (4.4.16) is the sufficient condition for a stable nominal system to remain stable under perturbation Δ. Equation (4.4.16) can be re-arranged, using norm equality relations, to give an upper bound on the allowed perturbation:

$$\bar{\sigma}[\Delta] < \frac{\delta(F)}{\bar{\sigma}[B]\ \bar{\sigma}[K]} \tag{4.4.17}$$

Using the modal decompositon of (4.3.20), the right hand side of equation (4.4.16) can be written as:

$$\delta(F) = \min_{s=j\omega} \underline{\sigma}(sI - V\Lambda V^{-1})$$

$$> \underline{\sigma}[V] \min_{s=j\omega} \underline{\sigma}[sI-\Lambda]\ \underline{\sigma}[V^{-1}]$$

$$> \underline{\sigma}[V] \min_{i} \mathrm{Re}[-\lambda_i]\ \underline{\sigma}[V^{-1}] \tag{4.4.18a}$$

to give a lower bound for nominal closed loop system behaviour. For discrete systems, the upper bound for allowed perturbations satisfies,

$$\delta(F) > \min_{i} \frac{\mathrm{Re}[1-|\lambda_i|]}{\kappa(V)} \tag{4.4.18b}$$

(This is derived similarly to (4.4.18a) using the discrete unit circle stability boundary instead of the imaginary axis of the s-plane). Combining equations (4.4.17) and (4.4.18) gives the upper bound for allowable perturbations in continuous systems as:

$$\bar{\sigma}[\Delta] < \quad \hat{\delta}(F) \quad > \min_i \frac{\mathrm{Re}[-\lambda_i]}{\kappa(V)\bar{\sigma}[B]\bar{\sigma}[K]} \tag{4.4.19a}$$

Equivalently for discrete systems, the allowable perturbations are bounded by

$$\bar{\sigma}[\Delta] < \quad \hat{\delta}(F) \quad > \min_i \frac{\mathrm{Re}[1-|\lambda_i|]}{\kappa(V)\bar{\sigma}[\Gamma]\bar{\sigma}[K]} \tag{4.4.19b}$$

The bound of equations (4.4.19) shows that low $\kappa(V)$, $\bar{\sigma}[B]$ ($\bar{\sigma}[\Gamma]$) and $\bar{\sigma}[K]$ will increase the amount of uncertainty that the system can tolerate whilst maintaining closed loop stability, again confirming the advantage of minimising $\kappa(V)$.

For a continuous system description the open loop system control matrix B of equation (4.4.19) is fixed and K, V, $\{\lambda_i\}$ are the design parameters. Kautsky et al (1985) calculate the upper bound on K as:

$$\bar{\sigma}[K] = < \frac{\bar{\sigma}[A] + \max_i \{|\lambda_i|\}\ \kappa(V)}{\underline{\sigma}(B)} \tag{4.4.20}$$

The conditions of (4.4.19) imply a lower bound on the stability margin of the closed-loop system and thus provide a measure of its *stability* robustness.

4.4.5 Summary of desired properties for global robustness

The desired maximum and minumum singular values, [$\underline{\sigma}$ $\bar{\sigma}$], of K, W, V, A, B and (jωI-A) for good robustness over the entire frequency range (as determined from the preceding sections) are not conflicting. The neccessary qualities can be achieved if:

$$\left.\begin{matrix}\kappa(V)\\ \kappa(M)\\ \kappa(W)\\ \kappa(B)\end{matrix}\right\} \text{ are minimised} \qquad (4.4.20a)$$

$$\left.\begin{matrix}\bar{\sigma}[K]\\ \bar{\sigma}[A]\end{matrix}\right\} \text{ are minimised} \qquad (4.4.20b)$$

4.5 DESIGN FREEDOM FOR THE MULTIRATE DISCRETE EIGENPROBLEM

The global robustness qualities outlined in the previous section were related to [$\bar{\sigma}$, $\underline{\sigma}$] of various open and closed loop system functions. For the continuous system, the open loop system parameters (A,B) are pre-determined and cannot be altered. Parameterisation of the robust eigenproblem in this case can only be based on the pair (K,V) (which implicitly includes M, W also). For discrete systems however, the sample period T can be included as an additional design parameter since this will directly affect the singular values of A (more accurately, Φ), B (Γ), $W=(sI-A)B^{-1}$, W_L and indirectly affect singular values of M. An examination of equations (4.4.7), (4.4.9), (4.4.13) and (4.4.19) shows that [$\bar{\sigma}$ $\underline{\sigma}$] of these elements implicitly influence MIMO system performance and stabililty robustness bounds.

Thus, it would seem that single rate feedback structures possess more design freedom to improve closed loop robustness than their continuous time counterparts. In the state feedback design procedure

this extra freedom corresponds to an ability to *select* an appropriate (A,B) invariant subspace for the formulation of equation (4.3.9). Thus, the discrete equivalent of equation (4.3.9) is posed as the selection of a right eigenvector,

$$\nu_{ai} = (\lambda_i I - \Phi)^{-1}\Gamma\tau_i \qquad i=1,..,n \qquad (4.5.1a)$$

by appropriate choice of the (mx1) design parameter,

$$\tau_i = KN_{\lambda i}k_i \qquad (4.5.1b)$$

The equations of (5.4.1) clearly show the role of sample period T in the discrete eigenproblem. This extra freedom will generally result in a flexibility to assign desired closed loop right eigenvectors (ν_{di}) with more accuracy, but it will not necessarily yield an overall "better" design. The reasons for this can be gleaned from considering the effect of varying sample period T for the systems of Examples 3.5.1 and 3.5.2 in Chapter 3.

Figures 4.5.1 and 4.5.2 shows the variation in $[\bar{\sigma}\ \underline{\sigma}]$ of single rate (Φ,Γ) of both systems for sample period $T\epsilon[0.01\ 2]$. For the system of Example 3.5.1 $\bar{\sigma}[\Phi]$ peaks at around T=0.3secs while $\bar{\sigma}[\Gamma]$ maintains a constant increase as T→2secs. The trend for the system of Example 3.5.2 is observed to be different with $\bar{\sigma}[\Phi]$, $\bar{\sigma}[\Gamma]$ both increasing exponentially as T→2secs. The summary of Section 4.4.5 indicates that $[\bar{\sigma},\ \underline{\sigma}]$ of open loop system matrices (Φ,Γ) will influence the robustess performance bounds. This effect cannot be generalised partly due to the non-uniform response of different open loop systems to a change in T (as indicated by Figures 4.5.1 and 4.5.2), and partly due to the dependency of the bounds on the actual closed loop design. However, for the second system it is clear that the following effects will be observed as T→2secs:

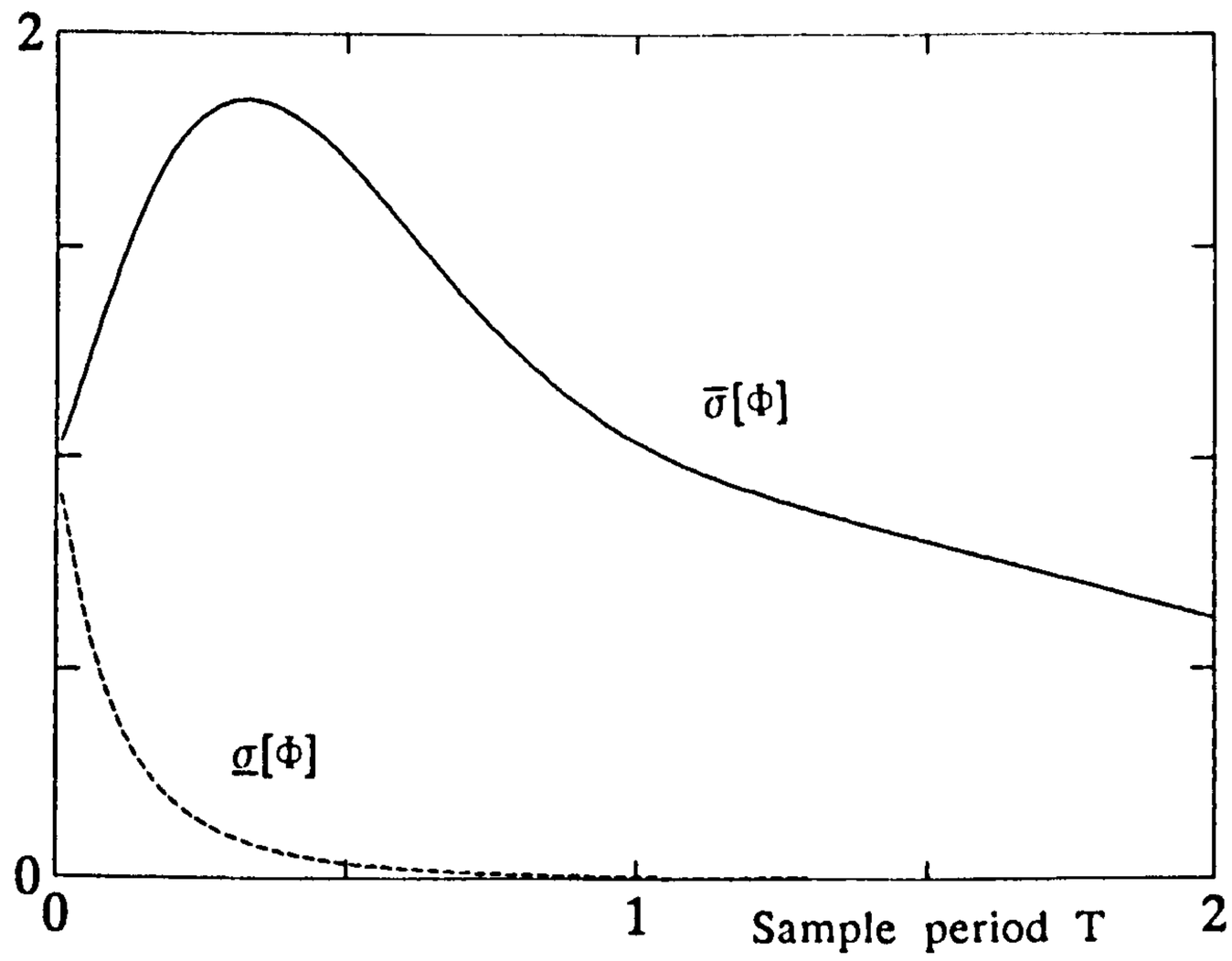

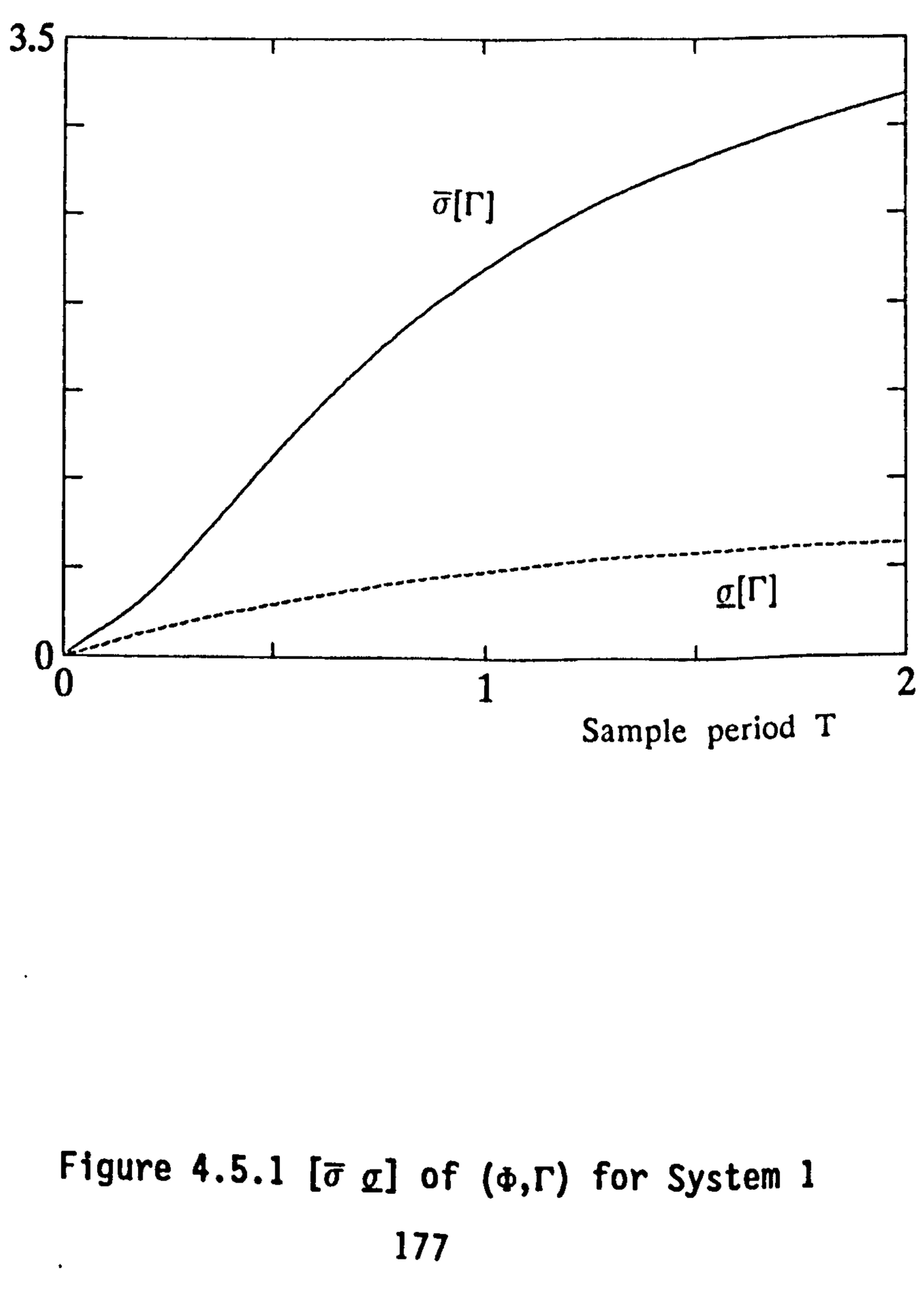

Figure 4.5.1 $[\bar{\sigma}\ \underline{\sigma}]$ of (Φ,Γ) for System 1

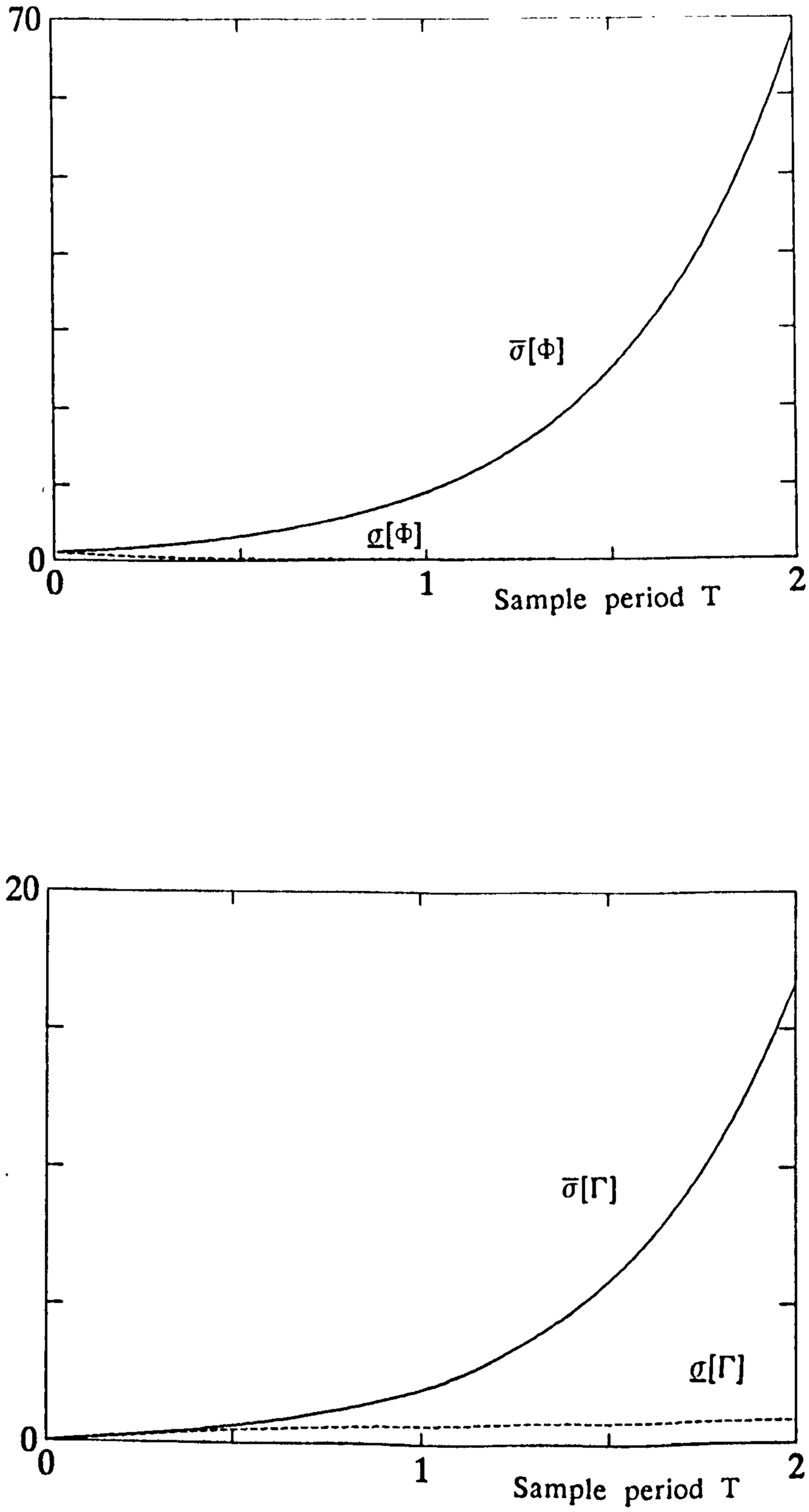

Figure 4.5.2 $[\bar{\sigma}\ \underline{\sigma}]$ of (Φ,Γ) for System 2

System 2: $\bar{\sigma}[K] \rightarrow$ large (since $\bar{\sigma}[\Phi] \rightarrow$ large)

$\bar{\sigma}[W] \rightarrow$ large ditto

$\bar{\sigma}[\Delta] \rightarrow$ small

The most important effect to note is that the general trend lead to $\bar{\sigma}[\Delta] \rightarrow$small as T→2secs (i.e. less uncertainty tolerated as T→2secs).

The bounding conditions of Section 4.4 are recognised to be conservative indicators of stable system performance. Nevertheless, they do provide an idea of the robustness trend expected from varying T. Thus, single rate discrete systems *may* offer some extra design freedom for trading off robustness properties in the freqency domain.

MIFO multirate system offer even more design freedom for the robust eigenproblem than the single rate discrete system. This freedom again manifests itself as the ability to select (A,B) invariant subspaces, but is significantly different in the *amount* of extra freedom generated. The ability of single rate structures to select the fixed dimension admissible subspace $[(\lambda_i I-\Phi)^{-1}\Gamma] \epsilon R^{nxm}$ by varying sample period T has been outlined above. The MIFO system, by variation of input sample rate multiplicities, provides a means of *increasing* the *dimension* of the admissible subspace in addition to the actual basis itself (from which design parameter τ_i selects the achievable right eigenvectors).

If $[(\lambda_i I-\Phi_{MR1})^{-1}\Gamma_{MR1}] \epsilon R^{nx\rho}$, $\rho>n$ the extra design freedom of MIFO structures will offer the capability of *exact* right eigenvector assignment at the main sample instants. The corresponding closed loop system will then, theoretically, be maximally insensitive to perturbations at the main sample instants. The possibility of achieving this perfect modal assignment is examined in Chapter 5.

4.6 MULTIRATE INSENSITIVITY MEASURES

The insensitivity measures of Section 4.3.3 monitor the performance of continuous-time and single rate discrete closed loop systems. The application of established MIMO eigenvalue placement design techniques requires the minimal open-loop state space description of Section 2.5. The MIFO multirate feedback control problem thus relates to the assignment of n eigenvalues $\{\lambda_1,..,\lambda_n\}$ designated by a transition matrix $(\Phi_{MR1}+\Gamma_{MR1}K)$ which represents the closed-loop system at the main sample instants. The set $\{\lambda_i\}$ corresponds to an equivalent set $\{\lambda_{mi}\}$ which can represent the faster poles of the closed-loop system sampled at the base rate T_b (Araki and Yamamoto, 1985; Boykin and Frazier, 1975; Francis and Gorgiou, 1988). The eigenvalues of the two sets are related by $\lambda_{mi} = (\lambda_i)^{1/n_0}$. The robustness and sensitivity measures of Section 4.3.3 relate to the n eigenvalues of the MIFO system and therefore, only provide an assessment of system performance *at the main sample instants.*

As highlighted by the remarks of Francis and Gorgiou (1988) no explicit method capable of monitoring intersample multirate performance exists. This section considers the expanded (non-minimal) closed-loop state space description of Section 2.4 to examine the *intersample* response of the MIFO system. A means of extending the robustness measures which apply to the continuous-time and single-rate discrete case to cover the intersample multirate case is then presented.

If, for a given open loop minimal pair $(\Phi_{MR1},\Gamma_{MR1})$, a feedback K is designed such that the resulting closed loop system $\Phi_{CL} = (\Phi_{MR1}+\Gamma_{MR1}K)$ has a desired set of main sample eigenvalues (λ_i), i=1,..,n then an equivalent expanded form (which represents the multirate system intersample response) can always be derived. This non-minimal equivalent system is denoted $(\Phi_{MR2}, \Gamma_{MR2}, K_{eq})$. Matrices Φ_{MR2} and Γ_{MR2} are of the form defined in equations (2.4.15), (2.4.17) respectively. Assume the open loop pair $(\Phi_{MR1}, \Gamma_{MR1})$ have input sample rate multiplicities (n_j),

j=1,..,m. Then, from equation (2.4.4), define $N=n_1+n_2+\ldots+n_m$. The $Nx(n_0xn)$ gain matrix K_{eq} can be derived by appropriate adjustment of K as follows:

$$K_{eq} = [\underbrace{0\ 0\ ..\ 0}_{(n_0-1)}\ \ K] \tag{4.6.1}$$

where the 0 blocks are zero matrices of dimension (Nxn_0). The expanded closed loop MIFO system is then defined as:

$$\Phi_{CLeq} = (\Phi_{MR2} + \Gamma_{MR2}K_{eq}) \tag{4.6.2}$$

$$= [0\ 0\ ..\ 0\ \ \hat{\Phi}_{CL}] \tag{4.6.3a}$$

$$\hat{\Phi}_{CL} = \begin{bmatrix} \Phi_{CL1} \\ \Phi_{CL2} \\ \cdot \\ \Phi_{CLn_0} \end{bmatrix} \tag{4.6.3b}$$

The matrices Φ_{CL1} ,..., Φ_{CLn_0-1} represent the *intersample* transitions of the closed loop system. Matrix Φ_{CLn_0} is the main sample transition matrix of the closed-loop system. Thus, the unforced closed loop MIFO sampled system response to an arbitary intial state perturbation $x_e(0)$ is governed by the following set of transition equations,

$$\begin{aligned} x_e[T_b] &= \Phi_{CL1}x_e(0) \\ x_e[2T_b] &= \Phi_{CL2}x_e(0) \\ &\cdot \qquad\quad \cdot \\ x_e[T] &= \Phi_{CLn_0}x_e(0) \\ &\text{etc} \end{aligned} \tag{4.6.4}$$

If the conditioning and sensitivity measures $\kappa(V)$, c_i of Section 4.3.3 are applied to closed loop matrices Φ_{CLi}, i=1,..,n_{0-1} then, the

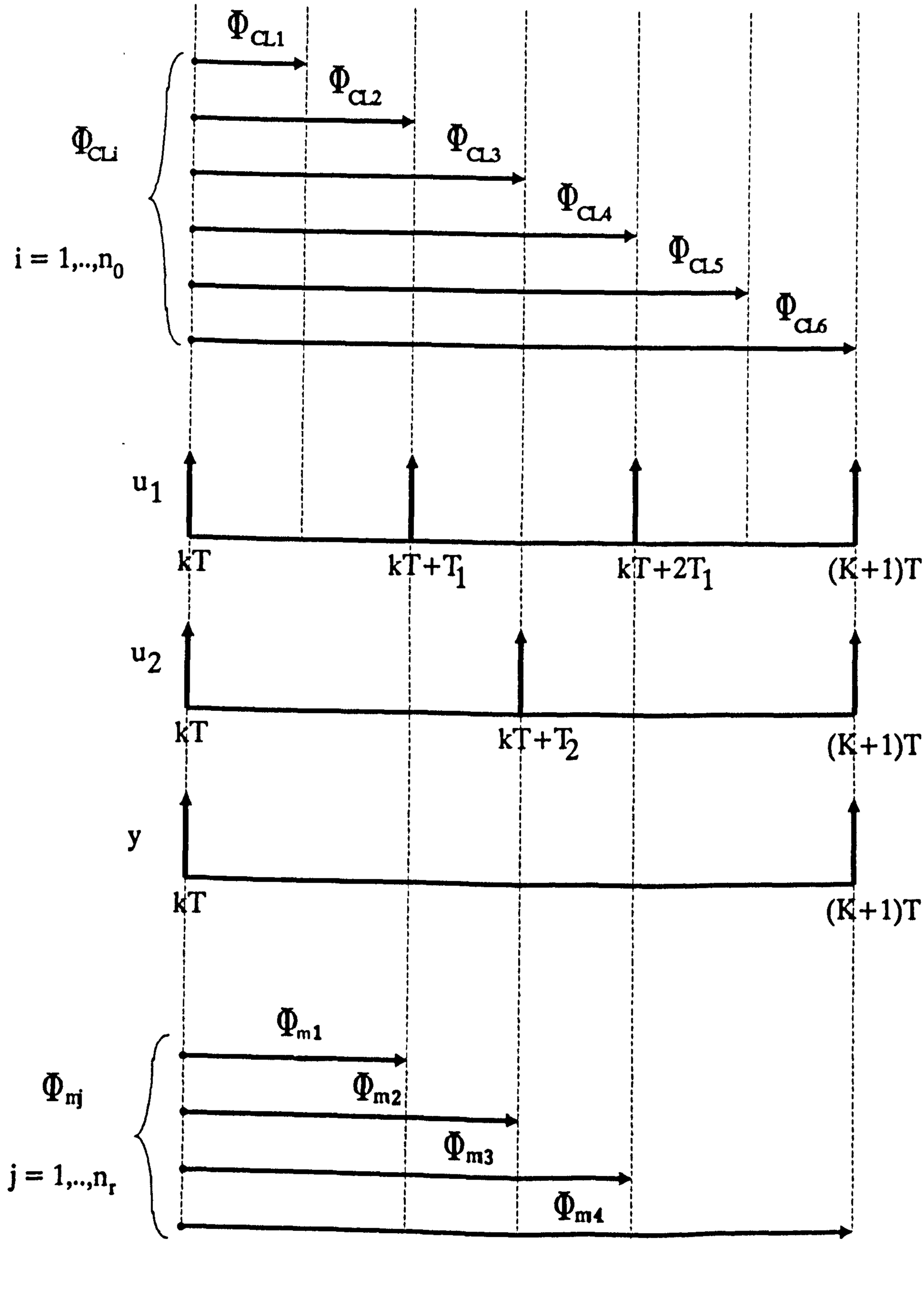

Figure 4.6.1 Φ_{CLi} and Φ_m of the MIFO System of Figure 2.5.1

insensitivity of the *intersample* MIFO system response can be indicated. Only a subset of Φ_{CLi} need be examined: the Φ_{CLi} which characterise the system transition between points at which a change in input signal occurs. Assume n_r of these matrices are required for a given MIFO system. (Figure 4.6.1 highlights the required Φ_{CLm} for the example MIFO system depicted in Figure 2.5.1). For notational ease this subset of closed loop transition matrices are denoted $\Phi_{CLm}=\{\Phi_{mj}\}$, $j = 1,..,n_r$.

The multirate intersample and main sample modal matrices and associated robustness measures of the set Φ_{CLm} are defined:

$$L_{mj}{}^T \Lambda_{mj} V_{mj} = \Phi_{mj} \qquad V_j = [\nu_{j1}\ \nu_{j2}\ ..\ \nu_{jn}]$$
$$L_j{}^T = [l_{j1}\ l_{j2}\ ..\ l_{jn}]$$

$$\kappa_{mj}(V) = \kappa(V_{mj})$$

$$c_{mj}=\{c_{ji}\}$$

$$c_{ji} = \frac{\|\nu_{ji}\|_2 \|l_{ji}\|_2}{|l_{ji}{}^T \nu_{ji}|} \qquad j = 1,..,n_r \qquad i = 1,..,n \qquad (4.6.5)$$

Note that the eigenvalues on the main diagonal of $\Lambda_{mj} = (\lambda_{mj})$ are not neccessarily the set $\{(\lambda_{mj})^i\}$, $j = 1,..,n$ where $\lambda_{mj} = (\lambda_j)^{1/n_o}$. This equivalence holds only when the n_i, $i = 1,..,m$ rows of the multirate gain matrix (associated with each of the m inputs) are all identical. That is, constant control is applied over the main sample interval. This is rarely the case for MIFO state feedback control designed using MIMO state-space techniques (including eigenstructure assignment).

The robustness measures $\{\kappa_{mj}(V),\ c_{mj}\}$, $j = 1,..,n_r$ will characterise the insensitivity of the *main sample and intersample* MIFO multirate system response to parameter perturbations around a given operating point.

4.7. SUMMARY

This Chapter has outlined the basic sensitivity and robustness concepts used in MIMO design techniques. A typical feedback system is subjected to three main types of uncertainty (sensor noise, disturbances and modelling errors), each entering the system at different points within the closed loop configuration. The effect of these uncertainties have been detailed. The "ideal" singular value plots of the closed loop return difference and complementary sensitivity functions to counteract these effects have been outlined. Matrix singular values were determined to be MIMO measures of "gain". Singular value plots are thus, the MIMO system equivalent of a SISO system magnitude Bode plot.

Section 4.3 outlined the overall design strategy of the eigenstructure assignment method and described output and state feedback eigenstructure design. The extra degrees of freedom made available (beyond the assignment of eigenvalues) by MIMO systems has been outlined. The extra freedom can be used to assign the closed loop system right and left eigenvectors $\{v_i\}$, $\{l_i\}$ respectively. (Note that when combined, the eigenvalues and eigenvectors constitute the system eigenstructure). Here, only right eigenvector assignment has been considered. The design criterion used for *robust* solutions to the eigenproblem is the right eigenvector conditioning measure $\kappa(V)$. This provides an upper bound on the sensitivities c_i of closed loop eigenvalues to perturbations in the nominal system matrices.

The *physical* interpretation of the robust eigenstructure assignment method has been shown to relate to the internal system operation. Two issues related to this physical interpretation are emphasised; the available design freedom and the manner in which the design freedom is utlised.

The available design freedom is determined by the number of inputs for state feedback, and the number of inputs and outputs for output

feedback. For the continuous-time and single rate discrete state feedback cases, the solution to the eigenproblem requires the direct use of *full* design freedom by utlising *all* m system inputs.

The second issue, which is intrinsically linked to the first, relates to the manner in which the design freedom is applied to arrange the internal system structure. It is well known that closed loop systems formed using canonical pole assignment algorithms generally produce extreme state transitions. This is due to a preliminary design phase which effectively *forces* a system to adopt an internal canonical structure (which allocates specific internal subsystems to each input) before applying appropriate control action. Such strong internal decoupling of system blocks is usually not necessary for the design of transient performance. A much more useful closed loop system internal structure is one which *enhances* system performance during the transient phase. Thus, by a suitable choice of right eigenvectors (v_i) the eigenstructure assignment method seeks to find an internal control structure which best suits the state feedback control task. In this way, the closed loop system insensitivity to *unstructered* uncertainties is improved at a specific operating point.

The relationship between the frequency domain robustness concepts and the $\kappa(V)$ sensitivity measure was outlined with the use of bounding conditions. A choice of $V = \{v_i\}$ such that $\kappa(V)$ is minimised was shown to improve directly the singular value plots of the sensitivity and return difference functions (ie move towards the "ideal" shape).

For the continuous-time and single rate state feedback eigenproblems, an achievable set of eigenvectors was shown to be limited by the nullity of the admissible space $N_{\lambda i}$. In general, $m<n$ indicating an overdetermined problem for which a maximum of m elements of the desired eigenvectors can be achieved exactly. For the single rate discrete eigenproblem, some extra design freedom is offered by the system sample interval. This effectively enables different bases for the

admissible subspace to be selected. For the MIFO multirate system, the *dimension* of $N_{\lambda i}$ can also be extended by the choice of its input sample rates. In particular, the input sample rate multiplicities $\{\mu_i\}$, $\{l_i\}$ defined in Chapter 3 will produce a solution space $N_{\lambda i} \epsilon R^{nxn}$, i=1,..,n.

The most important implication of this guaranteed extra design freedom is that the robust eigenstructure assignment design criterion can be *totally* satisfied. This would indicate that perfectly conditioned solutions can be obtained using MIFO multirate sampling schemes. However, sensitivity measures $\kappa(V)$, c_i, only monitor main sample behaviour of the MIFO system. Thus, the perfect decoupling property (if achieved) would only be observed at periodic intervals. Section 4.6 introduced new *intersample* robustness measures $\kappa_m(V)$, c_{mi}, to enable the total performance of the MIFO multirate feedback system to be assessed. The accuracy of these new measures is examined in Chapter 5.

CHAPTER FIVE

MIFO MULTIRATE CONTROL SYSTEM DESIGN USING EIGENSTRUCTURE ASSIGNMENT

5.1 INTRODUCTION

The application of eigenstructure assignment to the minimal MIFO multirate, multivariable system description is considered in this Chapter. The problems associated with the feedback design of general periodic systems are outlined together with an indication of the necessary qualities of a *practical* MIFO multirate design method. Eigenstructure assignment directly addresses these problems and this is the subject of the following discussion.

In Chapter 3 it was shown that the application of conventional state space feedback design methods to MIFO systems produce unrealistic control designs. This is due to the very high gain feedback matrices (monitored by $\|K\|_2$) which result from such a design. These gain matrices are an inherent product of the minimal state space description used to represent MIFO system behaviour (i.e. canonical type structures). Furthermore, the fact that MIFO system input updates occur at different points within the main sample interval presents a problem; there is a large risk of adverse intersample reaction of a "fast" subsystem propagating through "slower" subsystems and causing a rapid (due to large magnitude elements in the feedback gain matrix) destabilising response before it can be monitored and corrected.

Eigenstructure assignment can be applied to minimise these undesirable effects of high gains. If the MIFO system eigenstructure is selected to confine modal interaction to an operational minimum, the magnitude of elements in the feedback gain matrix can be decreased and, simultaneously, the destabilising effects are reduced. The degree of

multirate modal interaction or decoupling is monitored by $\kappa_{mi}(V)$ defined in Section 4.6. The measures $\kappa_{mi}(V)$ also indicate the insensitivity of the closed-loop system to inaccurate feedback information (since the insensitivity corresponds to changes in elements of the closed loop system transition matrix $\Phi + \Gamma K$). As the MIFO model relies on 'stale' state data to calculate the control over a main interval of sampling, this measure is particularly relevant in the multirate pole assignment problem.

Chapter 3 outlined the controllability condition which must be satisfied by a MIFO multirate system for pole placement. Two methods of selecting MIFO system input sample rate multiplicities to achieve this condition were outlined. Chapter 4 has indicated how MIFO sampling can extend the design freedom made available for the assignment of decoupled closed loop structures. Section 5.2 introduces a *generalised* criterion for input sample rate selection (which encompasses the controllability selection criteria of Chapter 3) for MIFO eigenstructure assignment design problems (Patel and Patton, 1991a, 1991b).

Section 5.3 outlines one method of solving the state feedback eigenproblem, based on a least squares minimisation of the error between desired and achieved eigenvectors. It is termed the "direct" assignment due to the non-iterative approach to the assignment of desired closed loop eigenvectors. The direct assignment method is well suited for comparison purposes due to its "single-pass" calculation, which leaves no opportunity for varying levels of attention in the formulation of the feedback control laws (as, for example, with optimised assignment techniques).

Sections 5.4 and 5.5 seek to establish the use and validity of the new multirate sensitivity measures of Section 4.6 ($\kappa_m(V)$ and c_{mi}) to monitor MIFO system performance and also to verify the selection criterion of Section 5.2.

To demonstrate the impact of decoupling and choice of input sample

rates on MIFO system performance, the feedback control designs of Examples 3.5.1 and 3.5.2 are repeated in Section 5.4 using direct eigenstructure assignment (Patel and Patton, 1991a, 1991b). Input sample rate multiplicities for these two examples are selected according to the basic controllability criteria of Chapter 3 and the generalised criterion of Section 5.2. The MIFO designs produced by the different choices of input sample rates are examined using time response data and the new sensitivity measures of Chapter 4. The $\|K\|_2$ measures of the eigenstructure assignment feedback designs are compared with those produced by the original designs of Chapter 3. The performance of the corresponding single rate feedback control (designed using the direct eigenstructure assignment method) is also examined to illustrate the effectiveness of MIFO multirate sampling schemes.

The first two design examples are based on low order and relatively simple systems. The simplicity serves well to demonstrate clearly the effects of MIFO sampling. A more complex (and realistic) MIFO control problem is introduced in the final example of Section 5.4 which considers the design of a flight control system.

Section 5.5 tests the controllability and MIFO eigenstructure assignment criteria of Chapter 3 and Section 5.2. Two examples demonstrate that the input sample rate multiplicities (indicated by a combination of these two separate conditions) are a neccessary requirement for perfectly decoupled closed loop modes. The effect of violating the essential controllability condition on MIFO pole placement is demonstrated.

The transient responses of the examples given in Sections 5.4 and 5.5 are investigated further in Section 5.6. In the author's experience, the intersample behaviour of multirate control systems is often *totally* ignored by many researchers. In the multirate pole assignment literature, the techniques are very rarely extended beyond a purely theoretical treatment and usually the topic of intersample response is

neatly avoided. Exceptions to this case include the work of Araki et al, 1988; Berg et al, 1988; Franklin et al, 1990. The intersample behaviour of multirate systems is particularly difficult to analyse since the dynamical coupling between different modes is constantly changing at different rates. The achievement of perfectly decoupled closed modes removes this difficulty and provides an opportunity for a precise analysis to be conducted.

An analysis of intersample behaviour of MIFO multirate systems is presented in Section 5.6. Section 5.4 supplements its design examples with time responses and sensitivity data corresponding to the intersample behaviour. A further (more detailed) examination of the Section 5.4 examples allows some new conclusions to be drawn regarding the design of intersample behaviour. The validity of these new conclusions is demonstrated by a further example in this final section.

5.2 INPUT SAMPLE RATE SELECTION CRITERION FOR MIFO EIGENSTRUCTURE ASSIGNMENT

Chapter 3 shows that the controllabilty conditions of the MIFO sampled system are satisfied by matrices M_{c1}, M_{c2} which determine the input sample rates. The *generalised* input selection criterion for perfectly conditioned solutions to the MIFO eigenproblem is based on the formulation of the matrix,

$$\beta_C = [\Gamma_1 \ \Phi_1\Gamma_1 \ldots \Phi_1^{\rho 1-1}\Gamma_1, \ .. \ , \ \Gamma_m \ \Phi_m\Gamma_m \ldots \Phi_m^{\rho m-1}\Gamma_m] \qquad (5.2.1)$$

Γ_i is the ith column of the single rate system control matrix sampled at T_i and Φ_i is the associated single rate state transition matrix. (The MIFO controllability conditions of Chapter 3 produce input sample rate multiplicities $\{p_i\} = \{\mu_i\}$, $\{p_i\} = \{l_i\}$).

The generalised selection criterion is as follows: The columns of β_C are selected such that, starting from Γ_1, a maximum of $p_1 = n$ further columns are added such that all vectors associated with Γ_1 are linearly independent. The process is continued for all control inputs required for the achievement of (A,B) controllability. When the condition,

$$\sum \rho_i = n \qquad i=j,\ j<m \qquad (5.2.2a)$$

is reached then all subsequent input sample rates have unity input multiplicity, i.e.,

$$n_i = 1 \qquad i=j+1,\ldots,m \qquad (5.2.2b)$$

Clearly, this method of selecting input sample rates yields $\{T_i\}=\{T/\rho_i\}$, $\sum\rho_i > n$ for all systems satisfying (5.2.2). *Note that a rearrangement of columns in the original control matrix may produce a different set $\{\rho_i\}$.*

If $\sum\rho_i = \rho > n$ then the subspace in which the achievable eigenvectors reside, $[(\lambda_i I-\Phi_{MR1})^{-1}\ \Gamma_{MR1}] \epsilon R^{nx\rho}$, will provide full design freedom for the eigenstructure assignment procedure. This effectively allows the *precise* assignment of *any* set of finite magnitude desired eigenvectors of the closed loop multirate system. For this set of sample parameters, the design parameter k_i of equation (4.6.4) (and thus ω_i of equation (4.5.1)) is determined uniquely, resulting in a simpler formula for the multirate gain matrix:

$$K = [M_{\lambda 1}(N_{\lambda i})^{-1}v_1\ ..\ M_{\lambda n}(N_{\lambda n})^{-1}v_n]V^{-1} \qquad (5.2.3)$$

Equation (5.2.3) holds for all multirate sampled systems that satisfy $\beta_C \epsilon R^n$. (Recall that MIFO systems determined by input sample rate multiplicities $\{\mu_i\}$, $\{l_i\}$ if put into the form of equation (5.2.1) will also produce matrix $\beta_C \epsilon R^n$).

The indices ρ_i, i=1,..,m, determine the dimension of the maximum solution subspace that the ith input is capable of generating with a multirate MIFO sampled system. The development of the β_c and the multirate controllability matrices is different; selection of columns for the latter terminates at $\sum\mu_i = n$ or $\sum l_i = n$ which may result in $\mu_i < \rho_i$, $l_i < \rho_i$.

For cases where the sample rate selection process does give $\rho > n$, a characteristic of the resulting feedback gain matrix produced using equation (5.2.3) is the generation of (ρ-n) null rows. This is a direct consequence of the overdetermined solution produced by this choice of sample rates. The presence of null rows effectively limits the number of gain elements of a feedback control matrix (designed using the direct assignment method) of *any* MIFO scheme satisfying the necessary conditions for multirate pole assignability to $\leq n^2$.

5.3 LEAST SQUARES APPROXIMATION TO DESIRED EIGENVECTORS

The solution of the eigenproblem requires two main stages; calculation of the admissible nullspace from which the desired right eigenvectors are to be selected and determination of the achievable eigenvectors.

For a given set of vectors V, an achievable eigenvector v_{ai} can be determined by the orthogonal projection of the desired eigenvector v_{di} onto the nullspace $R[N_{\lambda i}]$. The Singular Value Decomposition (SVD) method can be used to determine $R_{\lambda i} = [N_{\lambda i}^T \; M_{\lambda i}^T]^T$ in a numerically stable manner. This calculation is well documented (Golub and Van Loan, 1983; Silverthorn and Reid, 1980). Its application for the solution to the general eigenproblem is outlined:

For the matrix $S_{\lambda i} = [\lambda_i I - A : B] \in R^{nx(n+m)}$ orthogonal matrices, $U \in R^{mxm}$ and $V \in R^{nxn}$ will exist such that,

$$\begin{bmatrix} \lambda_i I - A & -B \end{bmatrix} = U \Sigma V^T = \begin{bmatrix} U_1 & U_2 \end{bmatrix} \begin{bmatrix} S & 0 \\ 0 & 0 \end{bmatrix} \begin{bmatrix} V_1^T \\ V_2^T \end{bmatrix} \tag{5.3.1}$$

where, $S = \text{diag}(\sigma_1, \sigma_2, .., \sigma_n)$ $\sigma_1 > \sigma_2 > , .., > \sigma_n$, is the matrix of non-zero singular values of $S_{\lambda i}$. The columns of U are the *left singular vectors* of $S_{\lambda i}$ and the columns of V the *right singular vectors*. If equation (5.3.1) is rewritten as:

$$\begin{bmatrix} \lambda_i I - A & -B \end{bmatrix} V = U_1 \begin{bmatrix} S & 0 \end{bmatrix} \tag{5.3.2}$$

then, since the last m columns of V (i.e. V_2) make $S_{\lambda i} V = 0$, the columns of V_2 span the nullspace of $S_{\lambda i}$. Thus, one numerically stable candidate for $R_{\lambda i}$ is V_2. For $S_{\lambda i} \epsilon \mathbb{C}$ (i.e. for complex poles), U and V will be *unitary* matrices.

The projection, $N_{\lambda i} k_i$, for the least squares problem,

$$\min_{k_i} \| \nu_{ai} - \nu_{di} \|_2 \tag{5.3.3}$$

has a solution given by,

$$k_i = (N_{\lambda i}^T N_{\lambda i})^{-1} N_{\lambda i}^T \nu_{di} \tag{5.3.4}$$

A minor modification to equation (5.3.4) is required for the complex eigenvalue case (see equations (4.3.16) to (4.3.19)). Define the combined real and imaginary parts of the desired complex eigenvector as $\nu_{cdi} = [\nu_{Rei}^T \ \nu_{Im}^T]^T$. Further, let $R^u_{C\lambda i}$ denote the upper portion of matrix $R_{C\lambda i}$ in equation (4.3.18), i.e.,

$$R^u_{C\lambda i} = \begin{bmatrix} N_{\lambda i} \\ P_{\lambda i} \end{bmatrix} \tag{5.3.5}$$

The achievable complex right eigenvector, ν_{cai}, resides in the space defined by the intersection of nullspaces corresponding to real and imaginary parts of λ_i (defined $N_{\lambda i}$ and $P_{\lambda i}$ respectively). Thus, for $\lambda_i \epsilon \mathbb{C}$ the least squares projection of ν_{cdi} onto the admissible subspace is given by:

$$k_{ci} = (R^{u}C_{\lambda i}{}^{T} R^{u}C_{\lambda i})^{-1} R^{u}C_{\lambda i}{}^{T}\nu_{cdi} \qquad (5.3.6)$$

A complex-conjugate pair of eigenvectors is obtained using this method.

For a given triple (Φ,Γ,C) and a desired eigenstructure, the least squares solution to the eigenproblem is obtained via a single pass calculation (hence, its name the "direct" assignment). If the desired eigenvectors are chosen to be as orthogonal to each other as possible, the feedback will provide a well-conditioned closed-loop system with maximum insensitivity of the poles to system parameter perturbations. A specific modal structure will emphasise some desired interaction of modes. A comparison of the two different approaches is outlined clearly in Burrows and Patton, (1991).

Note that the assignment of confluent eigenvalues with this method will give ill-conditioned solutions. Consider, for a given system, the assignment of an eigenvalue with multiplicity q i.e. $\{\lambda_1\ \lambda_2,..,\lambda_q\}$, $q<n$. The eigenvalue is said to have geometric multiplicity q and algebraic multiplicity 1. The geometric multiplicity of the right eigenvectors corresponding to the multiple eigenvalues is also 1. Therefore, equation (5.3.2) will not give q linearly independent right eigenvectors. In this case, (q-1) *generalised* eigenvectors can be found to preserve the singularity of matrix V (Klein and Moore, 1977).

The generalised eigenvectors satisfy the linear equation,

$$\begin{bmatrix} \lambda_i I-A & -B \end{bmatrix}\begin{bmatrix} N_{\lambda i,j} \\ M_{\lambda i,j} \end{bmatrix} = N_{\lambda i,j-1} \qquad j = 1\ ,..,\ (q-1) \qquad (5.3.7)$$

where, $N_{\lambda i,o}$ is the desired closed loop eigenvector. The solution of equation (5.3.7) requires the SVD of (5.3.1) to be calculated only once. The generalised eigenvectors are computed using

$$\begin{bmatrix} N_{\lambda i,j} \\ M_{\lambda i,j} \end{bmatrix} = V_1 \Sigma^{-1} U^T N_{\lambda i,j-1} + V_2 k_i \qquad j = 1, .., (q-1) \tag{5.3.8}$$

5.4 DIRECT EIGENSTRUCTURE ASSIGNMENT EXAMPLES

Three examples are presented to demonstrate the effects of applying the direct eigenstructure assignment procedure to MIFO sampled systems. The examples are based on the pole placement problems described in Chapter 3. These are repeated to show the improvement in feedback control design achievable by the eigenstructure assignment method. Solutions for the feedback gain matrix are found by a least squares approximation to the desired eigenstructure. For the first two examples, real eigenvalues are assigned and it is assumed that the desired eigenvectors are mutually orthogonal; the third example demonstrates the assignment of complex eigenvalues and furthermore, assumes some desired interaction of modes.

The effect of the different methods of selecting input sample rates on the multirate eigenproblem is demonstrated with examples 5.4.1 and 5.4.2. The low order dynamics of these examples are chosen to display clearly the design factors which influence the MIFO multirate pole placement. Time responses and conditioning measures of the MIFO feedback designs are compared with corresponding single rate discrete designs to illustrate the advantages and disadvantages of MIFO multirate sampling.

The open loop state transition matrix of Example 5.4.1 represents a strongly coupled system. The strong coupling presents a difficult decoupling task and is chosen to portray *accurately* the comparative

sensitivity and robustness properties produced by the single rate and multirate designs.

In contrast, Example 5.4.2 compares the closed loop sensitivity performance produced by single rate and multirate feedback applied to an open loop system with weak modal coupling. This example system is taken from Araki et al, (1988). The relative ease with which decoupling is achieved (by both single rate and multirate feedback) for the weakly coupled system is illustrated by this example.

5.4.1 Example 5.4.1

This example examines the design of single rate and MIFO multirate feedback for the system of Example 3.5.1 such that desired closed loop poles are assigned with a maximally orthogonal eigenstructure. Note that in the ideal case $\{\nu_{di}\} = I_n$. (Recall that for this example the open loop poles {-1 -2 -3} were required to be moved to {-0.5 -0.6 -0.7}). A least squares solution to the eigenproblem is determined for three sets of input sample rate multiplicities within a main interval of sampling T = 0.1secs. This does not render any of the modes uncontrollable, thus ensuring the assignability of desired eigenvalues.

The formulation of matrices M_{c1}, M_{c2} and B_c gives $\mu_1=l_1=2$, $\mu_2=l_2=1$ and $\rho_1=3$, $\rho_2=1$. The gain matrices produced by direct assignment for the single rate and the MIFO systems developed using each of the above input sample rate multiplicities are given below :

1. <u>Single rate</u> $T_1=T$, $T_2=T$

$$K_1 = \begin{bmatrix} 2.9832 & 5.9881 & 3.7679 \\ -0.2931 & -1.0622 & -1.1507 \end{bmatrix} \qquad (5.4.1a)$$

2. Multirate input sample rates determined by $\{\mu_i\}=\{l_i\}$ $T_1=T/2$, $T_2=T$

$$K_2 = \begin{bmatrix} 22.1843 & -40.2434 & -16.5515 \\ 20.1615 & 37.5406 & 17.6343 \\ 0.5250 & 0.3829 & 0.5409 \end{bmatrix} \qquad (5.4.1b)$$

3. Multirate input sample rates determined by $\{\rho_i\}$ $T_1=T/3$, $T_2=T$

$$K_3 = \begin{bmatrix} 25.3670 & 45.8164 & 18.3884 \\ 0 & 0 & 0 \\ -22.5552 & -41.7645 & -20.0087 \\ -0.5243 & -0.3821 & 0.5398 \end{bmatrix} \qquad (5.4.1c)$$

which has $(\rho\text{-}n) = 1$ null row as expected.

The results of implementing the three controllers in a simulation of the system, for an initial state perturbation of $[0.1\ 0.3\ 0.15]^T$ are shown in Figure 5.4.1. The responses of feedback design K_1 represent the maximum decoupling achievable by single rate sampling. Responses of K_2 design show the decoupling achievable by satisfying the MIFO multirate controllability conditions of Chapter 3 whilst the K_3 design responses demonstrate the decoupling obtained by satisfying the generalised β_C matrix selection criterion. Note that the responses of the K_2 and K_3 designs are identical; both exhibit the *perfect modal decoupling* that all designs are attempting to achieve.

The only difference in the control input responses of the two multirate systems (in addition to the different update rates) is a slight increase in the magnitude of u_1 demanded by feedback design K_3. The u_2 control signal for all designs is however, smooth and has an acceptable magnitude. Thus the faster sampling of input u_1 required for the K_3 closed loop system appears to offer no advantage over the K_2 system. Both achieve the required decoupled responses at the main sample instants.

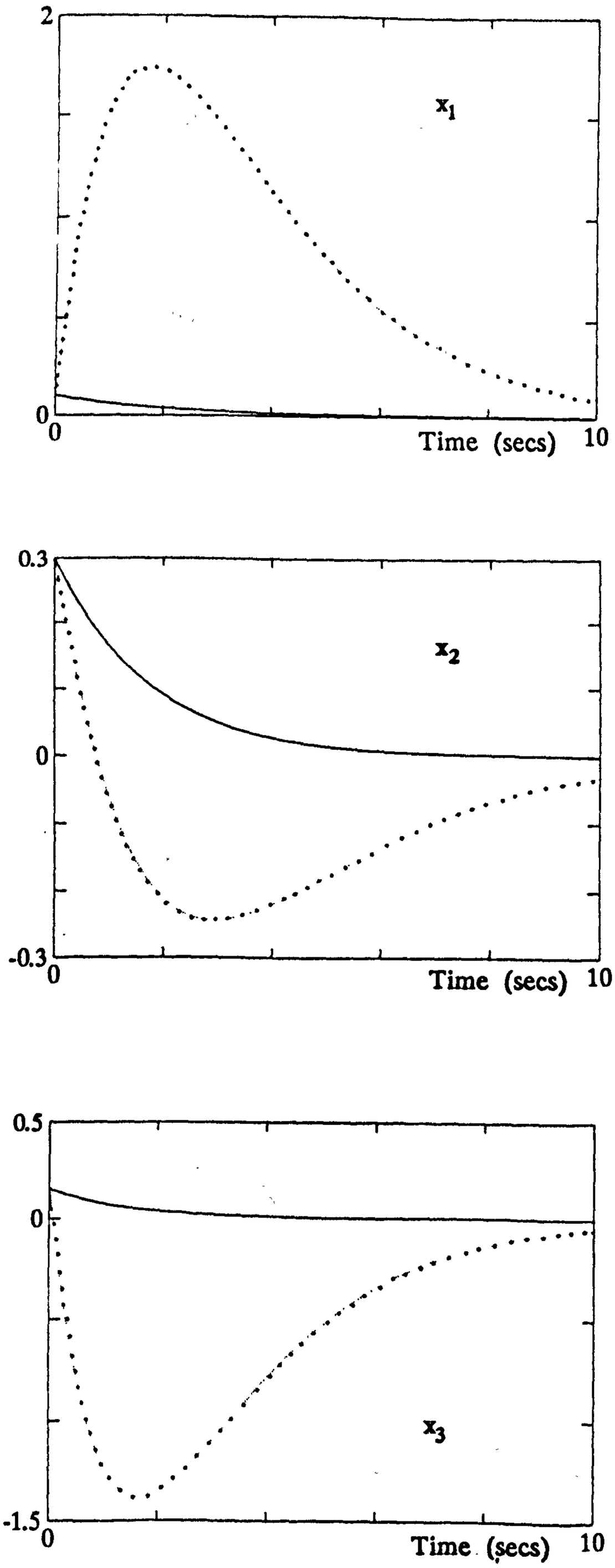

Figure 5.4.1a State responses of K_1 (single rate) and K_2, K_3 (multirate) closed loop systems.

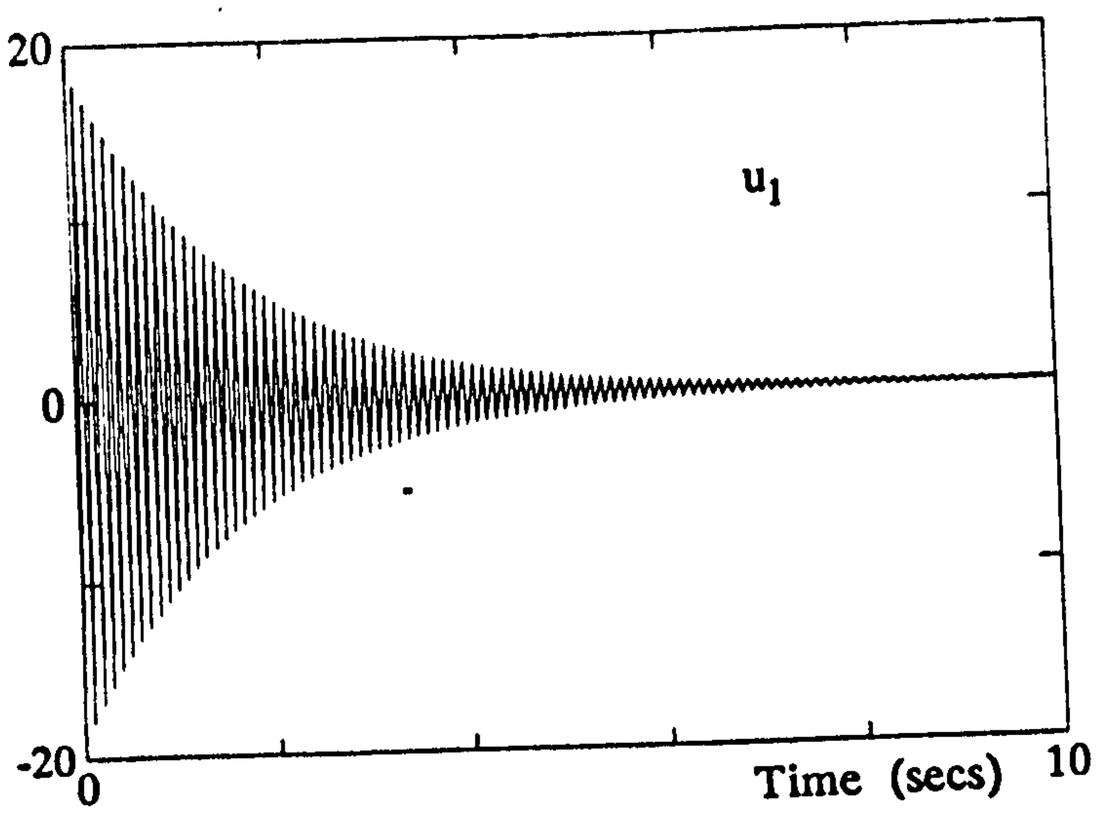

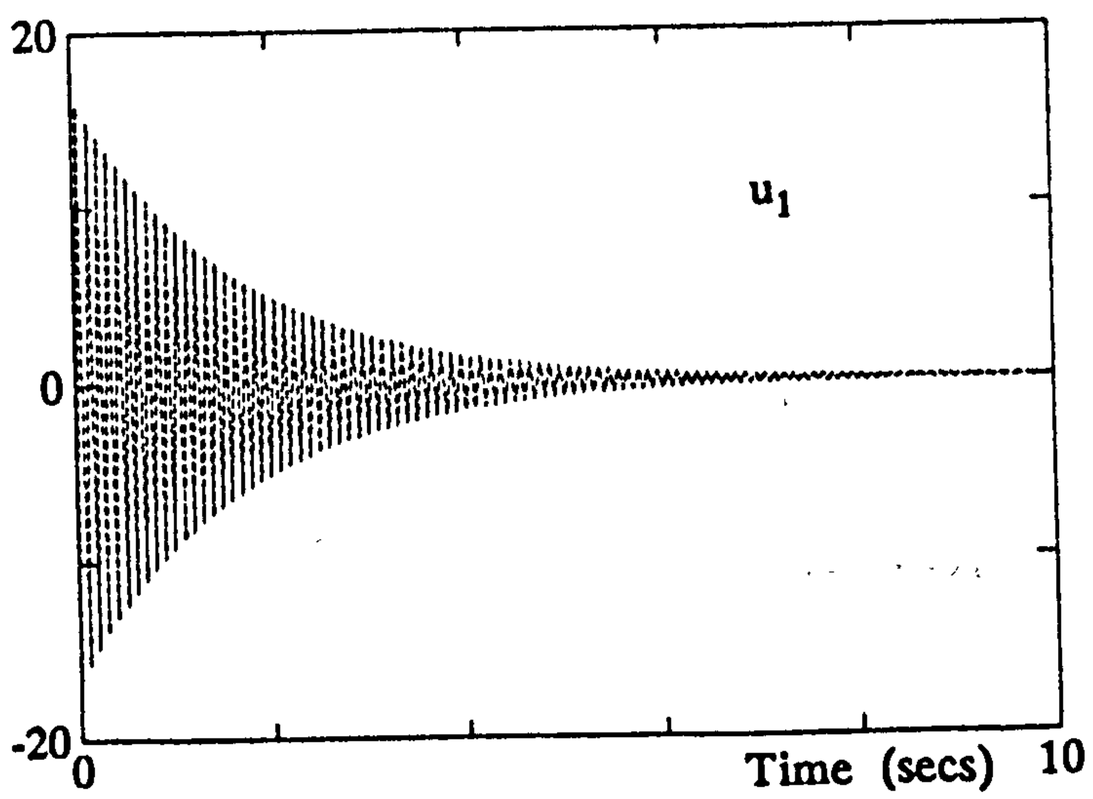

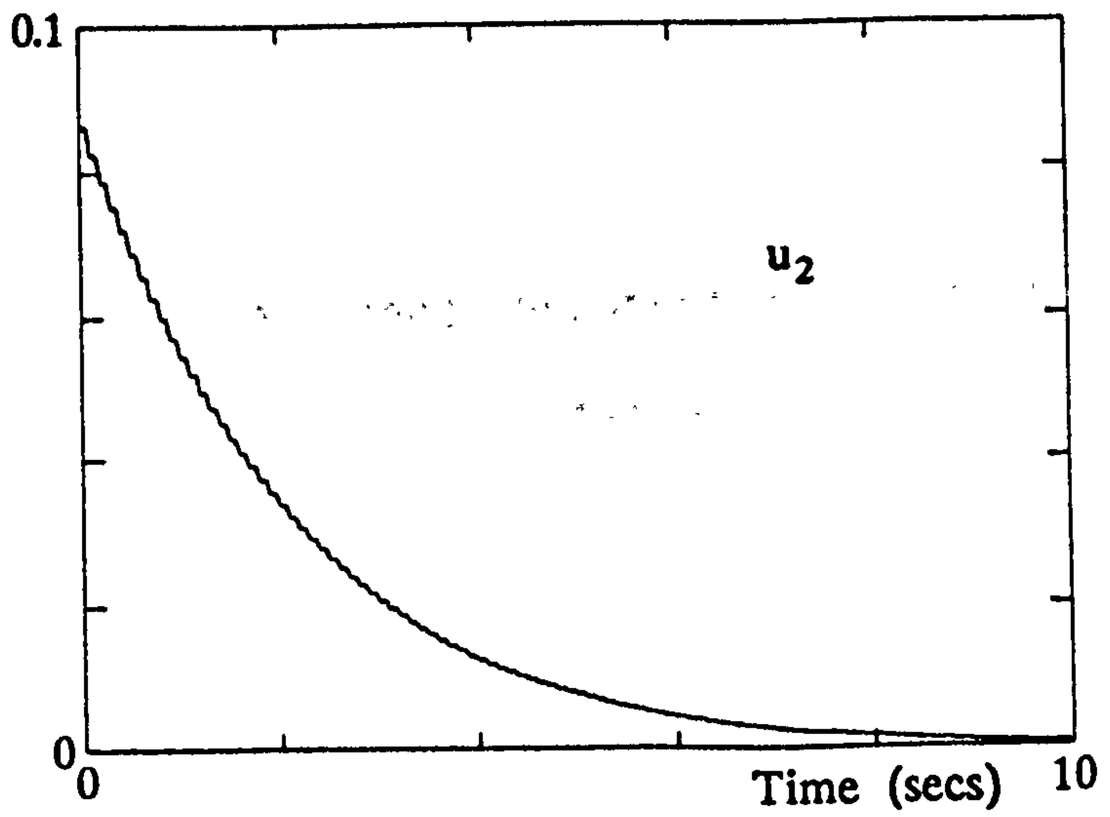

-----	K_2 system
———	K_3 system

Figure 5.4.1b Control input responses of K_2 and K_3 (multirate) closed loop systems.

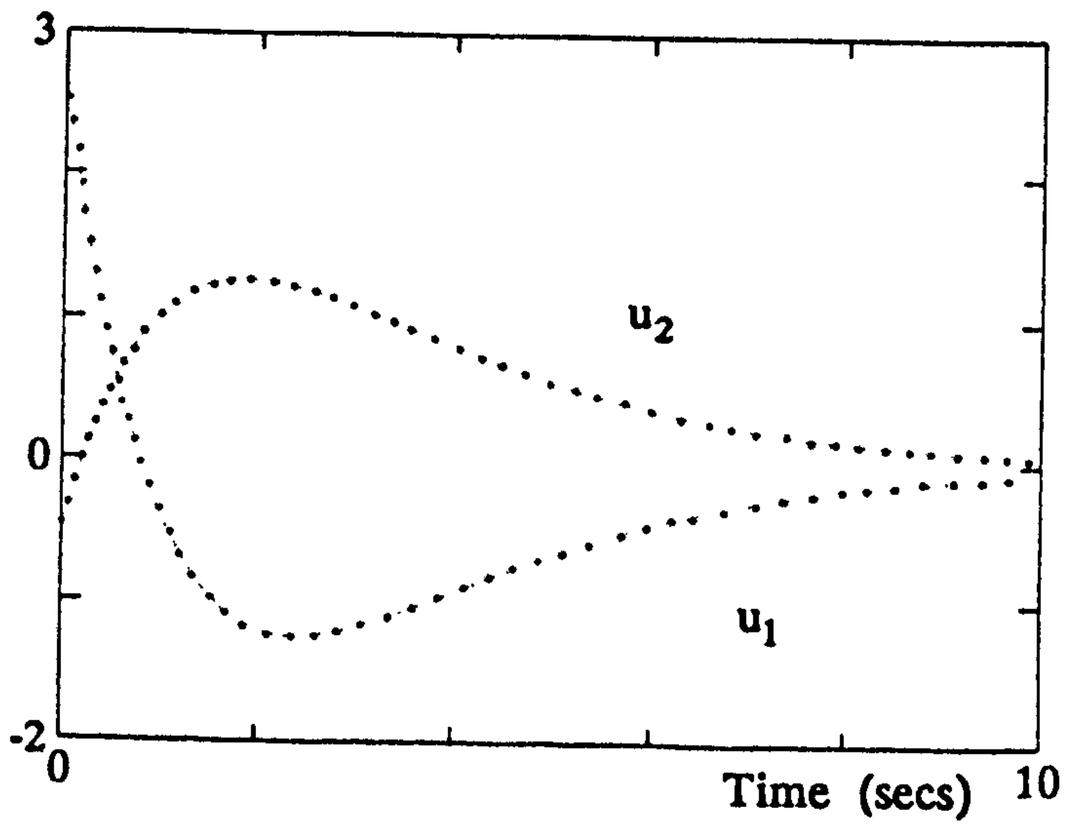

Figure 5.4.1c Control input responses of K_1 (single rate) closed loop system.

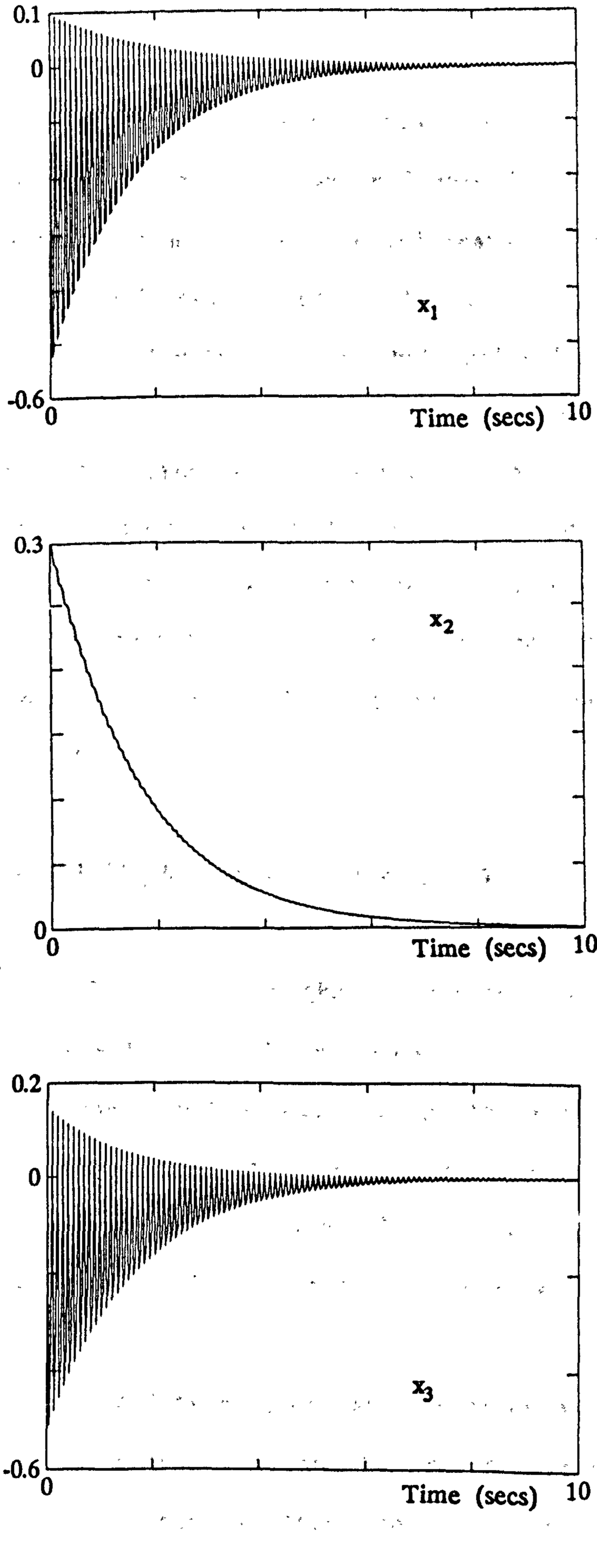

Figure 5.4.2 Intersample responses of K_2 and K_3 multirate closed loop systems.

The responses of Figure 5.4.1 are those obtained by sampling the system at a rate 1/T (which is the correct output sample rate of the MIFO system). An examination of the state responses *during* the interval T reveals the typical intersample oscillatory behaviour of the multirate designs. These are shown in Figure 5.4.2. These responses show that the improved decoupling of the multirate designs is obtained at the cost of large magnitude, switched intersample state behaviour. Note that x_2 of both multirate designs does not suffer from any intersample switching.

The extra control effort demanded by the feedback K_3 appears to be applied to produce less switched x_1 and x_3 state transients than K_2. The switched nature of both perfectly conditioned multirate solutions is obviously unacceptable and the cost on control effort impractical.

A sensitivity analysis of each design was conducted next to investigate whether the responses of Figure 5.4.1 could be analytically predicted.

<u>Sensitivity Analysis of Example 5.4.1</u>

Table 1 displays the eigenvector conditioning $\kappa_m(V)$ ($\kappa(V)$ for the single rate design) and $\|K\|_2$ figures for the above designs. Table 2 shows sensitivities c_{mi} (c_i for the single rate design), corresponding to the 3 closed loop eigenvalues of each feedback design. The ordering of the closed loop eigenvalues is $\lambda_1 = -0.5$, $\lambda_2 = -0.6$, $\lambda_3 = -0.7$. The results of Tables 1 and 2 are summarised as follows:

(i) *All* transition matrices produced by the multirate feedback gain matrices K_2 and K_3 provide *significantly* better overall modal decoupling than the single rate feedback matrix K_1. This is indicated by $\kappa_{mj}(V) < 1.94$ for all $j = 1,..n_r$, compared with $\kappa(V) \approx 173$ for the single rate case.

(ii) Both K_2 and K_3 produce $\kappa_{mj}(V)=1$; $j = n_r$.

(iii) The c_{mi} (eigenvalue sensitivity) figures of K_2, K_3 designs show that the closed loop poles of the multirate systems are much less sensitive to both main sample and intersample perturbations than the single rate design.

(iv) The gain norm $\|K\|_2$ increases from $K_1 \rightarrow K_3$. The difference between $\|K_2\|_2$ and $\|K_3\|_2$ is not as significant as that between $\|K_1\|_2$ and $\|K_2\|_2$, $\|K_3\|_2$.

Performance Measure	Feedback Gain Matrix		
	K_1	K_2	K_3
$\kappa(V)$ - for single rate design $\kappa_m(V)$ - for multirate designs	$\kappa(V) = 172.14$	$\kappa_1(V) = 3.68$ $\kappa_2(V) = 1$	$\kappa_1(V) = 3.35$ $\kappa_2(V) = 3.64$ $\kappa_3(V) = 1$
$\|K\|_2$	7.8253	67.1560	75.6217

Table 1 $\kappa(V)$, $\kappa_m(V)$ and $\|K\|_2$ of K_1, K_2 and K_3 closed loop systems

Transition period under examination	Sensitivities of closed loop eigenvalues produced by feedback gain matrix:								
	K_1			K_2			K_3		
	c_1	c_2	c_3	c_1	c_2	c_3	c_1	c_2	c_3
$kT \rightarrow kT+T_1$	—	—	—	—	—	—	1.781	1.558	1.724
$kT \rightarrow kT+2T_1$	—	—	—	1.751	1.910	1.876	—	—	—
$kT \rightarrow kT+3T_1$	—	—	—	—	—	—	1.724	1.714	1.934
$kT \rightarrow (k+1)T$	72.70	85.45	62.03	1	1	1	1	1	1

Table 2 Eigenvalue sensitivities c_{mi} of K_1, K_2 and K_3 systems

The most important point to note is that both the time responses and tabulated performance measures indicate the achievement of perfect decoupling by multirate feedback gains K_2 and K_3. Thus the analytic conditioning measures $\kappa(V)$ are an accurate means of assessing the sensitivity of MIFO system main sample behaviour.

The use of the *intersample* conditioning measures $\kappa_m(V)$ can also be validated by testing the relative insensitivity of the multirate and single rate closed loop systems to perturbations in the nominal *open loop* system dynamics. A comparison of the shift in position of the K_1 (single rate) and K_2, K_3 closed loop system poles caused by this perturbation will then establish the sensitivity of each system.

Sensitivity test of feedback K_2 design

The sensitivities of the closed loop systems produced by K_1, K_2 and K_3 are tested by perturbing the *open loop* system transition matrix A. The measures of Table 1 relate to the *discrete* closed loop system. If the system is subject to perturbations, then it is the *continuous* system transition matrix that is affected. Thus, for sensitivity analysis, the response of the three closed loop systems to changes in the A matrix is examined.

Table 1 suggests that the multirate designs are far more robust than equivalent single rate designs. A proportional perturbation in the system dynamics of the form $A = (1+\eta)A$ is considered to demonstrate this robustness. (Note that this form of variation in A will perturb the system in *one* direction only.) A perturbation $\eta = -0.1$, which corresponds to a 10% perturbation, *just* makes the single rate system unstable. The closed loop eigenvalues produced by each feedback gain matrix in response to this significant perturbation in the nominal system dynamics are as follows (together with the nominal eigenvalues):

Nominal Eigenvalues	Perturbed eigenvalues: K_1	K_2 and K_3
0.9512	1.0153	0.953±j0.007
0.9324	0.9136	
0.9418	0.9504	0.9364

Thus both multirate closed loop systems maintain stable performance while the single rate system becomes unstable. The multirate systems can in fact, tolerate an extreme proportional perturbation in the open loop system dynamics. A value of $\eta = -0.75$ (i.e. a 75% perturbation) will cause the above K_2, K_3 systems to become unstable. A perturbation of this magnitude can be regarded as producing a different system altogether rather than just a perturbation in the nominal system dynamics.

Thus, the perturbation test shows that the multirate designs deviate from the nominally designed closed loop poles but do maintain stable performance, whilst the single rate design has an unbounded x_3 trajectory (and hence unstable system performance).

5.4.2 Example 5.4.2

The MIFO feedback design for the 2 input, 4 state system of Example 3.5.2 is repeated. Recall that for this system the open loop eigenvalues {-2 -1 -3 -2} are to be moved to {-2.5 -1.5 -2.1 -0.5}. The sample rate selection criteria outlined in Sections 3.3 and 5.2 gives $\mu_1 = l_1 = \rho_1 = 2$, $\mu_2 = l_2 = \rho_2 = 2$. The main sample interval is chosen to be T=0.4secs. Feedback is to be designed such that the set of desired eigenvalues {0.3679 0.5488 0.4317 0.8817} is assigned with associated right eigenvectors possessing maximum mutual orthogonality. The single rate and multirate designs produced by the direct assignment method are:

1. <u>Single rate</u> $T_1=T,\ T_2=T$

$$K_4 = \begin{bmatrix} 1.4426 & 0.2931 & -0.2184 & 0.0043 \\ 4.6611 & 0.0054 & 0.0186 & 0.0176 \end{bmatrix} \qquad (5.4.3a)$$

2. <u>Multirate input rates determined by $\{\mu_i\}=\{l_i\}=\{\rho_i\}$</u> $T_1=T/2,\ T_2=T/2$

$$K_5 = \begin{bmatrix} -1.4525 & 2.4834 & 3.2151 & -3.6806 \\ 0.9481 & -1.3629 & -2.6323 & 2.3140 \\ 18.5629 & 0 & 0 & 3.1176 \\ -12.5842 & 0 & 0 & -4.6509 \end{bmatrix} \qquad (5.4.3b)$$

The state and control main sample responses of the closed loop system formed by gain matrices K_4 and K_5 to an initial state perturbation $[0.1\ 0.2\ 0.5\ 0.1]^T$ are shown in Figure 5.4.4. The intersample responses of the multirate system are shown in Figure 5.4.5.

Figure 5.4.4 shows that the single rate design K_4 produces almost perfect decoupling of closed loop modes, with a very slight modal interaction exhibited in all states. The multirate design K_5 produces perfect decoupling. This is achieved with significantly lower magnitude switching in the intersample response than that experienced by the system of Example 5.4.1. The ease with which almost perfectly decoupled modal responses are obtained by the single rate design is a reflection of the weak modal coupling of the open loop system. This gives some indication of the ease with which the multirate decoupling is likely to be achieved. Note also that, for this example $\{\mu_i\}$, $\{l_i\}$ and $\{\rho_i\}$, coincide.

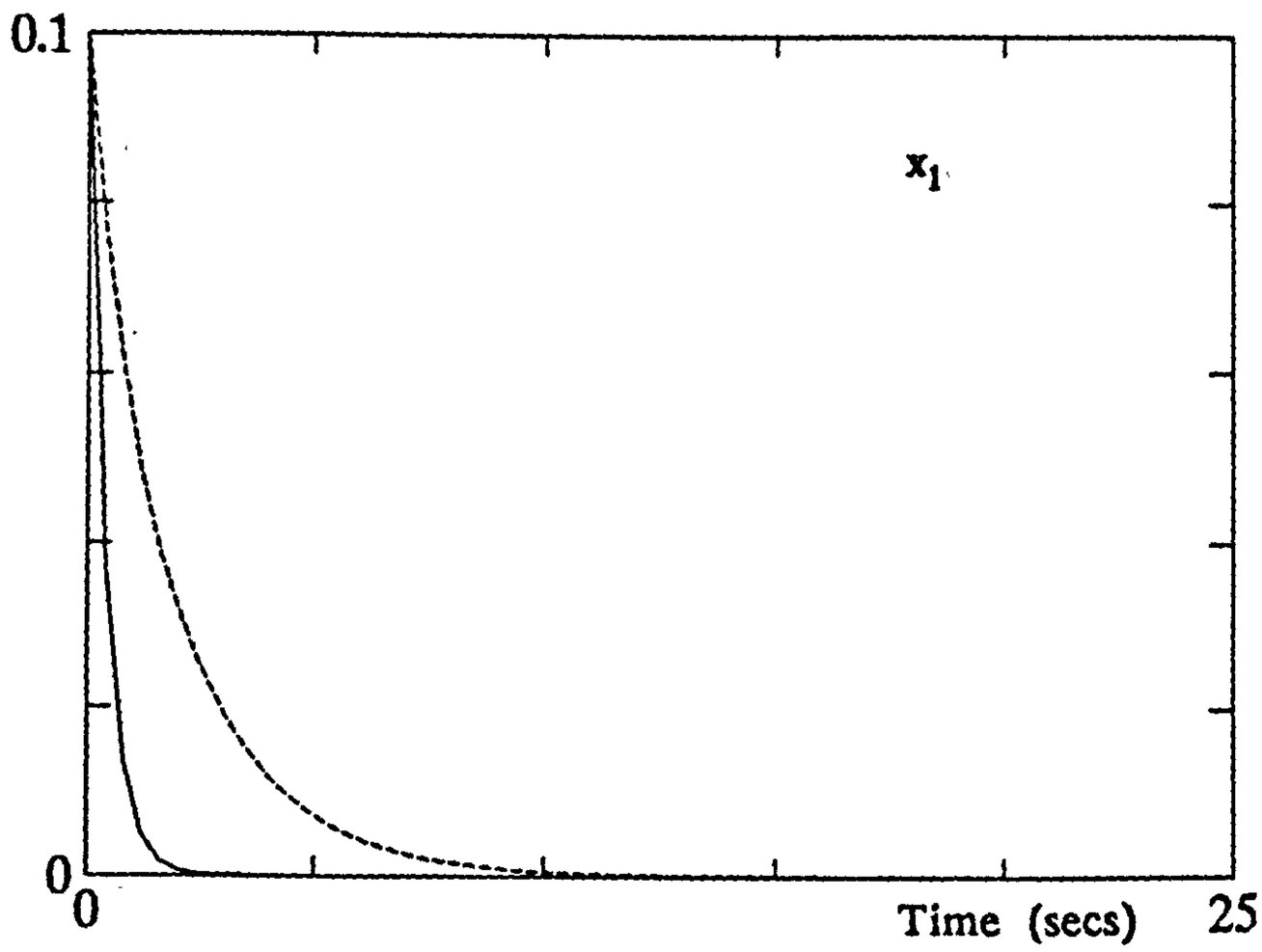

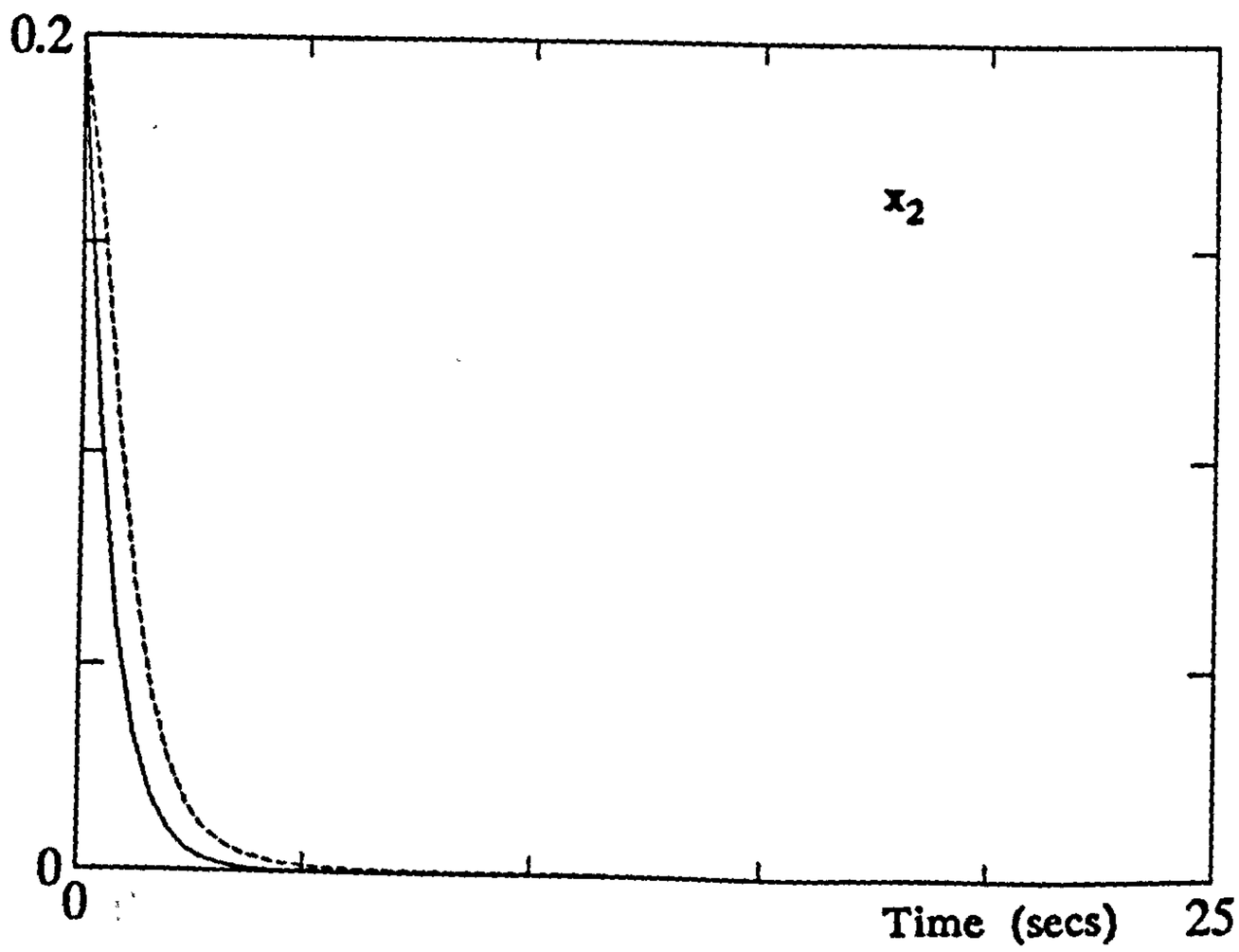

-----	K_4 system
———	K_5 system

Figure 5.4.4a State responses of K_4 (single rate) and K_5 (multirate) closed loop systems.

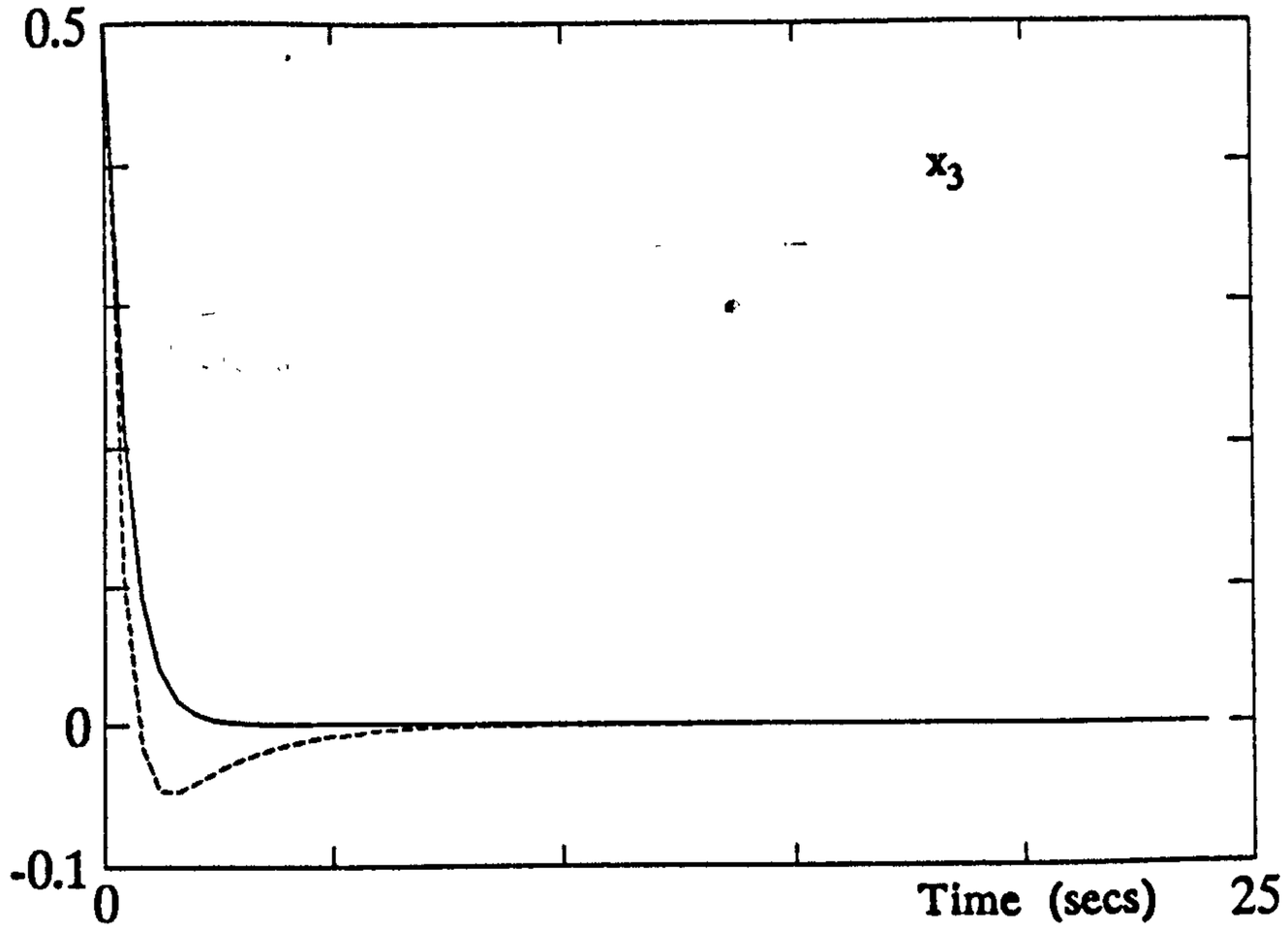

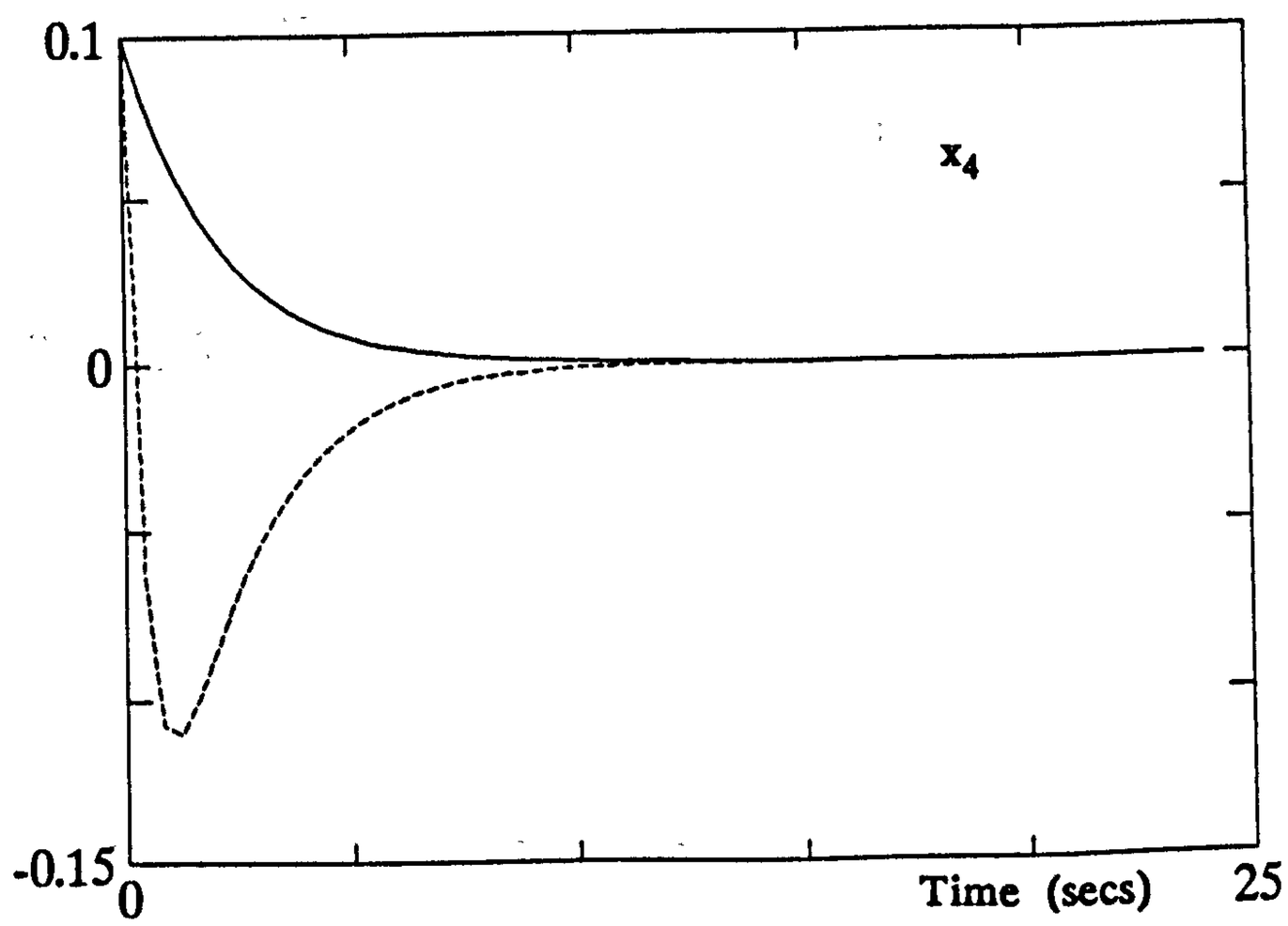

Figure 5.4.4a State responses of K_4 (single rate) and K_5 (multirate) closed loop systems (continued).

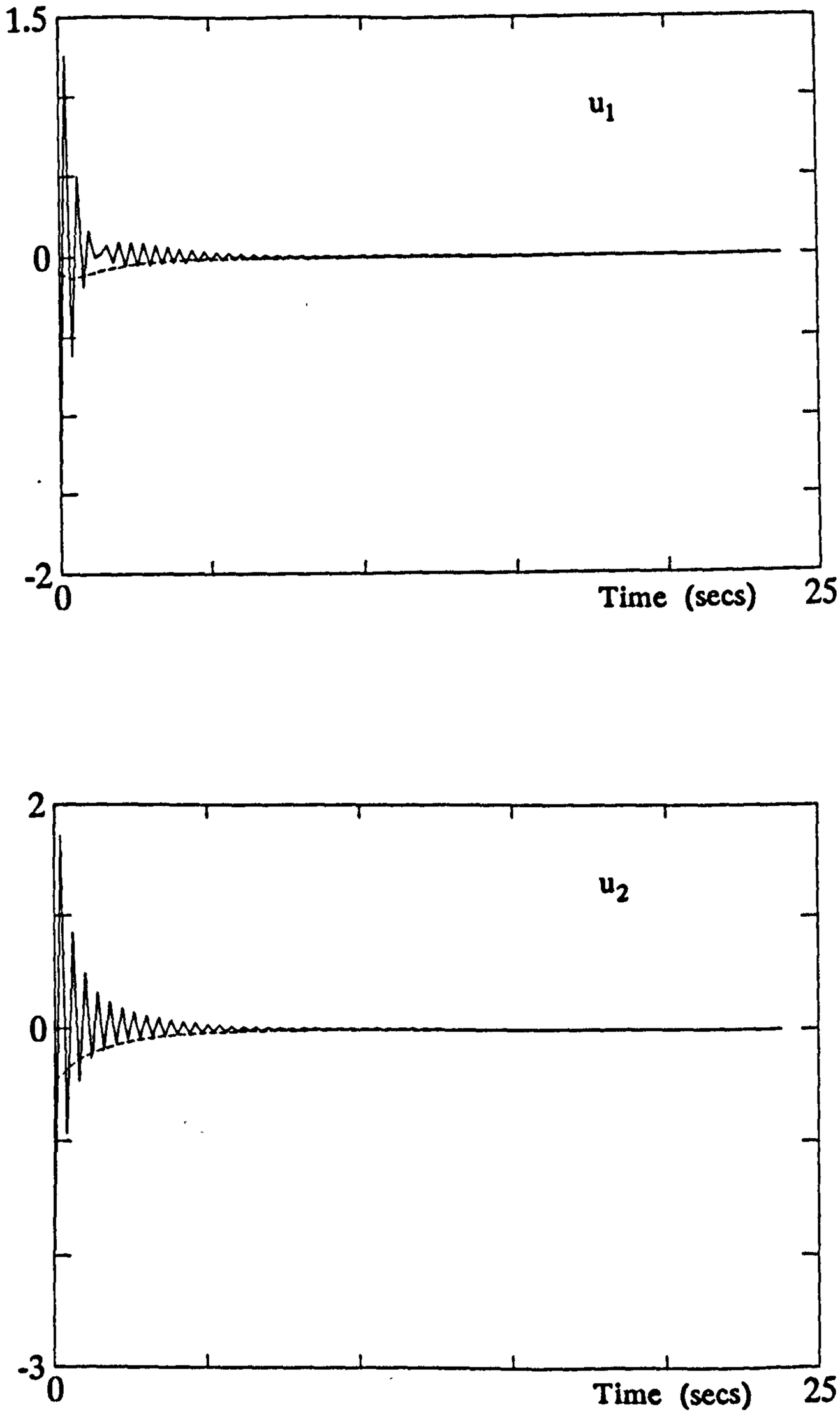

-----	K_4 system
———	K_5 system

Figure 5.4.4b Control input responses of K_4 (single rate) and K_5 (multirate) closed loop systems.

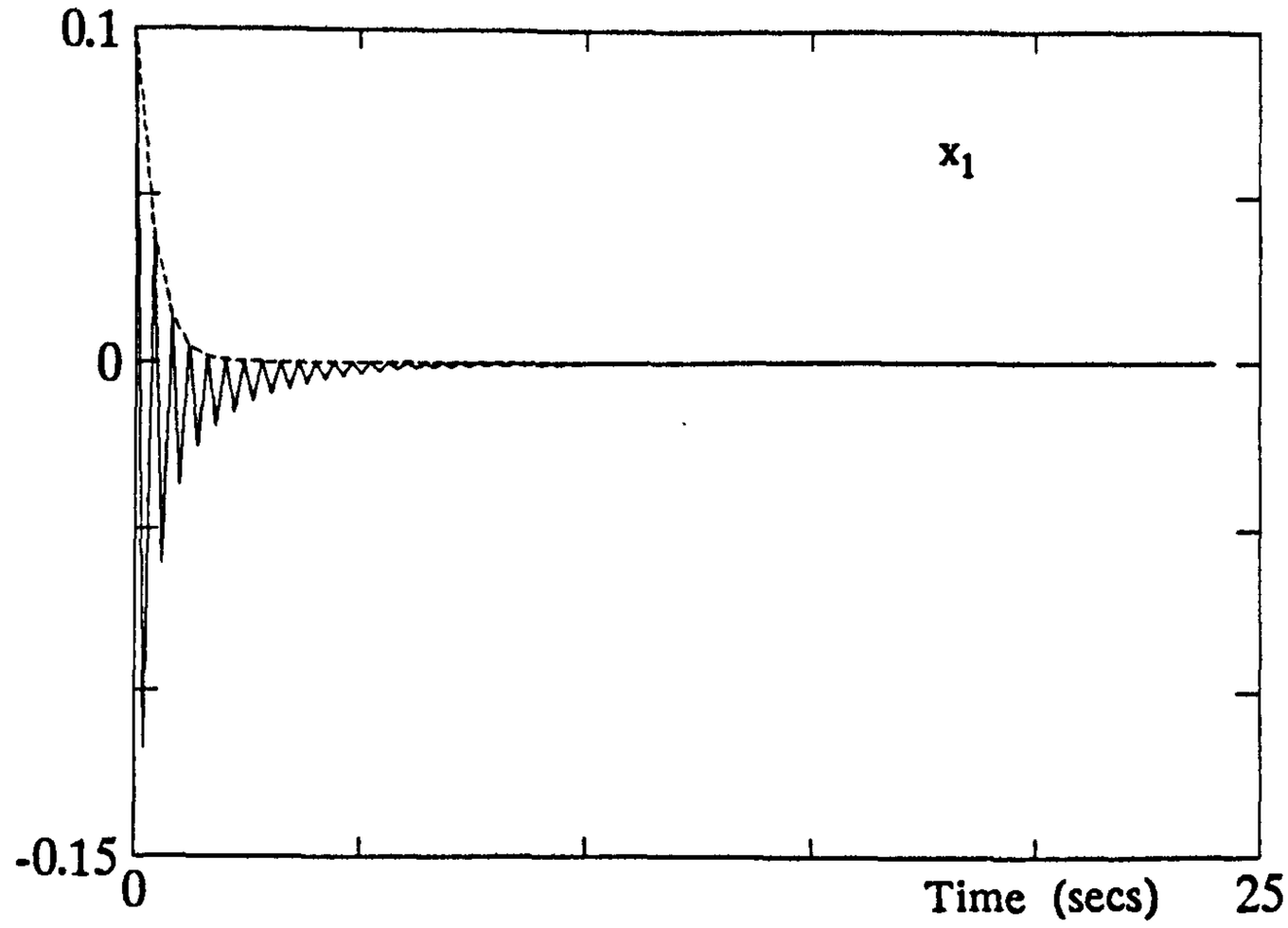

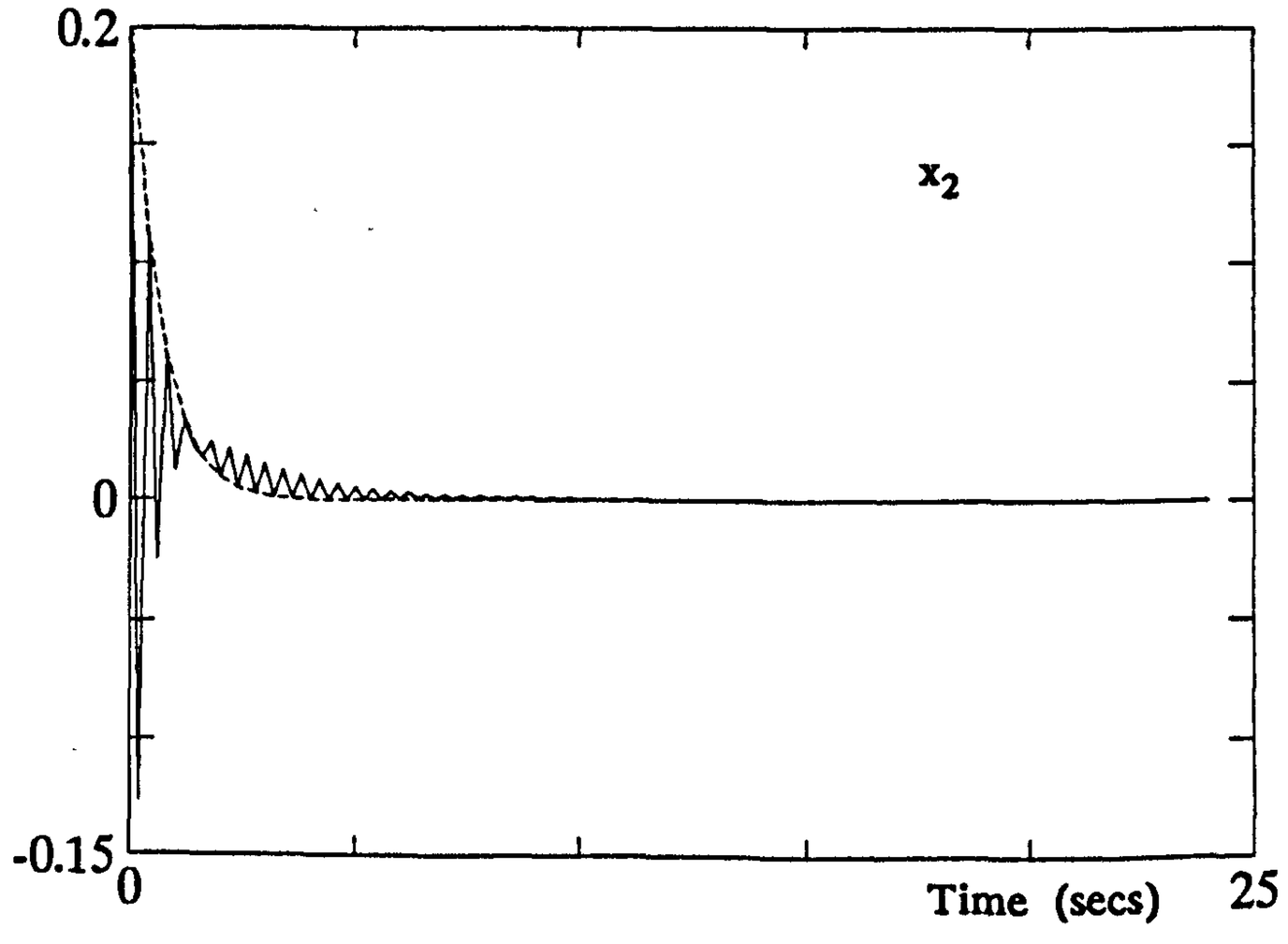

Figure 5.4.5 Intersample state responses of K_5 closed loop system.

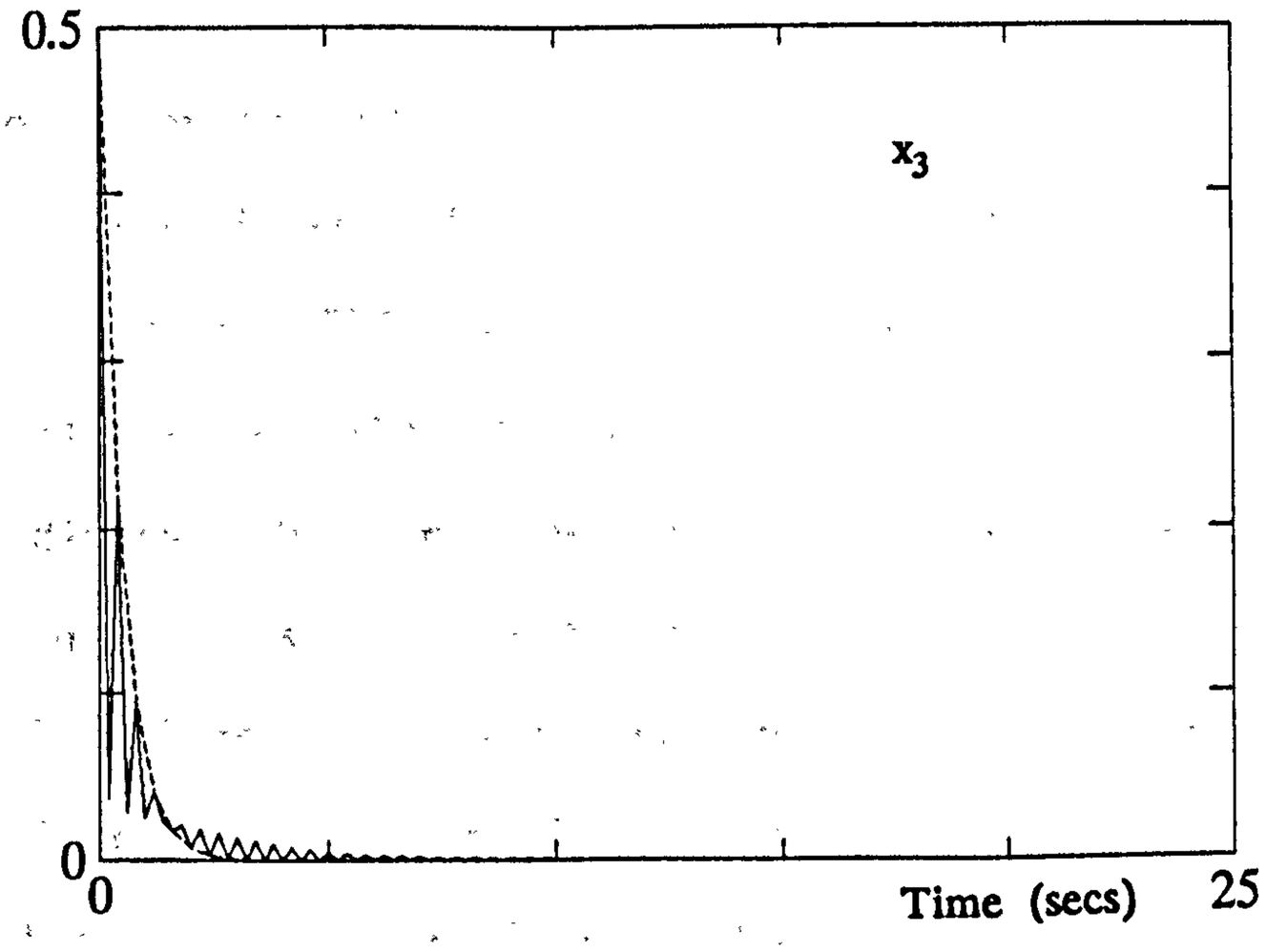

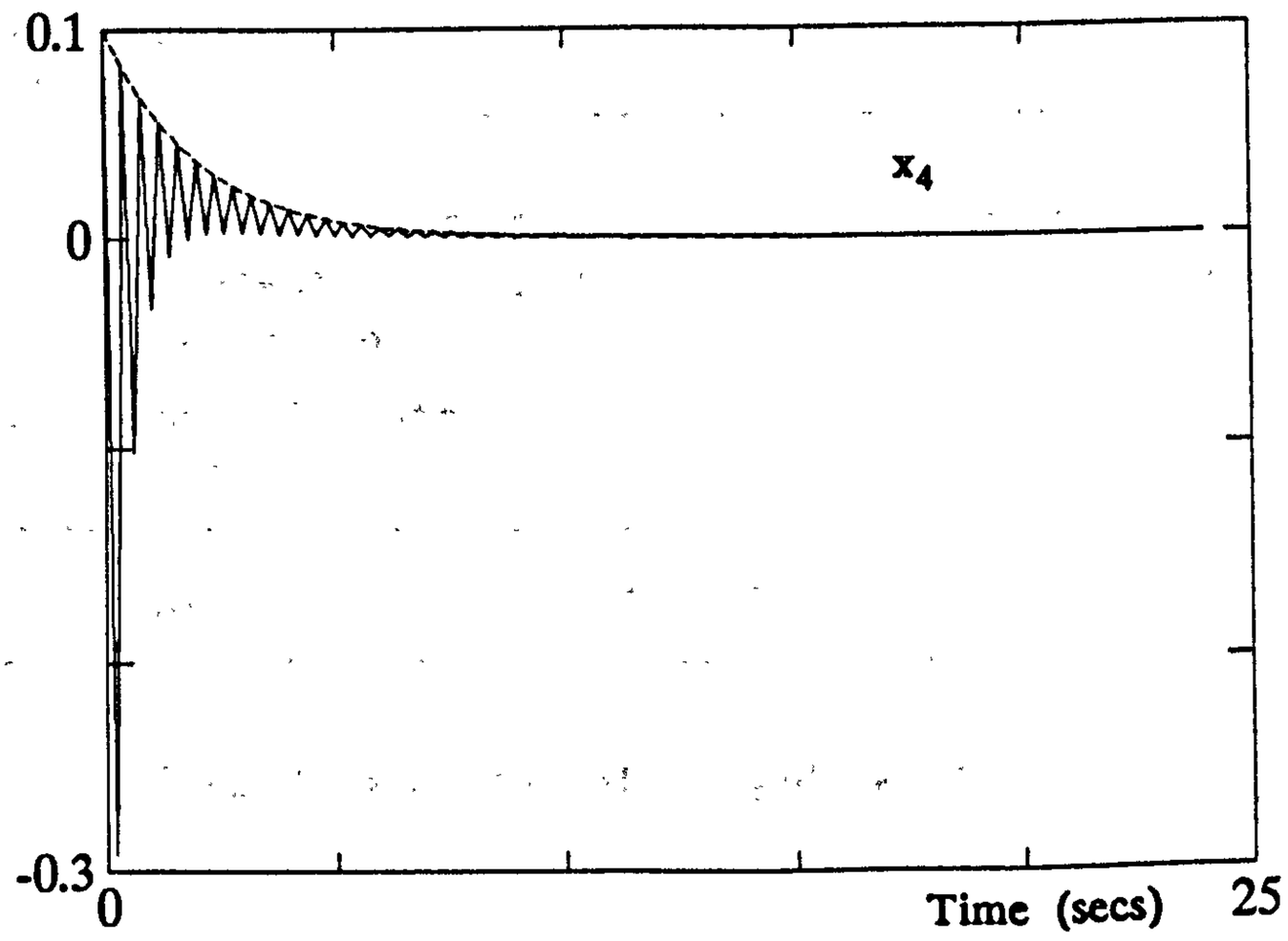

Figure 5.4.5 Intersample state responses of K_5 closed loop system (continued).

Sensitivity Analysis of Example 5.4.2

The conditioning and $\|K\|_2$ figures for Example 5.4.2 designs are shown in Tables 3 and 4. (The assumed ordering of closed loop eigenvalues is $\lambda_1 = 0.8187$, $\lambda_2 = 0.3679$, $\lambda_3 = 0.4317$, $\lambda_4 = 0.5488$).

The closeness of the $\kappa(V)$ and $\kappa_m(V)$ figures for the K_4 and K_5 designs indicates that an improvement in sensitivity gained by MIFO multirate sampling is not significant. Note that the sensitivity figures of closed loop transition matrix Φ_{m1} (produced by the multirate design) are very close to the maximally decoupled case. The increased cost in control effort of this decoupling can be estimated by $\|K_5\|_2 = 4.75\|K_4\|_2$.

Performance Measure	Feedback Gain Matrix	
	K_4	K_5
$\kappa(V)$ - for single rate design $\kappa_m(V)$ - for multirate designs	$\kappa(V) = 6.0199$	$\kappa_1(V) = 4.4503$ $\kappa_2(V) = 1$
$\|K\|_2$	4.8804	23.1916

Table 3 $\kappa_m(V)$ and $\|K\|2$ of K_4 and K_5 closed loop systems

Transition period under examination	Sensitivities of closed loop poles produced by feedback gain matrix:							
	K_4				K_5			
	c_1	c_2	c_3	c_4	c_1	c_2	c_3	c_4
$kT \rightarrow kT+T_1$	—	—	—	—	1.875	1.872	2.192	1.097
$kT \rightarrow (k+1)T$	3.000	2.115	2.427	1.291	1	1	1	1

Table 4 Eigenvalue sensitivities, c_{mi}, of K_4 and K_5 closed loop systems

5.4.3 Example 5.4.3

This example considers the design of a Stability Augmentation System (SAS) for the lateral motions of the Machan aircraft introduced in Chapter 2. The function of the SAS is to stabilise the aircraft and ease the pilot handling load by providing suitable speed and damping (characterised by natural frequency ω_n and damping ration ζ_n) of the various closed loop modes. Hence, the SAS contributes to the aircraft "handling qualities". The acceptable ω_n and ζ_n for different categories of aircraft are well documented, (MIL-F8785C, 1980).

For a stick-fixed configuration, the linearised lateral dynamics of the Machan at an airspeed of $33ms^{-1}$ (Aslin, 1985) are given by continuous-time system matrices:

$$A = \begin{bmatrix} -0.2770 & 0.0000 & -32.9000 & 9.8100 & 0.0000 \\ -0.1033 & -8.5250 & 3.7500 & 0.0000 & 0.0000 \\ 0.3649 & 0.0000 & -0.6390 & 0.0000 & 0.0000 \\ 0.0000 & 1.0000 & 0.0000 & 0.0000 & 0.0000 \\ 0.0000 & 0.0000 & 1.0000 & 0.0000 & 0.0000 \end{bmatrix}$$

$$B = \begin{bmatrix} -5.4320 & 0.0000 \\ 0.0000 & -26.6400 \\ -9.4900 & 0.0000 \\ 0.0000 & 0.0000 \\ 0.0000 & 0.0000 \end{bmatrix} \qquad (5.4.4)$$

where the state vector is,

$$\begin{bmatrix} v \\ p \\ r \\ \varphi \\ \psi \end{bmatrix} = \begin{bmatrix} \text{Sideslip} \\ \text{Roll rate} \\ \text{Yaw rate} \\ \text{Bank angle} \\ \text{Yaw angle} \end{bmatrix}$$

and the input vector, comprising the demanded lateral motion control surface deflections, is

$$\begin{bmatrix} \tau \\ \xi \end{bmatrix} = \begin{bmatrix} \text{Rudder} \\ \text{Aileron} \end{bmatrix}$$

The aircraft has a high level of modal interaction in the open loop, unstable state. Multirate feedback control is to be applied to stabilise the aircraft and furthermore, to enforce particular modal interactions which enhance aircraft manoeuvreability. In order to satisfy handling qualities criteria an appropriate set of desired closed loop poles for an SAS is:

$$\begin{aligned} \lambda_1 &= -4 && \text{Roll mode} \\ \lambda_{2,3} &= -1.5 \pm j1.5 && \text{Dutch roll mode} \\ \lambda_4 &= -1 && \text{Heading angle integration mode} \\ \lambda_5 &= -0.05 && \text{Spiral mode} \end{aligned} \qquad (5.4.5a)$$

This choice of poles ensure that ω_n and ζ_n of the lateral modes are well within the minimum values recommended for dynamic stability of the aircraft. In open loop the roll mode is characteristically sluggish. In closed loop, the roll reponse to a pilot demand is required to be quite fast (a time constant of 1.4 secs is typically recommended for all classes of aircraft during cruise flight conditions). In contrast, the spiral mode is required to be as slow as possible (to enable the pilot to perform steady turns without constantly having to correct for spiralling).

The Dutch roll mode (so called because it describes the motions of skaters on the Dutch canals) comprises a combination of yawing, sideslip and rolling motions. A perturbation in the heading angle will induce the Dutch roll action. This occurs from the trailing wing generating extra

lift, causing the aircraft to roll and sideslip. Weathercock correction from the tail then produces identical motion in the opposite yaw direction. During cruise, all classes of aircraft are recommended a minimum $\omega_n = 0.4$ rads/sec and $\zeta_n = 0.3$ for the Dutch roll mode. For this design the Dutch roll mode is selected to be critically damped.

The preferred eigenvector structure relating these lateral modes to the flight handling properties of the aircraft is well documented in MIL-spec (1980). The Dutch roll mode should appear predominantly in the sideslip and yaw states, while bank angle and roll rate coupling is supressed. The roll mode should be decoupled from yaw rate and sideslip and the spiral mode is required to have no lateral translation due to the effects of sideslip and yaw rate. From the above requirements, it is clear that the basic handling qualtities design objective is to minimise the interaction between the yaw and roll motions of the lateral aircraft subsystem. A desirable choice of eigenvectors based on the above requirements would therefore be,

$$\nu 1 = \begin{bmatrix} 0 \\ 1 \\ 0 \\ * \\ * \end{bmatrix} \quad \nu 2 = \begin{bmatrix} 1 \\ 0 \\ * \\ 0 \\ * \end{bmatrix} \pm j \begin{bmatrix} * \\ 0 \\ 1 \\ 0 \\ * \end{bmatrix} = \bar{\nu} 3 \quad \nu 2 = \begin{bmatrix} * \\ * \\ * \\ * \\ * \end{bmatrix} \quad \nu 5 = \begin{bmatrix} 0 \\ * \\ * \\ 1 \\ * \end{bmatrix} \tag{5.4.5b}$$

where '*' is used to denote that no particular preference is required. For simplicity, this example assumes that all '*' are equal to 0.

The input sample rate selection criteria gives $\mu_1 = l_1 = 3$, $\mu_2 = l_2 = 2$, $\rho_1 = 5$, $\rho_2 = 1$. The $\{\mu_i\}$, $\{l_i\}$ sets are chosen, indicating that the aileron and rudder sampling frequencies be related by,

$$T_\tau = \frac{I}{3} \qquad T_\xi = \frac{I}{2}$$

The main interval of samping is selected to be T = 0.1. This does not render any of the modes uncontrollable, hence all of the desired eigenvalues of (5.4.5a) may be assigned. The (unstable) open loop discrete poles are {1, 0.425, 1.012, 0.8932±j0.3267}

The direct eigenstructure assignment method is used to generate multirate feedback control such that the closed loop system has the desired discrete poles {0.6703, 0.851±j0.1286, 0.9048, 0.995} and the modal structure of (5.4.5b). The gain matrix thus computed is given by,

$$K_6 = \begin{bmatrix} 5.319 & 0.211 & -29.464 & 175.919 & 566.254 \\ -10.587 & 0.415 & 67.155 & -347.005 & -1107.931 \\ 5.853 & 0.208 & -37.725 & 173.406 & 549.219 \\ -0.105 & 1.3572 & 0.671 & -3.374 & 11.207 \\ 0.093 & -1.110 & -0.637 & 3.249 & 10.445 \end{bmatrix} \times 1000 \qquad (5.4.6)$$

The results of implementing K_6 in a linear simulation of the aircraft to an initial heading angle perturbation of 0.02 radians is shown in Figure 5.4.6. Note that a perturbation in heading angle will cause an immediate displacement in sideslip velocity (Aslin, 1985). The non-linear aircraft equations determines that a 0.02 radian perturbation in heading angle produces an immmediate offset of -0.8 m/sec^{-1} in sideslip velocity. Thus $x(0) = [-0.8\ 0\ 0\ 0\ 0.02]^T$ is a realistic initial state condition for simulation purposes.

Figure 5.4.6 shows that the desired decoupling of yaw and roll motions is achieved at the main sample instants. The initial heading angle perturbation causes a corresponding perturbation in yaw angle but the assigned modal structure ensures that the roll states remain virtually unaffected (bank angle and roll rate are perturbed by $\approx -3x10^{-12}$ radians and ms^{-1} respectively). The initial state perturbation would have induced a response in the Dutch Roll mode in the open loop. The reponse of the K_6 closed loop system show that the dutch

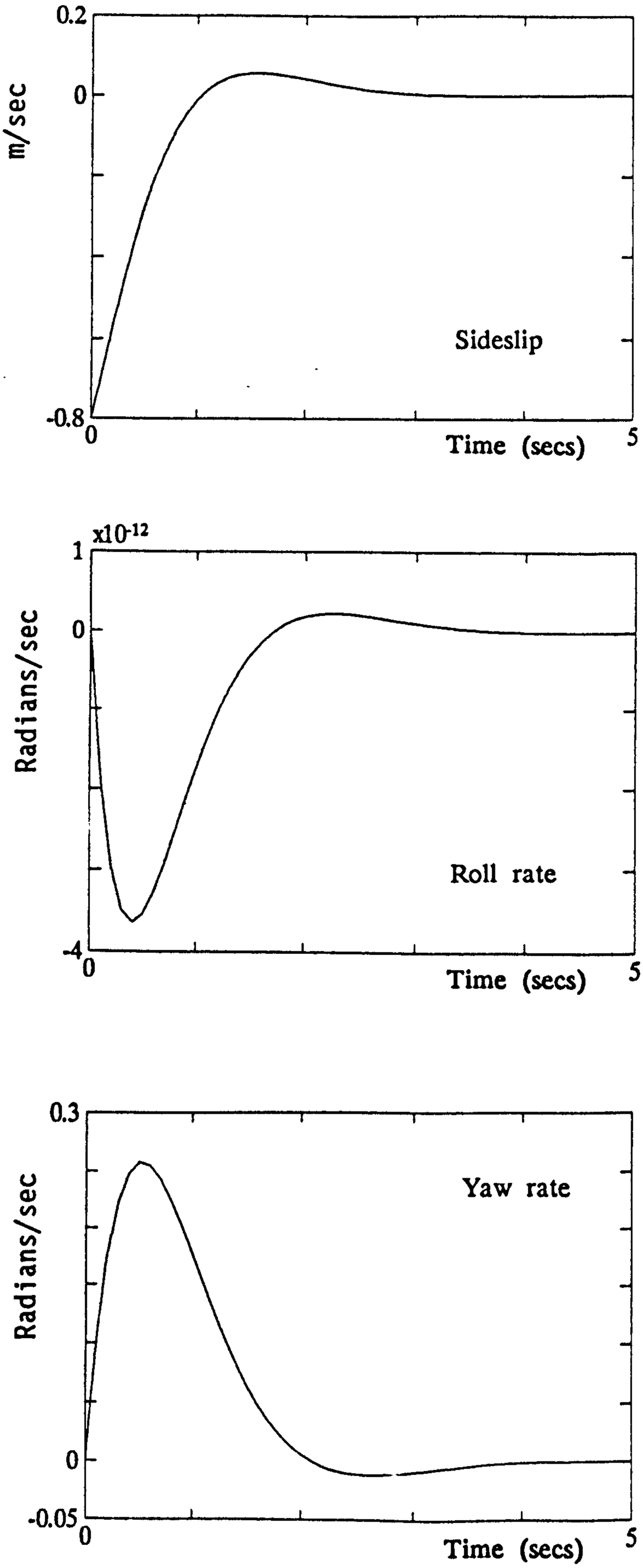

Figure 5.4.6a State responses of multirate feedback K_7 closed loop aircraft lateral subsystem.

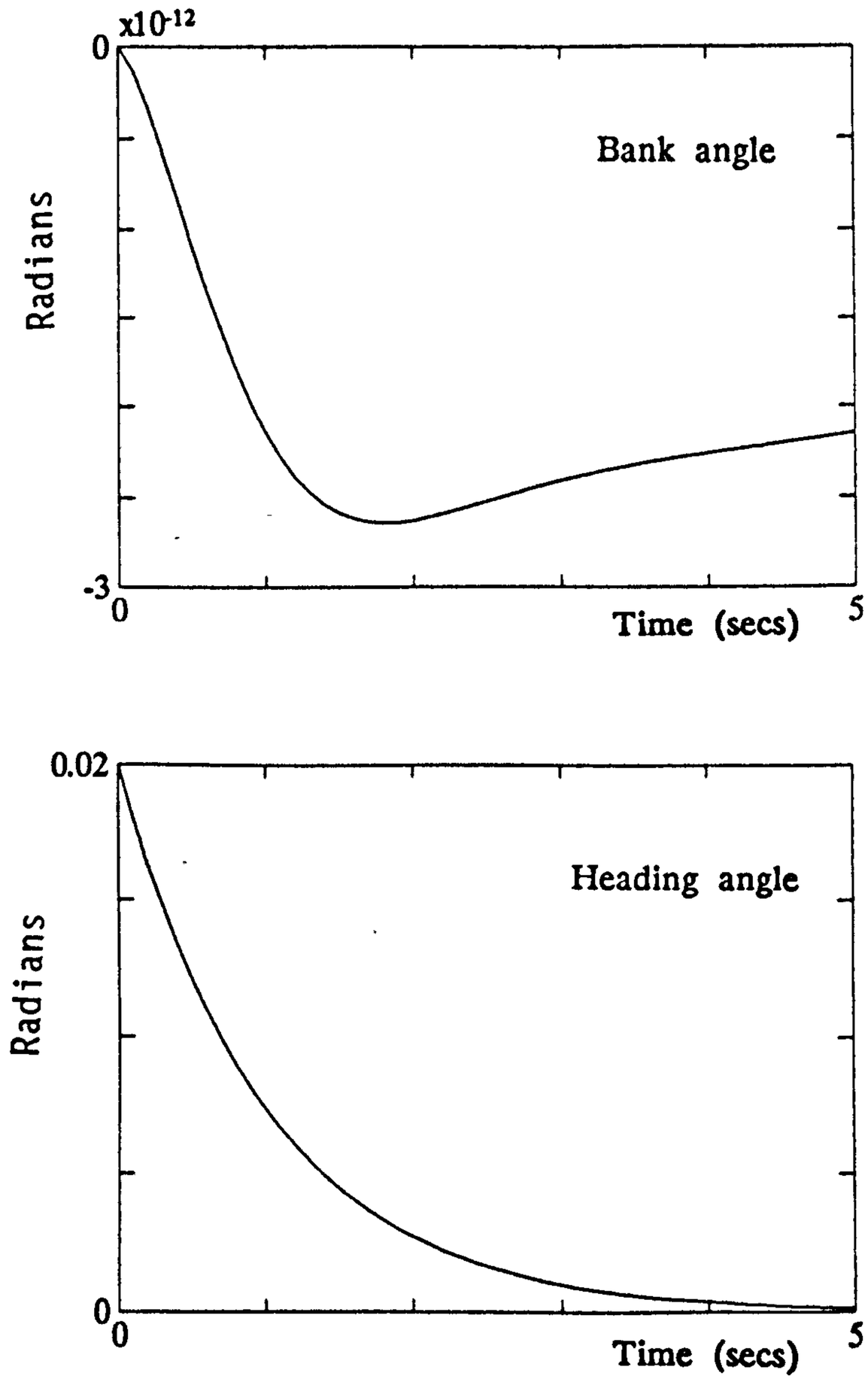

Figure 5.4.6a State responses of K_7 closed loop aircraft lateral subsystem (continued).

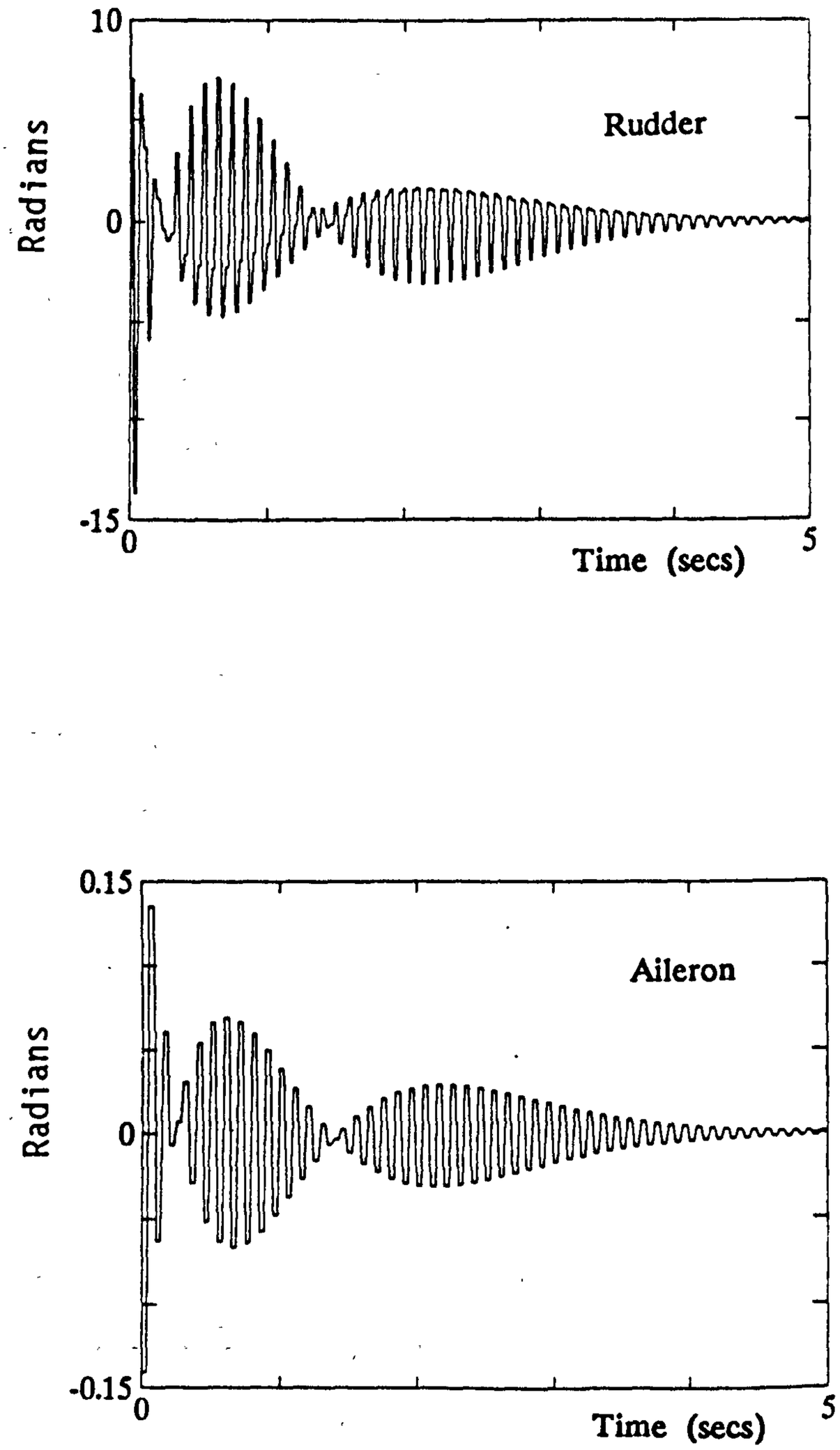

Figure 5.4.6b Control input activity of K_7 closed loop aircraft lateral subsystems.

roll mode is hardly excited; the offset in sideslip velocity and heading angle is smoothly recovered and both settle to a zero steady state without any further action in the opposite direction (which normally occurs in the dutch roll motion).

The rudder and aileron responses of Figure 5.4.6 show that the cost of this modal assignment is high magnitude and switched control input activity which, in practice, would be unacceptable. The demands on the rudder control surface, in particular, reach limits which could not be realistically supplied.

The intersample responses of this closed loop design are, as expected, highly switched (these responses will be displayed in Chapter 6). A non-linear simulation of the multirate feedback lateral system yields an unstable response, clearly demonstrating the impracticality of implementing the K_6 feedback design in real situations.

Sensitivity Analysis of Example 5.4.3

The eigenvector conditioning and eigenvalue sensitivity measures for the closed loop lateral subsystem produced by feedback design K_6 of Example 5.4.3 are shown in Table 5. The ordering of closed loop eigenvalues is $\lambda_1 = 0.6703$, $\lambda_2 = \lambda_3 = 0.851 \pm j0.1286$, $\lambda_4 = 0.995$, $\lambda_5 = 0.9048$. Furthermore $\|K_6\|_2 = 1427.73$.

This table shows that the intersample behaviour of the aircraft lateral subsystem is highly sensitive to perturbations about the nominal operating point. However despite this, maximal insensitivity of the closed loop poles is achieved at the main sample instants. The high $\kappa_m(V)$ figures reflect, to some degree, the difficult decoupling task posed by the highly interactive open loop aircraft lateral subsystem.

Transition period under examination	Eigenvector conditioning and eigenvalues sensitivities of closed loop system formed by gain matrix K_6:					
	c_1	c_2	c_3	c_4	c_5	$\kappa_m(V)$
$kT \rightarrow kT+T_1$	40.516	65.762	48.611	1.066	22.011	152.613
$kT \rightarrow kT+T_2$	83.034	40.591	47.526	22.549	8.852	202.691
$kT \rightarrow kT+2T_1$	20.995	31.632	45.388	1.147	23.537	106.032
$kT \rightarrow (k+1)T$	1	1	1	1	1	1

Table 5 Performance measures $\kappa_m(V)$ and c_{mi}, of the K_6 closed loop Machan aircraft lateral subsystem

5.5 TESTING THE MIFO INPUT SAMPLE RATE SELECTION CRITERIA

The MIFO pole assignment examples considered thus far have assumed that the multirate controllability and MIFO eigenstructure assignment criteria of Section 5.2 have been satisfied. This Section presents two examples to demonstrate the requirement of these criteria.

5.5.1 Example 5.5.1

The multirate controllability condition of Chapter 3 ensures that the response at every intersample point is controllable. Thus, a closed loop MIFO system that is asymptotically stable at main sample points, is also guaranteed to remain stable at all intersample instants, *regardless of whether unstable "intersample" poles appear to be assigned* (this aspect of intersample design is examined in Section 5.6). The controllability criterion can easily be demonstrated by contradiction:

Chapter 3 pointed out that all inputs used to generate the

continuous-time controllable pair (A,B) are required to participate in the achievement of the multirate controllability condition. This example demonstrates the effect of violating this requirement for the system of Example 5.4.1. MIFO uncontrollability can be achieved by discarding the second input altogether and selecting $T_1=T/3$ (as indicated by matrix β_C whose formulation is otherwise unaltered). A feedback gain matrix which assigns the desired eigenstructure for this single input MIFO system, using the direct assignment method, is designed. This feedback matrix is as follows:

<u>"Uncontrolled" sample set for Example 5.4.1</u> $T_1=T/3$

$$K_7 = \begin{bmatrix} -244.1339 & -205.2828 & 206.8605 \\ 405.5845 & 295.6439 & -417.6130 \\ -162.6860 & -93.1035 & 210.5171 \end{bmatrix} \qquad (5.5.1)$$

The response of the K_7 closed loop system to the same initial perturbation as Example 5.4.1 is unstable. The instability of these response affirms the multirate controllability conditions by contradiction (i.e. the controllability conditions have not been met).

Note that *theoretically*, the K_7 closed loop system assigns the desired poles and right eigenvectors at the main sample instants. Simulation results show that this is clearly not the case. Note also that a distinct characteristic of feedback matrices produced by "uncontrolled" input sample rate sets is the high $\|K\|_2$. (For this example $\|K_7\|_2 = 803.512$ compared to $\|K_3\| = 75.622$ for Example 5.4.1)

5.5.2 Example 5.5.2

The MIFO eigenstructure assignment selection criterion of

Section 5.2 indicates that a different $\{\rho_i\}$ may be produced by a rearrangment of the columns of B, (the control matrix). This is due to the formulation of β_C, requiring unity input sample rate multiplicity for the (i+1)th, (i+2)th ,.., (m)th inputs if $\sum\rho_i = n$ whilst i<m. This example is based on the system of Example 5.4.2. The two columns of the control distribution matrix is interchanged. The outcome of this column interchange on $\{\rho_i\}$ and the corresponding effect on the solution produced by the direct eigenstructure assignment is examined:

The $\{\rho_i\}$ of the "shuffled" system are determined to be ρ_1=4, ρ_2=1. Applying the direct assignment procedure produces the following gain matrix, K_8:

<u>"Shuffled" sample set $\{\rho_i\}$ for Example 5.4.2</u> T_1=T/4, T_2=T/1

$$K_8 = \begin{bmatrix} 68.4299 & -144.139 & -219.1276 & 220.7847 \\ -104.3980 & 152.4101 & 231.7019 & -238.3339 \\ -87.3843 & 144.8513 & 220.2105 & -223.4880 \\ 104.2260 & -141.6526 & -215.3477 & 226.2252 \\ -0.3143 & 0.3450 & 1.0848 & -0.7279 \end{bmatrix} \qquad (5.5.2)$$

The performance measures of this design are shown in Table 6. The responses of the K_8 closed loop system to the intial state perturbation of Example 5.4.2 are examined.

From the tabulated data and time response plots, the desired eigenstructure of the K_8 design is seen to be assigned (the desired poles are placed with associated right eigenvectors mutually orthogonal). Furthermore since $\|K_8\|_2 = 722.253 > \|K_5\|_2$, larger magnitude state and control input trajectories than that produced by the original K_5 design are expected. Time response data from simulation studies show that, for an identical initial state perturbation as that of Example 5.4.2, the K_8 design produces unacceptably large state overshoots (the maximum being of magnitude +12 units for state x_3). The

control effort demanded from the first input is also very high (peaking at 120 units). From an overall consideration of the performance of the two different MIFO feedback designs, control provided by K_5 is clearly much better than that provided by the gain K_8.

Thus, the order in which the control matrix columns are arranged when formulating β_c *can* have a significant effect on the MIFO feedback control design. The responses resulting from the K_5 and K_8 closed loop systems show that an even distribution of control effort is produced by equal sample rate multiplicities for each MIFO system input.

Transition period under examination	Sensitivities of closed loop poles produced by feedback gain matrix K_8				Eigenvector conditioning
	c_1	c_2	c_3	c_4	$\kappa_m(V)$
$kT \rightarrow kT+T_1$	1.5634	1.4161	1.1802	1.4837	3.0183
$kT \rightarrow kT+2T_1$	2.1224	2.1224	1.7106	1.1224	4.5981
$kT \rightarrow kT+3T_1$	1.4373	2.6671	2.6671	1.1277	5.5305
$kT \rightarrow (k+1)T$	1	1	1	1	1

Table 6 Conditioning and sensitivities of K_7 closed loop poles

5.6 INTERSAMPLE RESPONSE OF MIFO FEEDBACK DESIGNS

The examples of Sections 5.4 amd 5.5 all indicate that the direct assignment method does not allow intersample closed loop behaviour to be specifically designed. For the systems of Examples 5.4.1 and 5.4.2, this inability to design intersample response did not result in a significant degradation of the intersample system sensitivity. The test of Section 5.4.1 investigated this insensitivity by perturbing the open loop system transition matrix. (Recall that the test was conducted to

establish the accuracy of the intersample sensitivity figures obtained by applying the multirate sensitivity measures $\kappa_m(V)$ and c_{mi}). The aircraft lateral subsystem of Example 5.4.3 was however, assigned closed loop behaviour that is very sensitive to perturbations about the nominal operating point *at the intersample instants*. Though the linear simulation responses of the lateral subsystem (Figure 5.4.6) do show the high degree of decoupling achieved between the roll and yaw motions at the main instants, the responses clearly do not demonstrate the effects of the high pole sensitivities in a realistic situation. The non-linear simulation response was observed to be unstable. *This is due entirely to the sensitive and high magnitude intersample response.*

The intersample response plays an important role in transferring the initial system perturbations to the final steady state value. So far, any details pertaining to intersample behaviour have been restricted to the response of the multirate system to state conditions that exist *at the main sample instants only*. Recall that the (non-minimal) expanded MIFO equations of Section 2.4 are derived by collecting and rearranging state vectors defined for time intervals $(k-1)T \rightarrow kT$ and $kT \rightarrow (k+1)T$ (to isolate the [kT] and [(k+1)T] terms on the left and right hand side of the MIFO state equtations). Thus, the expanded MIFO state equations determine the state vector of the MIFO system at any sample point during the interval $kT \rightarrow (k+1)T$ from the state vector at instant kT and the series of inputs over interval $kT \rightarrow (k+1)T$. Section 4.6 used these expanded MIFO descriptions to formulate intersample transition matrices Φ_{CLm} and define the conditioning and sensitivity measures associated with each transition period. Hence the sensitivity measures of Section 4.6 characterise the intersample and main sample behaviour of the MIFO system to conditions that exist at the *main sample instant only* (see Figure 4.6.1). Clearly, any information concerning the transition response and sensitivity of the system to *intersample* state conditions is absent.

Reconsider the operation of the MIFO system: During the time interval $kT \rightarrow (k+1)T$ the MIFO system reacts to the state and control that exists at main sample and intersample instants. The initial conditions set up at each of the intersample instants is determined by matrices Φ_{CLi}, $i=1,..,n_o$. An examination of the MIFO system responses to these *intersample* initial conditions will shed some useful information on the intersample behaviour of each state. For this examination the perfectly decoupled closed loop responses produced by the K_3 design of Example 5.4.1 are reviewed (recall that $T_1=T/3$ for this system).

The x_3 state response of the K_3 closed loop system (see Figure 5.4.2) is decomposed into three separate transients corresponding to the state value at instants $[kT+T_1]$, $[kT+2T_1]$, $[(k+1)T]$, $k = 0,..,49$. These "decomposed" responses are shown in Figure 5.6.1. Since each transient response of Figure 5.6.1 represents the system response at intersample and main sample instants separated by intervals of period T, the three transients interleaved form the whole (i.e. main sample and intersample) response for state x_3. The initial condition for the $x_3[kT]$ transient is 0.15. From the definitions of Section 4.6,

$$x[T_1] = \Phi_{m1}x[0] \qquad\qquad x[2T_1] = \Phi_{m2}x[0] \qquad\qquad (5.6.1)$$

Thus the intitial conditions for the $[kT+T_1]$ and $[kT+2T_1]$ (intersample) transients are $x_3[T_1]$ and $x_3[2T_1]$. Now, the $x_3[kT]$ transient is known to be governed by eigenvalue $\lambda_3 = -0.7$. An interesting characteristic of the intersample x_3 transients are that both are *perfectly decoupled with the speed and damping of discrete eigenvalues very close to* $\lambda_2 = exp(-0.6T)$.

An examination of the x_1, x_2 transients for the K_3 closed loop system response of Figure 5.4.2 shows that these also comprise 3 *decoupled* transients interleaved. Furthermore, the intersample responses of the x_1 and x_2 states are also governed by eigenvalues very close to

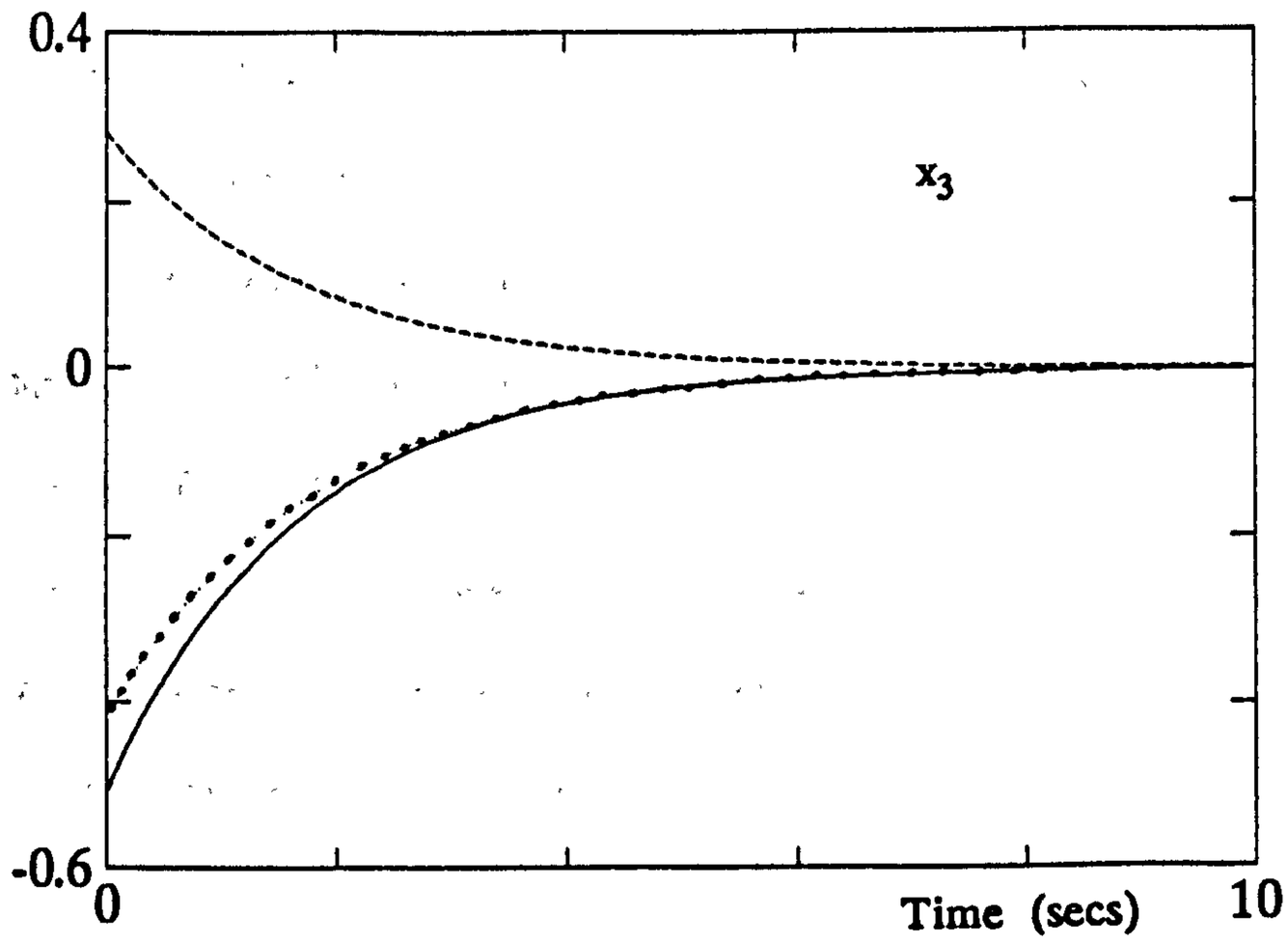

----- x_3 transient at kT instants

——— x_3 transient at $kT+T_1$ instants

..... x_3 transient at $kT+2T_1$ instants

Figure 5.6.1 Intersample transients of state x_3 of K_3 closed loop multirate system.

λ_2. Thus, the reason for the perfectly decoupled yet unswitched response of the x_2 state is that its main sample *and* intersample transients are all characterised by an *almost* constant eigenvalue λ_2. The assignment of "intersample" eigenvalues very close to those associated with unswitched states is consistently observed with all MIFO eigenstructure assignment examples. However, the reason for the imprecise assignment of eigenvalue λ_2 at intersample responses remains unclear. The discrepency may arise from modelling inaccuracies between the predicted and the actual state transtion matrices defined for time periods, T_1, $2T_1$ and T (which are used for both MIFO system modelling and simulation purposes).

The above conclusions can be summarised by the following set of transient equations which describe the main sample and intersample responses of states x_1, x_2 and x_3:

$$
\begin{aligned}
x[T+T_1] &= \exp(\hat{\lambda}_2 T)x[T_1] \\
x[2T+T_1] &= \exp(\hat{\lambda}_2 T)x[T+T_1] \qquad \hat{\lambda}_2 \approx -0.6 \\
x[T+2T_1] &= \exp(\hat{\lambda}_2 T)x[2T_1] \\
x[2T+2T_1] &= \exp(\hat{\lambda}_2 T)x[T+2T_1] \\
\\
x_1[2T] &= \exp(\lambda_1)x_1[T] \\
x_2[2T] &= \exp(\lambda_2)x_2[T] \\
x_3[2T] &= \exp(\lambda_3)x_3[T] \\
&\text{etc}
\end{aligned}
\qquad (5.6.2)
$$

The above observations indicate that the direct assignment method does maintain the perfectly decoupled nature at the intersample instants, albeit "blindly". The decoupled trajectories of (5.6.2) also imply that the state response of the K_3 closed loop system to a *state* perturbation at *any* main sample or intersample instant can be accurately predicted. Each K_3 closed loop system state will recover from a state perturbation

at the main sample instant with the speed and damping associated with its assigned closed loop eigenvalue. Furthermore, the response of each system state to any *intersample* state perturbation will be governed entirely by $\hat{\lambda}_2$.

The above analysis allows some further results to be predicted. Assume the system is released from an initial perturbation in one state only, say x_1 (which is governed by λ_1=-0.5). The unperturbed states x_2, x_3 will remain unaffected (i.e. remain zero) by this initial condition at the main sample instants. However, the two unperturbed states will have non-zero values at intersample instants $x[T_1]$ and $x[2T_1]$. Thus the two unperturbed states will, despite its zero main sample response, exhibit an *intersample* response.

The multirate designs of Example 5.4.1 also indicate a relationship between single rate inputs and unswitched state responses. Both multirate (K_2, K_3) closed loop systems have one unswitched state (x_2) and one single rate input (u_2). Thus it would appear that the number of single rate inputs determine the number of unswitched states that exist for a perfectly decoupled closed loop system. This relationship is tested in the following example:

5.6.1 Example 5.6.1

An "artificial" control input is selected for the system of Example 5.4.2 such that the control distribution matrix becomes:

$$B = \begin{bmatrix} 0 & 0.5 & 0.2 \\ 1 & 0 & 1 \\ 1 & 0 & 0 \\ 0 & 1 & 0 \end{bmatrix} \qquad (5.6.3)$$

The MIFO sample rate selection criteria determines the input sample rate multiplicities as $\mu_1 = l_1 = \rho_1 = 2$, $\mu_2 = l_2 = \rho_2 = 1$, $\mu_3 = l_3 = \rho_3 = 1$. Application of the direct assignment method to design feedback control for the multirate system produced by this choice of sample rates produces the following gain matrix:

$$K_9 = \begin{bmatrix} 77.3090 & -2.4834 & -3.2151 & 22.6002 \\ -41.4003 & -1.3629 & 2.6323 & -12.4032 \\ -0.6839 & 0 & 0 & 1.3416 \\ -13.4480 & 0 & 0 & -3.3541 \end{bmatrix} \qquad (5.6.4)$$

The response of the K_9 closed loop system to the same initial state perturbation as Example 5.4.2 is shown in Figure 5.6.2. These responses show that in correspondence with two single rate inputs (u_2, u_3) two unswitched state responses (x_1, x_4) corresponding to eigenvalues λ_1 and λ_4 are produced by feedback gain K_9. An examination of the (decomposed) intersample transients of switched states x_2 and x_3 reveal that they are governed by eigenvalues λ_1 and λ_4. Thus, the direct relationship between the number of single-rate inputs and unswitched state responses has been confirmed.

A final conclusion can drawn from the observations of this section: *the assignment of very close poles will reduce the* magnitude *of intersample ripple experienced in perfectly decoupled multirate control systems*. However note that, for a given system with a $\{\rho_i\}$ set which produces perfectly decoupled transients when distinct eigenvalues are assigned, the direct method will only produce perfect decoupling when confluent eigenvalues are assigned if generalised eigenvectors are used (see the concluding discussion of Section 5.3).

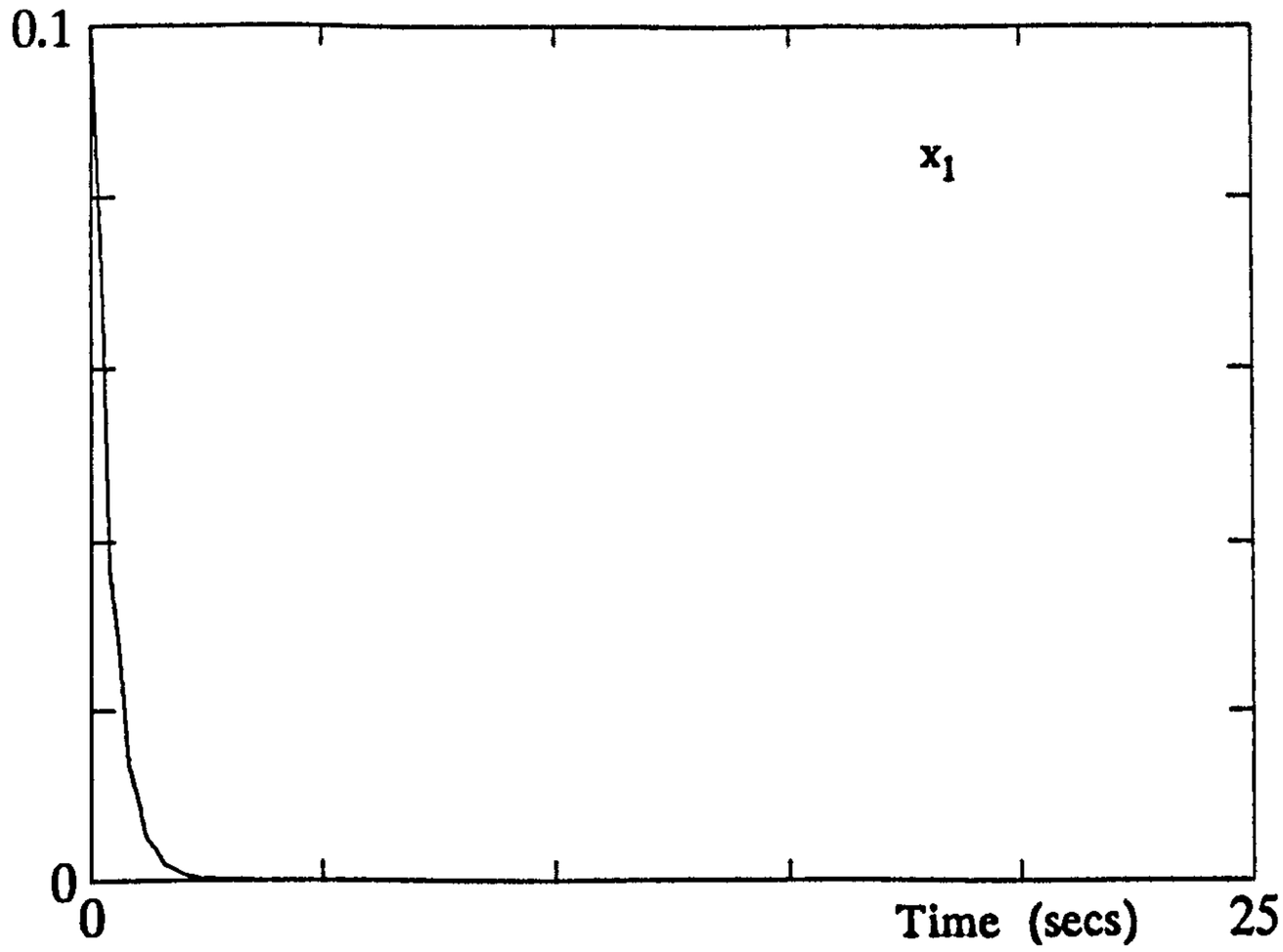

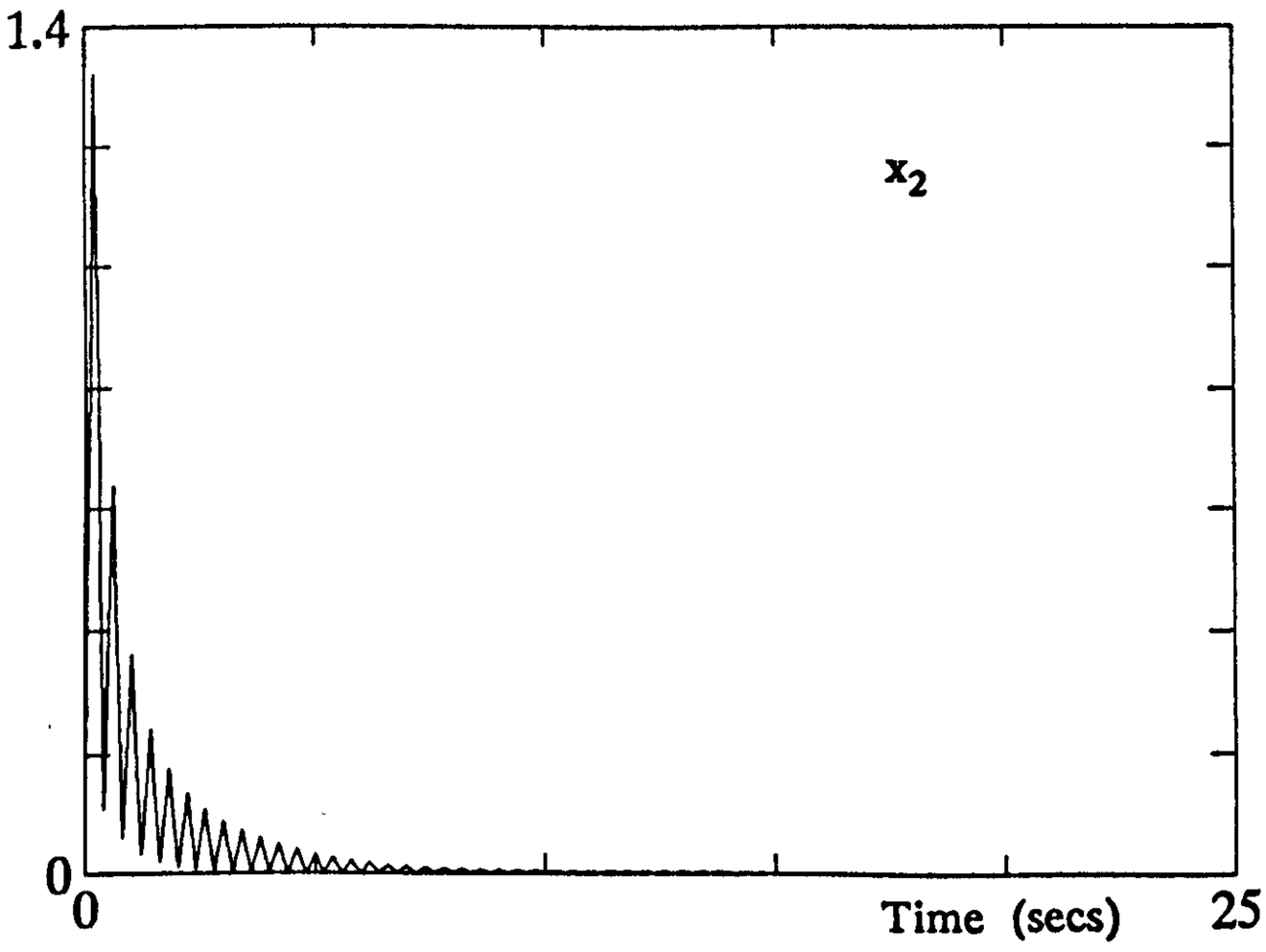

Figure 5.6.2 State responses of K_g closed loop system.

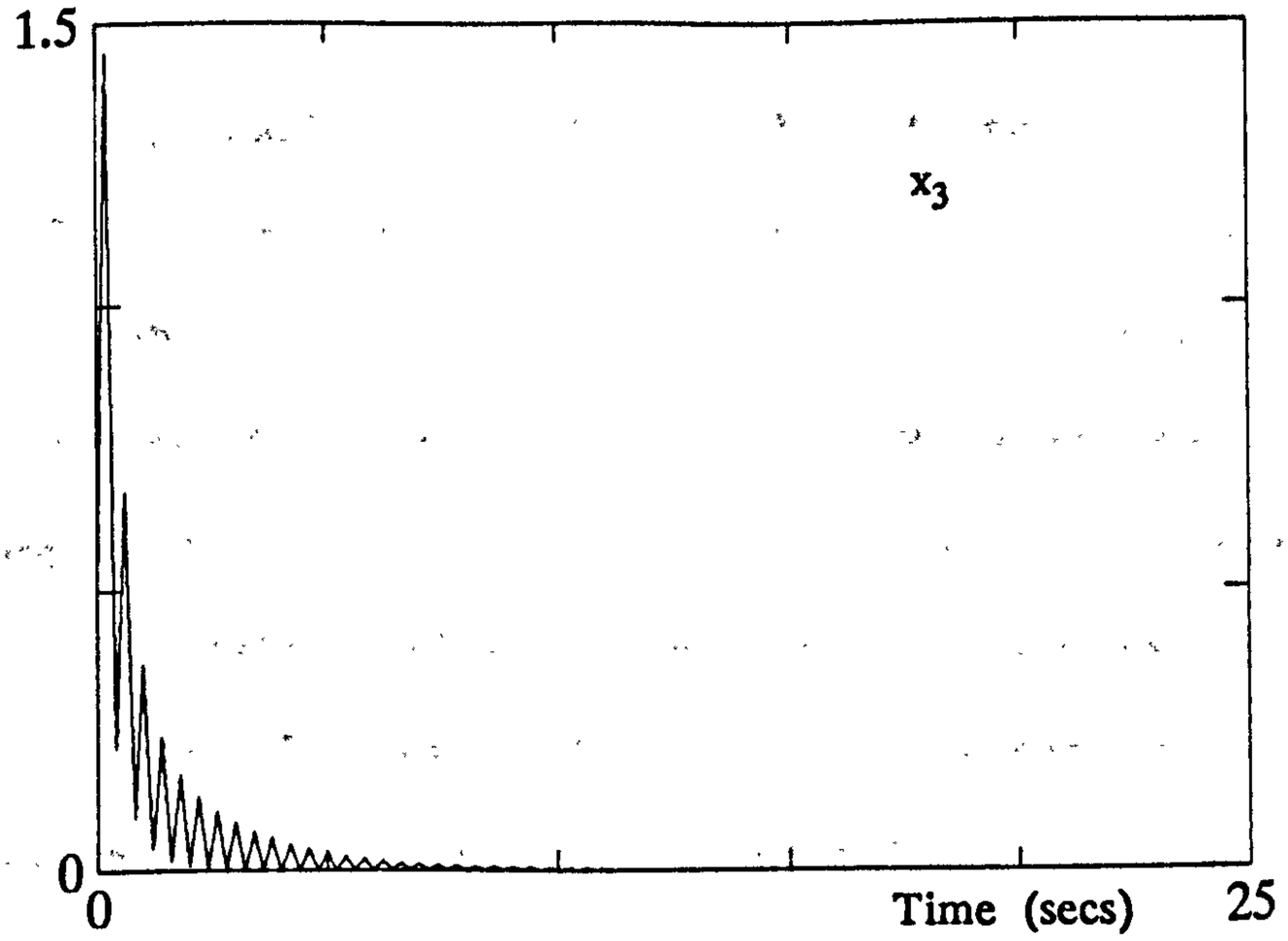

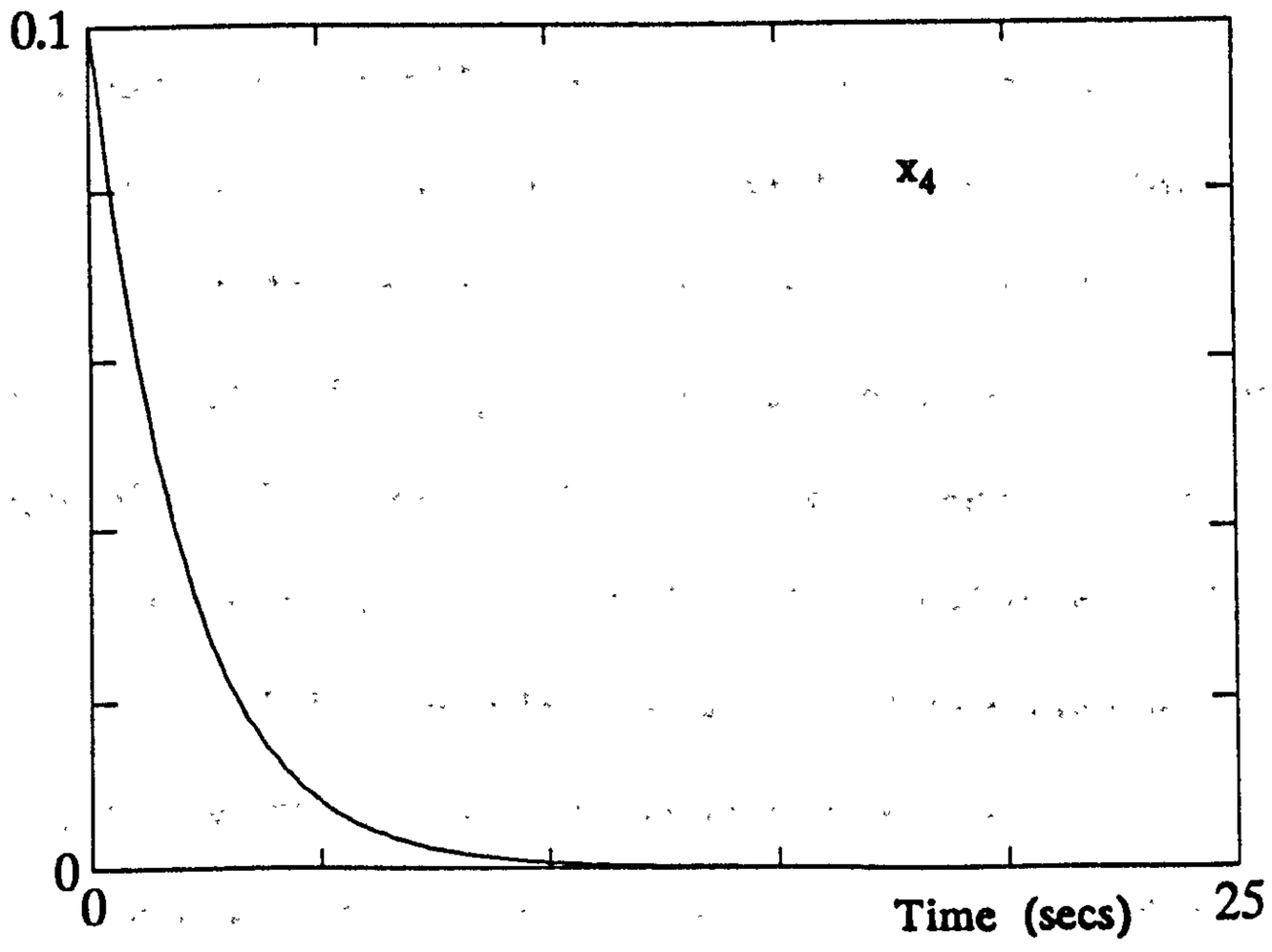

Figure 5.6.2 State responses of K_g closed loop system (continued).

5.7 SUMMARY

This Chapter has examined the influence of input sample rates on the MIFO eigenstructure assignment problem and investigated the applicability of the multirate sensitivity performance measures presented in Chapter 4. Section 5.2 introduced the *generalised* input sample rate selection criterion, based on the formulation of matrix β_C, for the state feedback eigenstructure assignment design method.

Section 5.3 has outlined a single-pass assignment technique which can be used to solve the eigenproblem of Chapter 4. This is based on a least squares projection of the desired closed loop eigenvectors onto the admissible space. The direct manner in which a solution is obtained by this technique serves well to demonstrate the advantages and disadvantages of MIFO input sampling schemes.

The use of the direct eigenstructure assignment design procedure on minimal state space descriptions of the MIFO systems was examined in Section 5.4. The $\kappa_m(V)$ and c_{mi} measures to the equivalent expanded (non-minimal) models of the closed loop system were applied to assess intersample behaviour. A detailed analysis of the main and intersample behaviour of the results established the degree of fidelity to be placed in the new multirate performance measures.

Three examples are presented in Sections 5.4. The first two examples demonstrate the degree of insensitivity achieved by MIFO input sampling compared to that achievable by single rate sampled control structures. The first example also demonstrated the difference in closed loop response produced by selecting input sample rates as determined by the β_C matrix (of Section5.2) and as according to the sets $\{\mu_i\}$; $\{l_i\}$ (of Chapter 3). Both choices produce perfectly conditioned solutions (and maximal insensitivity of closed loop poles) for the multirate eigenstructure assignment problem. Both multirate designs were demonstrated to be less sensitive to perturbations in the nominal system

dynamics.

The first two examples were confined to the assignment of a desired eigenvalue set $\{\lambda_i\} \in R$ with desired right eigenvectors $\{\nu_i\} = I_n$ for relatively simple examples. These were selected to portray the effects of MIFO multirate sampling in a simple manner. The third example was based on the design of a Stability Augmentation System *(SAS)* for the lateral subsystem of an aircraft. The desired closed loop eigenstructure (which required the assignment of $\{\lambda_i\} \in C$ with a specific modal structure) was designed and demonstrated to be achieved by linear simulation studies. This design produced relatively poor intersample insensitivity.

The performance of the multirate feedback designs of Section 5.4 were examined using both the analytic sensitivity measures of Section 4.6 and time response data. The totally decoupled responses of the MIFO multirate systems demonstrate that the sensitivity measures are an accurate measure of the main sample behaviour of MIFO multirate systems. The accuracy of the *intersample* sensitivity measures for MIFO system behaviour was also demonstrated to be valid by performing a sensitivity test. This test showed that a 10% (one-way) perturbation in open loop system dynamics produced an unstable single rate response whilst maintaining transient behaviour very close the nominal closed loop multirate system. In fact, the multirate designs were able to tolerate a 75% (one-way) perturbation in nominal system dynamics before the onset of unstable closed loop behaviour.

Section 5.5 investigated the applicability of the combined input sample rate selection criteria of Chapter 3 and Section 5.2 in more detail. Two examples were presented; the first example presented an uncontrollable multirate system, which *theoretically* was stable and perfectly conditioned. Simulation studies show that this design was, in fact, unstable. The second example examined the effects of rearranging columns of the Example 5.4.2 control distribution matrix. The resulting

system produced a different input sample set $\{\rho_i\}$ which yielded a inferior closed loop response. Thus, the ordering of control input columns has a direct bearing on the MIFO eigenstructure assignment designs. An even distribution of control effort is produced by roughly equal multirate sampling multiplicities (as in the case where input updates are determined by $\{\mu_i\}$ and $\{l_i\}$).

Section 5.6 examined the intersample responses of Example 5.4.2. Three important conclusions were drawn from this study. First, designs based on ideal sets produce state responses whose intersample transients are determined by eigenvalues very close to the eigenvalues associated with non-switched states. Secondly, the number of single rate inputs determine the number of non-switched state responses. Finally, the assignment of close eigenvalues will reduce intersample ripple.

From the examples of this Chapter, it is clear that a severe drawack of the MIFO feedback designs produced by the direct assignment method is the high magnitude and switched control and intersample state behaviour that is produced. However, the multirate designs can despite their switched nature, provide greater modal decoupling than that achievable by the corresponding single rate design. An advantage of the $\{\rho_i\}$ set of sample rates is the improved intersample behaviour that can be obtained. The examples verify the selection criteria of Chapter 3 and Section 5.2. Furthermore, the example clearly demonstrates the *flexibility* in decoupling and control properties of the closed loop MIFO multirate system obtained by varying input sample rate multiplicities.

CHAPTER SIX

CONSTRAINED AND OPTIMISED SOLUTIONS TO THE MULTIRATE EIGENPROBLEM

6.1 INTRODUCTION

The design examples of Chapter 5 have demonstrated that the extra design freedom offered by MIFO sampling can be usefully applied to assign precisely a desired (well conditioned) closed loop system eigenstructure. The examples also illustrated that a severe drawback of applying the direct eigenstructure assignment technique to the MIFO system is the production of feedback matrices with very high gain elements. These generate highly switched and usually unacceptable control inputs and states. This switched behaviour clearly makes the implementation of multirate control impractical (as demonstrated by the lateral SAS design example). However, direct eigenstructure assignment methods give rise to less switched MIFO designs when compared with other established feedback desgn techniques (as indicated by a comparison of the $\|K\|_2$ figures of the modal assignment designs of Chapter 5 and the sensitive designs of Chapter 3). Thus, a well conditioned closed loop MIFO solution does contribute significantly to the minimisation of the excessive control effort and high magnitude switching characteristic of MIFO sampled control schemes.

This chapter examines eigenstructure assignment techniques which specifically minimise the control effort required by a MIFO sampled system, whilst maintaining low sensitivity to intersample effects by reducing modal interaction. The examples of Chapter 5 indicate that a two-fold feedback design objective which incorporates both these qualities is necessary for an acceptable MIFO design. Two design approaches are considered in this Chapter to find a solution which

provides an adequate balance between the two desired qualities and thus alleviate the MIFO feedback problems.

The first design approach (Patel and Patton, 1990) incorporates an extra constraint into the direct assignment method to restrict the solution to a particular form. This is termed the "constrained" eigenstructure asssignment method and is formulated in Section 6.2. The constraint is determined by the feedback matrix corresponding to the state feedback control of an equivalent single rate system (the method uses the equivalence relations of Chapter 3). The solution attempts to *approximate* the single rate gain matrix and thus provides a damping effect on the control inputs. The advantage of this method is its simplicity. The inclusion of the extra constraint requires a very simple modification to the direct assignment eigenproblem. The solution requires a non-iterative calculation of the final gain matrix identical to the unconstrained direct assignment technique.

The formulation of the constrained eigenproblem indicates that approximation to the single rate gain matrix and precise eigenvector assignment present conflicting design objectives. Thus, the simultaneous minimisation of control effort and assignment of a prescribed modal structure is not possible. A solution must seek to achieve an acceptable compromise between these two objectives. Section 6.3 presents two examples to demonstrate the feasibility of achieving this compromise by application of the constrained eigenstructure assignment technique.

The second design approach is based on *optimised* solutions to the MIFO eigenstructure assignment problem (Patel et al, 1991a, 1991b). Two "optimised" eigenstructure assignment methods are presented. Both attempt to minimise the high amplitude switched state transients and control effort whilst maintaining a specific emphasis on decreasing sensitivity to intersample effects (by reducing modal interaction).

Section 6.4 introduces three MIFO system performance measures which may be formulated into cost functions for the optimised eigenstructure

assignment task. The measures provide *additional* design criteria for the MIFO eigenproblem. These extra measures are derived from noting specific state and control transient characteristics of the MIFO feedback design examples of Chapter 5.

Section 6.5 outlines the first optimised eigenstructure assignment method. This is a gain modification technique (Owens and Mielke, 1982) which may be applied subsequent to the first pass of an eigenvector assignment procedure to decrease the gain elements of the initial feedback gain matrix. This approach is well suited to the design of MIFO feedback gain matrices. The quality to be preserved throughout any modification procedure is the precise modal structure which is assignable at the first pass. Thus a design algorithm which performs a modification about a nominal design point will ensure that the emphasis of the final solution remains on the exceptionally good insensitivity obtainable by the MIFO system.

Section 6.6 applies the gain modification technique of Owens and Mielke to the design examples of Chapter 5 to demonstrate the effectiveness of solutions produced by this method. The examples also assess the usefulness of the new measures introduced in Section 6.3.

Section 6.7 outlines the second optimisation technique (Burrows, 1990). This technique is based on the minimisation of a *scalar* objective function formed from a combination of separate scalar functions for each desired system quality. Unlike the gain modification procedure of Section 6.5, this method provides solutions which do not emphasise the achievement of any one particular quality in the initial assignment. The incorporation of all desired properties is attempted at the onset of the optimisation procedure. The degree to which each desired quality is to be satisfied in the final solution is determined by weighting elements in the objective function which is to be optimised. The technique is termed "multi-objective" eigenstructure assignment (throughout this disseration) in the context that the eigenproblem solution requires the

achievement of more than one objective in the final design. *The term is not to be confused with its alternative meaning which is the formulation of a multi-objective optimisation task as the minimisation/maximisation of a single vector objective function which incorporates all objectives.*

Several researchers have developed design algorithms which provide solutions to a multi-objective (in the sense defined above) eigenstructure assignment problem (Burrows, 1990; Rew, 1989; Ropennecker, 1986). This section does not attempt to compare the merits of the different techniques; an excellent review of these methods is provided in the Ph.D. dissertation of Burrows (1990). The main objective of Section 6.7 is to demonstrate the use of multi-objective eigenstructure assignment techniques to address the specific problems of the MIFO sampled system and thus produce an implementable system.

Section 4.5 detailed the means by which the admissible space (which spans the achievable eigenvectors set) can be extended by MIFO sampled control schemes. An important feature of this second design method is that, unlike all previous eigenstructure assignment techniques detailed in this thesis, the desired closed loop eigenvalues do not have to be a fixed set. The eigenvalues are allowed to be varied (within user-specified bounds) to generate alternative admissible spaces from which the desired set of eigenvectors are selected. Section 6.8 demonstrates the impact of this extra design freedom on the solutions produced by the parametric eigenstructure assignment technique by repeating the design examples of Chapter 5.

6.2 CONSTRAINED EIGENSTRUCTURE ASSIGNMENT

This method reduces the switched and high magnitude nature of MIFO system control and state transients by constraining the gain matrix designed by the direct assignment technique to *approximate* a specific

form. If the form of this constraint is chosen to generate smooth control effort, the constrained MIFO gain matrix will achieve the desired objectives. An immediate difficulty that arises for this approach is the *a priori* selection of a gain matrix constraint suitable for the control task in hand. A trial and error method may yield an appropriate constraint but this would require an iterative approach relying largely on the expertise of the designer. A more convenient source of a "smoothing" constraint is provided by the pencil equivalence relations of Chapter 3. A suitable constraint can be determined by considering the equivalence between the desired closed loop multirate system and the corresponding *single-rate* closed loop system.

The equivalence relations of interest are given by equations (3.4.10), (3.4.15), (3.4.16) and (3.4.17). A combination of these equations (considering only those parts of the system pencils concerned with state feedback) gives the following equivalence relationship between the open loop single rate system and the closed loop MIFO multirate system:

$$\begin{bmatrix} zI-\Phi & \Gamma \end{bmatrix} = T_c \begin{bmatrix} zI-\Phi m & \Gamma_m \end{bmatrix} \begin{bmatrix} T_c^{-1} & 0 \\ Q_{22}KT_c^{-1} & Q_{22}G \end{bmatrix} \qquad (6.2.1)$$

which is consistent if

$$\Phi_m = T_c^{-1}\Phi T_c + \Gamma_m Q_{22}K \qquad (6.2.2)$$

Equation (6.2.2) represents an *equivalent* closed loop multirate matrix in terms of the single rate feedback matrix. The matrix $K_m = Q_{22}K$ can be used as a 'smoothing' parameter to constrain the direct multirate eigenstructure assignment problem. This serves to impose a restriction on the gain elements of the multirate feedback matrix and thus minimise the control effort demanded by the MIFO system.

To include the gain matrix constraint in the direct assignment solution, the eigenproblem of Section 4.3.2 is modified to one of selecting a set of eigenvectors $\{\nu_i\}$ such that:

$$\min_{k_i} \|M_{\lambda i} k_i - K_m \nu_{di}\|_2 \tag{6.2.3}$$

subject to the non-linear constraint,

$$\|N_{\lambda i} k_j - \nu_{dj}\| \leq \alpha \tag{6.2.4}$$

Now the direct assignment solution will attempt to achieve a desired eigenvector set with the additional objective of reducing the excessive oscillations by approximating the gain matrix of the single rate feedback matrix. The constrained problem will have a solution (Golub and Van Loan, 1983) iff $\min \|M_{\lambda i} k_i - K_m \nu_{ai}\|_2 \leq \alpha$. If this is the case, then either

$$\|N_{\lambda i} M_{\lambda i}^{-1} K_m \nu_{di} - \nu_{di}\|_2 \leq \alpha \tag{6.2.4a}$$

or,

$$\|N_{\lambda i} M_{\lambda i}^{-1} K_m \nu_{di} - \nu_{di}\|_2 > \alpha \tag{6.2.4b}$$

and the solution will satisfy

$$(M_{\lambda i}^T K_m M_{\lambda i} + \beta N_{\lambda i}^T N_{\lambda i}) k_i = (M_{\lambda i}^T K_m \nu_{di} - \beta N_{\lambda i} \nu_{ai}) \tag{6.2.5}$$

where β is chosen such that (6.2.4b) is satisfied. This is selected by the user, but generally proves to be a difficult parameter to specify for the MIFO eigenstructure assignment problem. A suitable compromise

between the constraints of (6.2.4) is provided by a direct combination of the two. This converts the problem to one of solving the single constraint:

$$\min_{k_j} \|P_{\lambda i} k_j - \xi \nu_{di}\|_2 \qquad (6.2.6a)$$

$$\xi = (I_n - Q_{22} K)$$

$$P_{\lambda i} = N_{\lambda i} - M_{\lambda i} \qquad (6.2.6b)$$

Matrix ξ (which is effectively a measure of the extent to which the approximation of the eigenvectors will be relaxed) is determined by the single rate feedback matrix.

Assume for simplicity, $\lambda_i \epsilon R$. If $P_{\lambda i} \epsilon R^{nxn}$ (as in the case of the MIFO system) equation (6.2.6) will have a unique solution which lies in the nullspace defined by the columns of $P_{\lambda i}$. Each closed-loop eigenvector will then be determined by

$$\nu_i = N_{\lambda i} P_{\lambda i}^{-1} \xi \nu_{di} \qquad (6.2.7)$$

The corresponding feedback matrix may be computed using equation (4.3.15). For $\lambda_i \epsilon \mathbb{C}$, a solution from the intersection of the nullspaces corresponding to real and imaginary parts of the eigenvalues is found. A method for this computation has been outlined in Section 4.3.2. The feedback matrix thus produced approximates the single rate feedback and therefore *constrains* the oscillatory solution that would otherwise occur.

The multirate feedback designs produced using this method inherit the relative sensitivity properties of the single rate constraint. For this reason, it is recommended that the design is based on an

insensitive single rate feedback matrix for systems with a high interaction of modes. Normal pole assignment techniques may be used to generate the smoothing feedback matrix for weakly coupled systems. The application of this constrained eigenstructure assigment method is illustrated in the next section. To assess the usefulness of this method in reducing the MIFO gain matrix element, the $\|K\|_2$ of feedback matrices produced by the constrained method are compared to those produced by the direct assignment technique.

6.3 APPLICATION OF CONSTRAINED EIGENSTRUCTURE ASSIGNMENT

Two examples demonstrate the use of the constrained eigenstructure assignment technique proposed in Section 6.2. The first example considers the design of feedback control for a weakly coupled open loop system such that its state transients are maximally decoupled. The second example repeats the design of a Stability Augmentation System (SAS) for the lateral aircraft subsystem of Example 5.4.3. Both systems are controllable in the continuous domain.

6.3.1 Example 6.3.1

The system to be examined is weakly coupled in the open loop state (Sinswat and Fallside, 1977) and is represented by the following continuous-time system matrices:

$$A = \begin{bmatrix} 1 & 1 & 0 \\ 0 & 2 & 0 \\ 1 & -2 & 3 \end{bmatrix} \qquad B = \begin{bmatrix} 0 & 0 \\ 1 & 0 \\ 0 & 1 \end{bmatrix} \tag{6.3.1}$$

The desired closed-loop poles are selected to be {-1 -2 -3}. The minimum column indices of the system are {μ_1=1 μ_2=2}. The main interval of sampling is chosen to be T = 0.1secs, implying sample rates of T_1=0.1 and T_2=0.05 for the MIFO system to be controllable. Multirate feedback matrices are designed, first with the direct assignment method and then using the constrained method of Section 6.2.

Two single rate feedback matrix constraints are considered. The first constraint is chosen to be an insensitive design determined using the direct assignment technique. The second constraint is designed using the canonical pole placement algorithm outlined in Section 3.4.2 and thus has no emphasis on system insensitivity. These single rate feedback matrices are given below (where the subscripts RSR and SR denote robust and non-robust single rate matrices respectively):

$$K_{RSR} = \begin{bmatrix} -1.5177 & 1.6302 & -5.2225 \\ -4.6943 & -5.2126 & 0 \end{bmatrix} \quad K_{SR} = \begin{bmatrix} -5.0658 & -0.1483 & -3.8160 \\ -8.5376 & -6.5022 & 0.0000 \end{bmatrix} \tag{6.3.2}$$

The MIFO multirate feedback matrix generated by the direct eigenstructure assignment method has a $\|K\|_2$ figure of 203.92 which produces extreme switching in both state and control transients. Applying the constrained eigenstructure assignment method with matrices K_{RSR} and K_{SR} generates the follow mulirate feedback gain matrices:

$$K_{RMR} = \begin{bmatrix} -5.715 & -0.111 & -4.559 \\ -5.595 & -5.685 & -0.063 \\ -6.434 & -6.052 & 0.071 \end{bmatrix} \quad K_{MR} = \begin{bmatrix} -7.119 & -0.605 & -4.578 \\ -5.880 & -6.018 & 0.097 \\ -6.141 & -5.677 & -0.110 \end{bmatrix} \tag{6.3.3}$$

The sensitivity performance measures of the single rate and multirate closed loop systems of K_{RSR}, K_{SR}, K_{RMR}, K_{MR} are shown in Tables 7 and 8. The response of the two multirate systems to an initial condition of

x_2=0.002 produced by feedback matrices K_{RMR} and K_{MR} are shown in Figures 6.3.1 and 6.3.2. The responses produced by the single rate systems are also included.

Performance Measure	Feedback Gain Matrix	
	K_{RSR}	K_{RMR}
$\kappa_m(V)$ multirate design $\kappa(V)$ single rate design	$\kappa(V)$= 14.1709	$\kappa_1(V)$= 15.913 $\kappa_2(V)$= 13.003
$\|\|K\|\|_2$	7.0227	12.8012

Table 7 Performance measures of K_{RSR} and K_{RMR} closed loop systems

Performance Measure	Feedback Gain Matrix	
	K_{SR}	K_{MR}
$\kappa_m(V)$ multirate design $\kappa(V)$ single rate design	$\kappa(V)$= 33.229	$\kappa_1(V)$= 19.077 $\kappa_2(V)$= 14.778
$\|\|K\|\|_2$	11.647	13.426

Table 8 Performance measures of K_{SR} and K_{MR} closed loop systems

The tabulated and time response data show that the minimisation of $\|\|K\|\|_2$ has been achieved by both multirate designs. Furthermore, both K_{MR} and K_{RMR} provide the desired smoothing of the state and control input

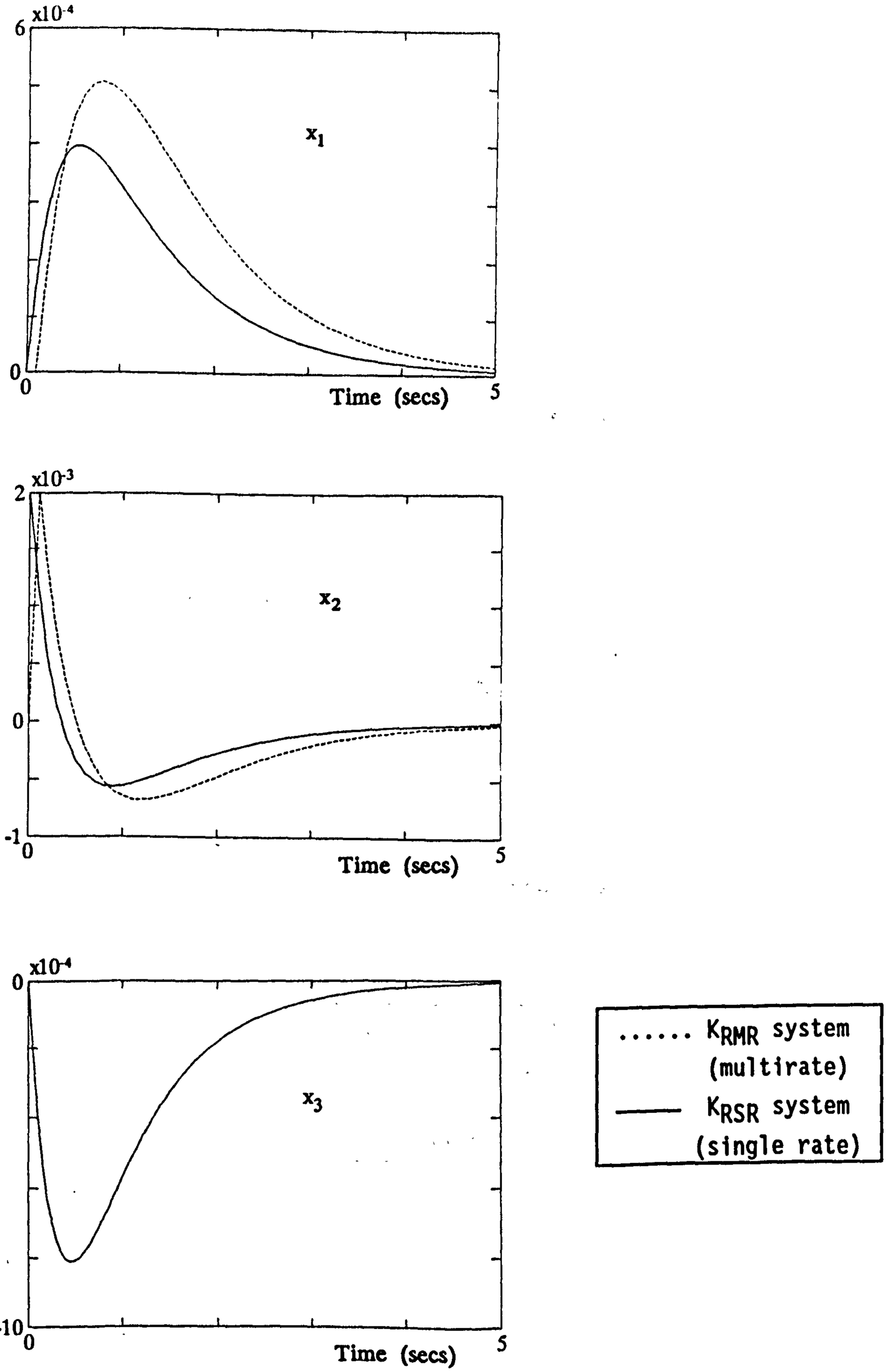

Figure 6.3.1a State responses of K_{RMR} closed loop multirate system (designed using constraint K_{RSR})

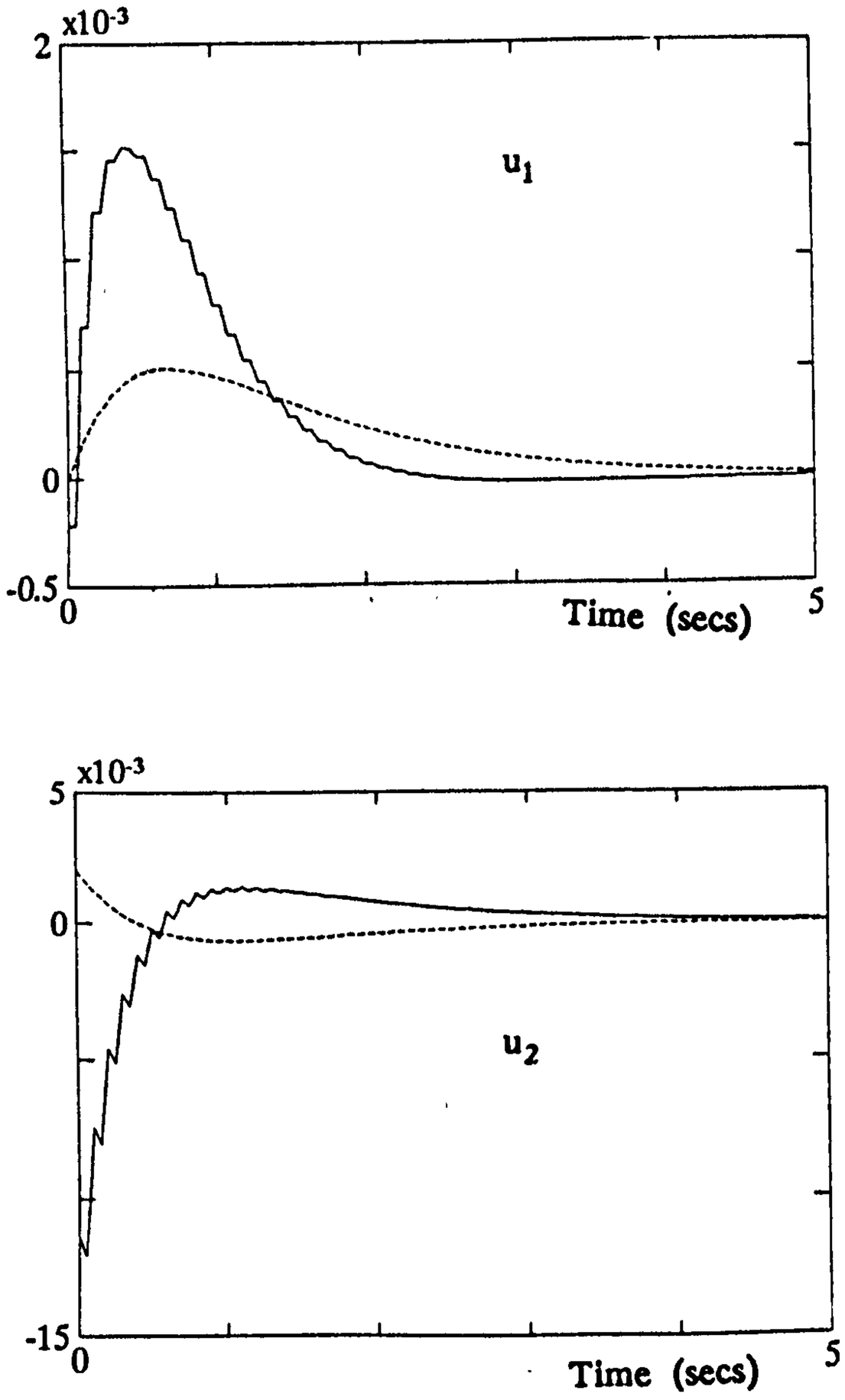

Figure 6.3.1b Control responses of K_{RMR} closed loop multirate system (designed using constraint K_{RSR})

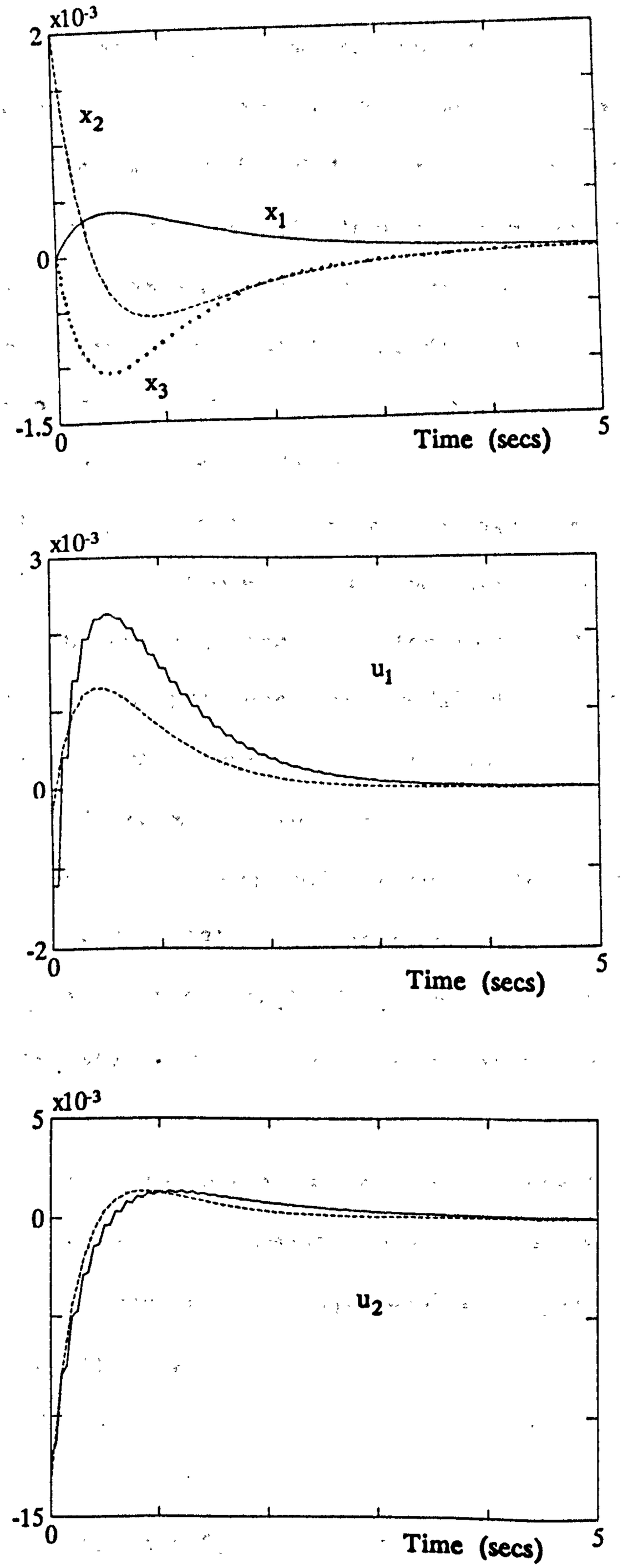

Figure 6.3.2 State and control responses of K_{MR} closed loop multirate system (designed using constraint K_{SR})

transients. In particular, the u_1, u_2 responses of multirate design K_{MR} are observed to have the same "shape" as the single rate control inputs. This demonstrates the design objective of the constrained assignment method on *approximating* the single rate gain matrix.

The tabulated and time response results for designs K_{RMR} and K_{RSR} show that the overall (good) insensitivity of the constraining single rate system has been maintained by the multirate design ($\kappa(V)$=14.1709 for K_{RSR} system whilst $\kappa_m(V)$ = {15.9131 13.0033} for K_{RMR} system). Despite this, there is an increase in the sensitivity of pole λ_3 = -3 for the multirate design. Thus, the use of a well conditioned single rate system in the constrained assignment procedure has resulted in a multirate system with the same overall (good) conditioning.

In contrast, the tabulated results for designs K_{MR} and K_{SR} show that the former provides more modal decoupling than its (not particularly insensitive) single rate counterpart. The sensitivities of poles λ_2 = -2 λ_3 = -3 are much lower for the multirate system than for the single rate system. The original conditioning of the single rate system ($\kappa(V)$ = 35.2293) is considerably improved by the K_{MR} design ($\kappa_m(V)$ = {19.072 14.7784}). The individual pole sensitivities of the multirate system are also observed to be approximately half that of the original single rate system.

Thus the use of a relatively sensitive single rate design for the constrained assignment procedure has resulted in a mulitrate design which produces a considerable improvement in closed loop system insensitivity.

6.3.2 Example 6.3.2

The aircraft SAS design of Example 5.4.3, for which an impractical design was obtained by using the direct eigenstructure assignment

method, is repeated. The constrained eigenstructure assignment method is used to generate multirate state feedback control such that the closed-loop system has the desired eigenstructure.

A design is based on a constraining single rate feedback matrix designed using the direct method. Proceeding with the MIFO system design using the constrained assignment method produces the following multirate feedback matrix:

$$K_{6C} = \begin{bmatrix} 0.4626 & 0.1988 & 4.4456 & -1.0495 & 0.0636 \\ -0.2708 & 0.0343 & -2.6074 & 0.3252 & -0.0710 \\ -0.2486 & -0.4486 & -1.2543 & 0.5240 & 0.0093 \\ 0.1382 & -0.0152 & -0.0149 & 0.8288 & -0.0175 \\ 0.1840 & -0.0001 & 0.0052 & -0.3487 & 0.0317 \end{bmatrix} \qquad (6.3.4)$$

The corresponding closed loop multirate system properties are presented in Table 9.

Performance Measure	Feedback Gain Matrix K_{6C}
$\kappa_m(V)$	$\kappa_1(V) = 8.2136$ $\kappa_2(V) = 7.6252$ $\kappa_3(V) = 7.5986$ $\kappa_4(V) = 25.7180$
$\|K\|_2$	5.4272

Table 9 Performance measures of K_{C6} closed loop system

The tabulated results show that the multirate gain matrix produced by

the constrained assignment method has a significantly lower norm than the original K_6 matrix (recall $\|K_6\|_2 = 1427.3$ whilst $\|K_{6C}\|_2 = 5.427$). The modal decoupling provided by feedback K_{6C} is also well within the bounds of "good" insensitivity. This design, nevertheless, produces unacceptable state and control switching which renders the design impractical. (The control inputs required for this design are oscillatory but do remain reasonably close to that demanded by the constraining single rate design.)

6.4 ADDITIONAL MIFO SYSTEM PERFORMANCE MEASURES FOR OPTIMISED EIGENSTRUCTURE ASSIGNMENT

The design examples of Chapters 3 and 5 and Section 6.3 all use the measure $\|K\|_2$ to monitor the control effort demanded by a particular MIFO feedback matrix. This norm measure is a standard means of assessing the magnitude of gain matrices for continuous-time and single rate discrete systems. For the MIFO state feedback problem, the gain matrix has a well defined distribution of high magnitude and low magnitude elements. An examination of Chapter 5 design examples indicate that the magnitude of gain elements associated with a particular input increases with an increase in the multiplicity of that input. For example, gain matrix K_2 is produced by multiplicities $\mu_1=2$, $\mu_2=1$ for inputs u_1 and u_2 respectively. In accordance with this choice of sample parameters, the gain matrix elements associated with input u_1 (i.e. the first two rows of K_2) are noticeably higher than those pertaining to the single rate input u_2.

Thus, any design procedure which attempts to reduce the control effort demanded by MIFO feedback gain should principally concentrate on minimising the magnitude of gain elements associated with each multirate input. A suitable (minimisation) cost function for this purpose is:

$$J_G = \sum_{i=1}^{m} \sum_{j=1}^{n} \alpha(i,j)\{K(i,j)\}^2 \qquad (6.4.1)$$

Matrix α is of dimension (mxn). It defines the design emphasis to be placed on the minimisation of each element in the feedback gain matrix by allocating a non-negative weighting to each ij'th position. The larger the weighting in the ij'th position of α the greater the corresponding ij'th element in K is penalised in the calculation of J_G. If α is chosen such that all weightings for gain matrix elements of rows associated with multirate inputs are significantly higher than those associated with single rate inputs then the desired emphasis for MIFO feedback design using eigenstructure assignment is achieved.

A further gain matrix measure is introduced in order to monitor the switched nature of the MIFO system states and control inputs. The switched behaviour is exhibited at intersample points. It is a direct consequence of large variations in the gain matrix elements of rows associated with each input. A reduction in switching can be obtained if the difference between the corresponding elements of each row of the gain matrix is minimised. As for the measures of (6.4.1), only the rows pertaining to the multirate inputs need to be considered. Thus, a suitable (minimisation) cost function for this purpose is:

$$J_{D1} = \sum_{p=1}^{m} \sum_{i=I_o}^{I_f} \sum_{j=1}^{n} \gamma(i,j)\{K(i,j) - K(i+1,j)\}^2 \qquad (6.4.2a)$$

$$I_o = \sum_{q=1}^{p-1} n_q + 1 \qquad (6.4.2b)$$

$$I_f = I_o \qquad \text{for } n_q = 1$$

$$I_f = I_o + n_q - 1 \qquad \text{for } n_q > 1 \qquad (6.4.2c)$$

Matrix γ is the allocated (non-negative) weighting matrix of the same dimension as gain matrix K. It contains all zero elements in every I_f'th row for each of the m inputs (since only the *difference* between multirate input rows are weighted and since every single rate input is excluded from the cost function). If the weighting elements are chosen such that rows with a large difference in corresponding positions are penalised by large values in matrix γ, the desired emphasis for MIFO feedback control design will be achieved.

Recall from Chapter 4 that the condition number $\kappa(K)$ is a measure of the "largest" and "smallest" numbers in K. Thus, state and control switching (i.e. the variation in the gain matrix rows associated with each multirate input) can also be monitored by conditioning measures,

$$\kappa_i(K_{mi}) \qquad i = 1,..,m$$

$$K_{mi} = \text{the } n_i \text{ rows of K associated with the i'th input} \qquad (6.4.3a)$$

Note that the measures of (6.4.3a) will provide a rough quide to the switching produced by each control input for a particular design and is by no means an adequate measure by itself. It is best used to monitor MIFO switching behaviour in conjunction with the measures of (6.4.1) and (6.4.2).

Thus, a suitable cost function to monitor the state and control switched behaviour is:

$$J_{D2} = \sum_{i=1}^{m} \kappa_i(K_{mi}) \qquad (6.4.3b)$$

A low J_{D2} will indicate the minimisation of switched state and control behaviour.

A final cost function is introduced. This measures the closeness of the right eigenvectors selected from the admissible space (i.e. the achievable eigenvectors) to the desired set. Let ν_{id} be the i'th desired right eigenvector. An appropriate measure of the proximity of the i'th achieved right eigenvector ν_i to ν_{id} is given by:-

$$J_M = \sum_{i=1}^{n} \beta(i)[\bar{\nu}_i - \bar{\nu}_{id}]^T[\nu_i - \nu_{id}] \qquad (6.4.4)$$

where $\beta(i)$ is the i'th non-negative weighting factors and a bar ('-') over a vector denotes the complex-conjugate. The elements of row matrix β indicates the emphasis to be placed on achieving the desired right eigenvector. A low $\beta(i)$ represents a low priority on the assignment of the i'th eigenvector and vice-versa. Thus, a low J_M will indicate the accuracy of achievement of prioritised right eigenvectors.

6.5 THE OPTIMISED GAIN MODIFICATION PROCEDURE

This Section outlines the optimised gain modification method of Owens and Mielke, 1982. The objective of this technique is to select a new set of achievable right eigenvectors such that the gain elements of the original design are minimised. For the continuous time and single rate discrete cases, this objective is achieved by performing a gradient search *local* to the initial achievable eigenvector set to retain the modal structure obtained by original design. The extent to which the gains can be modifed is dependent upon the desired eigenvectors, the initial admissible eigenvector space and the system matrices. For the MIFO system, the increased dimension of the admissible eigenvector space

allows a more flexible modification of the feedback matrix. The extra design freedom increases the range from which a new set of achievable eigenvectors can be selected. For some MIFO systems, this flexibility also allows a wider gradient search to be conducted without risk of a significant adjustment of the desired modal mixing in the final design.

The optimisation procedure requires a suitable cost function to monitor the degree to which the elements of an initial (mxn) gain matrix K are reduced. This is provided by the J_G cost function defined in equation (6.2.1). Each element of gain matrix K in equation (6.2.1) can be isolated by:

$$K(i,j) = L_i \, K \, C_j \tag{6.5.1}$$

$$L_i = [\underbrace{0 \; .. \; 0}_{i-1} \; 1 \; \underbrace{0 \; .. \; 0}_{m-i}] \qquad C_j = [\underbrace{0 \; .. \; 0}_{j-1} \; 1 \; \underbrace{0 \; .. \; 0}_{n-j}]^T \tag{6.5.2}$$

Recall from equation (4.3.15) that,

$$K = MV^{-1} = [M_{\lambda 1}k_1 \; M_{\lambda 2}k_2 \; \ldots \; M_{\lambda n}k_n]V^{-1} \tag{6.5.3}$$

For a given admissible eigenvector space $R_{\lambda i}$ ($R_{C\lambda i}$ for $\lambda_i \in \mathbb{C}$) for $\{\lambda_i\}$ i=1,..,n, the elements of gain matrix K are determined by the (mx1) design parameters k_i i=1,..,n (see Section 4.3). A combination of equations (6.5.1), (6.5.2) and (6.5.3) allows cost function J_G to be written as:

$$J_G = \sum_{i=1}^{m} \sum_{j=1}^{n} \alpha(i,j)\{L_i MVC_j\}^2 \tag{6.5.4}$$

The objective of the optimisation procedure is to minimise J_G by adjusting design parameters k_i. Define $k_{pq} \in k_i$. The effect on J_G of a

change in any element k_{pq} of k_i is determined by the partial derivative,

$$\Delta_{pq} = \frac{\delta J_G}{\delta k_{pq}} = \sum_{i=1}^{m} \sum_{j=1}^{n} 2\alpha(i,j)\{K_{ij}\} \frac{\delta\{K_{ij}\}}{\delta k_{pq}} \qquad (6.5.5a)$$

Collecting (mxn) such derivatives to form the Jacobian matrix and forming the following directional derivative

$$\Delta = \frac{\{\Delta_{pq}\}}{\|\{\Delta_{pq}\}\|} \qquad (6.5.5b)$$

will determine the direction of change in k_{pq} to induce the greatest change in J_G.

With the use of equation (6.5.3), partial derivatives Δ_{pq} can be expressed as;

$$\Delta_{pq} = \sum_{i=1}^{m} \sum_{j=1}^{n} 2\alpha(i,j)\{L_i M V^{-1} C_j\} \frac{\delta\{L_i M V^{-1} C_j\}}{\delta k_{pq}} \qquad (6.5.6)$$

The partial derivative of the product $\{L_i M V^{-1} C_j\}$ is:

$$\frac{\delta\{L_i M V^{-1} C_j\}}{\delta k_{pq}} = L_i \left[\frac{\delta M}{\delta k_{pq}} V^{-1} + M \frac{\delta V^{-1}}{\delta k_{pq}} \right] C_j \qquad (6.5.7)$$

The first partial derivative of equation (6.5.6) is given by,

$$\frac{\delta M}{\delta k_{pq}} = \left[0 \ldots\ldots 0 \quad -M_{\lambda q} \frac{\delta k_q}{\delta k_{pq}} \quad 0 \ldots\ldots 0 \right] \qquad (6.5.8)$$

$$= [\, 0 \ldots\ldots 0 \quad m_{pq} \quad 0 \ldots\ldots 0 \,]$$

where m_{pq} is the p'th column of $M_{\lambda q}$ (since only the (p,q)'th element of $M_{\lambda q}$ is affected by the (p,q)'th element of design vector k_q). Calculating the second derivative of equation (6.5.6) gives,

$$\frac{\delta V^{-1}}{\delta k_{pq}} = -V^{-1} \frac{\delta V^{-1}}{\delta k_{pq}} V^{-1} \qquad (6.5.9)$$

Since,

$$\frac{\delta V}{\delta k_{pq}} = \left[0 \ldots. 0 \quad -N_{\lambda q} \frac{\delta k_q}{\delta k_{pq}} \quad 0 \ldots.. 0 \right] \qquad (6.5.10)$$

$$= [\ 0 \ldots.. 0 \quad n_{pq} \quad 0 \ldots... 0\ ]$$

(where n_{pq} is the p'th column of $N_{\lambda q}$) then a combination of (6.5.7), (6.5.8) and (6.5.10) reduces the computation of derivative Δ_{pq} to:

$$\Delta_{pq} = \sum_{i=1}^{m} \sum_{j=1}^{n} 2\alpha(i,j)\{L_i M V^{-1} C_j\}\ L_i\{(m_{pq} - K n_{pq}) V^{-1}\} C_j \qquad (6.5.11)$$

The calculation of Δ then proceeds as indicated by equation (6.5.5). If a step of size s is taken along direction Δ, an update,

$$(k_{pq})_{NEW} = (k_{pq})_{OLD} - s\Delta \qquad (6.5.12)$$

will then give a new set of k_i which minimises J_G. The updated J_G thus produced is denoted $(J_G)_{NEW}$, whilst the preceding cost function is referred to as $(J_G)_{OLD}$. The search is terminated either when the desired reduction in gain elements has been obtained or when a further adjustment in k_i yields an insignificant improvement in the design, i.e. $(J_G)_{NEW} - (J_G)_{OLD}$ is sufficiently low.

As indicated earlier in this section, to retain the original modal mixing the step size s is required to be quite small for continuous-time and single rate discrete problems. For some MIFO multirate problems the search procedure can include very large steps without jeopardising the insensitivity of the final design. A method of automating the gain update procedure (once an initial design has been obtained) based on successive bisection of the search line is outlined below:

(i) Select an arbitary initial search step s_0.

(ii) Calculate $(k_{pq})_{NEW}$ for $s=s_0$.

(iii) Calculate $(J_G)_{NEW}$.

(iv) If $(J_G)_{NEW} >> (J_G)_{OLD}$ (i.e. a minimisation has not been obtained) or the desired termination criteria is not satisfied, continue with a search in the same direction but with an updated search step $s = s_{LAST}/2$ (initially $s_{LAST} = s_0$) until a minimisation has been obtained.

(v) Update $s = s_0/2$.

(vi) Continue from step (ii).

The successive bisection line search procedure is the simplest method of selecting the step to be taken in a given direction (as determined from gradient information) for the update algorithm of (6.5.12). For many gain modification problems this procedure obtains a significant reduction in J_G very rapidly (the average number of steps taken to reach a solution within 2% of a minimum is approximately 25/30 steps). The line search can be speeded up by interpolative search algorithms based

on for example, Powells quadratic interpolation method or the cubic interpolation method (Walsh, 1975). However, the above line search method is more than adequate for the single objective optimisation task.

A drawback of any optimisation task is that the search procedure will tend to converge to a minimum which may not necessarily be the global minimum. The minimum to which the optimisation routine converges to depends on the initial step s_0. A succession of searches with varying s_0 is recommended to find a collection of local minima. Selecting the lowest of this set of minima (which may be the global minimum) will ensure the achievement of a solution which minimises J_G.

Note that only the cost function J_G is directly minimised by the optimisation method. A minimisation of J_G will always ensure a great degree of reduction *initially* in J_{D1}, J_{D2}. However, the procedure will not necessarily minimise cost functions J_{D1} and J_{D2} to a large extent in subsequent updates. An overall gain minimisation is the primary objective of the optimisation task. For a good MIFO design, low figures for cost functions J_{D1} and J_{D2} are also required to ensure that the minimisation has been produced in the correct gain matrix elements (i.e. to specifically reduce state and control signal switching).

The design examples of the following section demonstrate the application of the gain minimisation technique with the above search procedure. The first example also examines the additional measures of Section 6.2, to assess their usefulness. For this example the following function plots are examined:

(i) $\|K\|_2$ versus J_G

(ii) $\|K\|_2$ versus conditioning measures $\kappa_m(V)$

(iii) J_G versus gain measures J_{D1}, J_{D2}

The first plot J_G and $\|K\|_2$ is included to show that (as expected) the $\|K\|_2$ figure of a gain matrix is reduced with a minimisation of J_G. In

practice, it is difficult to gauge the actual reduction in gain elements from the sum of weighted gain matrix elements (i.e. from J_G). The $\|K\|_2$ figure can be more readily interpreted for this purpose and is thus used to assess the actual gain minimisation. J_G is used to show the *degree* of minimisation achieved.

The second plot indicates the variation of MIFO system insensitivity with each new set of optimised eigenvectors, whilst the last two plots show the relationship between overall gain minimisation and the specific gain reductions required for the MIFO problem. The cost functions J_{D1} and J_{D2} do not participate in the actual optimisation design procedure. Thus it is not necessary to select the weighting matrix γ. For display purposes it is assumed that γ has all unity elements.

6.6 APPLICATION OF GAIN MODIFICATION PROCEDURE

The design exercises of Examples 5.4.2, 5.4.3 and 6.3.1 are repeated in this section to examine the effectiveness of the gain modification procedure of Section 6.5. The designs produced by the original assignment are modified. Time responses produced by gain matrices which minimise cost functions J_G, J_{D1} or J_{D2} are examined to investigate the effect of selecting solutions with different design emphasis on MIFO system performance.

6.6.1 Example 6.6.1

This example minimises $\|K_2\|_2$ of the multirate feedback matrix in Example 5.4.1. Recall that the closed loop system of design K_2 achieved perfectly decoupled state transients at main sample instants with highly switched x_1 and x_3 intersample responses. The cost of this exact decoupling was highly switched, high magnitude control effort from input

u_1. Recall also that input u_1 has a direct influence on states x_1 and x_3. Thus to minimise the switching experienced by both u_1 and x_1, x_3, the gain minimisation procedure must primarily reduce the gain elements associated with control input u_1. A suitable weighting matrix α to effect this emphasis for the optimisation task is:

$$\alpha = \begin{bmatrix} 100 & 100 & 100 \\ 100 & 100 & 100 \\ 1 & 1 & 1 \end{bmatrix} \qquad (6.6.1)$$

Applying the gain modification procedure with a choice of initial step size $s_0 = 10$ with the above weighting matrix gives the function plots of Figure 6.6.1. The termination criteria for this design is selected to be $(J_G)_{NEW}-(J_G)_{OLD} < 0.001$.

The following points are noted from the plots of Figure 6.6.1:

(i) Plot (6.6.1a) shows that the gain modification procedure has reduced $\|K\|_2$ of the original design by $\approx 96\%$ (original $\|K\|_2$=67.156, final $\|K\|_2$=2.5475).

(ii) Plot (6.6.1b) shows that the reduction in $\|K\|_2$ is obtained at the cost of increased sensitivity. The main sample sensitivity measured by $\kappa(V)$ suffers significantly but the intersample sensitivity (measured by $\kappa_m(V)$) remains extremely low.

(iii) Plots (6.6.1c) and (6.6.1d) show that both J_{D1} and J_{D2} decrease in correspondence with a decrease in $\|K\|_2$.

The optimisation procedure is repeated with several choices of s_0 to examine whether a "better" design (which for this system would be indicated by a lower $\|K\|_2$) can be obtained from a different choice of intial search step. The results obtained by this wider search do not

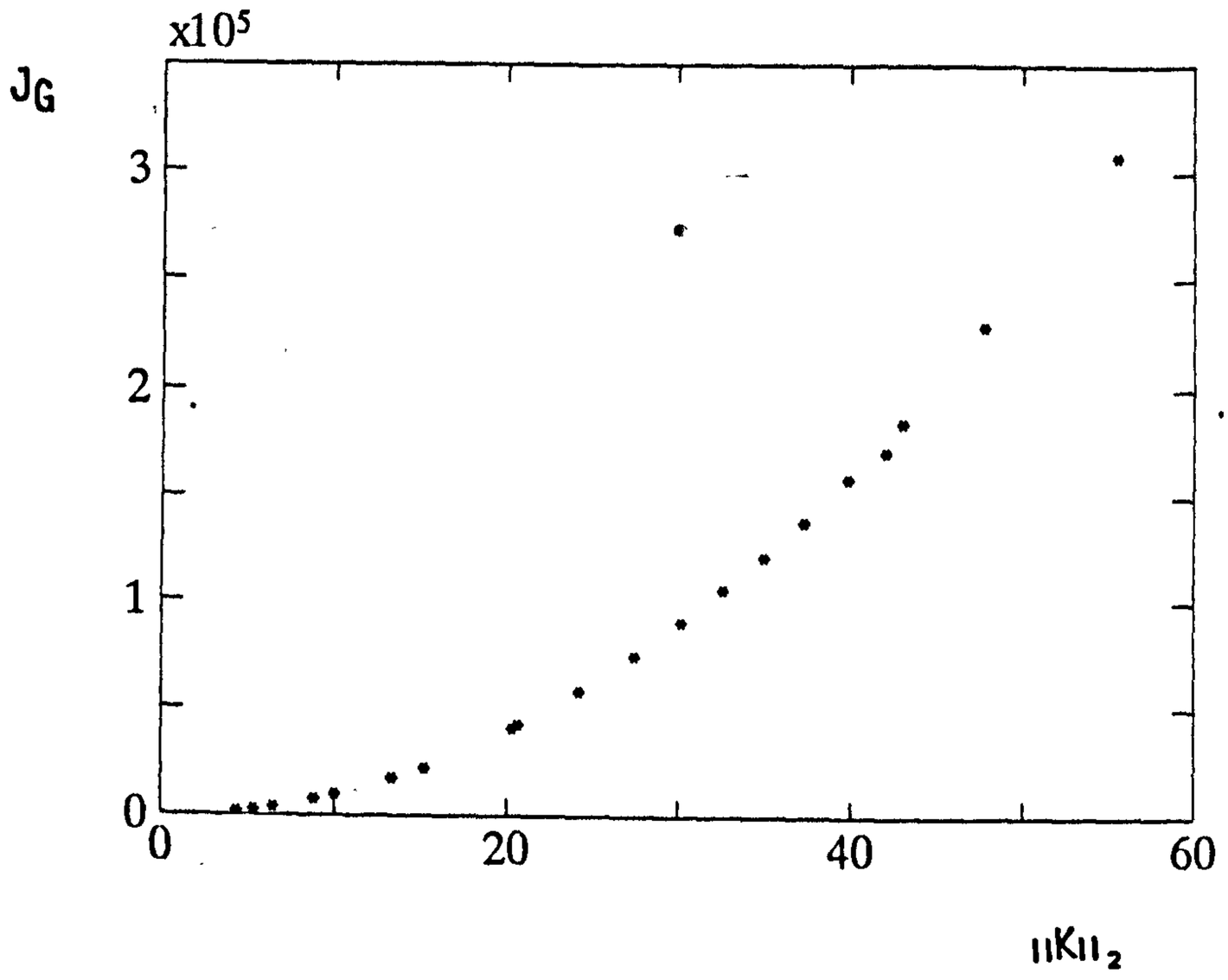

Figure 6.6.1a J_G vs $\|K\|_2$

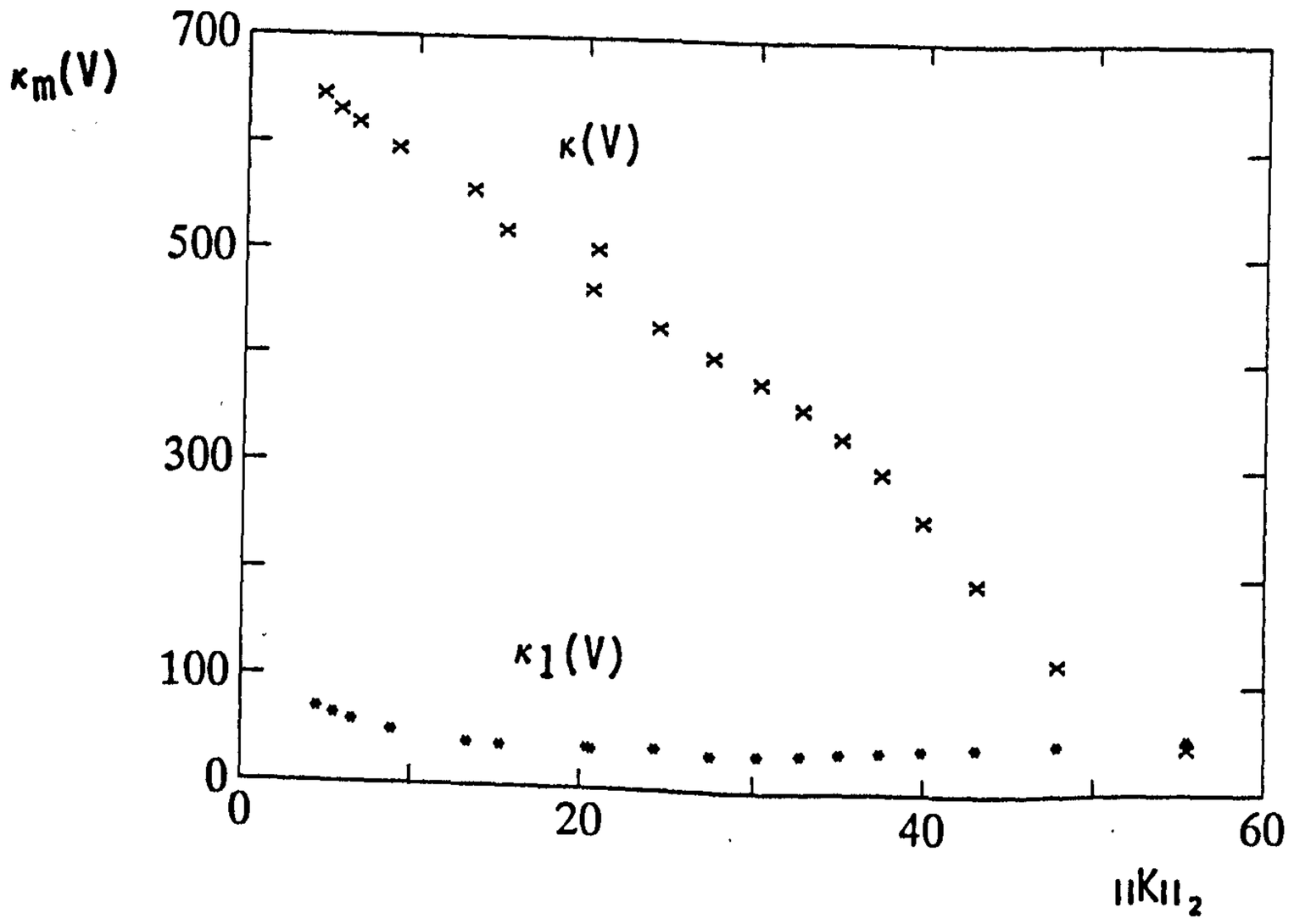

Figure 6.6.1b $\kappa_m(V)$ vs $\|K\|_2$

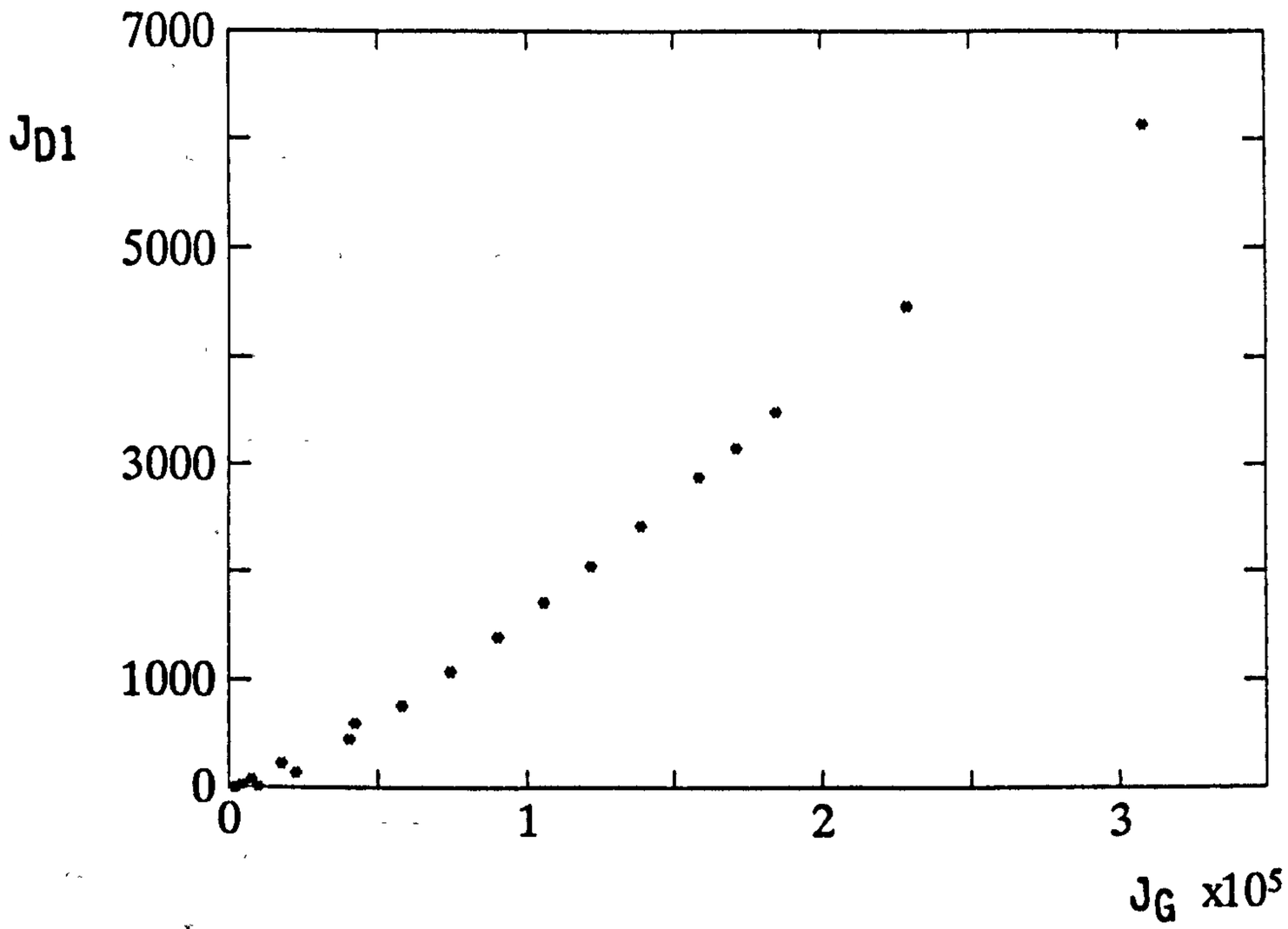

Figure 6.6.1c J_{D1} vs J_G

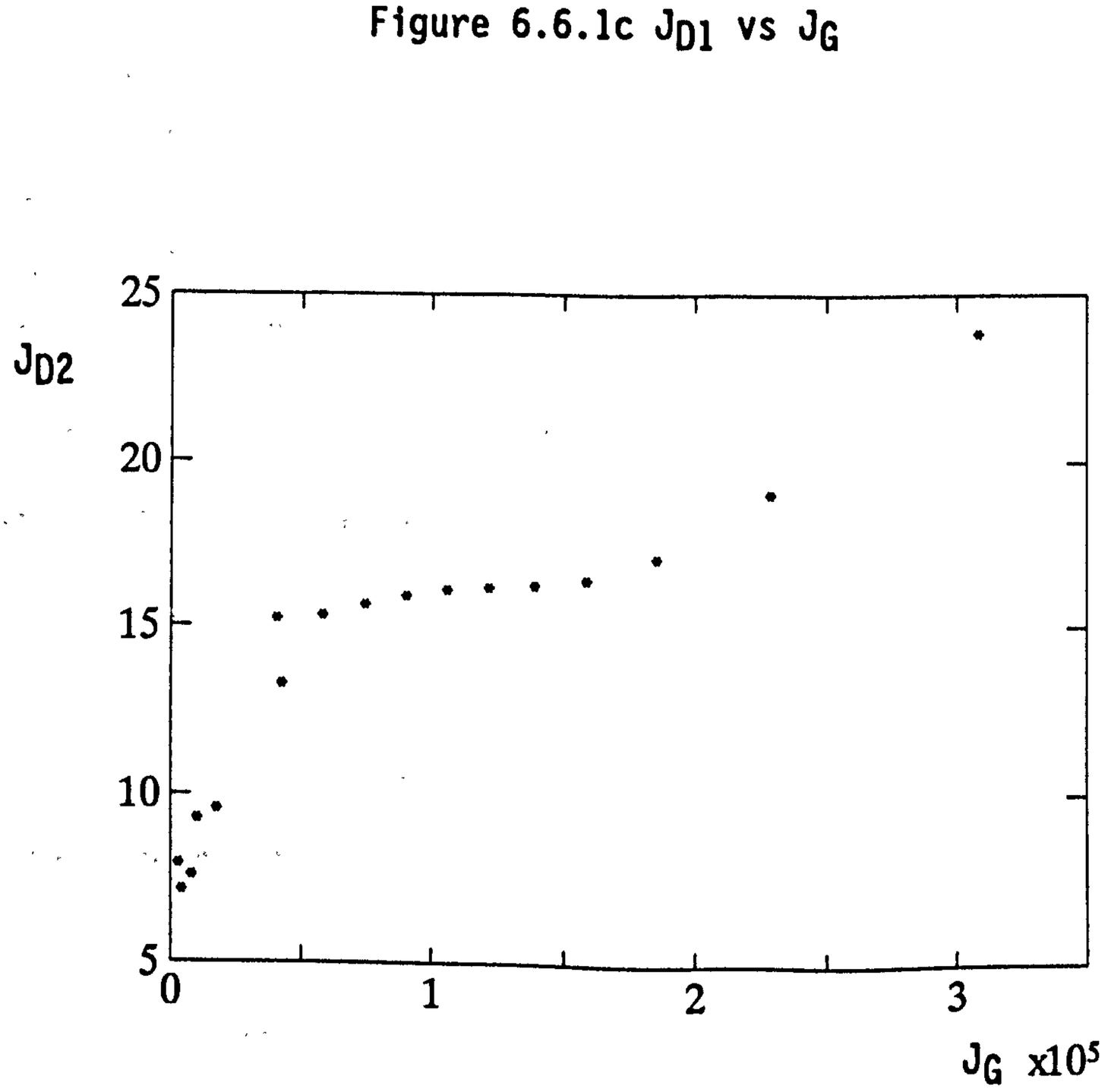

Figure 6.6.1d J_{D2} vs J_G

yield an improvement in $\|K\|_2$.

From the plots of Figure 6.6.1 it is clear that there is a tradeoff between the simultaneous minimisation of performance measures $\|K\|_2$ and $\kappa(V)$. A feedback design which gives low $\|K\|_2$ produces a high k(V), and vice-versa. To determine which performance quality is *primarily* required to give a practically implementable solution for this system, two feedback matrices K_{2G1}, K_{2G2} are selected from the optimisation runs for varying s_0. The performance measures of the two gain matrices are compared in Table 10 below.

Performance Measure	Feedback Gain Matrix	
	K_{2G1}	K_{2G2}
$\kappa_m(V)$	$\kappa_1(V)$= 18.2896 $\kappa_2(V)$=431.6414	$\kappa_1(V)$= 5.0797 $\kappa_2(V)$=42.9264
J_{D1}	0.0495	6147
J_{D2}	11.7108	23.8847
$\|K\|_2$	2.5475	55.4903

Table 10 Performance measures of K_{2G1} and K_{2G2} closed loop systems

The first feedback gain matrix is chosen because it has the lowest gain norm figure ($\|K\|_2$ = 2.5475). It is defined:

$$K_{2G1} = \begin{bmatrix} -0.4272 & -0.0511 & 1.2884 \\ -0.6138 & -0.1646 & 1.3301 \\ 1.4372 & 1.9409 & 0.0559 \end{bmatrix} \qquad (6.6.2)$$

The second gain matrix yields a closed loop system with a good balance of performance measures $\|K\|_2$ and $\kappa_m(V)$. This gain matrix is defined:

$$K_{2G2} = \begin{bmatrix} -17.315 & -31.4864 & -11.1699 \\ 17.7241 & 33.4031 & 15.4501 \\ 0.0940 & -0.4150 & -1.1161 \end{bmatrix} \qquad (6.6.3)$$

The time responses of closed loop systems formed with feedback gain matrices K_{2G1} and K_{2G2} are examined. Both systems are released from an initial state perturbation of $[0.1\ 0.3\ 0.15]^T$ (in accordance with the original simulation of Example 5.4.1). The state and control responses produced by the two designs are shown in Figure 6.6.2.

Figure 6.6.2a shows that gain matrix K_{2G1} produces state responses which are *completely devoid of switching*. Control input u_1, however, experiences very low magnitude oscillation (see Figure 6.6.2b). The K_{2G1} system demands on control u_2 remain of roughly the same magnitude as the original design K_2.

In contrast, Figures 6.6.2a and 6.6.2c show that multirate feedback K_{2G2} provides relatively switched state and control performance. The higher $\|K\|_2$ figure of this design produces switching in states x_1, x_3 and control u_1. (This switching is however, of much lower magnitude than that experienced by the original perfectly decoupled multirate closed loop system of design K_2.)

This example demonstrates that the highly switched, large magnitude state and control behaviour experienced by the original K_2 design has been completely removed by modified design K_{2G1}. Thus the minimisation of $\|K\|_2$ by application of the gain modification method has, for this system, produced a practically implementable multirate design. However, the tabulated performance measures show that this improvement in intersample behaviour is obtained at the cost of increased sensitivity of the closed loop system.

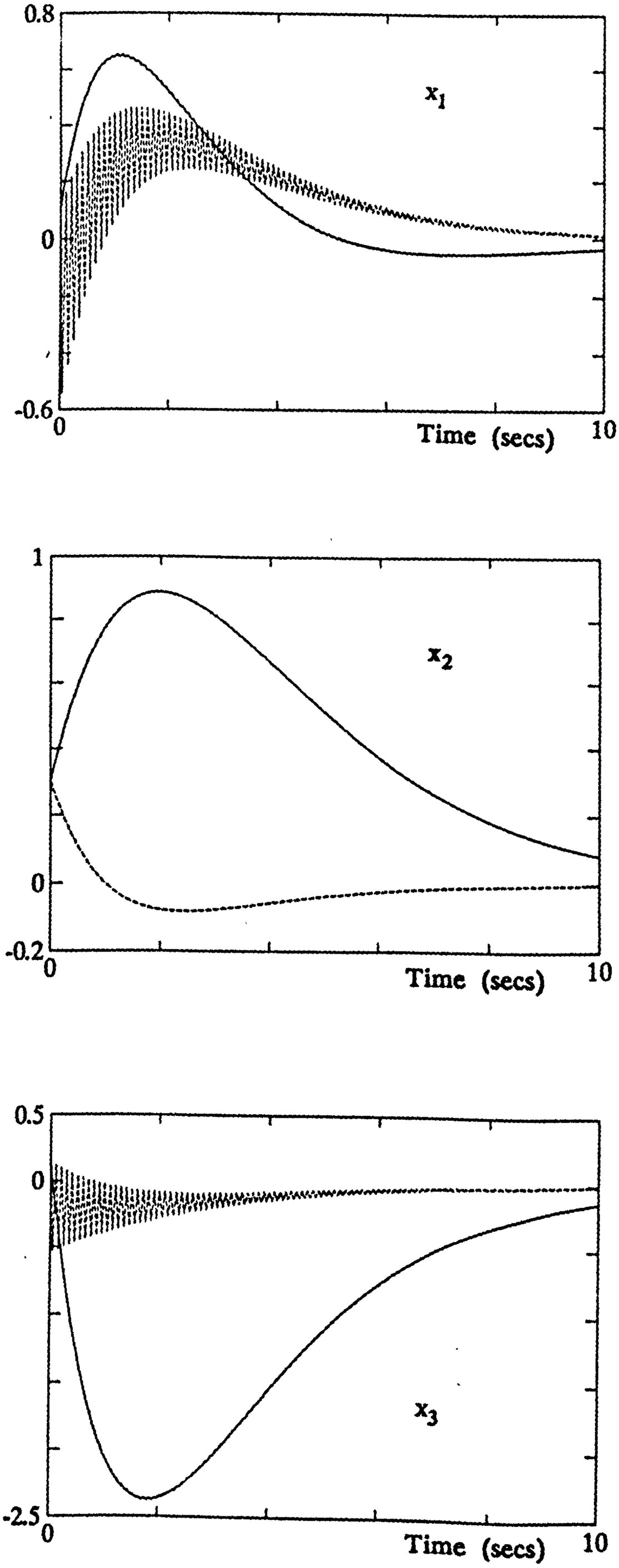

Figure 6.6.2a State responses of modified multirate feedback designs K_{2G1} and K_{2G2}.

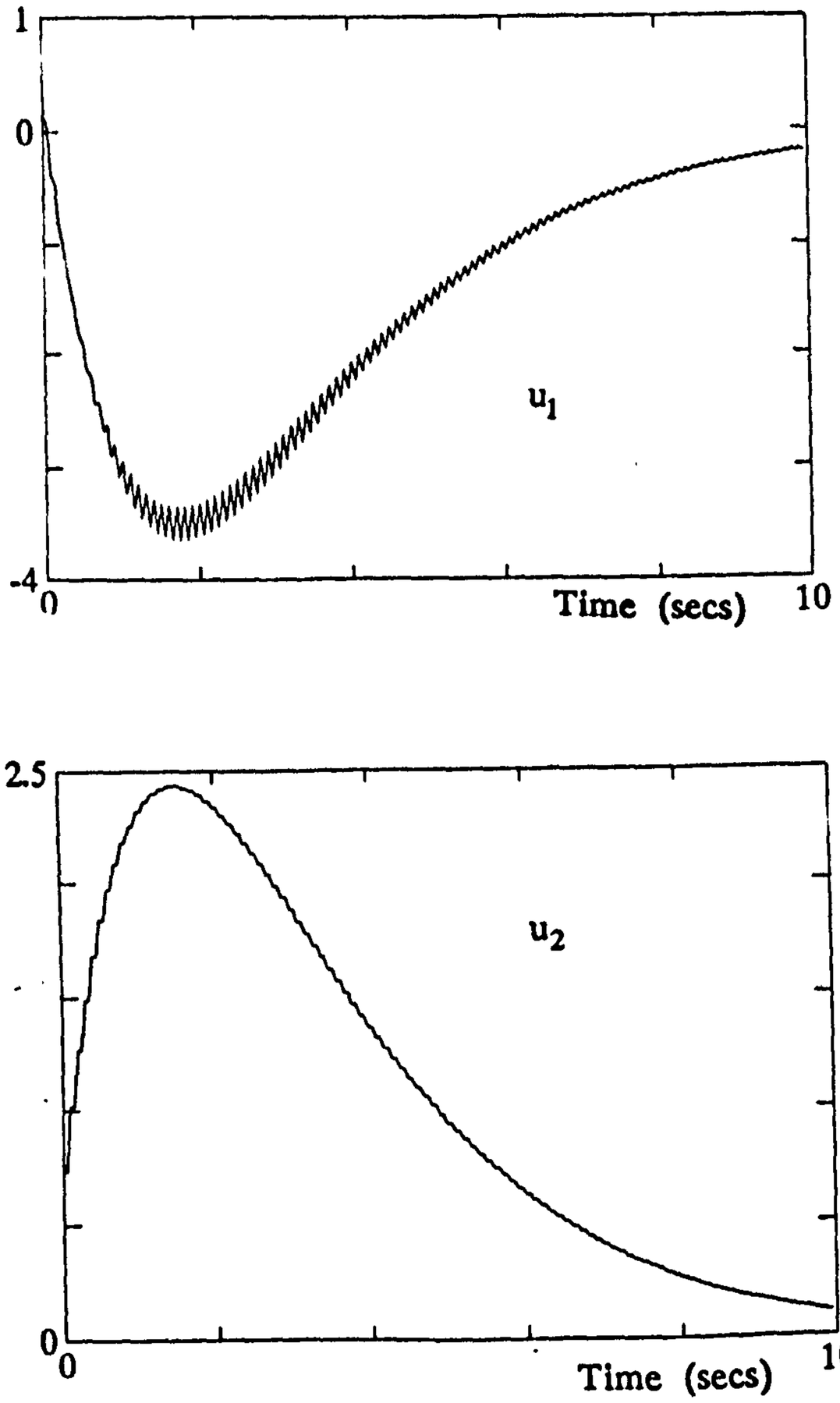

Figure 6.6.2b Control input responses of modified multirate feedback design K_{2G1}

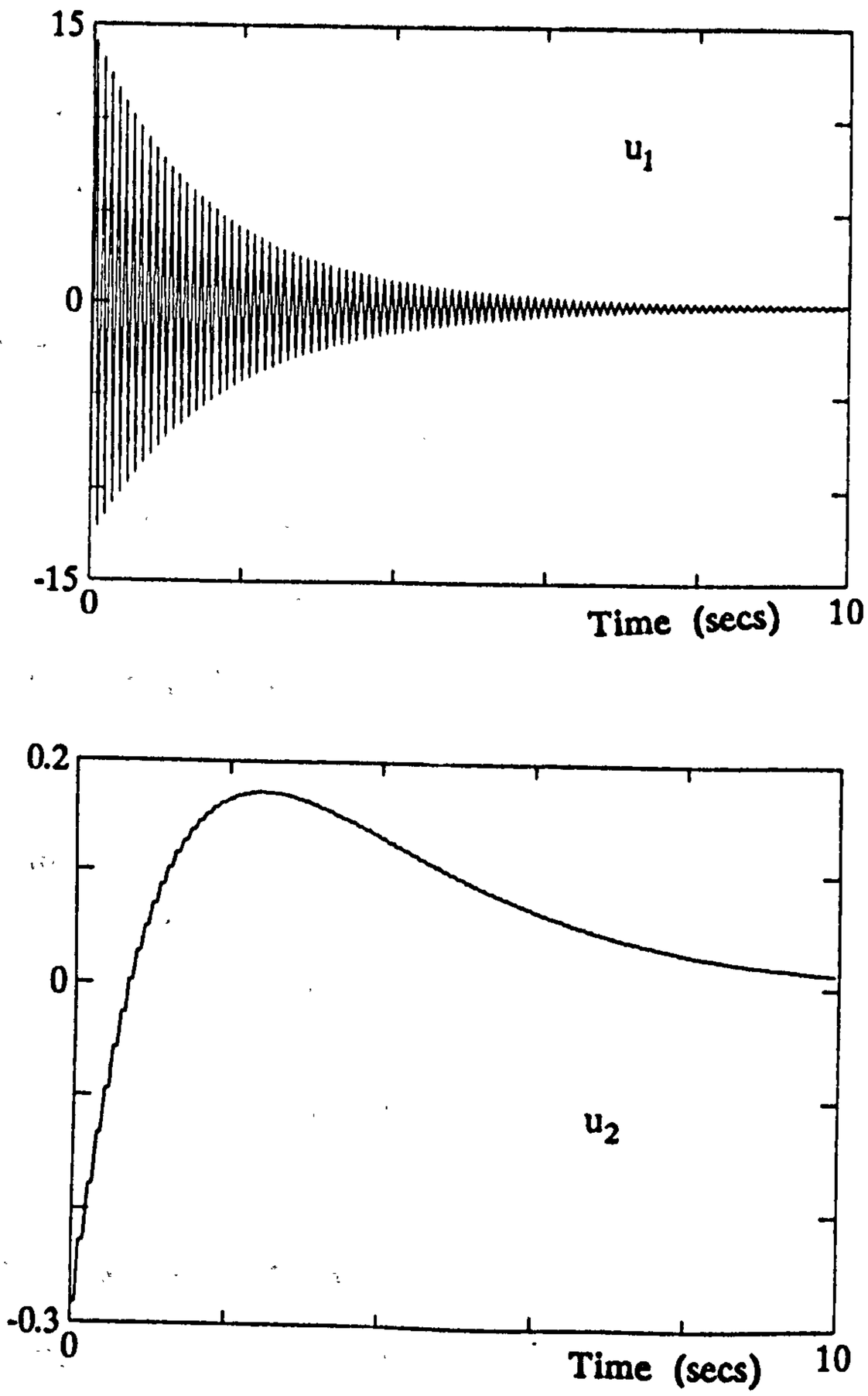

Figure 6.6.2c Control responses of modified multirate feedback design K_{2G2}

6.6.2 Example 6.6.2

This example applies the gain modification procedure to the multirate SAS design for the lateral aircraft subsystem of Example 5.4.3. The feedback gain matrix whose elements are to be minimised is K_6. Recall that the original K_6 design assigns the desired modal interaction but has a very high gain norm figure, $\|K_6\|=1427.73$ which renders it impractical (see Figure 5.4.6). For this design, the most switched and greatest control demand is experienced by the rudder input r (the largest rudder demand is $\approx$-14 degrees). The demanded aileron activity, though switched, is not of such high magnitude. Thus, a suitable choice of weighting matrix α for an optimised search for a feedback matrix with a lower $\|K\|_2$ figure is:

$$\alpha = \begin{bmatrix} 100 & 100 & 100 & 100 & 100 \\ 100 & 100 & 100 & 100 & 100 \\ 100 & 100 & 100 & 100 & 100 \\ 1 & 1 & 1 & 1 & 1 \\ 1 & 1 & 1 & 1 & 1 \end{bmatrix} \qquad (6.6.3)$$

The first three rows of matrix α are chosen to have larger elements than the last two rows to penalise the elements associated with r (u_1) greater than those of s (u_2). This will concentrate the design effort on minimising the control demanded from input r (rudder).

Several optimisation runs based on different choices of initial search step s_0 are executed. All obtained a rapid decrease in $\|K\|_2$ in the first 10 steps of the search procedure. Furthermore, unlike Example 6.6.1, for this system a large decrease in $\|K\|_2$ can be effected without a severe degradation in closed loop system insensitivity.

The design which yields the lowest $\|K\|_2$ figure is selected from the array of gain matrices produced by the set of optimised solutions. This is given below:

$$K_{6G1} = \begin{bmatrix} -0.0595 & 0.0168 & 0.4946 & -0.0620 & 0.0098 \\ 0.1660 & -0.0447 & -0.0079 & -0.2747 & 0.0868 \\ -0.0104 & -0.0034 & -0.2511 & 0.2860 & -0.0722 \\ 0.0355 & 0.3475 & -0.2196 & 1.2386 & 0.2642 \\ 0.0698 & -0.3851 & -1.2283 & -0.1962 & -0.2517 \end{bmatrix} \qquad (6.6.4)$$

The performance measures of modified design K_{6G1} are given in Table 11.

Time responses of the closed loop system produced by feedback gain matrix K_{6G1} are examined (these are obtained using linear simulations). The *main sample* responses of the lateral aircraft subsystem to an initial heading angle and sideslip velocity perturbation (of 0.02 radians and -0.8 ms^{-1} respectively) are shown in Figure 6.6.3. The main sample responses of the original K_6 design are also included. Figure 6.4.4 shows the *intersample responses* of designs K_{6G1} and K_6.

Performance Measure	Feedback Gain Matrix K_{6G1}
$\kappa_m(V)$	$\kappa_1(V) = 7.9213$ $\kappa_2(V) = 22.4263$ $\kappa_3(V) = 26.2921$ $\kappa(V) = 28.6271$
J_{D1}	4.6853
J_{D2}	9.4976
$\|K\|_2$	1.4346

Table 11 Performance measures of the K_{6G1} closed loop Machan aircraft lateral subsystem

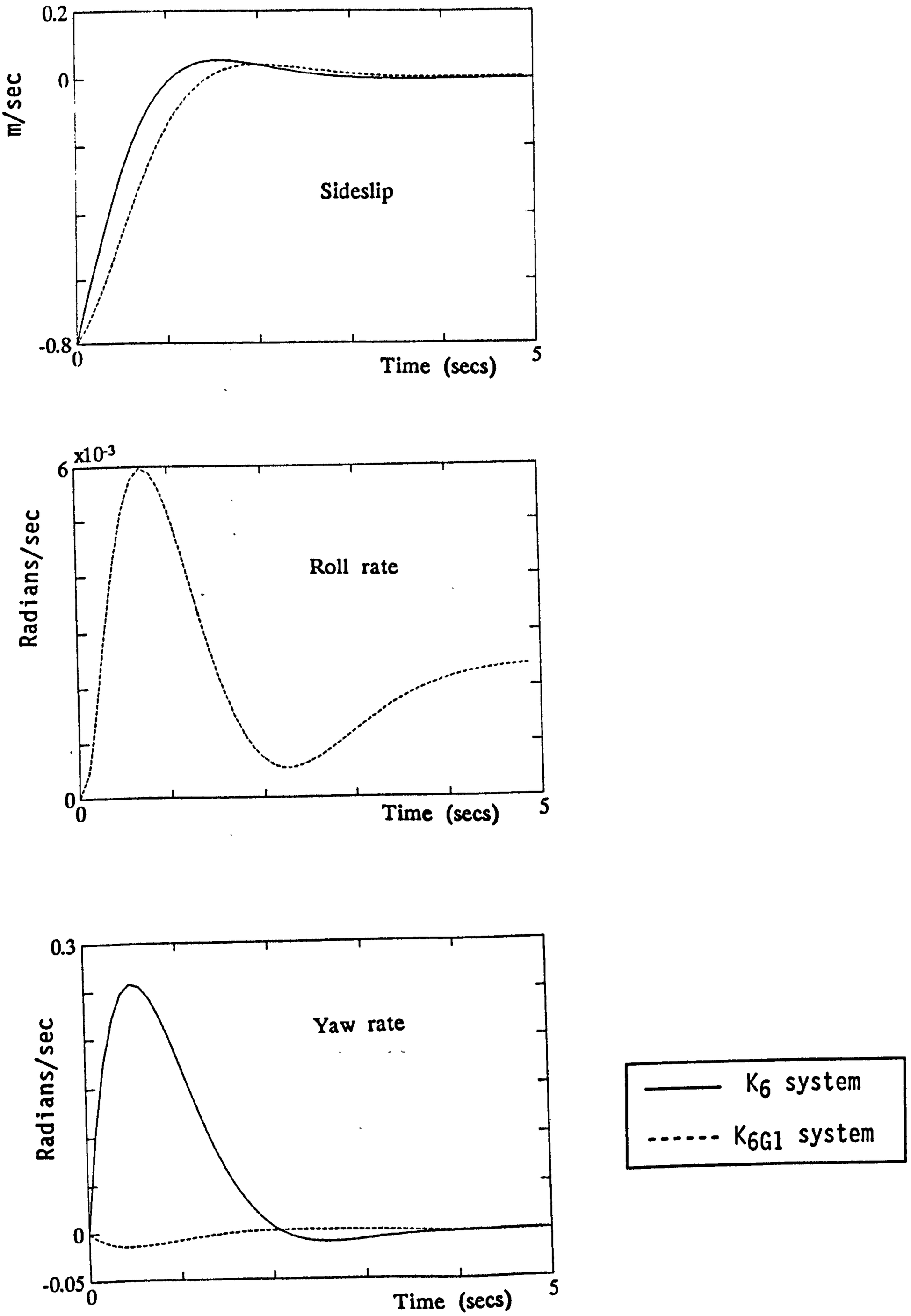

Figure 6.6.3a Main sample state responses of modified multirate feedback design K_{6G1} and original multirate design K_6

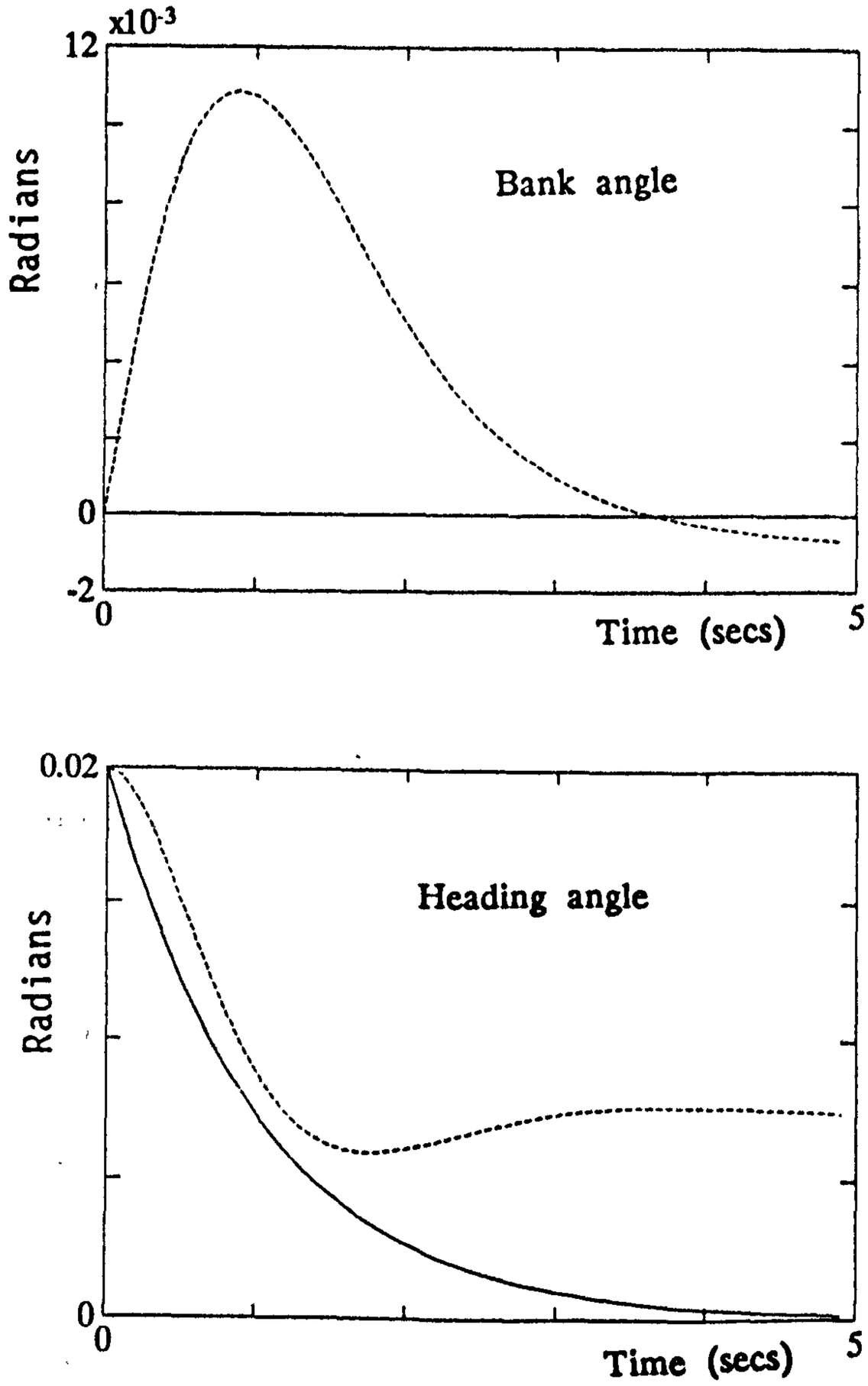

Figure 6.6.3a Main sample state responses of modified feedback design K_{6G1} and original multirate design K_6 (cont.)

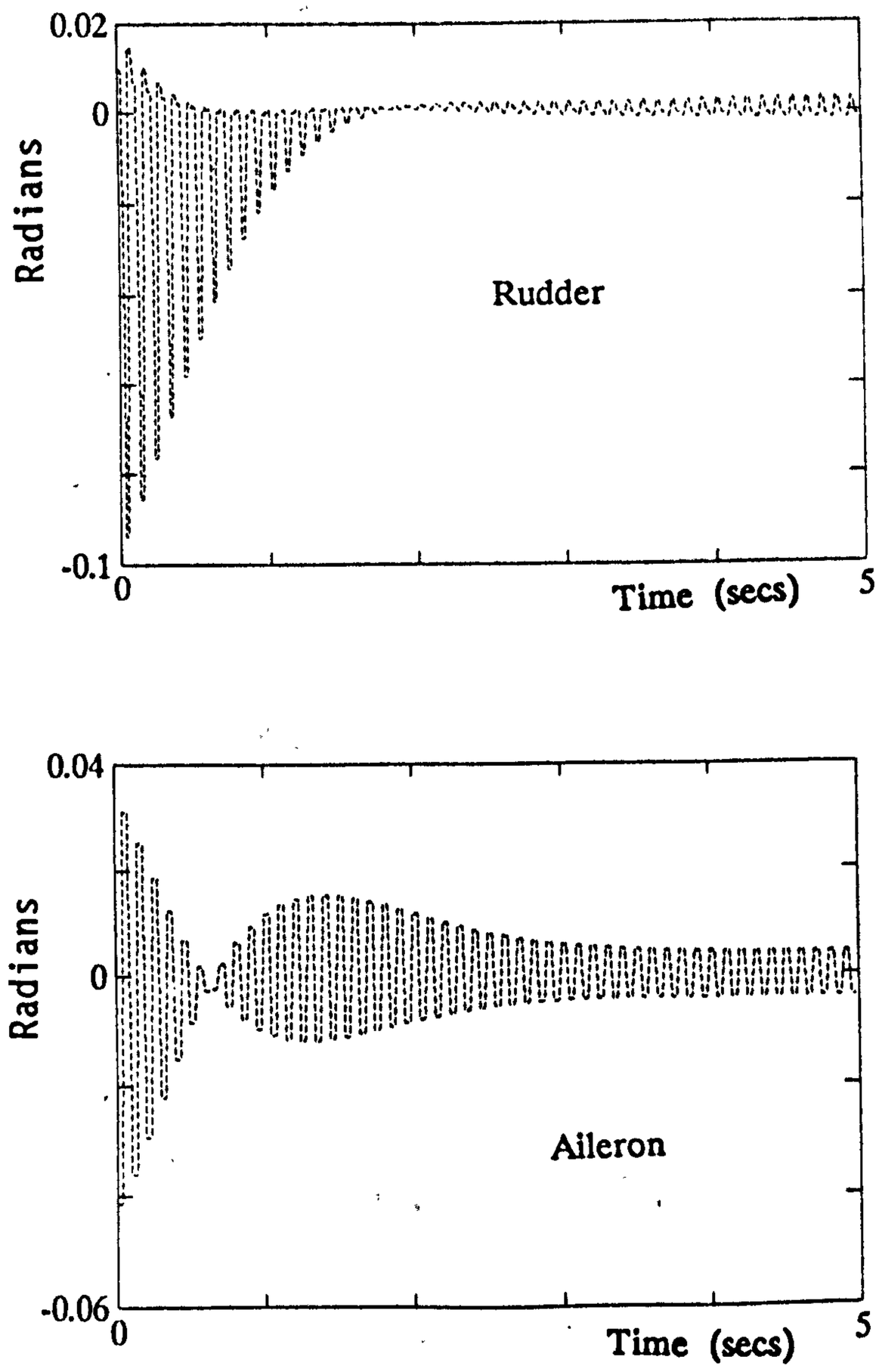

Figure 6.6.3b Control responses of modified multirate feedback design K_{6G1}

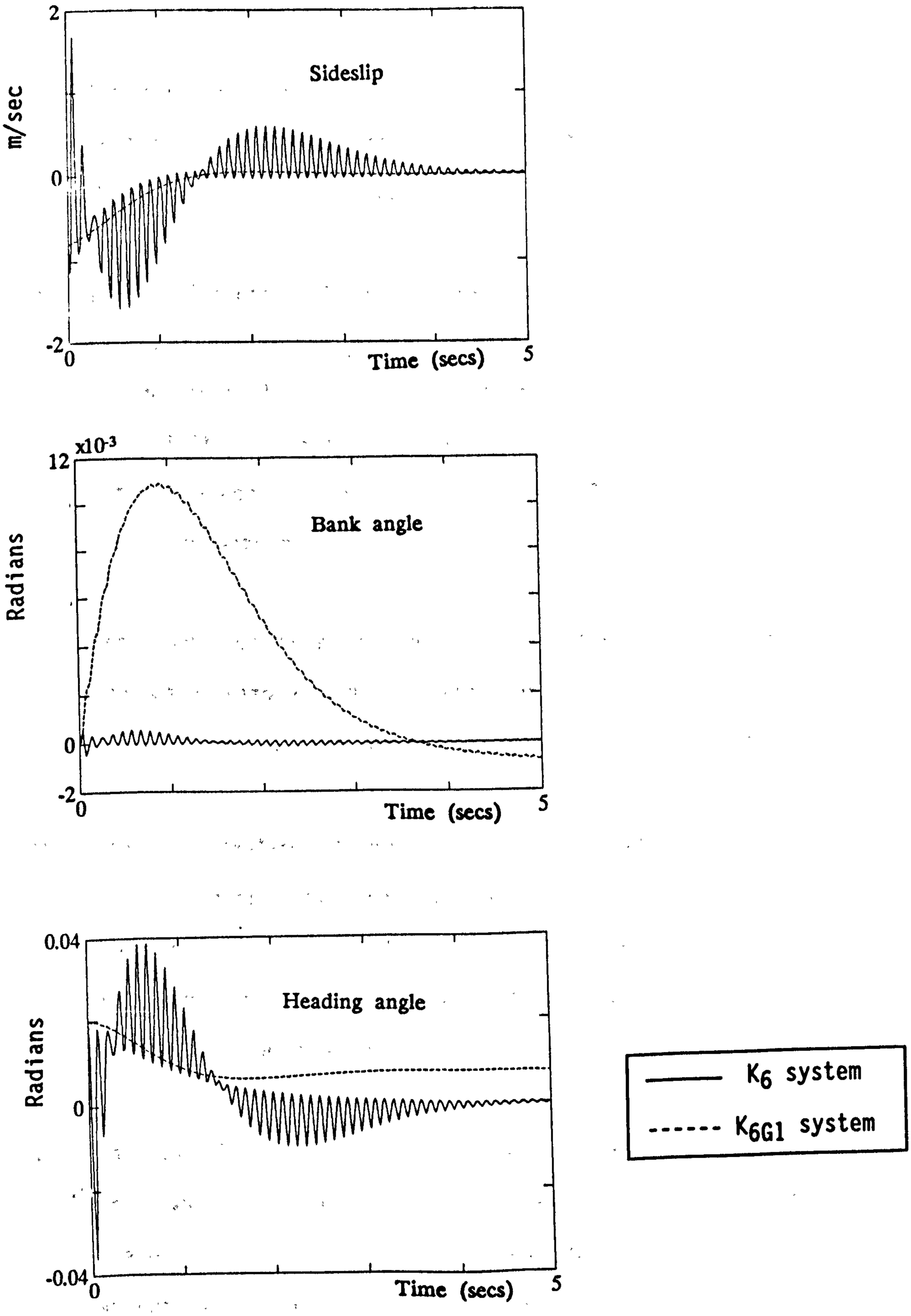

Figure 6.6.4 Intersample state responses of modified multirate feedback design K_{6G1} and original multirate design K_6

The following points are noted from the tabulated results and the time responses of Figures 6.6.3 and 6.6.4.

(i) The norm of feedback matrix K_{6G1} is approximately 0.1% of the original K_6 matrix norm (recall that $\|K_6\|_2 = 1427.73$ whilst $\|K_{6G1}\|_2 = 1.4346$). Clearly, this is a significant reduction.

(ii) The conditioning figures show that both main and intersample system sensitivity remain extremely low for design K_{6G1}. These figure predict a slight increase in modal interaction. These sensitivity figures are, nevertheless, extremely good for the lateral aircraft subsystem (Mudge and Patton, 1988; Smith, 1991; Sobel and Shapiro, 1987).

(iii) The predicted increased modal interaction of K_{6G1} is evident in the main sample time response of Figure 6.6.3a which show an increase in coupling between the yaw and roll motions.

(iv) The K_{6G1} system demands significantly lower rudder control than that demanded by the original design (compare response of Figures 5.4.6b and 6.4.3b). A reduction of at least 200% is achieved. Furthermore, slightly less aileron activity is demanded by the modified design.

(v) The K_{6G1} SAS experiences no switching whatsoever in the sideslip and yaw states and only very small oscillations in the roll states. In comparison, the original K_6 SAS produces a significant amount of high magnitude switching in all states. The sideslip and yaw states are under the control of the rudder surface. Thus, a reduction in rudder activity has effected the removal of switched behaviour in sideslip and yaw motions.

Though the modified design produces much lower control activity and acceptable main sample and intersample modal coupling the K_{6G1} design could not in practice be implemented. The magnitude of demanded control effort is acceptable but the fast switching of the rudder and aileron is undesirable and cannot in reality be supplied.

A final point regarding the influence of weighting matrix α on the design produced by the optimisation procedure is mentioned here. For the Stability Augmentation System example an indiscriminant choice of α (e.g. an α matrix with all '1' elements) gives a much poorer design (low $\|K\|_2$ figures) than the α matrix choice of (6.6.3). Thus, a judicious choice of α is important for the design of this system.

6.6.3 Example 6.6.3

This example minimises the elements of the multirate feedback matrix designed using the direct assignment in Example 6.3.1. Though the feedback matrix itself was not given in Example 6.3.1, recall that $\|K\|_2$ figure for this design was 203.9203. Since u_1 and u_2 are sampled at rates T and T/2 respectively the α weighting matrix is chosen to be:

$$\alpha = \begin{bmatrix} 1 & 1 & 1 \\ 100 & 100 & 100 \\ 100 & 100 & 100 \end{bmatrix} \qquad (6.6.5)$$

Applying the gain modification procedure with the above weighting matrix determines the feedback matrix with the lowest $\|K\|_2$ figure to be:

$$K_G = \begin{bmatrix} -6.1747 & 2.6201 & -10.1617 \\ -5.1486 & -6.3488 & 2.3540 \\ -4.0273 & -4.6846 & 0.1555 \end{bmatrix} \qquad (6.6.6)$$

The performance measures of the corresponding closed loop multirate system are presented in Table 12.

Performance Measure	Feedback Gain Matrix K_G
$\kappa_m(V)$	$\kappa_1(V) = 11.2335$ $\kappa_2(V) = 10.7254$
$\|\|K\|\|_2$	12.2335

Table 12 Performance measures of K_G closed loop system

The tabulated results show that the multirate gain matrix produced by the constrained assignment method has a significantly lower norm than the original feedback matrix ($\|\|K\|\|_2$ has been reduced from 203.9203 to 12.2335). The modal decoupling provided by feedback K_G also remains very good. The responses of closed loop systems formed by the original (perfect decoupling) design and the gain modified design K_G to an initial state perturabation of [0.2 0.3 0.4]' are shown in Figure 6.6.5.

A comparison of these results show that the high magnitude, switched x_2, u_2 response produced by the original design are *completely* removed by feedback matrix K_G. The cost of this removal is the increased modal interaction.

6.7 MULTI-OBJECTIVE EIGENSTRUCTURE ASSIGNMENT

This section applies the multi-objective eigenstructure assignment method of Burrows (1990c) to address the problems encountered with MIFO

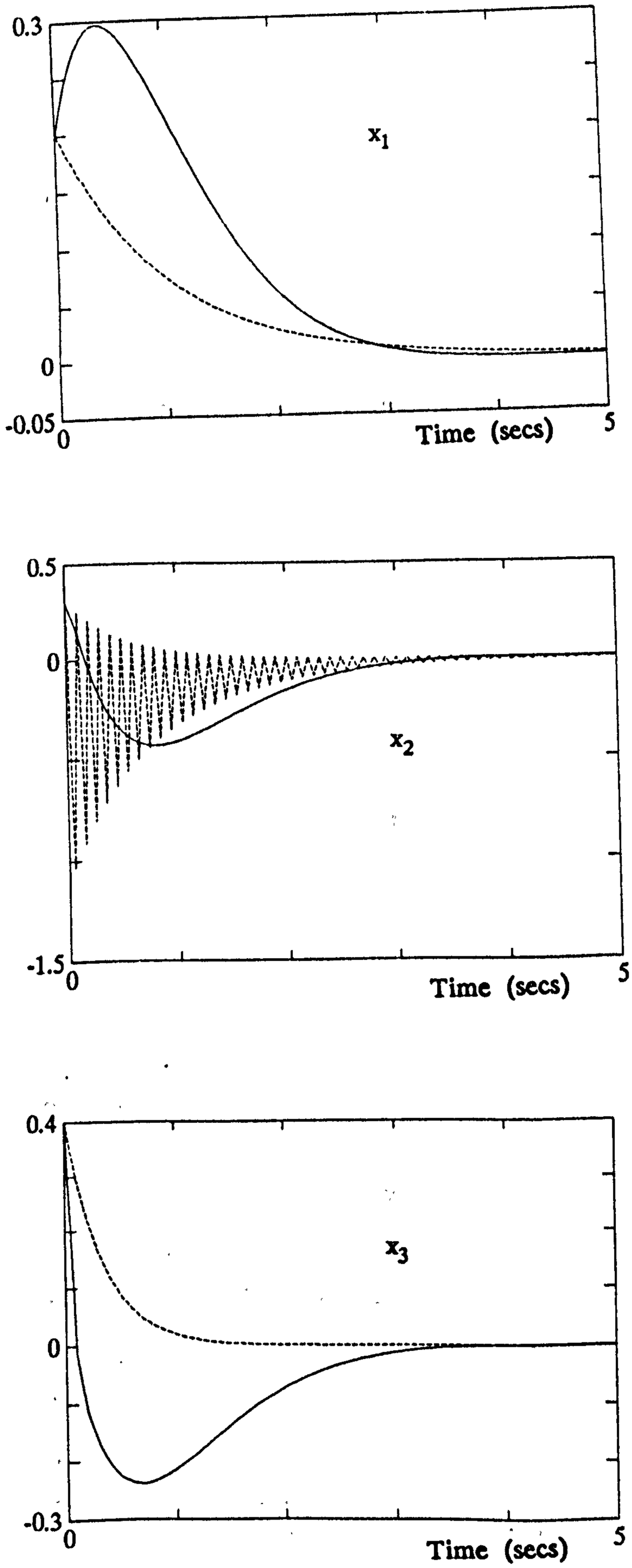

Figure 6.6.5a State responses of modified multirate feedback design K_G and original (perfectly decoupling) multirate design

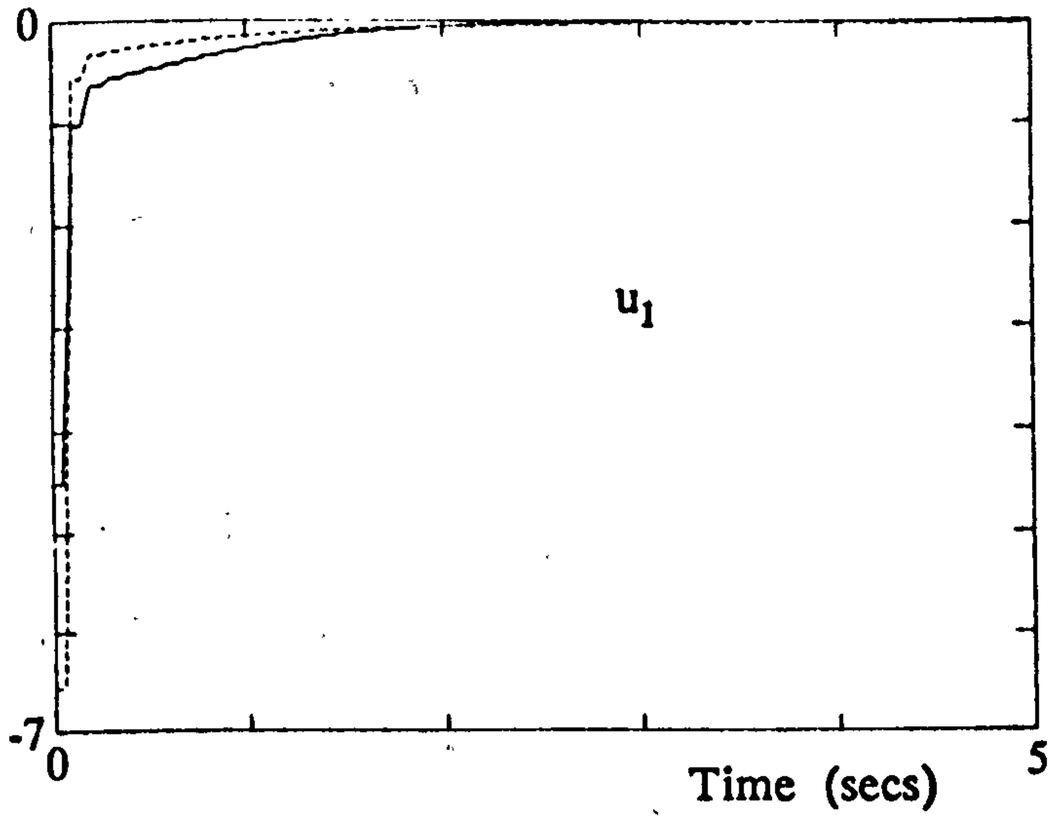

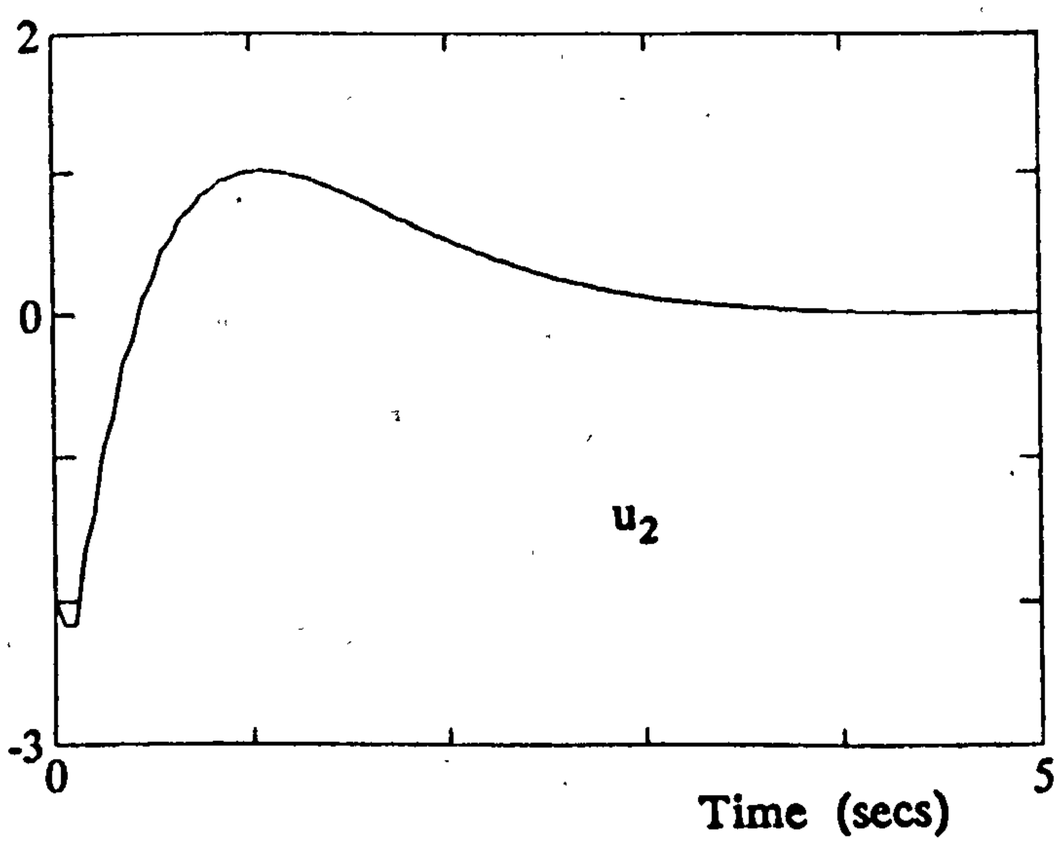

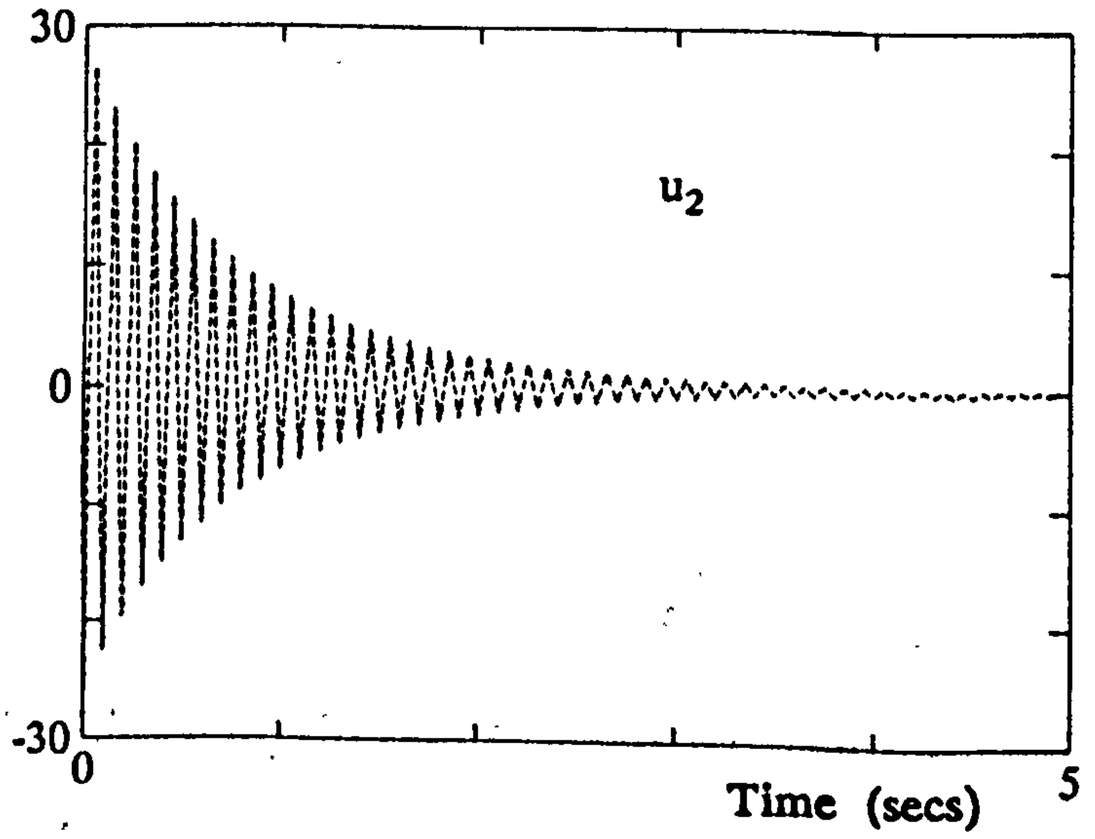

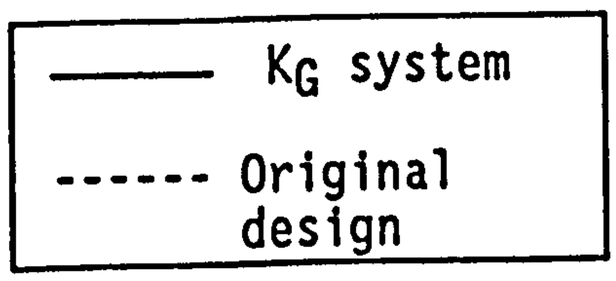

Figure 6.6.5b Control inputs of modified multirate feedback design K_G and original (perfectly decoupling) multirate design

sampled state feedback design. The development of this technique is documented in the D.Phil dissertation of Burrows (1990c) and will not be repeated in detail in this section. An outline of the design method is provided for the purposes of this demonstration.

An important feature of this design method is that, unlike all previous eigenstructure assignment techniques detailed in this thesis, the desired closed loop eigenvalues do not have to be a fixed set. The eigenvalues are allowed to be varied (within user-specified bounds) to generate alternative admissible spaces from which the desired set of eigenvectors are selected. Clearly, some *a priori* knowledge of the allowable variation in the closed loop eigenvalues is required for the application of this technique.

It has been established that the desirable properties of a multirate control law require small elements in the feedback gain matrix (i.e. low $\|K\|_2$ and low J_G) and the accurate assignment of desired right eigenvectors (i.e. low J_M). The results of previous examples show that the two design objectives represented by J_G and J_M (defined in Section 6.4) are *in competition*; a gain matrix of low norm will not, in general, assign a desirable set of eigenvectors which reduce modal interaction *and vice versa*. This conflict can be addressed by formulating the eigenproblem as an optimisation task which minimises an overall scalar cost function comprising the two individual measures:

$$J = J_G + J_M \qquad (6.7.1)$$

The minimisation of cost function J will then produce a control law with the desired balance of each closed loop multirate system quality. The contribution of each design objective to the optimisation criteria is controlled by the weighting elements α and β of J_G and J_M. Provided J is small, control laws which adequately satisfy both reduced modal interaction and low control effort are produced.

The multiple objective eigenstructure assignment method of Burrows (1990) minimises cost function J using analytically-derived gradients along with the Davidon-Fletcher-Powell numerical optimisation technique (Gill et al, 1981; Walsh, 1975). The assignment of eigenvalues from *regions* of the complex plane is yet another way of generating different admissible subspaces (from which the right eigenvectors are selected). When this flexibility in defining the design subspace is combined with the ability of the MIFO sampled systems to increase the actual dimension of the subspace itself, an abundant amount of design freedom is made available. The effect of this extra design freedom is a very accurate assignment of the desired eigenstructure. Furthermore, this accuracy is achieved with considerably less time and design effort being demanded for the optimisation procedure than that required for the corresponding single rate or continuous-time problem. This is because for the single rate and continuous-time cases, the achievement of a suitable solution depends heavily on the selection of an optimal set of closed loop eigenvalues. This influence of the eigenvalues on the optimised solution to the MIFO eigenproblem is compensated for by the extra dimension of the admissible subspace.

6.8 APPLICATION OF MULTIPLE OBJECTIVE EIGENSTRUCTURE ASSIGNMENT

The aircraft example of previous sections is (again) repeated. Using the multiple objective optimised eigenstructure assignment procedure two control laws are designed. Both attempt to minimise the modal interactions of the closed loop system and reduce the size of the gain matrix. They differ in the emphasis placed on each. The first has a main emphasis on reducing the norm of the gain matrix. The second on achieving the desired modal structure. The gain matrices are denoted K_{NORM}, K_{MODAL}, respectively, and are given below.

$$K_{NORM} = \begin{bmatrix} -0.0064 & 0.0226 & -0.0078 & -0.0485 & -0.0041 \\ 0.0051 & 0.0294 & -0.0065 & -0.0500 & -0.0080 \\ 0.0187 & 0.0366 & -0.0041 & -0.0501 & -0.0052 \\ -0.0636 & -0.0236 & 0.0089 & 0.0413 & -0.0016 \\ -0.0834 & -0.0285 & 0.0093 & 0.0484 & -0.0005 \end{bmatrix} \qquad (6.8.1)$$

$$K_{MODAL} = \begin{bmatrix} 0.0373 & 0.2553 & 0.1615 & -0.0443 & 0.0017 \\ 0.0285 & 0.0046 & 0.1437 & 0.0059 & 0.0113 \\ 0.0190 & -0.2508 & 0.1240 & 0.0567 & 0.0208 \\ -0.0032 & 0.0098 & 0.1356 & 0.1483 & 0.0224 \\ -0.0020 & -0.1582 & 0.1158 & 0.2113 & 0.0332 \end{bmatrix} \qquad (6.8.2)$$

The performance measures of the closed loop systems formed by K_{NORM} and K_{MODAL} are displayed in Table 13.

Performance Measure	Feedback Gain Matrix	
	K_{NORM}	K_{MODAL}
$\kappa_m(V)$	$\kappa_1(V)$= 15.8711 $\kappa_2(V)$=18.8311 $\kappa_3(V)$=21.8778 $\kappa_4(V)$=59.0667	$\kappa_1(V)$=154.3092 $\kappa_2(V)$=124.9601 $\kappa_3(V)$=82.7186 $\kappa_4(V)$=28.6046
$\|K\|_2$	0.1508	0.4184

Table 13 Performance measures of K_{NORM} and K_{MODAL} closed loop Machan aircraft lateral subsystems

The tabulated results show that the different emphasis placed on the two design objectives has been achieved by designs K_{NORM} and K_{MODAL}. From these results it is clear that, theoretically, control matrix K_{MODAL} has superior robustness properties than feedback control K_{NORM}; Comparing the right eigenvectors produced by each design, K_{MODAL} is seen to

achieve the required decoupling far more closely than K_{NORM}. This is to be expected from the emphasis of K_{MODAL} on accurate modal assignment. However, gain matrix K_{NORM} has a far lower norm figure than K_{MODAL}.

The trade-off between the reduction of control effort and the decoupling of modes is examined using a fully non-linear simulation of the aircraft. This is a severe test for the MIFO multirate controllers.

The performance of both gain matrices in correcting an initial perturbation of 0.02 radians in heading angle are shown in Figure 6.8.1. The responses clearly demonstrate the difference in emphasis placed on the two control laws. Control law K_{MODAL} produces modal interactions which enhance the performance of the aircraft lateral subsystem and, correspondingly, alleviates the overall control task required to achieve the desired closed loop responses. This serves to reduce the control effort demanded by the aircraft system far more effectively than a direct minimisation of the gain matrix norm, as for control law K_{NORM}.

The effect of the modal structure of both control laws on the aircraft response can be assessed by the degree of yaw, roll and sideslip motions induced by the initial perturbations in heading angle. The handling qualities requirement for the roll mode to be decoupled from both yaw and sideslip velocity is achieved by feedback design K_{MODAL} with far more success than design K_{NORM}.

Figure 6.8.1 shows that the K_{MODAL} design induces significantly less Dutch roll than the K_{NORM} design. This is apparent from the smooth recovery of sideslip, roll and yaw motion from the initial heading angle perturbation produced by controller K_{MODAL}. In contrast, roll and sideslip motions of the K_{NORM} controlled system are both seen to react quite significantly to the initial perturbation. For this manoeuvre, the accomodating aircraft modal structure of feedback design K_{MODAL} also effects a significant saving in aileron control activity. It demands less than 2% of the control effort required by design K_{NORM}.

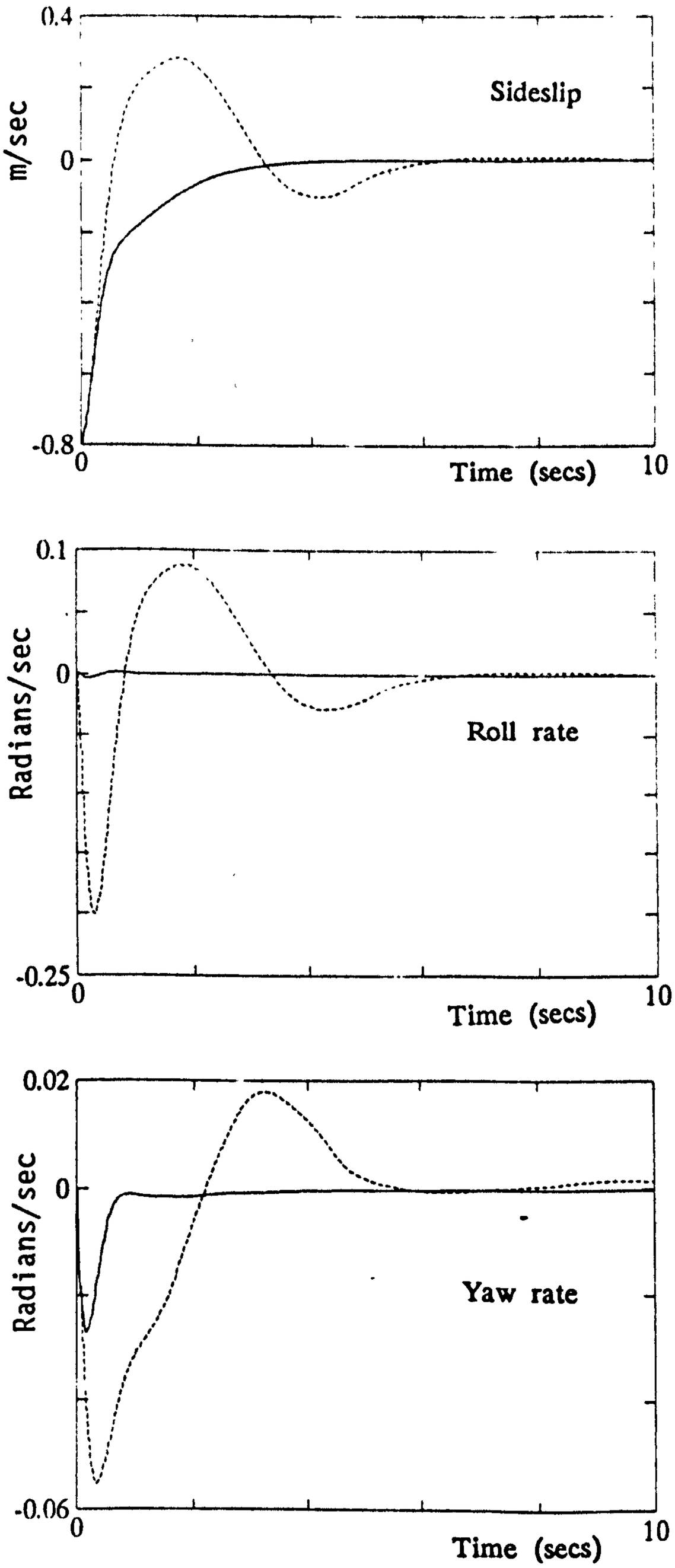

Figure 6.8.1a State responses of multirate feedback designs K_{NORM} and K_{MODAL}

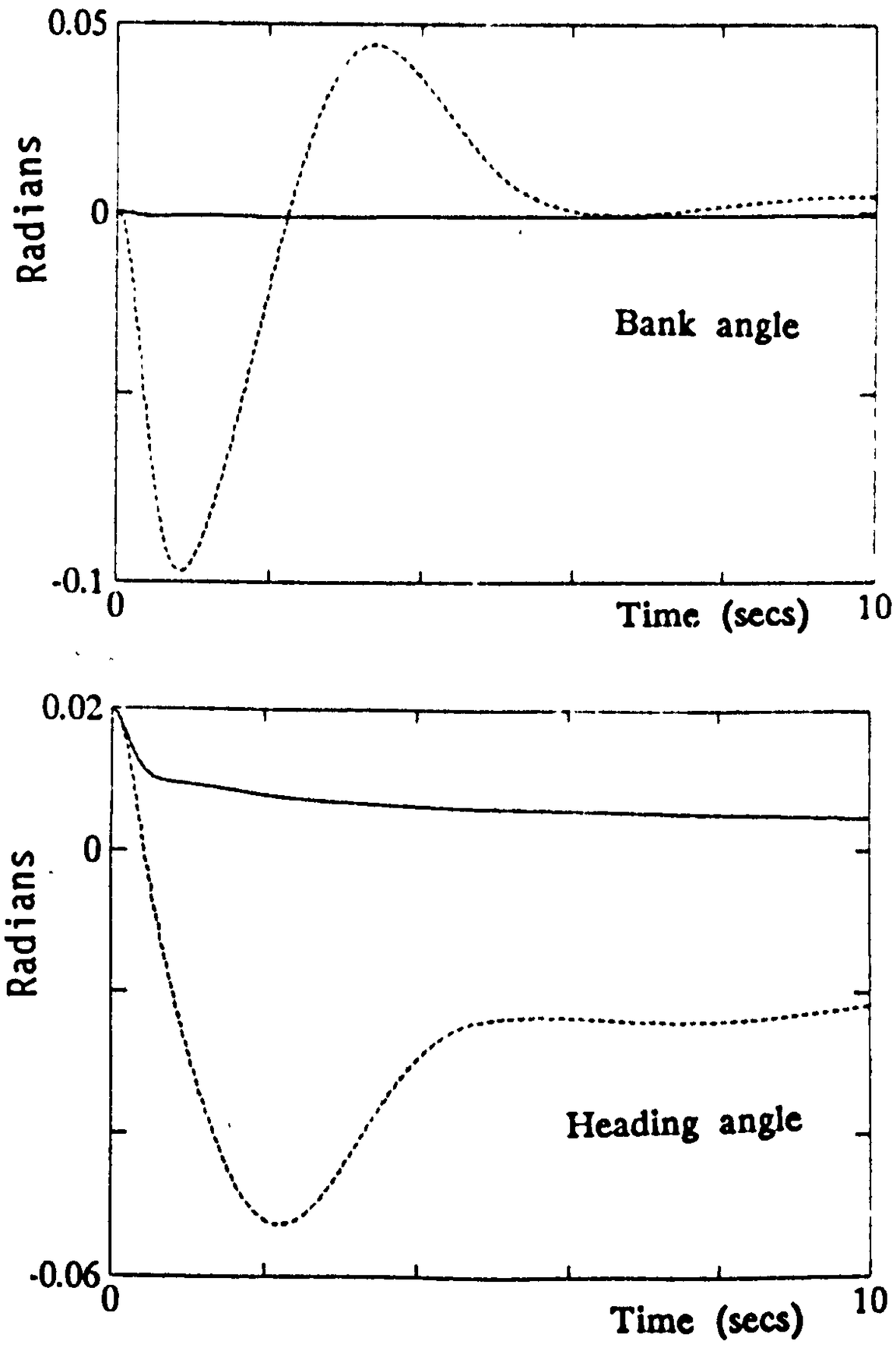

——— K_{MODAL} lateral SAS

------ K_{NORM} lateral SAS

Figure 6.8.1a State responses of multirate feedback designs K_{NORM} and K_{MODAL} (cont.)

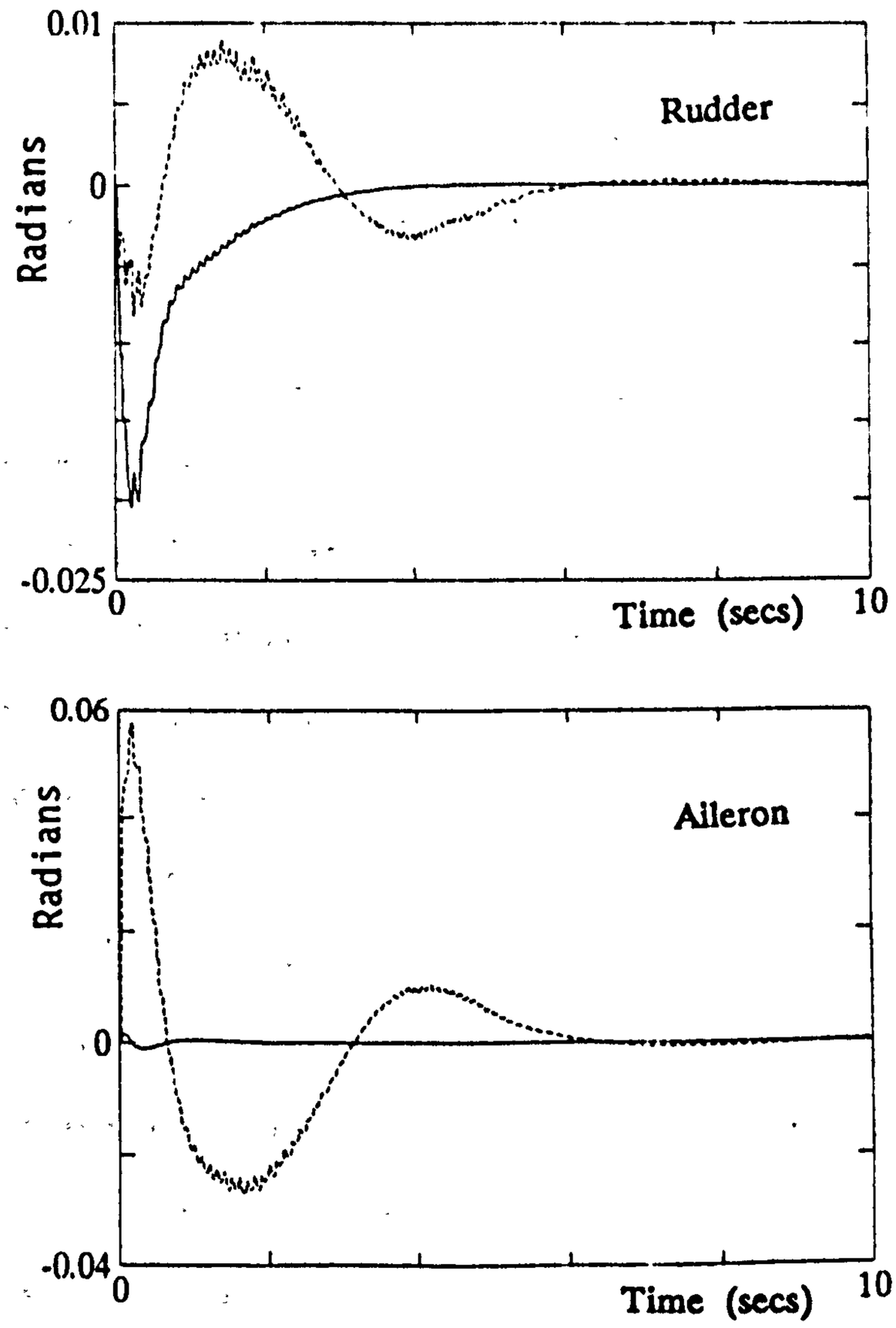

——— K_{MODAL} lateral SAS

------ K_{NORM} lateral SAS

Figure 6.8.1b Control input responses of multirate feedback designs K_{NORM} and K_{MODAL}

The performance of K_{NORM} and K_{MODAL} in correcting the heading angle perturbation demonstrate the improved decoupling (and hence improved insensitivity properties) of the latter design. The responses confirm the results of Table 13 and demonstrate the effectiveness of the optimised eigenstructure assignment method in fulfilling the conflicting design objectives of the multirate pole placement problem. Furthermore, the responses clearly show the impact of the closed loop modal structure on aircraft performance during co-ordinated manoeuvres.

Two solutions to the multirate feedback control of an aircraft lateral subsystem have been detailed. Both address the problems experienced by MIFO feedback systems but differ in the emphasis that is placed on the minimisation of each individual objective. The design perspective considered includes the specification of the *degree* of trade-off between the two system performance characteristics through the use of the weighting elements associated with each quality. This has been shown to provide an accurate means of compromise between control input minimisation and the assignment of a particular set of closed-loop eigenvectors. The performance of the two control laws has been clearly demonstrated by non-linear simulation studies.

6.9 SUMMARY

This chapter has presented three eigenstructure assignment techniques to provide solutions which alleviate the two main problems associated with a MIFO feedback control system; high magnitude, switched control effort and adverse intersample effects. (Note that the minimisation of the control effort required both the damping of oscillations and a reduction in magnitude of the control inputs.) The solutions provided by all three techniques were shown to address the MIFO system problems with varying degrees of success. All have

adequately circumvented the problems described above but differ in the complexity and flexibility in the application of the design techniques. Furthermore, all the design examples have demonstrated that a trade-off between the minimisation of control switching and the assignment of a particular set of closed-loop eigenvectors exists. Thus, the objective of all three techniques is to provide a MIFO eigenproblem solution which achieves an acceptable balance of these two desired qualities.

This design task is not straightforward since an *a priori* specification of the two performance qualities requires some heuristic judgement. A given MIFO system will possess performance trade-offs which are determined by its open loop system structure, main sample rate, input multiplicities and its desired closed loop specification. Thus, it is not possible to recommend a design emphasis on any one single qualitiy to guarantee a satisfactory solution to the MIFO state feedback eigenproblem.

Section 6.2 presented the first technique: a constrained eigenstructure assignment method. This approach requires a constraint to be included in the formulation of the direct eigenstrucucture assignment problem to ensure that the gain matrix elements remains low. An appropriate constraint was provided by incorporating the corresponding single rate discrete design into the pencil equivalence relations of Chapter 3.

The application of this technique was demonstrated by two design examples in Section 6.3. The first example is based on a two input, three state system whilst the second example is a repeat of the Stability Augmentation System design for the aircraft lateral subsystem of Example 5.4.3. For the first example, the constrained design was shown to remove *completely* the oscillations experienced by the original design. However, the total removal of switched behaviour was not obtained for the second example (the aircraft lateral subsystem), despite a significant 99.62% reduction in the norm of the constrained

gain matrix.

The non-iterative solution of the constrained eigenstructure assignment problem does not facilitate the specification of the *degree* of trade-off between the two desired system qualities. However, it will allow the reduction of specific elements in the gain matrix to be emphasised by a judicious choice of the constraint matrix.

The two remaining techniques of this chapter both allow a means of allocating different design emphasis on the achievement of the two desired system qualities. Both use optimisation methods for the solution of the MIFO eigenproblem. Four new MIFO system performance measure are introduced in Section 6.4. The additional measures can either be used to monitor the balance of desired qualities in the final solution or be incorporated into an optimisation cost function.

Section 6.5 describes the gain modification procedure of Owens and Mielke (1982). This technique performs a gradient based line search around an initial eigenstructure assignment to minimise the elements of the feedback gain matrix whilst maintaining the modal properties achieved by the intial design. A weighting matrix is used in the calculation of the direction of search to influence the amount by which each individual element of the gain matrix is minimised. Owens and Mielke recommended a single search local to the initial assignment to provide a solution which preserves the original modal assignment. The extra design freedom available for the solution of the MIFO eigenproblem allows a number of line searches of *any* step size to be conducted. A procedure to automate this line search, based on a successive bisection of the size of step taken in a given direction is outlined in Section 6.5.

Two examples in Section 6.6 demonstrate the application of the gain modification procedure. The design task of both examples was to reduce the elements of the feedback gain matrices produced by design Examples 5.4.1 and 5.4.3 (the lateral aircraft sub-system). A

significant minimisation in the norm of the original feedback designs of both examples was produced. An examination of the results produced by the first design example (using the additional measures of Section 6.4) showed clearly the performance trade-offs involved in the design of MIFO feedback control. The time responses of two particular designs (each with a different balance of the two desired qualities) selected from the optimisation runs of this design example were compared to demonstrate this trade-off.

The application of the gain modification procedure to minimise the gain elements in the lateral aircraft Stability Augmentation System produced a significant 99.9% reduction in $\|K\|_2$. The linear time response produced by the low norm Stability Augmentation System design was shown to eliminate all switched behaviour in the sideslip and yaw states and remove almost all switching from the roll states. However, this reduction was not enough to remove the oscillations experienced by the control inputs *completely* and thus is still unacceptable. An unstable response from a non-linear simulation of the aircraft demonstates the infeasibility of implementing this low norm SAS design in a realistic situation.

Section 6.7 outlines the multiple objective eigenstructure assignment method of Burrows, (1990). This technique is based on a parameterisation of the state feedback eigenproblem in terms of the assignability of a desired eigenstructure and the minimisation of the gain matrix norm. The solution of the multiple objective eigenstructure assignment requires the minimisation of a *scalar* cost function which measures both the control effort required for implementing a particular control law and the modal interactions of the closed-loop system. (As clearly indicated in Section 6.1, the multiple objective optimisation methods described and referred to in this Chapter are not to be confused with multi-objective optimisation techniques based on *vector* objective functions.) Weighting factors control the contribution of each of these

properties to the overall value of the cost function. (The individual components of the cost function are defined in Section 6.4.) The objective function is then minimised using analytically derived gradients and the Davidson-Fletcher-Powell optimisation algorithm. In this way, the feedback control design can be tailored to address the specific needs of the MIFO sampled system.

The design approach of the multi-objective eigenstructure assignment method is very different in one aspect; it does not require a strict *a priori* set of desired closed loop poles. Instead, a desired *region* within which the closed loop poles may reside is specified. The optimised solution locates pole positions within the specified region such that an acceptable balance of the desired design qualities is obtained easily. The variation in pole positions is one method of generating (different) admissible subspaces from which the admissible eigenvectors are to be selected.

Section 6.8 applies the multi-objective eigenstructure assignment method to design two Stability Augmentation System feedback control laws for the aircraft lateral subsystem. The two control laws differ in the emphasis placed on the two components of the design objective function thus providing a means of comparing the trade-off between the reduction of control effort and the decoupling of modes. The modal decoupling and the effect of the different weighting on the objective function components was examined using a fully non-linear simulation of the aircraft. This was a severe test for the MIFO multirate controllers. Both control laws produced stable and smooth, unswitched time responses thus demonstrating the practical applicability of the outlined design method.

The ability of the multi-objective eigenstructure assignment method to produce an acceptable solution for the Stability Augmentation System can be attributed largely to the variation in eigenvalue positions allowed by this technique.

CHAPTER SEVEN

DEADBEAT CONTROL USING MIFO SAMPLED FEEDBACK

7.1 INTRODUCTION

This chapter examines the use of MIFO state feedback for deadbeat regulation and tracking control. A discrete system is said to exhibit deadbeat behaviour if the error between some reference signal and its output goes to zero in a finite number of steps and remains there for all subsequent sample periods. Deadbeat controllers of this class are used for minimum-time regulation and tracking in linear multivariable systems. Many deadbeat design methods have been proposed for systems sampled at a single uniform rate (Emami-Naeini and Franklin, 1982; Jordan and Korn, 1980; Kimura and Tanaka, 1981; Kucera and Sebek, 1984; Leden, 1977; Minamide, 1984; O'Reilly, 1981; Sebakhy and Abdel-Monem, 1980) but the application of deadbeat control to multivariable multirate systems remains an open topic.

Multirate sampling is ideally suited to the implementation of this type of control due to its inherent deadbeat type structure imposed by the multirate controllability conditions (see Chapter 3). It is not surprising then that from the few multirate design techniques contributed by researchers, many fall into the category of deadbeat tracking and regulation (Albertos, 1990; Eckardt, 1989; Felui et al, 1990; Kono and Suzuki, 1991; Saadane and Richard, 1991). A limitation of all the methods proposed in these references is that they can only be applied to SISO multirate systems. Albertos (1990) describes a relatively simple but neat method based on the direct combination of past ouputs and desired outputs. The work of Eckardt (1989) and Felui et

al (1990) is based on a classical synthesis type of approach to design a deadbeat series compensator (i.e. the controller is placed in the forward path). There are two limitations of the Eckardt method. The first is that the design algorithm cannot be applied to systems with finite transmission zeros. The zeros cause very high overshoots and an oscillatory transient response which takes considerable time and control effort to settle. The second limitation is that it requires a judicious choice of desired closed loop poles.

The technique of Felui et al (1990) is based on a single rate feedback and multirate series compensator type of control structure. This technique again requires a judicious choice of desired closed loop poles and also demands some trial and error for the final choice of input sample rate multiplicities. The design algorithms of Kono and Suzuki (1991) and Saadane and Richard (1991) apply to the general periodic system (using the monodromy system matrix derived using Floquet theory).

The preceding chapters have emphasised that multirate control structures possess more design freedom for the design of state feedback (characterised by (A,B) invariance properties) than single rate systems. This chapter extends the single rate deadbeat feedback design algorithm of Marrari et al (1989) to the multirate case and applies the multirate design freedom to improve closed loop system insensitivity properties (Patel and Patton, 1991b). The algorithm is easy to apply since it disposes system poles at the origin to prescribe deadbeat regulation and thus requires no a priori knowledge of suitable closed loop poles (as for the compensator synthesis approach). Ill-conditioned solutions generally result from assigning multiple roots (see Section 4.4) as with deadbeat controllers which place as many poles as possible at the origin to drive every state to zero in the minimum number of time steps. For a given MIFO system, the maximum (A,B) invariant subspace that lies in the kernel (nullspace) of C can be usefully applied to improve the

conditioning of the closed loop solution when all zero poles are assigned. Alternatively, this design freedom can be used to drive a subset of the system state to its final settling point *faster* than is otherwise possible, by placing *all* the system poles at the origin.

The MIFO state feedback matrix designed using the extension of the method of Marrari et al ensures that the closed loop system output response to any initial condition will go to zero in a minimum number of sample periods. As such, the system is confined to purely regulation tasks and thus limited in its application. To incorporate tracking capabilities in the closed loop multirate system a technique to design an *independent* input precompensator to accompany the feedback design is also presented.

Two examples (based on the systems of Eckardt and Felui et al respectively) demonstrate the deadbeat design technique outlined in this chapter. The first example, in particular, shows how the overshoot problem associated with applying the Eckardt algorithm to design a deadbeat system with finite zeros can be *completely* removed with the extension to the method of Marrari et al. The examples also illustrate the improvement in system sensitivity that can be achieved by adopting a multirate control strategy.

7.2 MULTIRATE DEADBEAT DESIGN ALGORITM

This section outlines a multirate deadbeat algorithm to design a MIFO state feedback controller (for regulation properties) and an accompanying input precompensator (for tracking properties). The combined multirate control structure is shown in Figure 7.1. The algorithm is based on the *minimal* state space description of Section 2.6.

The *feedback* design is based on an output zeroing approach (Marrari

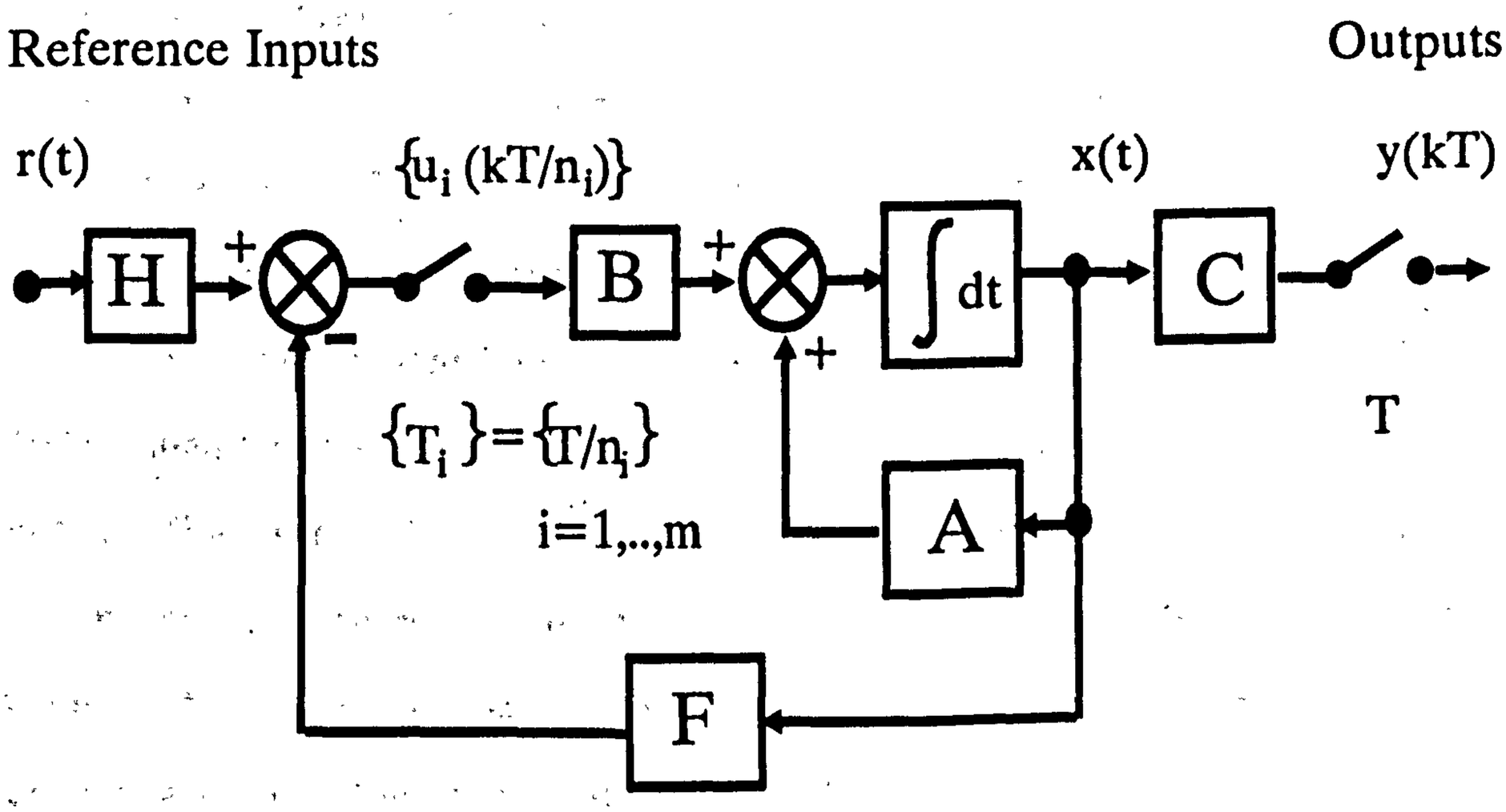

Figure 7.1. Combined feedback and precompensator structure of the multirate deadbeat control system.

et al, 1989). For the output zeroing problem the freedom to assign poles at the origin is restricted by the form of the system output matrix (the C matrix). The output matrix will determine the observability of system modes and hence the number of poles that may be moved by output feedback. The technique of this section designs a feedback matrix which renders all stable transmission zeros unobservable in the closed loop system and simultaneously prescribes deadbeat behaviour to the remaining observable modes (Kimura, 1981; Ragazinni and Franklin, 1958). In other words, the zero poles are confined to lie in the (A,B) invariant subspace that lies in the subspace spanned by the columns of C. The combined objectives of this methodology ensures that the typical overshoot transient effect of the transmission zeros are nullified (thus reducing the control task of the deadbeat system), whilst maintaining minimum time (deadbeat) performance.

The input precompensator is determined from a specification of the desired steady-state behaviour of the system states, control signals and outputs. The specification of the steady-state output necessarily incorporates the form of input signal to be tracked by the combined precompensator and feedback controllers. The dynamics of the input precompensator element does not affect the regulation properties of the feedback control. However, the form of the feedback matrix is an inherent part of the input compensator design and cannot be separated. Consequently, the *robustness* of the feedback design determines the integrity of the compensator element performance under varying system conditions.

The following sub-sections describe the theoretical and computational aspects of the multirate deadbeat design method for the control structure of Figure 7.1.

7.2.1 Preliminaries of the Output Zeroing Problem

For a linear MIFO sampled multirate system the output zeroing problem is to select a control law,

$$u(kT) = -Fx(kT) \tag{7.2.1}$$

such that the outputs are forced to zero, from any initial condition x(0), in a minimum number of time steps μ. That is,

$$y(kT) = C(\Phi_{CLM})^{\mu}x(0) = 0 \tag{7.2.2a}$$

or,

$$C(\Phi_{CLM})^{\mu} = 0 \tag{7.2.2b}$$

where $\Phi_{CLM} = (\Phi_{MR1}-\Gamma_{MR1}F)$ is the multirate closed loop system matrix formed by feedback matrix F. The equations of (7.2.2) describe the desired behaviour of the deadbeat closed loop system. The conditions specified are achieved either by assigning all poles to the origin or by ensuring that the closed loop system right eigenvectors lie in the nullspace of C, N[C]. The state feedback matrix designed to fulfil these objectives will ensure that the closed loop system output response to an initial condition x(0) will go to zero in μ sample periods.

This deadbeat control design technique can also designate *transmission blocking properties* to the closed loop multirate system. The blocking properties simplify the output zeroing task. This design philosophy can be understood as follows: Consider a system mode characterised by a frequency s_i. Unobservability of this mode is achieved if an input of the form,

$$u(t) = u_i \exp(s_i t) \quad t \geq 0 \tag{7.2.3}$$

and an initial state, x_i, yields an output response

$$y(t) = 0 \qquad t \geq 0 \tag{7.2.4}$$

This is equivalent to the cancellation of a transmission zero of frequency s_i. The condition of equation (7.2.4) can be achieved by considering the *zero structure* of the discrete system (Kailath, 1980). This is characterised by the matrix:

$$T(z) = \begin{bmatrix} zI-\Phi & -\Gamma \\ C & 0 \end{bmatrix} \tag{7.2.5}$$

Assume r stable transmission zeros exist for the system triplet $\{\Phi,\Gamma,C\}$. The null transmission properties of the zero $z=z_i$, i=1,..,r, are defined by,

$$T(z)\begin{bmatrix} v_i \\ w_i \end{bmatrix} = 0, \qquad \begin{bmatrix} v_i \\ w_i \end{bmatrix} \neq 0 \qquad i=1,..,r \tag{7.2.6}$$

where v_i, w_i are defined as the *zero state directions* and *zero input directions* respectively, corresponding to the transmission zero z_i. Thus by definition, the subspace which spans the set of zero state directions, $\{v_i,..,v_r\}$, lies in the nullspace of C, N[C].

Since the zero directions are invariant under feedback, *maximum unobservability* can only be obtained if all r stable transmission zeros are cancelled by the feedback matrix F. Ensuring that all remaining zeros are at infinity will then prescribe the necessary deadbeat behaviour.

7.2.2 Deadbeat Multirate Feedback Design

The design of feedback matrix F requires three stages:

(i) A suitable change of basis to decompose the MIFO multirate system into subsystems of observable and unobservable modes.

(ii) The cancellation of all stable transmission zeros.

(iii) The assignment of all remaining observable poles to the origin to ensure deadbeat regulation performance.

The first stage of the design can be achieved by a transformation comprising the set of r zero state directions, $\{v_1 .. v_r\}$, augmented by (n-r) linearly independent vectors, $\{l_1 .. l_{n-r}\}$ to complete the basis, i.e.,

$$R = [v_1 .. v_r \; l_1 .. l_{n-r}] \tag{7.2.7}$$

For repeated transmission zeros, generalised eigenvectors (Klein, 1984) can be used to form the R^r subspace of zero state directions. (Since the MIFO multirate system transition equations are defined over the main interval period T the transmission zeros of interest are those related to the single rate system sampled at rate 1/T.)

Applying transform R to the open loop multirate system gives,

$$\Phi_r = R^{-1}\Phi R, \quad \Gamma_r = R^{-1}\Gamma, \quad C_r = CR \tag{7.2.8}$$

where,

$$\Phi_r = \begin{bmatrix} \Phi_{11} & \Phi_{12} \\ \Phi_{21} & \Phi_{22} \end{bmatrix} \begin{matrix} \} \ r \\ \} \ n-r \end{matrix} \qquad \Gamma_r = \begin{bmatrix} \Gamma_1 \\ \Gamma_2 \end{bmatrix} \begin{matrix} \} \ r \\ \} \ n-r \end{matrix}$$

$$C_r = \underset{\substack{\uparrow \\ r}}{\left[0 \right.} \ : \ \underset{\substack{\uparrow \\ n-r}}{\left. C_2 \right]} \qquad (7.2.9)$$

A choice of $F_r = [F_1 \ F_2]$ such that $(v_i..v_r)$ are unobservable gives,

$$\Phi_r = \begin{bmatrix} \Phi_{11}-\Gamma_1F_1 & \Phi_{12}-\Gamma_1F_2 \\ 0 & \Phi_{22}-\Gamma_2F_2 \end{bmatrix} \begin{matrix} \} \ r \\ \} \ n-r \end{matrix} \qquad (7.2.10)$$

thus completing stage two. Ensuring $(\Phi_{22}-\Gamma_2F_2)$ has all zero poles fulfils the objectives of the third stage of the procedure. Transformation of the resulting closed loop system to its original basis completes the design of the MIFO feedback gain matrix.

The sensitivity of the state feedback control system can be monitored by the conditioning of the closed loop right eigenvectors $\kappa(V)$ (recall from Chapter 4 that this measure indicates the closed loop system insensitivity to variations in the nominal system dynamics). A common drawback of deadbeat control schemes are the ill-conditioned solutions, characterised by high $\kappa(V)$, which arise from assigning confluent eigenvalues. Thus a deadbeat design method which produces a $\kappa(V)$ figure approaching unity will enhance closed loop system insensitivity.

7.2.3 Deadbeat Tracking

This section deals with the formulation and design of a multirate input precompensator (Emami-Naeini and Franklin, 1982) to accompany the multirate feedback design of Section 7.2.2. This compensator will

incorporate additional tracking capabilities in the MIFO deadbeat control structure. The design methodology is outlined for the most general case, which allows the class of input reference signal described by,

$$r(k+1) = \Omega r(k)$$
$$u_r(k) = \Sigma r(k) \qquad (7.2.11)$$

to be tracked. This includes polynomials, sinusoids and exponential functions. The combined control law takes the form,

$$u[kT] = -Fx[kT] + Hr[kT] \qquad (7.2.12)$$

If the closed loop system is to track the input signal by time instant [NT] then the desired steady-state output is:

$$y[NT] = u_r[(N-1)T] \qquad (7.2.13)$$

The precompensator matrix H is determined from a combination of equations (7.2.11) to (7.2.13) and a specification of the desired steady-state values for the input and dynamic state vectors. The desired input and state vectors at instant [NT] are specified by matrices $L \in R^{nx1}$ and $M \in R^{mx1}$ using:

$$x[NT] = Lr[(N-1)T] \qquad (7.2.13)$$

$$u[NT] = Mr[(N-1)T] \qquad (7.2.14)$$

which then gives the following relations:

$$\Phi_{MR1}L + \Gamma_{MR1}M = L\Omega \qquad (7.2.15)$$

$$CL = \Sigma \tag{7.2.16}$$

$$H\Omega = M + FL \tag{7.2.17}$$

Equations (7.2.15) to (7.2.17) clearly indicate that the input signal dynamics determine the order and complexity of the input precompensator matrix H.

7.3 APPLICATION OF DEADBEAT DESIGN ALGORITHM

Two examples are presented to demonstrate the application of the design technique outlined in Section 7.2. The systems and the control tasks used for these examples have appeared in the literature of Eckardt (1989) and Felui et al (1990). These original articles demonstrate the application of two different multirate deadbeat tracking control methods. The methods proposed in these articles both design multirate series compensators. The results of the two methods detailed in the original articles are compared to those produced by the technique outlined in Section 7.2. Corresponding single rate deadbeat control is also designed for the second example to illustrate the significant improvement in closed loop system robustness that can be effected by adopting a multirate input control strategy. (This improvement in insensitivity is obtained by use of the unique (A,B) invariant subspaces of the MIFO system.)

7.3.1 Example 7.3.1

The continuous linear system described by the following matrices (Eckardt, 1989),

$$A = \begin{bmatrix} -3 & -2 \\ 1 & 0 \end{bmatrix} \quad B = \begin{bmatrix} 1 \\ 0 \end{bmatrix} \quad C = \begin{bmatrix} 2 & 3 \end{bmatrix} \tag{7.3.1}$$

is required to track a unit step input in a finite time. The sample parameters chosen (corresponding to those of the original work) are $T = 0.1667$secs, $n_0 = n_1 = 2$, $T_1 = T_b = 0.0833$secs. The discrete system sampled at $T = 0.1667$secs has a transmission zero, $z = 0.7789$, which is to be removed by the deadbeat control feedback matrix.

Deriving the MIFO multirate system model and proceeding with the design of the feedback controller outlined in Section 7.2, gives the following gain matrix:

$$F_{E1} = \begin{bmatrix} 4.9492 & 7.6295 \\ 5.5985 & 8.6305 \end{bmatrix} \tag{7.3.2}$$

The closed loop system formed by this feedback matrix has poles {0.7789 0}. Thus, the single transmission zero has been cancelled. Furthermore, in reponse to any initial state perturbation feedback gain matrix F_{E1} drives the system outputs to zero in one main interval time step.

To enable deadbeat output tracking, the multirate precompensator element is designed following the procedure outlined in Section 7.2.3. The closed loop system is required to track *step* changes in the reference signal. Thus, the input signal dynamics of equation (7.2.11) are described by Ω=1, Σ=1. Generating the H matrix with these parameters gives the following input feedforward controller:

$$H_{E1} = \begin{bmatrix} -3.1432 \\ -3.4768 \end{bmatrix} \tag{7.3.3}$$

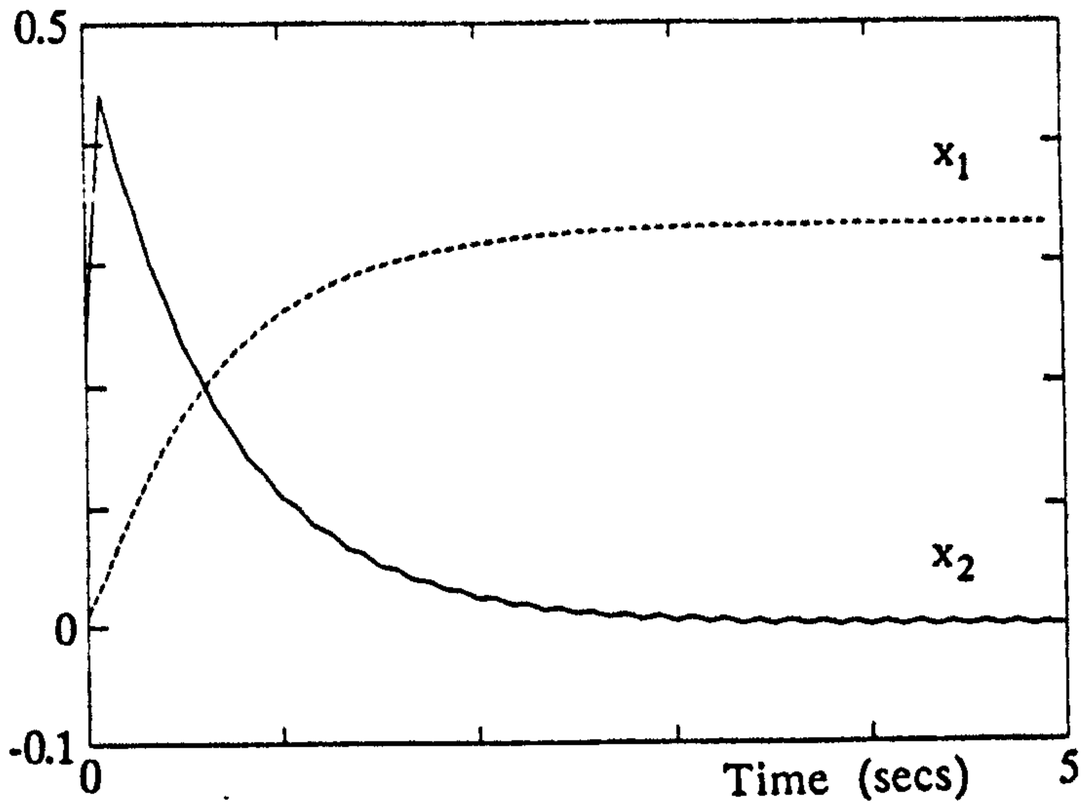

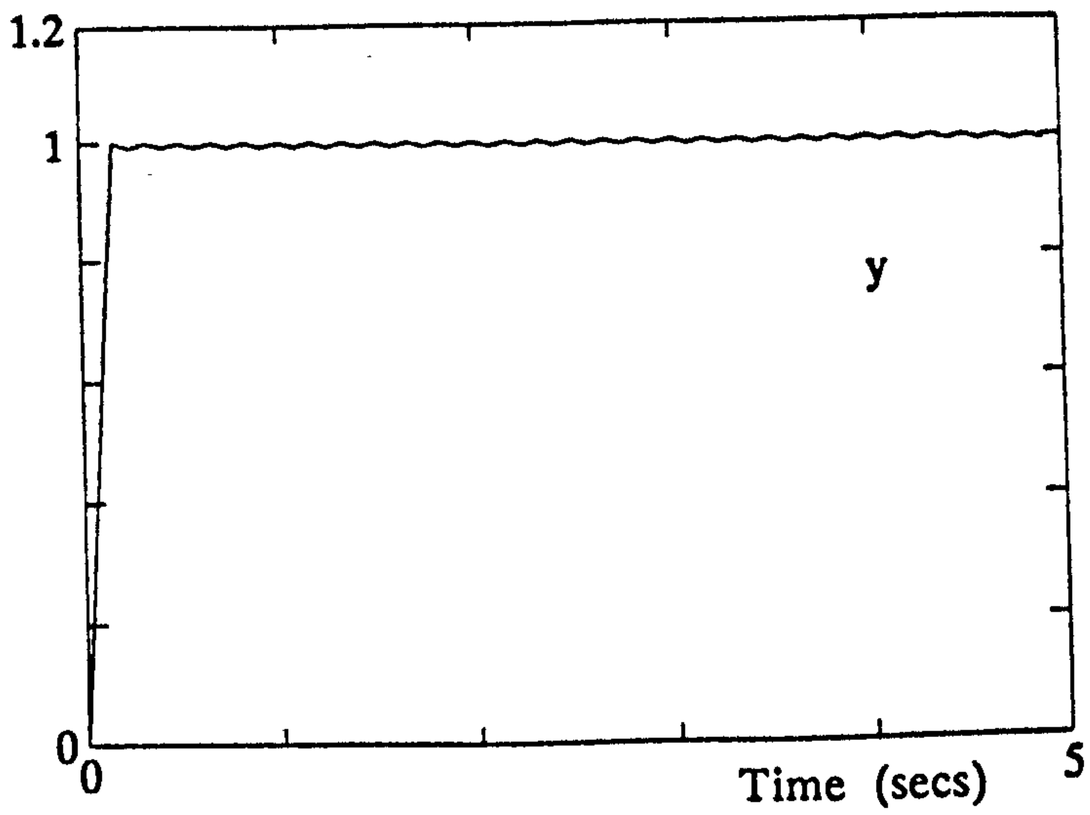

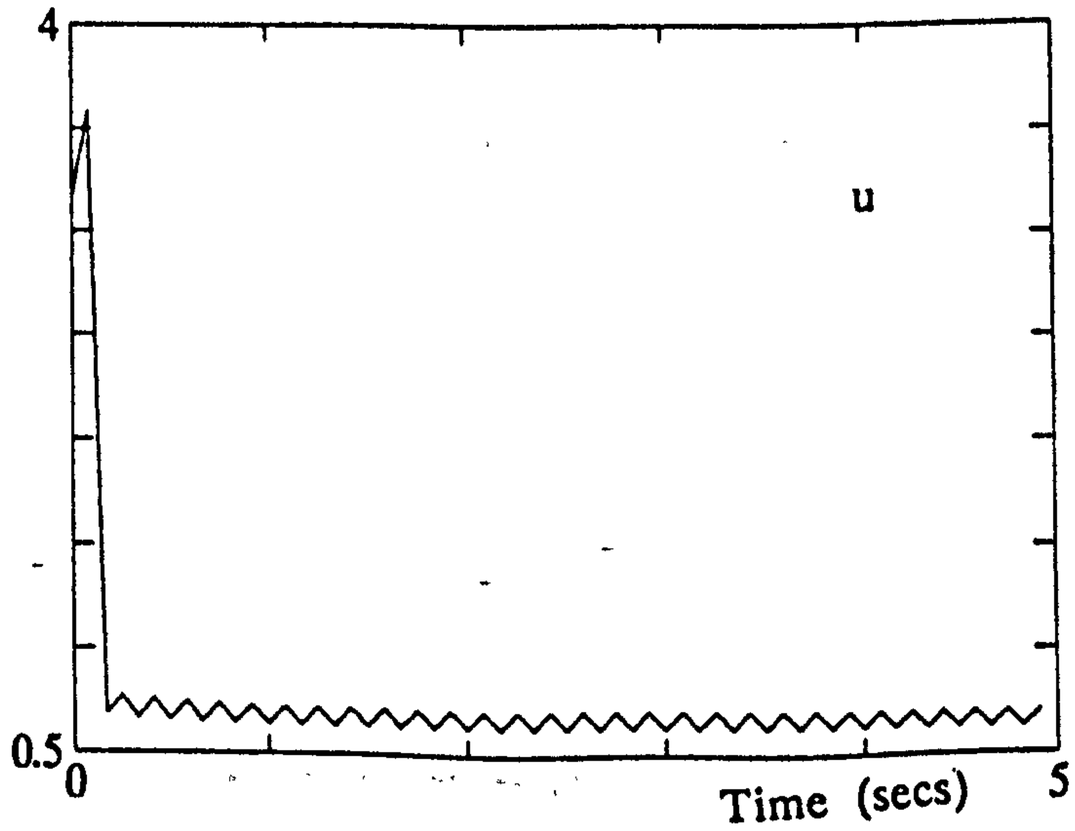

Figure 7.3.1a Closed loop system response produced by F_{E1}, H_{E1} controllers of Example 1.

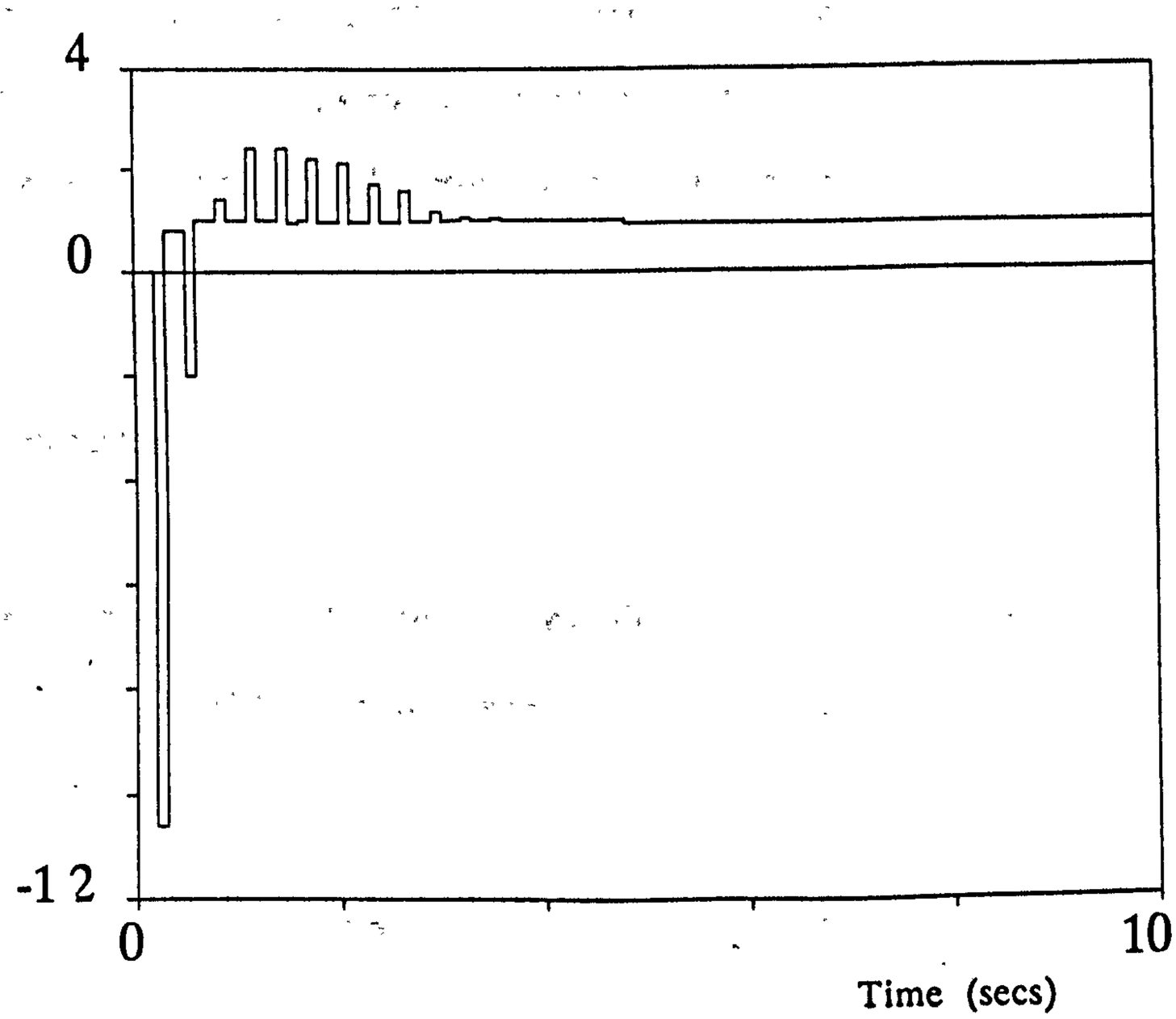

Figure 7.3.1b Closed loop system response of original Eckardt multirate design for Example 7.3.1.

The responses of the MIFO sampled closed loop system formed by controllers F_{E1} and H_{E1} are shown in Figure 7.3.1a. The corresponding results generated by the design of Eckardt (1989) is included in Figure 7.3.1b to provide a comparison of the results of the two methods.

The responses of Figure 7.3.1 show that multirate deadbeat controllers F_{E1} and H_{E1} provide much more effective tracking properties than the original Eckardt design. The output response generated by the Eckardt design suffers from transients of magnitude up to -11 units. In comparison, the output of the F_{E1} and H_{E1} closed loop system tracks the step input in one step smoothly and without the large overshoots of the original design. Thus, the problems outlined by Eckardt (which can be attributed to the zero properties of the closed loop system) are *completely* removed by the method presented in this chapter.

7.3.2 Example 7.3.2

The second example considers deadbeat control of a d.c. servomotor (Felui et al, 1990) whose dynamics are given by,

$$A = \begin{bmatrix} -6.67 & 0 \\ 1 & 0 \end{bmatrix} \quad B = \begin{bmatrix} 1 \\ 0 \end{bmatrix} \quad C = \begin{bmatrix} 0 & 1000 \end{bmatrix} \tag{7.3.4}$$

The sample parameters (as chosen by Felui et al) are T = 0.5secs, $n_0 = n_1 = 2$, $T_1 = T_b = 0.25$. The single rate discrete system of sample rate T has one transmission zero at -0.3567. Note that the 0 element in the output matrix of (7.3.4) ensures that the system is already decomposed into observable and unobservable subsystems thus obviating the need for the transformation R. Feedback and precompensator gain matrices F and H are determined for the single rate and multirate cases as follows:

Single Rate Design

The single rate system to be examined it that obtained by discretising the SISO system of (7.3.4) with a time interval T = 0.5 secs. Applying the method of Section 7.2 to the resulting single rate system *uniquely* determines (since there is only one output) the following gain matrices:

$$F_S = [-2.7134 \quad -18.7668] \qquad H_S = [0.0188] \tag{7.3.5}$$

The closed loop system formed using F_S and H_S produces a right eigenvector conditioning measure $\kappa(V)$=15.2798.

Multirate Design

For the multirate case extra freedom exists for the determination of state feedback F when compared to the single rate design of (7.3.5). This can be used to improved the closed loop system robustness at stage 3 of the design procedure outlined in Section 7.2. With this objective in mind, the following gain matrix is designed:

$$F_{EM2} = \begin{bmatrix} -2.7134 & -32.8862 \\ -2.7134 & 6.2062 \end{bmatrix} \tag{7.3.6}$$

This feedback control produces closed loop system poles at {-0.3567 0}, making the effect of the transmission zero unobservable and driving the output to zero from any intial condition. Furthermore, it produces a closed loop system with $\kappa(V) = 1$, ensuring *maximum* insensitivity at the main sample instants.

The accompanying tracking precompensator is designed using the method of Section 7.3. This produces:

$$H_{E2} = \begin{bmatrix} -0.0220 \\ -0.0129 \end{bmatrix} \qquad (7.3.7)$$

The responses of the closed loop systems formed by the feedback and input precompensator controllers of both the single rate and multirate systems are displayed in Figure 7.3.2. The responses show that, for both cases, the output tracks the step input in one main sample interval. Both multirate system states are also seen to attain their steady-state values in one step. In comparison, state x_2 of the single rate design takes 5 main sample intervals to settle to its final value. The control effort of the multirate design is also significantly reduced and in correspondence with the rapid state behaviour, reaches its final value much faster.

7.4 SUMMARY

This chapter has outlined a technique which uses the extra design freedom made available by MIFO multirate sampling to design superior deadbeat control than corresponding single rate systems. The method presented is used to design a regulation and tracking deadbeat system using state feedback and input precompensated control. The multirate deadbeat regulation design technique is based on the single rate output zeroing method of Marrari et al (1989). A technique to formulate an accompanying input precompensator is also presented. The precompensator element provides additional tracking qualities capabilities to the pure multirate feedback control structure.

This chapter has applied the deadbeat design algorithm of Marrari et al (1989) to a MIFO multirate system and illustrated the improvement in tracking and regulation control that can be effected by the multirate sampling strategy. The application of the technique has been

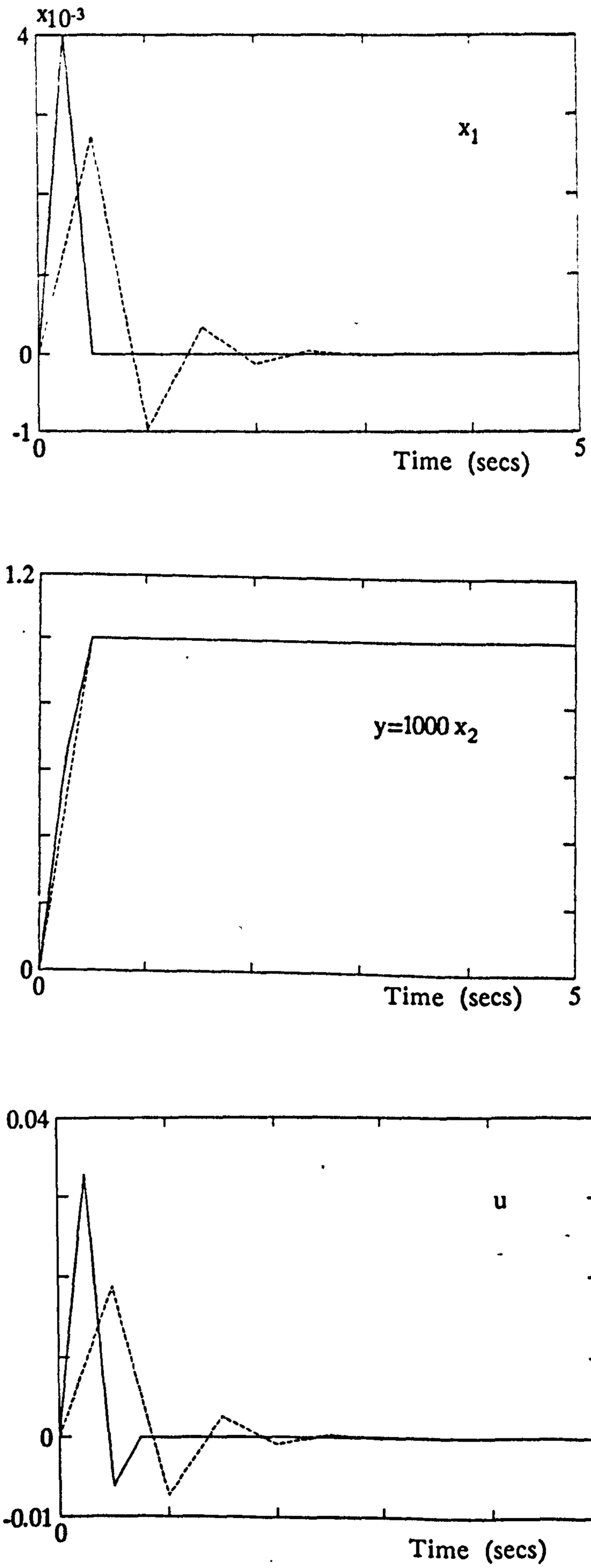

Figure 7.3.2 Closed loop response produced by single rate and multirate controllers of Example 7.3.2.

demonstrated with the design of multirate controllers for two examples taken from two recent articles (which outline alternative multirate deadbeat design methods). Note that though both the examples of this chapter have been based on SISO systems, the technique can be applied to MIMO systems (without *any* modifications) to produce equally good results.

The control structure arising from the technique of this chapter is different from both the original designs since it includes both multirate feedback and input precompensator elements.

The alternative methods of the original articles do not consider the application of state feedback to provide unobservability of undesired transmission modes in the closed loop system. This omission results in tracking designs which demand greater control effort to nullify the oscillatory effects of the unwanted modes. The design method of this chapter has a primary objective of eliminating the transmission zeros and thus provides a much more effective deadbeat control design. The technique, as demonstrated by the first example, directly addresses the overshoot problems experienced by the Eckardt design.

A method of usefully exploiting the extra design freedom of multirate control schemes to produce more insensitive closed loop systems than corresponding single rate designs has also been outlined. The effectiveness of improved sensitivity of the feedback design has been clearly and simply demonstrated by the simulation results of the second example.

CHAPTER EIGHT

CONCLUSION

8.1 CONTRIBUTION

The main aim of this thesis has been to examine and develop techniques for the design and analysis of multirate control systems.

The thesis Introduction details the historical development of multirate control systems and the tools used for their analysis. The direction and results of previous research in this area have been summarised. Chapter 1 has described and demonstrated the use of the early classical multirate modelling methods. The complexity and intractability of the closed loop multirate system descriptions produced by these early methods highlighted likely reasons for the slow development of design and analysis techniques for multirate control systems.

Chapter 2 has described the state space representation of multirate systems. A number of state space models, of varying complexity, were derived. The complexity of each model was observed to indicate the amount of information it contained and thus its usefulness for the design and analysis of the multirate system. Complex, high dimensional and non-minimal state space models were shown to provide the maximum amount of information on the input/output behaviour of multirate systems. This type of model is mostly used for the *analysis* of multirate systems; the non-minimality of these models is not suited for the application of many conventional state space design techniques. Low dimensional, minimal state space models were shown to represent the multirate system outputs only at the main sample instants. The multirate input, fixed rate output (MIFO) sampled system, which falls into the latter category of multirate systems was introduced.

State space design techniques are applicable to multirate systems of this category. The advantages and disadvantages associated with the design of MIFO control systems were outlined. Chapter 2 also presented a new state space technique for the design of compensators for MIFO systems.

Chapter 3 has described the role of input/output sample rates in the design of MIFO control systems. The sample rates were shown to influence the controllability, observability and internal structural properties of the multirate system. The set of *minimum* sample rates required to satisfy the controllability conditions were indicated and two different method of generating this set outlined. The links between these sample sets, canonical structures and (A,B), (A,C) invariance properties were clearly shown by the use of pencil equivalence relations. In addition, a means of creating useful (A,B) invariance properties for the solution of the MIFO pole assignment problem was outlined.

Chapter 4 has described the design strategy of the state and output feedback eigenstructure assignment techniques. In particular, the direct way in which the (A,B) invariance properties of a system are usefully employed by eigenstructure assignment methods is emphasised. The benefits of assigning an *insensitive* closed loop system eigenstructure were outlined. The precise effect of this insensitivity on the robustness of the closed loop system performance has been detailed from both the time and frequency domain perspectives.

The possibility of applying eigenstructure assignment techniques in an attempt to use the MIFO system (A,B) invariance properties for the design of maximally insensitive closed loop systems was also outlined in Chapter 4. The limited ability of the existing insensitivity measures to monitor the total behaviour of MIFO multirate systems was noted. More specifically, the existing measures were shown to monitor only the main sample behaviour indicated by minimal MIFO state space models. A means of assessing the *intersample* behaviour of MIFO systems by applying the

insensitivity measures to the equivalent non-minimal description was outlined.

Chapter 5 has generalised the input/output sample rate selection criterion for the achievement of maximally insensitive (*perfectly* decoupled) closed loop solutions to the MIFO eigenproblem. The direct method of solving the MIFO eigenproblem, based on a least squares minimisation of the desired and assignable right eigenvectors has been described. The application of this direct method has been demonstrated using several examples and the performance of the first MIFO design compared with that of the corresponding single rate design. This comparison showed that increased modal decoupling (in fact, perfect decoupling) is achievable by the MIFO multirate system at the main sample instants. The design examples of Chapter 5 have shown that the increased accuracy of the assigned MIFO system eigenstructure was obtained at the cost of high magnitude, switched control effort. This control behaviour produced unacceptable intersample state (and thus output) performance. A trade-off between accurate assignment of a desired eigenstructure and the magnitude and switching of control signals of the MIFO system was observed. The examples of Chaper 5 verify the accuracy of the new multirate insensitivity measures introduced in Chapter 4 in monitoring the intersample behaviour of the MIFO system.

Chapter 6 has described three eigenstructure assignment techniques which address the problem of high magnitude, switched control signals in MIFO feedback systems. The first technique, constrained eigenstructure assignment, produces implementable designs for simple systems in a direct and simple manner. The remaining two techniques both use an optimisation approach to produce a practically implementable solution. The optimisation task of both methods is to minimise scalar cost functions which incorporate suitable weightings of components required for a MIFO feedback design: the minimisation of control input effort and reduction of modal coupling.

The first optimised technique, the *gain modification procedure*, assigns a maximally conditioned solution during the first pass of eigenstructure assignment. The optimisation procedure then uses analytically derived gradients to minimise a single objective function which modifies the initial assignment such that the elements of the initial gain matrix are reduced. The second optimised technique, the multiple objective eigenstructure assignment method, attempts to design, from the onset, a feedback matrix of low norm which assigns the desired eigenstructure. The minimised objective function comprises two components which independently control the modal assignment and the reduction of control effort. The scalar objective function is minimised using analytically derived gradients and an optimisation algorithm. In this way, the feedback control design is tailored to address the specific needs of the multirate sampled system.

The application of all three techniques was demonstrated by repeating the design examples of Chapter 5.

A trade-off between the capability of each design technique to alleviate the problems and the complexity of the design procedure was noted. The technique which offered the most design flexibility (i.e. the multiple objective eigenstructure assignment method) demanded a high level of expertise and interaction from the designer. The technique which offered the least design flexibility (i.e. the constrained eigenstructure assignment method) required no user expertise or interaction. In the author's opinion, the best compromise between the demanded designer effort and the capabilities of the design technique is offered by the optimised gain modification procedure. A drawback of this method, as demonstrated by the aircraft Stability Augmentation System example, is that it may not always give the required reduction in the demanded control effort to yield a suitable solution. However, the application of this technique is recommended in the first instance.

Chapter 7 has described a deadbeat tracking and regulation design

technique which can be usefully applied to MIFO feedback control systems. The objective of the control designs produced by this technique is to render a maximum number of undesired transmission zeros unobservable in the closed loop system (by moving poles under the zeros) whilst assigning all remaining poles to the origin. Thus deadbeat behaviour of all the observable system modes is ensured. A comparison of the performance achievable by the multirate and corresponding single rate systems has shown that MIFO sampling can be used to prescribe faster settling of states and to improve the insensitivity of the closed loop system.

In conclusion, this dissertation has described several state space models of use for the analysis of multirate systems and investigated and demonstrated (in some detail) the generation and application of extra design opportunities offered by MIFO sampled control schemes. In particular, the capabilities of the MIFO systems to enhance the insensitivity of closed loop systems (beyond that achievable by corresponding single rate and continuous-time systems) with the use of eigenstructure assignment techniques has been emphasised. This work has filled a notable gap in the development of multirate state-space control design methods.

8.2 DISCUSSION AND SUGGESTIONS FOR FURTHER WORK

Several areas of multirate design and analysis work remain to be successfully developed. The two most important and useful topics (in the author's opinion) that require investigation are:-

(i) The development of analytic techniques to examine the frequency domain behaviour of MIMO multirate systems

(ii) The development of observer design techniques for multirate systems.

The following subsections briefly discuss both area of suggested work.

8.2.1 Stability of Multirate Systems

Stability analysis of SISO multirate systems has been examined by a number of researchers. Early attempts were hindered by the difficulty encountered in deriving an analytic closed loop expression. Once this had been overcome with the development of simpler modelling methods, classical stability analysis was applied. These examinations were restricted to determining asymptotic stability from pole/zero locations. The application of Bode plots for stability analysis of sampled data systems is not as simple or as useful as in the continuous domain. This is due to the lack of correspondence of discrete singularities to break frequencies on the bode plots and the absence of simple linear approximations of discrete element characteristics (Maciejowski and Samra, 1990). The Nyquist Stability Criterion is more useful in this case. Later stability analysis methods included the determination of gain and phase margins from Nyquist plots.

For MIMO multirate systems, these classical SISO measures are not applicable. They assume the isolation of independent functions between each input and output, effectively a diagonally dominant system. The multirate structure, with interactions between different modes occuring at different rates, severely violates this strict assumption. The characterisation of a unique frequency response for every input/output function is even more difficult than in the continuous or single rate cases.

For the continuous case, approximations to the diagonally dominant form can precede the use of classical stability analysis of multivariable systems. One cannot place confidence in the interpretation of true stability performance in this case. A more accurate (but conservative) measure is indicated by the maximum and minimum singular values ($\bar{\sigma}$ and $\underline{\sigma}$)

of the multivariable system state matrix. As described in Chapter 4, these measures indicate upper and lower bounds on the damping present in the *whole* system. A plot of its variation over the frequency spectrum provides a means of assessing the global performance and stability of the system.

The extension of these multivariable stability measures and diagonalisation techniques to the multirate case, however, is not simple. The problem stems from the non-minimality of time domain models derived for multirate systems. This is due to periodic descriptions being defined in terms of the dynamics associated with a common smallest sample time interval. Chapters 1 and 2 indicated that this is the only way in which a unified description, incorporating multirate inputs and multirate outputs, can be defined. Contrary to this modelling requirement, for the different aliasing properties of the individual subsystems to be accurately accounted for, the frequency description must *only* contain sample effects at the instants that they *physically* occur. This is equivalent to the requirement of a strictly non-minimal multirate description. Once this requirement is satisfied the MIMO system singular values plots can be used to good effect.

The non-minimalilty can be removed by restricting the sampling scheme to a particular form (as for the MIFO system), but this is not always a realistic physical interpretation and is more suited to design than analysis of existing multirate configurations. The two restrictions that are generally applied to simplify the derivation of a multivariable, multirate description (i.e. that the various sample intervals be related (or can be approximated) to rational ratios and that they are *low* multiples of the base period) compromise the fidelity of the true multirate system representation by introducing "oversampling". These restrictions are necessary in order to codify the behaviour of the system as periodic over a defined interval. In particular, the second condition reflects the dimension and non-minimalilty of the multirate description (as shown in Chapter 2). This indicates that, the more disparate the sample frequencies,

the more difficult it becomes to represent accurately the true multirate frequency responses. (If a rational relationship cannot be approximated, the multirate system has an infinite periodic interval and its state matrix has quasi-randomly varying elements. This is clearly unsuitable for any accurate frequency domain stability analysis.)

Further research could develop techniques to resolve the conflicting requirements for multirate system analysis and design. This would require the investigation of different modelling methods and/or the development of transformations for application to existing multirate models.

8.2.2 Observer Design Techniques

Multirate sampling of system outputs provides an ideal mechanism for optimising the performance of observer based control systems. One application of multirate observer techniqes has been examined by Viswanadham and Minto (1990) for the design of fault diagnosis systems. The ability of multirate systems to assign a desired system eigenstructure can be usefully applied for the design of observers which are insensitive to disturbances or unknown inputs (Patton and Chen, 1991). The research of Serrano and Ramadage (1991), which considers the disturbance decoupling properties of multirate control systems, also contributes to this area of control. This very recently published work applies the invariance properties achievable by the multirate systems (which are described in this dissertation) to decouple the effects of disturbances *with known structures*. (Note that this approach is very similar to that used for the application of (A,C) invariance properties in the design of the MIFO deadbeat design algorithm of Chapter 7.)

Further research could extend the application of eigenstructure assignment techniques for the development of robust multirate observers.

REFERENCES

Albertos P. (1990), Block Multirate Input/Output Model for Sampled Data Control Systems, *IEEE Transactions*, Vol. AC-35, pp 1085-1088.

Al-Rahmani H., Franklin G. (1990), A New Optimal Multirate Control of Linear Periodic and Time-Invariant Systems, *IEEE Transactions*, Vol AC-35, pp 406-415.

Araki M., Yamamoto K. (1986), Multivariable Multirate Sampled-Data Systems: State-Space Description, Transfer Characteristics, and Nyquist Criterion, *IEEE Transactions*, Vol AC-31, pp 145-154.

Aslin P.P. (1985), Aircraft Simulation and Robust Flight Control System Design., D.Phil Thesis, University of York, UK.

Amit N., Powell J.D. (1981), Optimal Control of Multirate Systems, *Proceedings of the AIAA Guidance and Control Conference*, Alberquerque, New Mexico, Paper No 81-1797.

Andry A.N., Shapiro E.Y., Chung J.C. (1983), Eigenstructure Assignment for Linear Systems, *IEEE Transactions*, Vol AC-19, pp 711-728.

Berg M., Amit N., Powell J.D. (1988a), Multirate Digital Control System Design, *IEEE Transactions*, Vol AC-33, pp 1139-1149.

Berg M., Yang G.S. (1988b), A New Algorithm for Multirate Digital Control Law Synthesis, *Proceedings of the 27th Conference on Decision and Control*, Austin, Texas, pp 1685-1690.

Bittani S., Colerani P., Guardbassi G. (1984), Periodic Solutions of Periodic Ricatti Equations, *IEEE Transactions*, Vol AC-29, pp 665-667.

Bittani S., Bolzern P. (1985), Dicrete Time Linear Periodic Systems: Gramian and Modal Criteria for Reachability and Controllability, *International Journal of Control*, Vol 41, pp 909-928.

Boykin W.H., Frazier B.D. (1975), Analysis of Multiloop, Multirate Sampled Data Systems, *AIAA Journal of Guidance, Control and Dynamics*, Vol 14, No 14, pp 453-456.

Burrows S.P., Patton R.J. (1990a), Optimal Eigenstructure Assignment for Multiple Design Objectives, *Proceedings of American Control Conference*, San Diego, California, USA, pp 1678-1683.

Burrows S.P., Patton R.J. (1990b), Robust, Low-Norm Output Feedback Design for Flight Control Systems, *Proceedings of the AIAA Guidance, Navigation and Control Conference*, Portland, OR, USA, pp 1711-1719.

Burrows S.P. (1990c), Robust Control Design Techniques using Eigenstructure Assignment, D.Phil Thesis, Department of Electronics, University of York, York, UK.

Burrows S.P., Patton R.J. (1991), A Comparison of Some Robust Eigenvalue Assignment Techniques, *To appear in Journal of Optimal Control Theory & Applications*.

Byers R., Nash S.G. (1989), Approaches to Robust Pole Assignment, *International Journal of Control*, Vol 49, pp 97-117.

Chammas A.B., Leondes C.T. (1978), On the Design of Linear Time-Invariant Systems by Periodic Output Feedback, *International Journal of Control*, Vol 27, pp885-894.

Chammas A.B., Leondes C.T. (1979), Pole Assignment by Piecewise Constant Output Feedback, *International Journal of Control*, Vol 29, No 1, pp 31-38.

Coffey T.C., Williams I.J. (1966), Stability of Multiloop, Multirate Sampled Systems, *AIAA Journal*, Vol 4, pp 2178-2190.

Cruz J.B., Freudenbergh J.S., Looze D.P. (1981), Multivariable Feedback System Design: Concepts for a Classical Modern Synthesis, *IEEE Transactions*, Vol AC-26, pp 66-74.

Davison E.J. (1976), The Steady-State Invertibility and Feedforward Control of Linear Time-Invariant Systems, *IEEE Transactions*, Vol AC-21, pp 529-534.

D'Azzo J.J., Houpis C.H. (1981), *Linear Control System - Analysis and Design*, (2nd Edition), McGraw Hill.

Diduch C.P., Doraiswami R. (1987), Sample Period Effects in Optimally Designed Digital Control Systems, *IEEE Transactions*, Vol AC-32, pp 838-841.

Doyle J.C., Stein G. (1981), Multivariable Feedback System Design: Concepts for a Classical Modern Synthesis, *IEEE Transactions*, Vol AC-26, pp 4-16.

Eckardt D. (1989), Design of Finite Impulse Response Controllers by Pole Assignment in Multirate Sampled-Data Systems, *International Journal of Control*, Vol 49, No 4, pp 1185-1193.

Engwerda J.C. (1988), Control Aspects of Linear Discrete Time-Varying Systems, *International Journal of Control*, Vol 48, No 4, pp 1631-1658.

Emami-Naeini A., Franklin G.F. (1982), Deadbeat Control and Tracking of Discrete-Time Systems, *IEEE Transactions*, Vol AC-27, No 1, pp 176-181.

El-Sakkary A.K. (1990), A New Criterion for Estimating Robust Time Delays for Closed-Loop Stability, *IEEE Transactions*, Vol 35, pp 209-214.

Fahmy M.M., O'Reilly J. (1988a), Multi-Stage Eigenstructure Assignment by Output Feedback, *International Journal of Control*, Vol 48, pp 97-116.

Fahmy M.M., O'Reilly J. (1988b), Parametric Eigenstructure Assignment by Output Feedback: The Case of Multiple Eigenvalues, *International Journal of Control*, Vol 48, pp 1519-1535.

Fahmy M.M., O'Reilly J. (1983), Organization of the Non-Uniqueness of a Canonical Structure of Linear Multivariable Systems, *International Journal of Systems Science*, Vol 14, pp 585-601.

Feliu V., Cerrada J.A., Cerrada C. (1990), A Method to Design Multirate Controllers for Plants Sampled at a Low Rate, *IEEE Transactions*, Vol AC-35, pp 57-65.

Feng W. (1984), Robustness Analysis of Multivariable Feedback Systems with Time Delays, *IEEE Transactions*, Vol AC-29, No 1, pp 77-79.

Fessas P. (1979), An Analytic Determination of the (A,B) Invariant and Controllability Subspaces, *International Journal of Control*, Vol 30, pp 77-79.

Flowers D.C., Hammonds J.L. (1972), Simplification of the Characteristic Equation of Multirate Sampled Data Control Systems, *IEEE Transactions*, Vol AC-17, No 4, pp 249-250.

Francis B.A., Gorgiou T.T. (1988), Stability Theory for Linear Time-Invariant Plants with Periodic Digital Controllers, *IEEE Transactions*, Vol AC-33, pp 820-832.

Franklin G.F., Powell J.D., Workman. (1990), Feedback Control of Digital Control Systems, *Addison-Wesley Inc.*

Garg S. (1989), Stability Robustness Improvement of Direct Eigenspace Assignment Based Feedback Systems, Using Singular Value Sensitivities, *NASA Contractor Report 182303*.

Gantmacher (1959), Theory of Matrices, Vols 1 & 2, *Chelsea Publishing Company*, New York.

Garrard W.L., Low E., Prouty S. (1989), Design of Attitude and Rate Command Systems for Helicopters Using Eigenstructure Assignment, *AIAA Journal of Guidance, Control and Dynamics*, Vol 12, pp 783-791.

Gill P.E., Murray W., Wright M.H. (1981), Practical Optimisation, *Academic Press*.

Glasson D.P. (1982), A New Technique for Multirate Digital Control Design and Sample Rate Selection, *AIAA Journal of Guidance, Control and Dynamics*, Vol 5, pp 379-382.

Glasson D.P. (1980), Research in Multirate Estimation and Control, Report No.TR-1356-1, *The Analytic Sciences Corporation*, Reading, Massachusetts.

Godbout L.F., Jordan D., Apostolakis I.A. (1988), A Closed-Loop Model for General Multirate Digital Control Systems, *Proceedings of the IEE Control 1988 Conference*, Oxford, UK pp 494-499.

Golub G.H., Van Loan C.F. (1983), *Matrix Computations*, North Oxford Academic.

Golub G.H., Wilkinson J.H. (1976), Ill-Conditioned Eigensystems and the Computation of the Jordan Canonical Form, *SIAM review*. Vol 18, pp 578-619.

Grasselli O.M., Longhi S. (1986), Disturbance Localisation with Deadbeat Control For Linear Periodic Discrete-Time Systems, *International Journal of Control*, Vol 44, pp 1319-1347.

Hagiwara T., Araki M. (1986a), On the Necessary Condition for Discete-Time Pole Assignability by Piecewise Constant Output Feedback, *International Journal of Control*, Vol 43, pp 1905-1909.

Hagiwara T., Araki M. (1986b), Pole Assignment by Multirate Sampled-Data Output Feedback, *International Journal of Control*, Vol 44, pp 1661-1673.

Hagiwara T., Araki M. (1988), Design of a Stable State Feedback Controller Based on the Multirate Sampling of the Plant Output, *IEEE Transactions*, Vol AC-33, pp 812-819.

Hagiwara T., Fujimura T., Araki M. (1990), Generalized Multirate-Output Controllers, *International Journal of Control*, Vol 52, pp 597-612.

Houpis C.H. (1985), Refined Design Method for Sampled-Data Control Systems: the Pseudo-Continuous-Time (PCT) Control System Design, *IEE Proceedings*, Vol 132, pp 69-74.

Jury E.I. (1967), A Note on Multirate Sampled Data Systems, *IEEE Transactions*, Vol AC-12, pp 319-320.

Jordan D., Korn J. (1980), Deadbeat Algorithms for Multivariable Process Control, *IEEE Transactions*, VOL AC-25, pp 486491.

Kailath T. (1980), Linear Systems, *Prentice-Hall Inc.*

Kalman R.E., Bertram J.E. (1959), A Unified Approach to the Theory of Sampling Systems, *Journal of the Franklin Institute*, Vol 269, pp 405-436.

Kalman R.E. (1972), Kronecker Invariants and Feedback, *Ordinary Differential Equations*, (Editor L.Weiss), Academic Press, New York, pp 459-471.

Kano H., Nishimura T. (1985), Controllabilty, Stabilizability and Matrix Ricatti Equations for Periodic Systems, *IEEE Transactions*, Vol AC-30, pp 1129-1131.

Kantor J.C., Andres R.P. (1983), Characterization of "Allowable Perturbations" for Robust Stability, *IEEE Transactions*, Vol AC-28, pp 107-109.

Kargonekar P.P., Poolla K., Tannenbaum A. (1985), Robust Control of Linear Time-Invariant Plants using Periodic Compensation, *IEEE Transactions*, Vol AC-30, pp 1088-1096.

Katz P. (1981), Digital Control using Microprocessors, *Prentice-Hall.*

Kautsky J., Nichols N.K., Van Dooren P. (1985), Robust Pole Assignment in Linear State Feedback, *International Journal of Control*, Vol 41, pp 1129-1155.

Kimura H. (1975), Pole Assignment by Gain Output Feedback, *IEEE Transactions*, Vol AC-20, pp 509-516.

Kimura H., Tanaka Y. (1981), Minimal-Time Minimal-Order Deadbeat Regulator with Internal Stability, *IEEE Transactions*, VOL AC-26, pp 1276-1282.

Kimura H. (1981), Minimal-Time Minimal-Order Deadbeat Regulator with Internal Stability, *IEEE Transactions*, Vol AC-26, pp 1276-1282.

Klein G. (1984), On the Relationship Between Controllability Indexes, Eigenvector Assignment, and Deadbeat Control, *IEEE Transactions*, Vol AC-29, pp 77-79.

Klein G., Moore B.C. (1977), Eigenvalue-Generalised Eigenvector Assignment with State Feedback, *IEEE Transactions*, Vol AC-22, pp 140-141.

Kono M., Suzuki T. (1991), Monodromy Eigenvalue Assignment for Periodic Continuous-Time Systems by Multirate Sampled State Periodic Hold Control, *Proceedings of the IMACS-IFAC Symposium on Modelling and Control of Technological Systems*, pp 322-326.

Kono M. (1980), Eigenvalue Assignment in Linear Discrete-Time Systems, *International Journal of Control*, Vol 32, pp 149-158.

Kono M., Suzuki T., Morishita T. (1990), Block Decoupling of Linear ω-Periodic Discrete-Time Systems, *IEEE Transactions*, Vol AC-35, pp 1262-1265.

Kranc G.M. (1957), Input-Output Analysis of Multirate Feedback Systems, *IRE Transactions on Automatic Control*, Vol PGAC, pp 21-28.

Kucera V., Sebek M. (1984), On Deadbeat Controllers, *IEEE Transactions*, Vol AC-29, pp 719-722.

Kuo B.C. (1980), *Digital Control Systems*, Holt, Rinehart & Winston Inc.

Leden B. (1977), Multivariable Deadbeat Control, *Automatica*, Vol 13, pp 183-188.

Lehtomaki N.A., Sandell N.R., Athans M. (1981), Robustness Results in Linear-Quadratic Guassian Based Multivariable Control Designs, *IEEE Transactions*, Vol AC-26, pp 75-92.

Lennartson B. (1988), Periodic Solutions of Ricatti Equations Applied to Multirate Sampling, *International Journal of Control*, Vol 48, pp 1025-1042.

Lennartson B. (1989), Multirate Sampled-Data Control of Two Time-Scale Systems, *IEEE Transactions*, Vol AC-34, pp 642-644.

Litkouhi B., Khalil H. (1985), Multirate and Composite Control of Two Time-Scale Discrete-Time Systems, *IEEE Transactions*, Vol AC-30,

Luenberger D.G. (1967), Canonical Forms for Linear Multivariable Systems, *IEEE Transactions*, Vol AC-12, pp 290-293.

Luse D.W. (1988), State Space Realisation of Multiple-Frequency-Scale Transfer Matrices, *IEEE Transactions*, Vol AC-33, pp 185-187.

Ly Uy-Loi. (1983), Robustness Analysis of Multiloop Flight Control Systems, *Proceedings of the AIAA Guidance, Navigation and Control Conference*, Paper No 83-2189, pp 155-165.

MacFarlane A.J.G. (1970), Return Difference and Return Ratio Matrices and Their Use in Analysis and Design of Multivariable Feedback Control Systems, *IEE Proceedings*, Part D, Vol 117, No 10, pp 2037-2049.

Maciejowski J.M., Samra B.S. (1990), Gain/Phase Relationships for Discrete-Time Systems, *International Journal of Control*, Vol 51, pp 119-137.

Mahmoud M. (1982), Structural Properites of Discrete Systems with Slow and Fast modes, *Large Scale Systems*, Vol 3, pp 227-236.

Marrari M.R., Emami-Naeini A, Franklin G.F. (1989), Output Deadbeat Control of Descrete-Time Multivariable Systems, *IEEE Transactions*, Vol AC-34, pp 644-648.

Meyer D.G. (1990), A Parametrization of Stabilizing Controllers for Multirate Sampled-Data Systems, *IEEE Transactions*, Vol 35, pp 233236.

Meyer R.A., Burrus C.S. (1975), A Unified Analysis of Multirate and Periodically Time Varying Digital Filters, *IEEE Transactions*, Vol CAS-22, pp 162-168.

Meyer D.G. (1990), A New Class of Shift Varying Operators, Their Shift Invariant Equivalents, and Multirate Digital Systems, *IEEE Transactions*, Vol AC-35, pp 429-433.

MIL-F8785C, (1980), Flying Qualities of Piloted Vehicles, USA, pp 1678-1683.

Mielke R.R., Tung L.J. (1985), Design of Multivariable Feedback Control Systems via Spectral Assignment using Reduced Order Models and Reduced Order Observers, *NASA Contractor Report 3889*, NASA Langley Research Centre.

Minamide N. (1984), Design of a Deadbeat Adaptive Tracking System, *International Journal of Control*, Vol 39, pp 63-81.

Mita T., Pang B.C., Liu K.H. (1987), Design of Optimal Strongly Stable Digital Control Systems and Application to Output Feedback Control of Mechanical Systems, *International Journal of Control*, Vol 45, pp 2071-2082.

Mita T. (1980), A Relation between Overshoot and Sampling Period in Sampled Data Feedback Control Systems, *IEEE Transactions*, VOL AC-25, pp 603-604.

McRuer D.T., Askenas I., Graham D. (1973), Aircraft Dynamics and Automatic Control, *Princeton University Press*.

Moore B.C. (1976), On the Flexibility Offered by State Feedback in Multivariable Systems Beyond Closed-Loop Eigenvalue Assignment, *IEEE Transactions*, Vol AC-21, pp 659-692.

Mudge S.K., Patton R.J. (1988), An Analysis of the Technique of Robust Eigenstructure Assignment with Application to Aircraft Control, *IEE Proceedings*, part D, Vol 135, No 4, pp 275-281.

Mukhopadyay V., Newsom J.R. (1984), A Multiloop Stability Margin Study using Matrix Singular Values, *Journal of Guidance and Control*, Vol 7, pp 582-587.

O'Reilly J. (1981), The Discrete Linear Time Invariant Time-Optimal Control Problem - An Overview, *Automatica*, Vol 17, pp 363-370.

Owens T.J., Mielke R.R. (1982), A New Gain Modification Algorithm for Spectral Assignment, *Proceedings of the 14'th Symposium on Sytems Theory*, pp 51-54.

Owens T.J., O'Reilly J. (1989), Parametric State-Feedback Control for Arbitary Eigenvalue Assignment with Minimum Sensitivity, *IEE Proceedings*, part D, Vol 136, pp 307-313.

Owens D.H., Raya A. (1982), Robust Stability of Smith Predictor Controllers for Time Delay Systems, *IEE Proceedings*, Part D, Vol 129, No 6, pp 298-304.

Paduano J.D., Downing D.R. (1989), Sensitivity Analysis of Digital Flight Control Systems Using Singular-Value Concepts, *AIAA Journal of Guidance, Dynamice and Control*, Vol 12, pp 297-303.

Patel Y. (1990), An Analysis of Multirate Control Applied to a Simplified Helicopter Model, Report for Westland Helicopters Limited, Yeovil, Somerset.

Patel Y, Patton R.J. (1990), A Robust Approach to Multirate Controller Design using Eigenstructure Assignment, *Proceedings of the American Control Conference*, San Diego, California, USA, pp 945-951.

Patel Y. (1991), State Space Techniques for Multirate Control Systems Analysis, Report for Westland Helicopters Limited, Yeovil, Somerset.

Patel Y., Patton R.J. (1991a), Design of Robust, Multirate Feedback Control using Eigenstructure Assignment, *Proceedings of the IMACS-IFACS Symposium on Modelling and Control of Technological Systems*, Lille, France, pp 309-315. Also to appear in *Mathematics of the Analysis and Design of Process Control*, Editors Borne P. and Tzafestas S.G.

Patel Y., Patton R.J. (1991b), Deadbeat Control Algorithms for Multirate Control Systems, *Proceedings of the 1st European Control Conference*, Grenoble, France, pp 1598-1603.

Patel Y., Patton R.J., (1991c), Insensitivity Properties of Multirate Feedback Control Systems, *Proceedings of the 30'th IEEE CDC Conference*, Brighton, UK, pp 2954-2959. Also to be published in *IEEE Transactions on Automatic Control*.

Patel Y., Patton R.J., Burrows S.P. (1991a), Robust, Low Norm Multirate Control using Eigenstructure Assignment, *Proceedings of IEE Control 91 Conference*, Edinburgh, UK, pp 1165-1170.

Patel Y., Patton R.J., Burrows S.P. (1991b), The Design of Robust Multirate Aircraft Control Using Optimised Eigenstructure Assignment, *Proceedings of the AIAA Guidance, Navigation and Control Conference*, New Orleans, USA, pp 1805-1811. Also to be published in *Journal of Guidance, Control and Dynamics*.

Patton R.J., Chen J. (1991), Robust Fault Detection Using Eigenstructure Assignment: A Tutorial Consideration and Some New Results, *Proceedings of the 30'th IEEE CDC Conference*, Brighton, UK.

Popov V.M. (1972), Invariant Description of Linear Time-Invariant Controllable Systems, *SIAM Journal of Control*, Vol 10, pp 252-264.

Porter B. (1969), Eigenvalue Sensitivity of Modal Control Systems to Loop Gain Variations, *International Journal of Control*, Vol 10, pp 159-162.

Porter B. (1977), Eigenvalue Assignment in Linear Multivariable Systems by Output Feedback, *International Journal of Control*, Vol 25, pp 483-490.

Powell J.D., Katz P. (1975), Sample Rate Selection for Aircraft Digital Control, *AIAA Journal of Guidance, Control and Dynamics*, Vol 13, No 8, pp 975-979.

Ragazzini J.R., Franklin G.F. (1958), Sampled-Data Control Systems, *McGraw-Hill Inc.*

Raman K.V., Calise A.J. (1987), Modal Decoupling Insensitivity, *IEEE Transactions*, Vol AC-32, pp 524-526.

Rattan K. (1984), Digitisation of Existing Continuous Control Systems, *IEEE Transactions*, Vol AC-29, pp 282-285.

Rew D.W., Junkins J.L., Juang J.N. (1989), Robust Eigenstructure Assignment by a Projection Method: Applications using Multiple Optimisation Criteria, *Journal of Guidance, Control and Dynamics*, Vol 12, pp 396-403.

Roppenecker G. (1986), On Parametric State Feedback Design, *International Journal of Control*, Vol 43, pp 793-804.

Roppenecker G., O'Reilly J. (1989), Parametric Output Feedback Controller Design, *Automatica*, Vol 25, pp 259-265.

Saadane A., Richard J.P. (1991), A Note on Eigenvalue Assignment for Periodical Linear Systems, *Proceedings of the IMACS-IFAC Symposium on Modelling and Control of Technological Systems*, pp 327-333.

Safanov M.G. (1981), Stability Margins of Diagonally Perturbed Multivariable Feedback Systems, *IEE Proceedings*, Vol 129, No 6, pp 251-256.

Sebakhy O.A., Abdel-Moneim T.M. (1980), Design of Optimal Dead-Beat Controllers, *IEEE Transactions*, Vol AC-25, pp 604-606.

Serrano L.J., Ramadge P.J. (1991), Sampled Disturbance Decoupling with Stability using Multirate Control, *IEEE Transactions*, Vol AC-36, pp 1061-1065.

Slansky J., Ragazzini J.R. (1955), Analysis of Errors in Sampled-Data Feedback Systems, AIEE Trans, Vol 74, pp 75-71.

Silverthorn J.T., Reid J.G. (1980), Computation of the Subspaces for Entire Eigenstructure Assignment via the Singular Value Decomposition, *Proceedings of the 17th Conference on Decision and Control*, Austin, Texas, pp 1206-1207.

Sobel K.M., Shapiro E.Y. (1987), Robustness/Performance Tradeoffs in Eigenstructure Assignment With Flight Control Application, *Proceedings of the American Control Conference*, Minneapolis, USA, pp 380-385.

Shapiro E.Y., Chung J.C. (1981), Application of Eigenvalue/Eigenvector Assignment by Constant Output Feedback to Flight Control System Design, *Proceedings of the 15'th Annual Conference on Information Sciences and Systems*, pp 164-169.

Shapiro E.Y., Sobel K.M. (1986), Flight Control Synthesis via Eigenstructure Assignment, The Discrete Version, *Proceedings of the 28th Israel Conference on Aviation & Aeronautics*, pp 1-6.

Sinswat V., Fallside F. (1977), Eigenvalue/Eigenvector Assignment by State-Feedback, *International Journal of Control*, Vol 29, pp 389-403.

Smith P.R. (1991), Use of Eigenstructure Assignment on VSTOL Aircraft Control Law Design, *Proceedings of the Control '91 Conference*, Edinburgh, U.K., pp 1028-1034.

Sobel K.M., Shapiro E.Y. (1987), Application of Eigenstructure Assignment to Flight Control Design: Some Extensions, *AIAA Journal of Guidance, Dynamics and Control*, Vol 10, pp 73-79.

Sogaard-Andersen P., (1985), Design of Multivariable State Feedback Controllers, Ph.D. Thesis, Control Engineering Institute, Technical University of Denmark, Denmark.

Sogaard-Andersen P., Trostmann E., Conrad F. (1986), A Singular Value Sensitivity Approach to Robust Eigenstructure Assignment, *Proceedings of 25th Conference on Decision and Control*, Athens, Greece, pp 121-126.

Srinathkumar S., Jategaonkar R.V. (1985), Robust Eigensystem Assignment in Multi-Input Systems, Technical Memorandum SE 8506, National Aeronautical Laboratories, Systems Engineering Division, Bangalore, India.

Taylor P. (1991), Method of Analysing Multirate Discrete Sampled-Data Systems, Internal Report, Westland Helicopters Limited, Yeovil, Somerset.

Tischler M.B. (1989), Assessment of Digital Flight Control Technology for Advanced Combat Rotorcraft, *Journal of the American Helicopter Society*, Vol 34, pp66-76.

Thompson P.M. (1986), Multirate Sampled Data Feedback Systems, *International Journal of Control*, Vol 44, pp 833-846.

APPENDIX A

STATE SPACE REPRESENTATION OF SINGLE RATE DISCRETE SYSTEMS

The derivation of sampled-data system equations from a continuous-time state-space description is a simple and well documented procedure: Consider a linear, time-invariant system described by,

$$\dot{x}(t) = Ax(t) + Bu(t) \tag{A.1}$$

$$y(t) = Cx(t) \tag{A.2}$$

where $x \in R^n$, $u \in R^m$, $y \in R^n$ are the state, control and output matrices respectively. The solution of the non-homogeneous state equation (A.1) forms the state transition equation of the open-loop continuous system,

$$x(t) = \exp(At)x(0) + \int_0^t \exp[A(t-\tau)]Bu(\tau)\, d\tau \tag{A.3}$$

This gives the state vector at any time $t > 0$ as the sum of two terms, the complementary function and the particular solution. The first represents the contribution due to the initial state $x(0)$ and is defined as the natural system response. It is the solution to the homogeneous equation that is formed in the absence of any system excitation (ie $u = 0$). The particular solution represents the contribution due to the input over the interval $[0,t]$ and is thus known as the forced response. The exponential term in the natural response is the system state transition matrix.

To determine the state at any time t, $x(t)$ in terms of an arbitary initial state at time t_0 over the time interval $[t_0,t]$ equation (A.3) can

Viswanadham N., Minto K.D. (1990), Fault Diagnosis in Multirate Sampled Data Systems, *Proceeding of 29th Conference on Decision and Control*, Honolulu, Hawaii, pp 3666-3671.

Walsh G.R. (1975), Methods of Optimisation, *John Wiley & Sons Ltd.*, Chichester, England.

Wilkinson J.H. (1965), The Algebraic Eigenvalue Problem, *Clarendon Press*, Oxford, England.

Wilkinson J.H. (1984), Sensitivity of Eigenvalues, *Utilitas Mathematica*, Vol 25, pp 5-76.

Whitbeck R.F., Hofmann L.G. (1978), Digital Control Law Synthesis in the W' Domain, *Journal of Guidance and Control*, Vol 1, pp 319-326.

White B.A. (1991), Eigenstructure Assignment for Aerospace Applications: MATLAB Implementation, *Proceedings of the IEE Control '91 Conference*, Edinburgh, UK, pp 738-743.

Zhu G., Skelton R.E. (1991), Robust Properties of Periodic Discrete and Multirate Systems, *Proceedings of the IMACS-IFAC Symposium on Modelling and Control of Technological Systems*, pp 2755-2759.

be restated as,

$$x(t) = \exp[A(t-t_0)]x(t_0) + \int_{t_0}^{t} \exp[A(t-\tau)]Bu(\tau)\, d\tau \qquad (A.4)$$

If the continuous-time system is subjected to an input that changes from one constant value to another at successive, uniformly-spaced time instants t=kT, then,

$$u(\tau) = u(kT) \qquad kT \leqslant \tau < (k+1)T \qquad (A.5)$$

Since the inputs are held constant over the time period T (by a zero-order hold) the input term, u(kT), can be moved outside the integral to gives the transition of the states *during* the sampling interval $kT \leqslant t \leqslant (k+1)T$,

$$x(t) = \exp[A(t-kT)]x(kT) + \int_{kT}^{t} \exp[A(t-\tau)]B\, d\tau\; u(kT) \qquad (A.6)$$

Due to the uniformity of the sampling, this can be modified to describe the transition of the states at the sampling instants only,

$$x[(k+1)T] = \Phi(T)x(kT) + \Gamma(T)u(kT) \qquad (A.7)$$

$$y(kT) = Cx(kT) \qquad (A.8)$$

where,

$$\Phi(T) = \exp(AT) \qquad (A.9)$$

$$\Gamma(T) = \int_{0}^{T} \exp[A(T-\tau)B\, d\tau \qquad (A.10)$$

$\Phi(T)$ is the discrete state transition matrix defined at the sample instants

of the more explicit description,

$$\Phi_T[(k+1),k] = \Phi[(k+1)T,kT] = \exp\left[\int_{kT}^{(k+1)T} A(\tau)d\tau\right] \qquad (A.11)$$

similarly,

$$\Gamma_T[(k+1),k] = \Gamma[(k+1)T,kT] = \int_{kT}^{(k+1)T} \Phi[(k+1)T,\tau]B\, d\tau \qquad (A.12)$$

To derive an expression for x(kT) for any kT>0 given x(0) and u(kT) over the interval [0 (k-1)T] the equations for $x(k_iT)$ are successively substituted for $k_i = 0,..,(k-1)$,

$$x(T) = \Phi(T)x(0) + \Gamma(T)u(0)$$

$$x(2T) = \Phi(T)x(T) + \Gamma(T)u(T)$$

$$= \Phi^2(T)x(0) + \Phi(T)\Gamma(T)u(0) + \Gamma(T)u(T)$$

.

.

etc. (A.13)

ie,

$$x(kT) = \Phi^k(T)x(0) + \sum_{j=0}^{k-1} \Phi^j(T)\Gamma(T)u[(k-j-1)T] \qquad (A.14)$$

where, $\Phi^k(T)$ is the kth fold matrix product known as the fundamental matrix.

Equation (A.14) is the sampled-data system transition equation, which

can be shifted to determine the state at any sample instant $(k+i)T > kT$ for an arbitary initial time point, i.e.,

$$x[(k+i)T] = \Phi^k(T)x(iT) + \sum_{j=0}^{k-1} \Phi^j(T)\Gamma(T)u[(k-j+i-1)T] \qquad (A.15)$$

APPENDIX B

NUMERICAL DETAILS OF EXAMPLE 3.5.1

The system of Example 3.5.1 is described by the continuous-time matrices:

$$A = \begin{bmatrix} 0 & 1 & 0 \\ 0 & 0 & 1 \\ -6 & -11 & -6 \end{bmatrix} \qquad B = \begin{bmatrix} 1 & 1 \\ 0 & 1 \\ 1 & 1 \end{bmatrix} \tag{B.1}$$

Using the formulation of Section 2.5, the MIFO multirate discrete system matrices for input sampling multiplicities $\{n_1=2\ n_2=1\}$ and a main sample of interval T=0.1 secs are determined to be:

$$\Phi_{MR1} = \begin{bmatrix} 0.9991 & 0.0489 & 0.0011 \\ -0.0246 & 0.9541 & 0.0738 \\ -0.4429 & -0.8366 & 0.5112 \end{bmatrix} \quad \Gamma_{MR1} = \begin{bmatrix} 0.0501 & 0.0500 & 0.1051 \\ 0.0022 & 0.0010 & 0.1016 \\ 0.0130 & 0.0362 & 0.0033 \end{bmatrix} \tag{B.2}$$

Recall that the objective of Example 3.5.1 is to apply the canonical pole assignment algorithm of equation (3.5.3) to design multirate feedback control such that the unstable open loop poles of A are moved to {-0.5 -0.6 -0.7}. Thus, the desired discrete poles are defined to be exp({-0.5 -0.6 -0.7}*0.1) = {0.9512 0.9418 0.9324} which yields the closed loop system characteristic equation, P_{CL}:

$$P_{CL} = z^3 - 2.8254z^2 + 2.6609z - 0.8353 \tag{B.3}$$

Using P_{CL}, the desired (canonical) closed loop system matrix is defined:

$$\Phi_M = \begin{bmatrix} 0 & 1 & 0 \\ 0 & 0 & 1 \\ 0.8353 & -2.6609 & -2.8254 \end{bmatrix} \qquad \text{(B.4)}$$

Calculating the multirate feedback control using $K = \Gamma_{MR1}^{-1}(\Phi_M - \Phi_{MR1})$ then gives the gain matrix of equation (3.5.5).